Design and Synthesis of Novel Polymerizable and Polymeric Antimicrobial Agents

by

Peter Snedden

A thesis submitted to the Department of Pure and Applied Chemistry, University of Strathclyde, in accordance with the requirements for the degree of Doctor of Philosophy.

September 1997

Glaubt es mir!—das Geheimniß, um die größte Fruchtbarkeit und den größten Genuß vom Dasein einzuernten, heißt: *gefährlich leben!*

— Friedrich Wilhelm Nietzsche
Die fröhliche Wißenschaft (bk. 4)

Acknowledgements

I would like to take this opportunity to acknowledge a few individuals. For those who offered either help, advice, assistance or inspiration, I extend my warmest thanks.

First, and foremost, I must mention my supervisor, Professor David Sherrington. His advice, encouragement and general sage counsel is sincerely and gratefully acknowledged.

The basis of this thesis took root during my time as a research assistant on *Project Spider*. As part of the *Spider* team I had the privilege of working alongside dedicated and skilled scientists. I would like to take this opportunity of thanking everyone, past and present, associated with the project. My appreciation goes to (in no particular order) Dr. Brian Rowatt, Dr. Elinor Scott, Dr. Tony McKee, Frank Murdoch, Dr. Jan Eggestadt, Dr. Mike Matty and Professor Bjorn Kristiansen. In particular, I am beholden to Andy Sneddon and Angela Brown, both of whom provided invaluable assistance and expertise on many technical matters.

For their help and assistance, I would also like to thank Bob Snedden (for computer scanned images), Dennis McLoughlin and Graham Fleming (for photographs), Margaret Smith, Sheila McCulloch, Alison Drummond and Jeff from the polymer engineering laboratory. Thanks also to the staff of the NMR and microanalytical laboratories of the Chemistry Department at the University of Strathclyde.

Finally, I wish to acknowledge my former supervisor at the University of Glasgow, Professor Gordon Kirby. This thesis would be non-existent if it were not for him.

Peter Snedden
September, 1997.

Summary

A range of structurally diverse, novel antimicrobial agents – non-polymerizable, polymerizable and polymeric – have been synthesized and tested for antimicrobial activity against the yeast strain *Saccharomyces cerevisiae* EL1 in orange and apple juice media. The aim of this work was to provide attractive candidates for use in liquid food preservatives.

The acrylamido thiazolyl monomer **67** (Scheme 1) was prepared but tested as inactive. Attempts to prepare the novel thiazolylsulfanilamide monomer **69** (Scheme 2) met with failure.

The non-polymerizable antimicrobial agents benzofuroxan **71** (Scheme 3), nonyl 3-amino parabens **78** (Scheme 4) and benzokathon **99** (Scheme 6) were prepared and tested for antimicrobial activity. Benzofuroxan **71** and, in particular, the parabens compound **78** displayed significant activity, whereas benzokathon **99** showed little activity. Polymerizable analogues of compounds **71**, **78** and **99** would make useful targets towards the development of polymeric antimicrobial agents.

Attempts to prepare the chloropropyl kathon **93a** and the bromoethyl kathon **93b** (Scheme 5) met with failure. In principle, the kathons **93a** and **93b** could be modified, through relatively straightforward chemistry, to polymerizable analogues.

The triethyl, tri-*n*-butyl, tri-*n*-octyl and triphenyl polymerizable phosphonium salts **105a–d** (Scheme 7) were prepared as *m/p*-isomeric mixtures. The pure *p*-isomeric analogues **111b–d** were prepared also. Only the tri-*n*-octyl phosphonium salt **105c** displayed antimicrobial activity. This result supports the general finding that cationic biocides with long alkyl chains are more active than those with shorter chains. The tri-*n*-butyl phosphonium salt monomer **105b** was polymerized. The resulting homo-polymer **112b** (Scheme 8) was found to inhibit yeast growth more than the corresponding monomer **105b**. This result supports the general finding that polymeric biocides are more active than the corresponding low molecular weight compounds.

The diiodomethyl sulfone **125** (Amical) and the analogous monoiodo species **126** (Scheme 10) were prepared and tested for antimicrobial activity. Compounds **126** and, in particular, **125** displayed very potent activities. A polymerizable analogue of Amical would

make a useful target towards the development of polymeric antimicrobial diiodomethyl sulfones.

The chemical breakdown of Amical **125**, in chloroform, to molecular iodine was investigated by UV spectrophotometry. The rate of iodine production was found to be accelerated by ultraviolet light and to be decelerated by darkness. As a result of this discovery, a photochemical mechanism was proposed for the degradation. Further studies revealed that the rate of iodine production was inversely proportional to the Amical solution concentration. The monoiodo analogue **126** of Amical was also observed to break down in chloroform to produce iodine. However, iodine production resulting from the degradation of **126** was not as great compared with that of Amical. As a result, it was concluded that iodine production increases with the degree of iodonation. This conclusion was supported by UV spectrophotometric studies of the 'model' compound, iodoform (CHI_3) – for solutions of identical concentration, iodine production increased in the order: **126** < **125** < CHI_3.

The chemical modification of Amberlyst 15 and Dowex 50-X8 sulfonic acid ion exchange resins **138** was conducted, in parallel, with the aim of producing a polymer-supported diiodomethyl sulfone **142a** (Scheme 12). Analytical evidence suggested that the transformation **138** → **142a** was more successful on the Amberlyst resin. Despite this, however, only very low iodine loadings were obtained for the Amberlyst resin **142a**. The Amberlyst- and Dowex-derived resin beads **138**, **139**, **141** and **142a** were tested for anti-microbial activity in the 'dry' and 'wet' states using plate assay and liquid assay techniques respectively. Although some beads were active, and others were not, the microbiological data was too inconsistent, in general, to form any concrete conclusions regarding activity trends.

The series of novel polymerizable nicotinate quaternary ammonium salts **148a–i** (Scheme 13), with esters of different chain length and structure, were prepared and tested for antimicrobial activity. A selection of the analogous isonicotinate compounds **149** were also prepared and tested. It was found that an increase in ester chain length lead to an increase in activity, with the C_8, C_9 and C_{12} nicotinate quats (**148g**, **148h** and **148i** respectively) testing as the most active. In addition, it was found that the straight-chain compounds were more active than their branched-chain counterparts (*e.g.* **148e** was more

active than **148f**). The position of the ester group on the pyridinium ring (*c.f.* **148** and **149** series) did not appear to significantly influence antimicrobial activity. The octyl nicotinate quat **148g** was polymerized with the aim of producing a water-soluble polymeric pyridinium salt. However, the resulting homo-polymer **150** (Scheme 14) was insoluble and, as a result, was not tested for antimicrobial activity. The *m/p*-isomeric version **151** of the quat **148g** was co-polymerized, separately, with acrylamide and 2-hydroxyethyl methacrylate (Scheme 15). It was hoped that co-polymerizing **151** with a hydrophilic monomer would produce a water-soluble pyridinium salt co-polymer. However, both the co-polymers **153** and **154** were insoluble in water and, again, testing of these materials was not pursued.

Abbreviations and Symbols

Abbreviations and symbols in common usage throughout this thesis are listed below.

Δ	reflux
AAm	acrylamide
abs.	absorbed
Ac	acetyl
AIBN	azobis-*iso*-butyronitrile
AMA	antimicrobial agent
approx.	approximately
Ar	aromatic
bp	boiling point
br	broad
Bu	butyl
BV	bed volume
cfu	colony forming units
conc.	concentrated
d	days *(time context)*
d	doublet *(NMR context)*
decomp.	decomposed
Et	ethyl
ex	extremely
exch.	exchangeable
FTIR	Fourier transform infrared
h	hours
HEMA	2-hydroxyethyl methacrylate
Hz	hertz
lit.	literature
m	medium
Me	methyl
MEA	malt extract agar
meq	milliequivalent
mg	milligram
MHz	Megahertz
MIC	minimum inhibitory conc.
MOJ	Mills orange juice
min	minutes
mp	melting point
N/A	not available
NAJ	Norwegian apple juice
NMR	nuclear magnetic resonance
Ⓟ	polymer
Ph	phenyl
ppm	parts per million
Pr^i	*iso*-propyl
Pr^n	*n*-propyl
py	pyridine
q	quartet
qn	quintet
r.t.	room temperature
s	strong
sh	shoulder
S/N	supernatant
SOJ	Sainsbury's orange juice
sp	septet
sp gr	specific gravity
sx	sextet

T	temperature	v	very
t	triplet	vbz	vinylbenzyl
THF	tetrahydrofuran	w	weak
TLC	thin layer chromatography	w.r.t.	with respect to
UV	ultraviolet		

Contents

3. Results and Discussion

1. INTRODUCTION

1.1 Antimicrobial Agents

1.1.1 Introduction

An *antimicrobial agent* (abbreviated to 'AMA'), or *antibacterial agent*, is a chemical compound (commonly a low molecular weight species; *polymeric* antimicrobial agents and antimicrobial *surfaces* are known also) that is capable of inhibiting, or retarding, the growth of a micro-organism. Some antimicrobial agents are also capable of the outright killing of micro-organisms. Antimicrobial substances affect the growth of micro-organisms via a discrete *mode* (or *mechanism*) *of action*. The *site of action* for antimicrobial agents is usually the cell membrane or the cell interior. The action of antimicrobial substances causes the disruption of key biochemical processes and mechanisms taking place inside the cell. As a result, the functioning of the cell is impaired and this leads, eventually, either to the inhibition of cell growth (*biostatic action*) or to the outright death of the cell (*biocidal action*). For a full understanding of the structure and function of antimicrobial agents it is therefore necessary to have a knowledge of how these compounds interact with host cells. In particular, it is desirable to understand the nature of the biochemical processes at work that affect the metabolism of micro-organisms. In this respect, the *specificity* and *selectivity* of the mode of action of antimicrobial agents with cell membranes and cell interiors becomes of vital importance.

Antimicrobial compounds and substances are vast in both number and type. Subsequently, they have found usage in a wide range of diverse fields and applications. The most common areas that antimicrobial materials are utilized are:

- Preservative formulations:
  - Cosmetics (*e.g.* hand creams & lotions)
  - Consumables (*e.g.* detergents, soaps and toiletries)
  - Food-stuffs
  - Technical
- Pharmaceuticals
- Antislime agents
- Antifungal agents
- Hygienic surfaces
- Insecticides and pesticides

The objective of this thesis was the design, synthesis and microbiological testing of a range of novel, polymerizable antimicrobial agents. The aim of this work was to provide

attractive candidates for utilization in liquid food preservative formulations. Hopefully, the present studies will serve as the groundwork for future research.

This thesis is primarily concerned with the chemical synthesis and testing of antimicrobial agents. Consequently, the biochemical aspects of antimicrobial action will take second place to the chemistry. Presented in section 1.2, however, is the relevant biochemical background (with an emphasis on the structure of micro-organisms, and the methodologies used to determine antimicrobial modes of action) this thesis demands. This is followed, in section 1.3, by a discussion of the different classes and types of antimicrobial agents and their biochemical modes of action. Section 1.4 summarizes the elementary aspects and principles of polymer chemistry. Following on from this, in section 1.5, is a discussion of polymeric and surface-immobilized antimicrobial agents.

The remainder of this section is devoted to a brief synopsis of the historical development of antimicrobial agents; particular attention is paid to the pioneering research in bacteriology, and the development of synthetic drugs used to combat infectious diseases. Further information and details on the history of antimicrobial substances can be found in the textbook written by Franklin and Snow.[1]

1.1.2 A Brief Overview of the Historical Development of Antimicrobial Agents

During their conquest of Inca Peru in the sixteenth century the Spanish *Conquistadores* observed the native Indians made use of the bark from the cinchona tree to treat malaria. Nearly three centuries later, in 1820, the alkaloid quinine **1**[2,3] (Figure 1) was isolated from *Cinchona officinalis*. For over a century, quinine remained the sole treatment for malaria until alternative drugs were developed in the twentieth century. Although quinine occurs mainly in cinchona bark it has also been isolated form trunkwood (Rubiaceae). Quinine is especially important in treating *Plasmodium falciparum* which is resistant to other anti-malarial drugs. Quinine also acts as a weak cardiac depressant and antifibrillatory agent and as a stimulant for horses (it has been used in horse doping).

In 1817, the alkaloid emetine **2**[4,5] (Figure 1) was isolated from the Brazilian ipecacuanha root (*Psychotria ipecacuanha*), the latter of which was used for its curative effects against diarrhoea and dysentery. Later, in 1891, emetine was shown to be active

against amoebic dysentery and it is still used, today, to treat this disease. Emetine has also been isolated from *Alangium lamarckii*, *Psychotria granadensis* and *Cephaelis acuminata*. The occurrence of emetine in common ivy (*Hedera helix*) and in the roots of *Borreria verticillata* still remains unconfirmed. Emetine is an amoebicide and a general parasiticide. It also shows antiviral, antitumour and antibacterial activity, and neuromuscular and cardiovascular effects. Emetine is an inhibitor of RNA, DNA and protein synthesis.

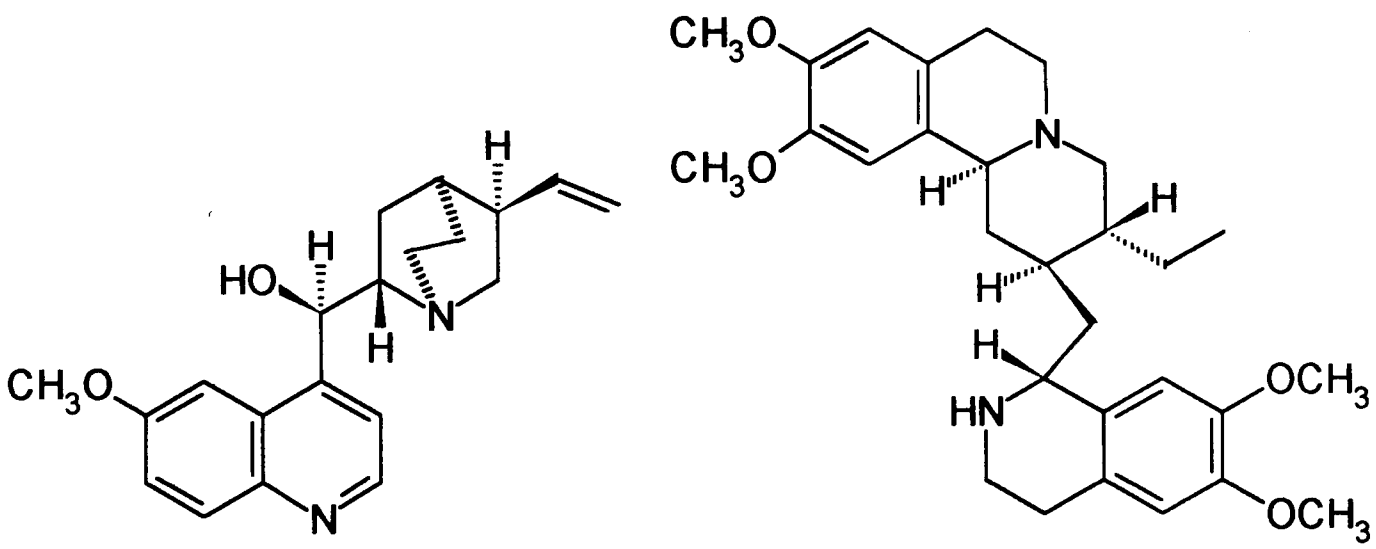

Quinine **1** Emetine **2**

Fig. 1 Early examples of natural antimicrobial compounds: *quinine* **1** (cinchona bark) was used to treat malaria up until the early twentieth century; *emetine* **2** (ipecacuanha root) is still used today to treat amoebic dysentery.

Quinine and emetine are probably the earliest sources of antimicrobial compounds to be used in medicine. It is noteworthy to point out that these early medicines were utilized well before the nature of the diseases they were used to cure were fully recognized and understood. For example, the exact nature of malarial disease was not realized until 1899.

In 1750, it is believed that the Scot John Pringle (1707–1782), acknowledged as the founder of modern military medicine, coined the term 'antiseptic'. Pringle used this terminology to describe chemical species that prevented the process of rotting (*putrefaction*). As far back as the Middle Ages, mercuric chloride ($HgCl_2$) was used in Arabia to prevent sepsis (pus-forming bacteria) in open wounds. It was not until the nineteenth century, however, that antiseptics became of widespread use in medicine. For example, in 1825, Labarraque used hypochlorite (ClO^-) to treat wounds. Later, in 1839, iodine tincture

was introduced for the treatment of the same. Then, in 1863, the French chemist and microbiologist Louis Pasteur (1822–1895) published a paper on the microbial origin of putrefaction. As a result of Pasteur's work, the foundations were laid for an understanding of infectional diseases. In 1870, phenol became the first example of an antiseptic to find widespread use in surgical techniques. The introduction of phenol antiseptic was due to work by the acknowledged founder of antiseptic medicine, the English surgeon and medical scientist Joseph Lister (1827–1912). It was not until the late nineteenth century, however, that initial attempts were made to fully realize and understand the function of antiseptic compounds. For example, in the 1880s, Koch laid the foundations of bacteriology by devising methodologies for obtaining pure cultures and for working under sterile conditions. Kronig and Paul utilized Koch's techniques and methodologies in their own researches. In 1897, they published a paper on the action of antiseptics and disinfectants. From the early twentieth century to the present day steady improvements have been made in the science of antiseptics. A wide variety of new antiseptic substances are now available today. However, many historical antiseptics are still in use either in pure, or chemically modified, form.

Once it had been established that infectious diseases were caused by micro-organisms numerous attempts were made to eradicate the micro-organisms and so end the infection. The Prussian medical scientist Paul Ehrlich (1854–1915) was responsible for pioneering research in the fields of hematology, immunology and chemotherapy. In particular, Ehrlich investigated the use of antimicrobial agents to combat infectious diseases. Ehrlich examined various chemical agents and the effects they had against infections (for example, the use of methylene blue to combat malaria). As a result of his studies, Ehrlich concluded that antimicrobial agents were intrinsically toxic materials that bound, and interacted, in some way with the cells of micro-organisms in order to exert an effect. Such chemical agents, Ehrlich postulated, had to have a selective action, *i.e.* they should only effect microbial cells and not the cells of the host species. Consequently, Ehrlich provided trypan red **3**[6] (Figure 2) as the first synthetic compound to have a curative effect against microbial infection, *viz.* trypanosomiasis in horses. Arguably, Ehrlich's greatest achievement came in 1909 with his discovery of the arsenical drug, salvarsan **4**[7] (Figure 2). Salvarsan became the standard treatment for syphilis until penicillin was introduced in

1945. Salvarsan is a polymer (usually stored as the hydrochloride salt) of variable molecular weight and, contrary to structural representations widespread in the literature, is unlikely to contain As=As double bonds.

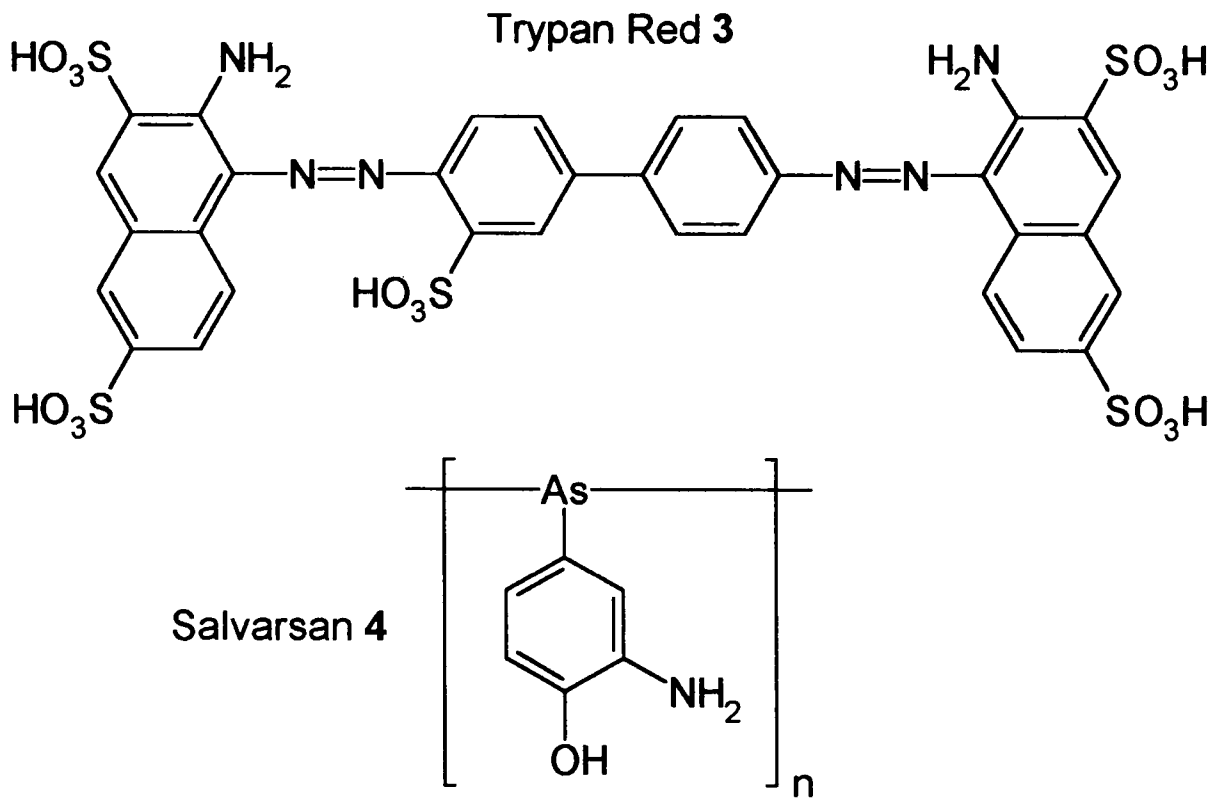

Fig. 2 Antimicrobial compounds introduced by Paul Ehrlich: *trypan red* **3** was the first synthetic compound used to combat an infectious disease (trypanosomiasis in horses); *salvarsan* **4** was the standard treatment for syphilis up until the introduction of penicillin in 1945.

The 'screening' methodology pioneered by Ehrlich is a useful tool that can be used in the search for new antimicrobial compounds. 'Screening' involves the application of a relatively simple microbiological test to a wide range of compounds of different molecular structure and design. In this way, molecular structure can be correlated against biological activity. By extending this idea, new compounds can be synthesized, and tested, with the aim of optimizing their antimicrobial effectiveness. For example, it is desirable to increase the activity of an antimicrobial substance and, at the same time, to decrease its toxicity. Using this methodology, it is possible, in principle, to arrive at the best possible compound (the 'optimum' structure) for the desired purpose. An assumption, here, is that if a compound shows activity against a micro-organism then a structurally similar, or analogous variant, will also show activity. As a result of Ehrlich's work, many useful and effective antimicrobial compounds were discovered in the twentieth century. For example, suramin

5[8–10] was first introduced in 1920 to treat human trypanosomiasis. Suramin was the first useful antimicrobial agent not to contain a toxic metal atom. Mepacrine **6** (Figure 3) came out in 1933 and was used to treat malaria in the Second World War. Owing to its skin-discolouring side-effect, however, mepacrine has since been replaced by alternative malarial drugs.

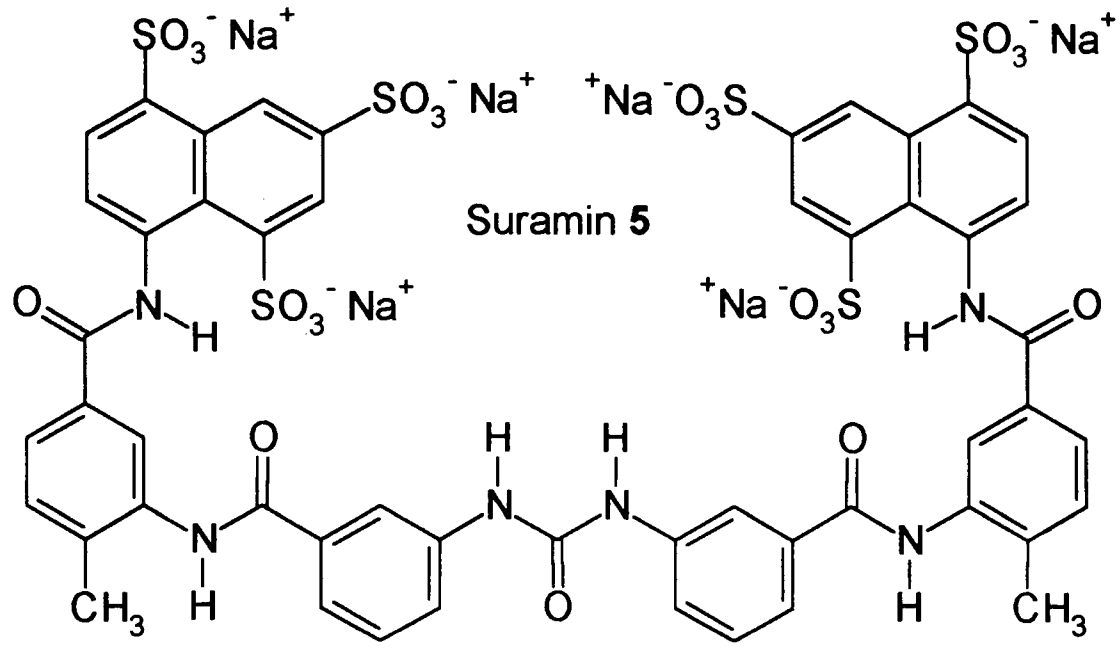

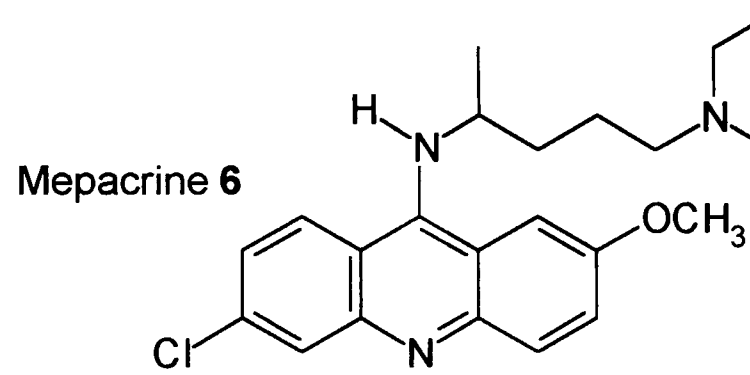

Fig. 3 Early synthetic compounds used to treat infectious diseases: *suramin* **5** was used to treat human trypanosomiasis from 1920 onwards; *mepacrine* **6** was the standard malarial drug used during the Second World War.

Little progress was made in the therapy of bacterial infection until 1935 when the German bacteriologist and pathologist Gerhard Domagk (1895–1964) discovered that *Prontosil rubrum* was active against infection in animals. Domagk was awarded the Nobel Prize in 1937. It was later shown by Tréfouël that *Prontosil rubrum* was metabolized in the body to produce sulfanilamide **7** (Figure 4). The latter proved to be the active agent. The results of this work opened the door to a new class of antimicrobial molecule and,

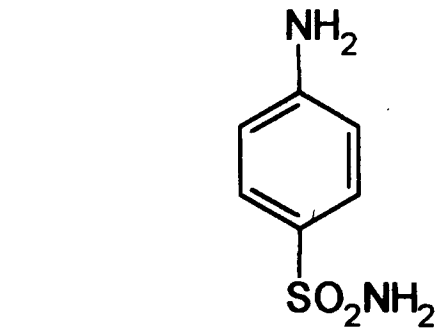

Sulfanilamide **7**

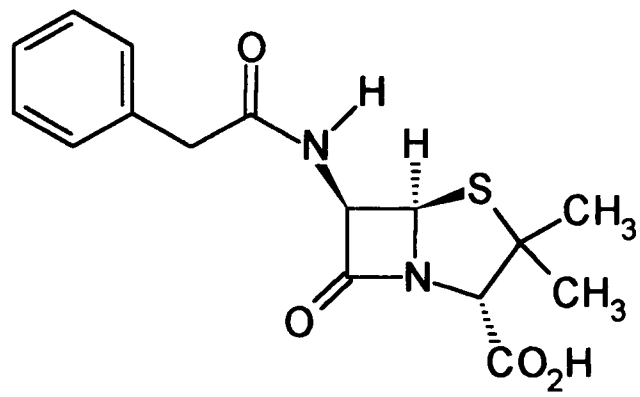

Penicillin (G) **8**

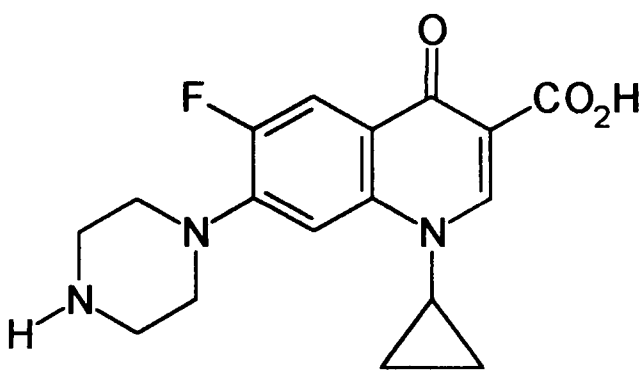

Ciprofloxacin **9**

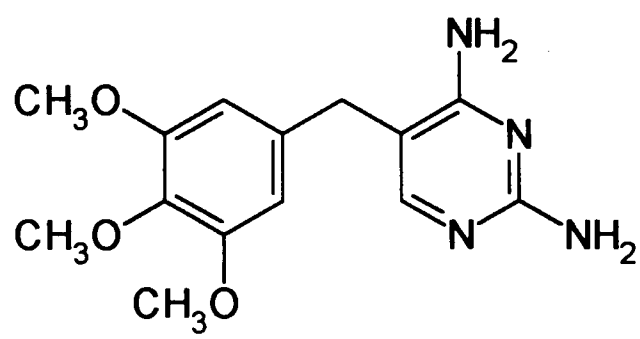

Trimethoprim **10**

Ceftazidime **11**

Fig. 4 Synthetic compounds commonly used to combat bacterial infection.

consequently, the sulfonamides proved to be extremely successful drugs. However, the development of sulfonamide drugs was overshadowed by that of penicillin **8** (Figure 4). Penicillin was first discovered by the Scottish bacteriologist Alexander Fleming (1881–1955) in 1928. It was not until 1940, however, that penicillin was isolated and purified due

to the collaborative work of the Australian pathologist Howard Florey (1898–1968) and the German-born British biochemist Ernst Chain (1906–1979). In the light of Florey and Chain's work the full potential of penicillin as an effective antibiotic was realized. Due to their efforts, Florey and Chain shared the Nobel Prize with Fleming in 1945.

Examples of modern synthetic compounds used commonly to combat bacterial infection are shown in Figure 4 and include ciprofloxacin **9**[11,12], trimethoprim (also known as 'syraprim' and 'trimpex') **10**[13] and ceftazidime **11**.[14,15] The quinolone ciprofloxacin is used in the treatment of Legionnaire's disease. Ceftazidime is an example of a semisynthetic cephalosporin β-lactam drug. It is used clinically as an antibiotic and is highly active against *Pseudomonas*.

Although not having as diverse an effect as that of bacteria, fungal microorganisms are still a significant threat to mankind and to animals. Antibiotics tend, in general, not to be very effective agents against fungal infections. As a result, research has concentrated on the design, and preparation, of synthetic antifungal agents. From studies of developments made in the design and synthesis of these compounds several reasonably safe azole drugs have been devised to combat human fungal infections (see below).

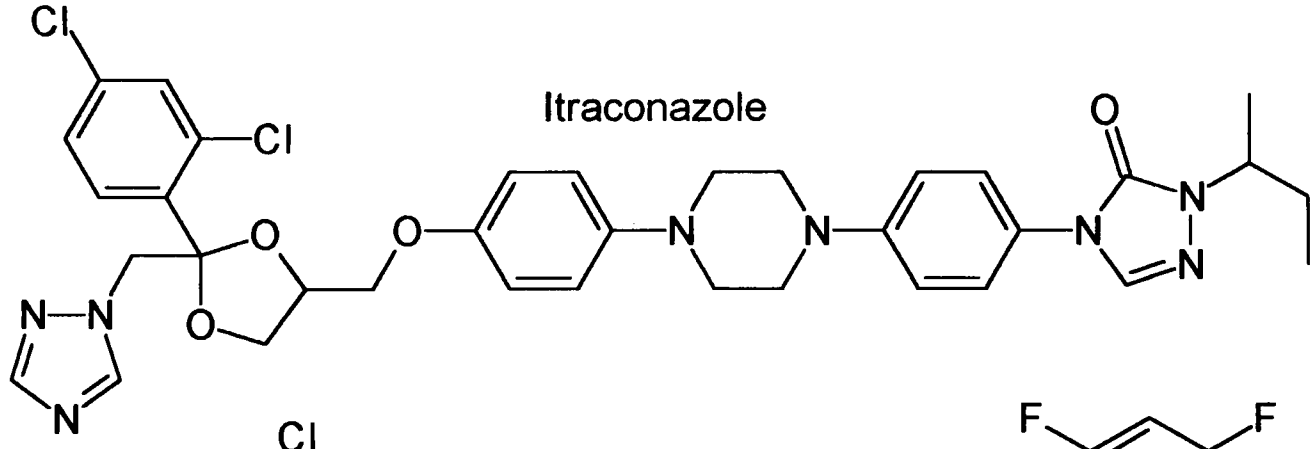

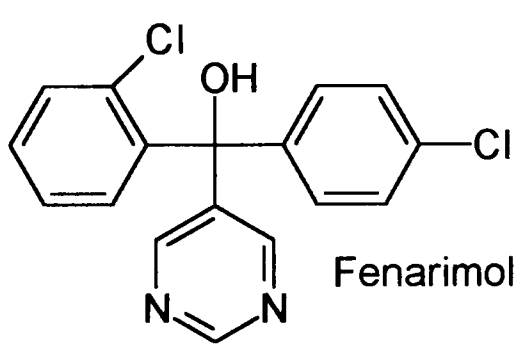

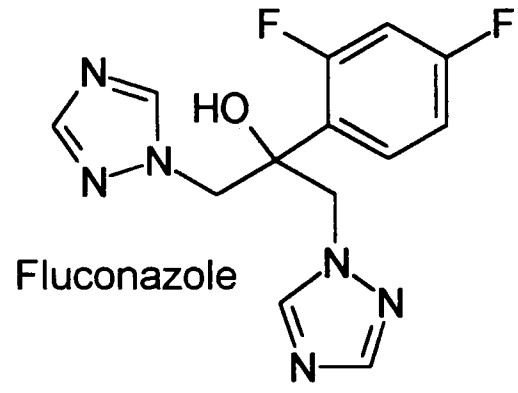

1.2 Biochemical Background For the Understanding of Antimicrobial Action

1.2.1 The Structure of Micro-organisms

Introduction

Discussion of the mode of action of antimicrobial agents assumes a knowledge of the structure and constitution of micro-organisms. The classes and structures of different types of micro-organism will now be described. Although antimicrobial agents can be effective against different kinds of organisms, their action against *bacteria* is of special importance and interest. Consequently, the structure of bacterial organisms will be described in specific detail later on in this section. General information on the structure and biochemistry of micro-organisms can be found in biochemistry textbooks written by Campbell,[16] Devlin[17] and Voet & Voet.[18] The biochemical aspects of antimicrobial action are described in texts by Franklin & Snow,[1] Edwards[19] and Hammond.[20] Natural antimicrobial agents and antimicrobial food preservatives are covered in the textbook edited by Dillon & Board.[21]

The smallest independent unit of life is the cell. The cell is protected from the outside environment by a membrane attached to a rigid cell wall. The membrane is in a fluid state and, as a result, the cell has a significant amount of flexibility. This flexibility is due to the predominantly non-covalent nature of the bonds between the components that make up the membrane. Coulomb and van der Waals forces therefore confer the membrane with a certain degree of flexibility and resilience.

We are all familiar with the names of different types of living organisms such as plants, animals, bacteria, yeasts, fungi and algae. The structures and constitution of the cells that compose these organisms can be quite different. For example, there are distinct differences between bacterial cells and animal cells. Animal cells are relatively large with a thin, non-rigid outer membrane. Within, specific parts and areas of the cell are responsible for different biochemical processes. The medium outside the cell is referred to as the *extracellular fluid*. This fluid acts as a food source for the cell, supplying the nutrients required to sustain it. Factors such as temperature and osmosis control the uptake of these nut-

rients. Bacterial cells, on the other hand, are smaller than animal cells and possess tougher, rigid outer membranes. Bacterial cells can develop high internal osmotic pressures. Consequently, in order to avoid disruption, bacterial cells are characterized by a constitutionally sound outer membrane. This membrane, or cell wall, therefore acts as a protective shield for the bacterium. Certain types of antimicrobial agents owe their effectiveness to their ability to interfere with the biochemical processes responsible for the synthesis of the cell wall.

Eucaryotic and Procaryotic Micro-organisms

Living organisms can, in general, be divided into the following two classes:

- *Eucaryotic Organisms* (*eucaryotes*, or *eukaryotes*)
- *Procaryotic Organisms* (*procaryotes*, or *prokaryotes*)

The governing distinction between eucaryotic and procaryotic organisms concerns the peripheral constitution of the cell nuclei. Eucaryotic organisms are characterized by cells that contain a distinct membrane-bound nucleus (*i.e.* the cell nucleus is clearly defined). Procaryotic organisms, on the other hand, lack a true membrane-enclosed nucleus. Plants, animals, yeasts, fungi and algae (with the exception of the *blue-green* algae) are all examples of eucaryotic organisms. Bacteria are among the best-known procaryotic organisms.

The eucaryotic cell is composed of a true membrane-bound nucleus and discrete, specialized membranous structures called *organelles* (examples of organelles include *mitochondria*, *chloroplasts*, *lysosomes*, *ribosomes* and the nucleus itself). The *cytoplasmic matrix* constitutes the nuclear membrane and is composed of *microfilaments* and fine, tubular structures known as *microtubules*. The latter, commonly found within animal and plant cells, help give shape to the cell and are the major components of *cilia* and *flagella* (small hair-like organs, or *locomotory projections*, on cell surfaces that help propel cells through fluids). The main function of microtubules is to aid the flow of materials in nerve cells. The cytoplasmic matrix also contains complex molecular structures responsible for important cell process such as energy generation, photosynthesis (plants only), protein and *lysosome* synthesis. Lysosomes are organelles (principally found in animal cells) that

contain enzymes capable of breaking down proteins and other biological substances. Lysosome enzymes play important roles in the digestive process and in the attack of ingested bacteria (in *phagocyte* white blood cells). The eucaryotic nucleus is a large organelle that contains well-defined *chromosomes* (bodies containing the hereditary DNA code material). The nucleus, itself, is bound by a complex double-membrane envelope. The eucaryotic cell wall is constructed of polysaccharides (*e.g.* cellulose) and is simpler in structure than the *peptidoglycan* component of procaryotes (see below). Eucaryotic cells also contain *mitochondria*, an *endoplasmic reticulum*, and a *Golgi apparatus*. Mitochondria are rod-like, spherical membrane-enclosed organelles. They contain enzymes responsible for energy production and serve as cellular energy exchangers. The endoplasmic reticulum consists of compartments composed of a membranous system of tubes, channels and flattened sacs. It acts as a canal-like communication system within the cell by storing and transporting proteins. The endoplasmic reticulum also carries enzymes responsible for fat synthesis. A Golgi apparatus[†] (or *Golgi body*) is composed of a stack of flattened membranous sacs, and acts a secretory device. Inside the sacs, molecules are assembled or modified. Many molecules travel through the Golgi apparatus on their way to other organelles or to the endoplasmic reticulum. The flagella of procaryotes are distinct from those of eucaryotes in both structural design and movement.

Procaryotes have simpler cellular structures than eucaryotes. Procaryotes lack a nuclear membrane and most of the components of eucaryotic cells. A characteristic feature of procaryotic cells is the possession of a *plasma membrane* (or *cytoplasmic membrane*). The latter is composed of a *phospholipid bilayer* containing integral proteins. The plasma membrane can form simple structures which carry out certain metabolic functions. Procaryotes have a *cell wall* attached to the outer surface of the plasma membrane. The cell wall is chemically and structurally complex and is composed mainly of a thick polymer meshwork called *peptidoglycan* (or *murein*). The cell wall constitutes the cell's primary osmotic barrier and functions to give shape and protection from *osmotic lysis* (a process that destroys cells by rupturing their membranes or cell walls). The part of the cell outside the nucleus is referred to as the *cytoplasm*. This term refers specifically to the jelly-like matter in which organelles are embedded. An important cytoplasmic constituent are the

---

[†] Named after the Italian physician, Camillo Golgi (1844–1926).

ribosomes. These are the protein-making 'machinery' of the cell and are located specifically on the endoplasmic reticulum. Ribosomes are composed of proteins and a special type of RNA called *ribosomal RNA*. They receive messenger RNA (copied from DNA) and amino acids and translate the messenger RNA using a set of chemically coded instructions. As a result, amino acids are linked in a specific order to make a strand of a particular protein. The procaryotic nucleus is termed the *nucleoid* and is not enclosed by a membrane (*c.f.* eucaryotes). Held within the nucleoid is the genetic material, composed usually of circular, double-stranded DNA. The nucleoid is susceptible to attack by small, low molecular weight foreign molecules (*e.g.* antimicrobial agents). Many procaryotic organisms also contain accessory, self-replicating genetic structures called *plasmids* (a small, mobile DNA strand found in bacteria) and *encoding proteins* to inactivate antibiotics.

As mentioned previously, bacteria are probably the best-known examples of procaryotic organisms. Antimicrobial agents are used to combat a wide variety of micro-organisms. Bacteria, in particular, pose a vital threat to mankind. As a result, extensive research and development is devoted to the design and synthesis of *antibacterial* agents. The principle barrier standing between bacterial organisms and foreign substances is the *bacterial cell wall*. The structure and constitution of the latter will now be described in detail.

Bacterial Micro-organisms

Bacterial organisms can be divided into the following two classes:

- *Gram-positive bacteria*
- *Gram-negative bacteria*

The above classification is historical in origin and derives from the *Gram stain*. The Gram stain is a widely used microbiological staining technique. It is used in the characterization and identification of bacteria. The test was devised by the Danish physician Hans Christian Gram in 1884.[18] The *Gram reaction* reflects fundamental differences in the biochemical and structural properties of bacteria. Bacterial cells are smeared onto a slide and the slide treated with a staining agent, commonly a dye named *crystal-violet*. The dye stains the bacterial cells a purple colour. The slide is then washed with an iodine solution, followed

by an organic solvent (commonly alcohol or acetone). *Gram-positive* bacteria possess relatively thick cell walls. Consequently, the cell wall is not readily penetrated by the solvent and, as a result, the bacterial cells remain purple. *Gram-negative* bacteria, on the other hand, possess relatively thin cell walls. Solvent is readily able to penetrate the cell wall thereby flushing the violet stain from the bacterial cells. In a final step, a counterstain is commonly employed. For example, *safranin* stains gram-negative bacterial cells red in colour. The Gram stain test in summary is as follows:

Bacteria	Cell wall	Violet stain
Gram-positive	thick	retained
Gram-negative	thin	removed

The Gram stain test therefore reflects the differences in the cell wall structures of different types of bacteria. The constitution and structure of gram-positive and gram-negative bacterial cell walls will now be described.

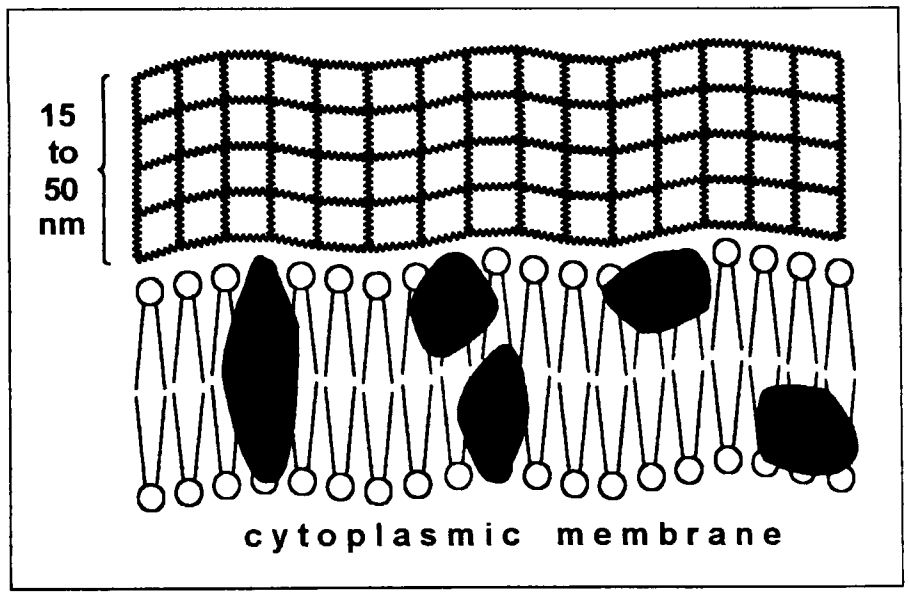

Fig. 5 A schematic representation of the gram-positive bacterial cell wall in cross-section. Refer to the text.

A schematic representation of a cross-section of the gram-positive bacterial cell wall is shown in Figure 5. The gram-positive cell wall forms a rigid protective covering for the fluid *cytoplasmic membrane* (or *plasma membrane*) beneath. The latter is the most important barrier separating the bacterial cell from its environment. The cytoplasmic membrane is composed of a double layer of *lipid* molecules. The non-polar, hydrophobic lipid tails are orientated towards each other and thus form the inside of the membrane. The polar, hydrophilic lipid heads face away from each other and so form the outside of the membrane. The gram-positive cell wall can vary in thickness from 15–50 nm. It is relatively simple in form and is comprised, in the main part, of an extensive cross-linked polymer network consisting of two covalently linked components – *peptidoglycan* (or *murein*) and *teichoic acids*. Peptidoglycan constitutes about 50% of the cell wall mass. Because of its cross-linked nature, peptidoglycan confers the cell with strength and shape. The peptidoglycan network, however, is not an effective barrier against low molecular weight compounds and, as a result, small foreign molecules can penetrate through to the cytoplasmic membrane relatively easily. Covalently linked to the peptidoglycan is an acidic polymer. This is usually a teichoic acid, either a poly(D-ribitol 5-phosphate) or a glycerol 3-phosphate. The teichoic acid component constitutes about 30–40% of the cell wall mass. The remaining 5–10% of the cell wall mass is comprised mainly of proteins and polysaccharides (each usually found in the outermost layers of the cell wall).

A schematic representation of a cross-section of the gram-negative bacterial cell wall is shown in Figure 6. The gram-negative bacterial cell wall is far more complex in structure than that of the gram-positive cell wall. The *periplasmic space* is comprised mainly of soluble enzymes and separates the cytoplasmic membrane from the cell wall. In gram-positive bacteria, approximately one half of the cell wall mass is composed of peptidoglycan. By contrast, in gram-negative bacteria, the peptidoglycan component constitutes only 5% of the cell wall mass. The peptidoglycan layer is also much thinner, typically on the order of 2 nm thick. Despite its small percentage composition and thickness, the peptidoglycan component nevertheless makes a considerable contribution to the strength of the cell wall. The main difference, however, between gram-positive and gram-negative cell walls is the possession by the latter of an *outer membrane*. The outer membrane is on the order of 6–10 nm thick and lies outside the cell wall. In an identical manner to the cyto-

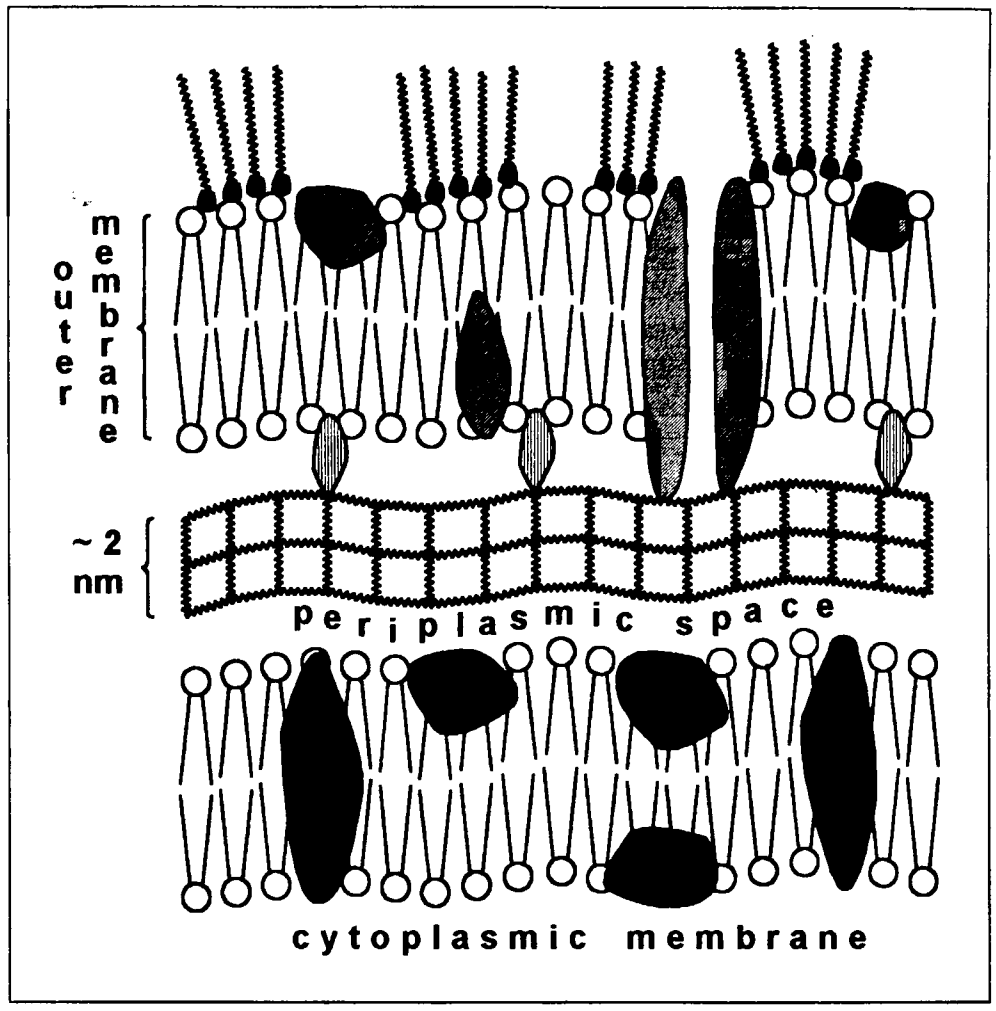

Fig. 6 A schematic representation of the gram-negative bacterial cell wall in cross-section. Refer to the text.

plasmic membrane, the outer membrane consists of a double layer of lipid molecules (hydrophobic on the inside, hydrophilic on the outside). Unlike the cytoplasmic membrane, however, the lipid bilayer of the outer membrane is composed of several components. These include *lipopolysaccharides* (structurally complex), proteins, fatty acids and *phospholipids*. In some cases the proteins that comprise the outer membrane form pores. Such

proteins are called *porins* and increase the permeability of the cell wall. As a result, hydrophilic molecules with molecular weights up to 700 are able to diffuse through the outer membrane. In general, however, the outer membrane of gram-negative bacteria is very resilient to penetration by foreign substances. *Lipoprotein* is another type of protein that constitutes the outer membrane. Approximately one third of lipoprotein is attached to the peptidoglycan component of the cell wall. The remaining two-thirds is in an unattached form.

1.2.2 Methodologies for Determining the Mode of Action of Antimicrobial Agents

During the latter half of the twentieth century scientists discovered and learnt a great deal more about the structure of biological macromolecules. Consequently, the synthesis and function of these molecules is now better recognized and understood. Nowadays, there are available a variety of modern procedures and techniques that enable the elucidation of the parts of micro-organisms antimicrobial agents are active against.

The part or molecular fragment of a biological molecule that an antimicrobial agent exerts its mode of action against is referred to as the *active site*. In some instances there may be more than one active site. In such a case the main, or principle, target for the antimicrobial agent is called the *primary active site*. The first step in the understanding of the action of an antimicrobial substance is to determine the primary active site in the micro-organism. Once this has been determined it is often possible to explain the antimicrobial agent's effect and influence on the metabolic and biochemical processes at work inside the cell. Presented below are brief descriptions of the methodologies employed to determine and understand the modes of action of antimicrobial substances.

- **Chemical structure** — It is desirable to know the chemical structure of the antimicrobial agent. With this knowledge it is then possible to correlate the antimicrobial agent's structure with that of other biologically important molecules (*e.g.* an intermediate in a metabolic pathway). An excellent example which illustrates this method of structure correlation is provided by the penicillin drugs: the β-lactam antibiotics (of which penicillins are the most well-known examples) are structural analogues of the D-alanyl-D-alanin molecular fragments that ultimately form the peptidoglycan component

of cell walls (refer to section 1.3.3, *Electrophilic Agents*, for further details). It is important to point out, however, that any structural similarities that exist between the antimicrobial agent and other biological molecules may, or may not, turn out to be important factors in determining the agent's mode of action. Structural information obtained in this way can therefore be deceptive or misleading.

- **Cell growth and morphology** — The antimicrobial agent's effect on cell growth and cell morphology can be examined. In this way it is possible to assess the extent to which the cell has been damaged by the agent. For example, certain antimicrobial agents act by rupturing, or damaging, cell membranes. This is referred to as a *cytocidal effect* and is common with many antibiotics (for example, the β-lactam drugs referred to previously). The rupturing of cell membranes leads to leakage of vital cell constituents such as potassium ions, amino acids and nucleotides. Experimental procedures exist that allow the observation and monitoring of the loss of ions and molecules from cells. *Lysis* occurs when the cell becomes severely damaged. A common cause of lysis is interference with the biological processes responsible for the synthesis and maintenance of the cell wall. Changes and perturbations in cell morphology are commonly detected using scanning electron microscopy.

- **Reversal of antimicrobial action** — If the antimicrobial agent does not harm the cell membrane then attempts can be made to try and reverse the biochemical action of the agent. The reversion process can be achieved by adding a series of supplements to the system. Examples of commonly employed supplements include fatty acids, amino acids, nutrients (*e.g.* compounds containing oxidizable carbon) and intermediary metabolites (*e.g.* vitamins, purines, pyrimidines). If reversal of the agent's biochemical action occurs then it may provide valuable information on the reaction sequence, or intermediate, that is being directly affected (or *blocked*) by the agent's action.

- **Cell ATP levels** — The biological activity in micro-organisms is greatly influenced and affected by changes, or perturbations, in energy metabolism. Metabolic changes can be detected by monitoring the supply and consumption of adenosine triphosphate (ATP)

within the cell. This is commonly achieved by testing the antimicrobial agent against the micro-organism's glycolytic and respiratory systems and by measuring cell ATP levels.

- **Radio-labelling** — It can sometimes be informative to examine the influence of an antimicrobial agent on the uptake of a radio-labelled nutrient (such as an amino acid, fatty acid, glucose or phosphate molecule). Kinetic studies employing radio-labelled compounds may give some indication of the identity of the primary active site.

- **Inhibition of the polymerization process** — If an antimicrobial agent inhibits protein or nucleic acid synthesis without affecting cell membrane functioning, protein/nucleic acid precursor biosynthesis or ATP formation, then it is likely that the polymerization process (leading to macromolecular formation) is inhibited. For example, if the anti-microbial agent directly affects RNA biosynthesis, the result is the indirect inhibition of protein biosynthesis.

- ***In vitro* testing of antimicrobial agents** — Assume that the biochemical sequence affected by the antimicrobial agent has been recognized in intact cells. The next step is to test the agent in a *cell-free* preparation. This is usually achieved by firstly isolating a key biomolecule, such as a target enzyme or a purified nucleic acid. The biomolecule is then tested *in vitro* with the antimicrobial agent. *In vitro* testing of antimicrobial agents enables more detailed information to be gained into the mechanism of the agent's mode of action.

1.2.3 Selectivity and the Mode of Action of Antimicrobial Agents

Once it has been determined how the action of an antimicrobial agent affects and influences a micro-organism's metabolism it is then required to explain the agent's *selectivity*.

By nature, an antimicrobial agent is effective against a micro-organism only if it's mode of action is selective. It is usually necessary to examine the effect of the agent's action on host cells as well as those of parasitical cells. There is a large diversity in the structure, size and function of antimicrobial agents. Consequently, their selectivity varies from one compound to another. If an antimicrobial agent is effective against microbial cells it does not necessarily imply that the host cells will remain unaffected. In some cases, anti-

microbial agents act on the biochemistries of both animal and microbial cells, but only affect the latter. Scientists can still not offer a satisfactory explanation for this observation. In other cases, antimicrobial agents act on and affect both host and microbial cells. However, if the agent is sufficiently concentrated in the microbial cells the selectivity is guaranteed and the host cells remain unaffected. An antimicrobial agent's selectivity of action of can therefore be affected by both chemical and physical factors.

There was a time when antimicrobial action was explained solely in biochemical terms. For a fuller comprehension of the nature of antimicrobial action, however, it has proven desirable to understand the *molecular* factors associated with the agent–target site interaction. An understanding of molecular interactions requires a knowledge of the three-dimensional structures of the antimicrobial agent (referred to as the *acceptor* molecule) and the target site (referred to as the *receptor* molecule – an enzyme, for example). Antimicrobial agents can, in most cases, be readily synthesized in the laboratory. The structures of these compounds can then be studied in detail using structure elucidation techniques such as X-ray crystallography and NMR spectroscopy. Performing a detailed structural analysis on a biochemical or macromolecular species (for example, a cell membrane or a large enzyme) can be, by comparison, an extremely demanding task. Modern science now possesses sufficiently advanced technologies and analytical techniques in order to accomplish this challenge.

The biochemical action of antimicrobial agents can be very sensitive to structural change. For example, if a minor structural alteration is made to a compound the result can lead to a partial, or complete, loss of biological activity. On the other hand, performing a structural alteration may have the opposite effect and enhance the compound's activity. Consequently, it is important to understand the precise structural requirements for antimicrobial activity. Although this is relatively straightforward to assess for small molecules it can be difficult to do for large molecules.

An effective antimicrobial agent, or substance, must have an optimum combination of the following characteristics:

- Efficient distribution and absorption within the system (especially important for drugs and pharmaceuticals)

- Ability to enter and concentrate in the micro-organism
- Selective action with the target site

It is not surprising that each of the above demands or requires a specific structural or molecular feature. For the antimicrobial agent to function at optimum efficiency its structure will therefore need to be comprised of subunits which will impart to it all of the above properties. It is important, however, that these molecular subunits do not interfere with, or affect, one another.

1.3 Classes of Antimicrobial Agents and their Modes of Action

1.3.1 Introduction

Now that the required biochemical background has been presented, it is time to examine and discuss the different classes of antimicrobial agents and their modes of action. For a review of the action of antimicrobial agents the work of Schmitt should be referred to.[22] The structures and properties of a wide range of antimicrobial substances can be found in the comprehensive 'dictionary' compiled by Elks and Ganellin.[23]

Antimicrobial agents can be classified either by *structure*, or according to their *mode* (or *mechanism*) *of action* against micro-organisms. The common structural classes of antimicrobial agents are as follows:

- *Acids*
- *Activated-halogen compounds*
- *Alcohols*
- *Aldehyde-releasing compounds*
- *Amidines*
- *Carbanilides*
- *Guanidines*
- *Isothiazolinones – 'kathons'*
- *Mercury compounds*
- *Phenols*
- *Quaternary ammonium salts – 'quats'*
- *Salicylanilides*

When classified by their mode of action, antimicrobial agents fall into one of the following two categories:

- *Membrane-active compounds*
- *Electrophilic agents*

Membrane-active compounds are so-named because their mode of action occurs at the cytoplasmic membrane of a cell. When adsorbed onto the cytoplasmic membrane, membrane-active compounds inhibit the following:

- *Electron transport chain process*
- *Adenosine triphosphate(ATP) synthesis*

As their name implies, electrophilic agents are strongly electrophilic in nature. They react with nucleophilic cell components and, consequently, deactivate key enzymes and substrates responsible for the life and maintenance of the cell.

Membrane-active compounds and electrophilic agents are described and discussed in more detail below.

1.3.2 Membrane-active Compounds

The principle structural classes of membrane-active compounds are as follows:

- *Acids*
- *Alcohols*
- *Carbanilides*
- *Guanidines*
- *Phenols*
- *Quaternary ammonium salts*
- *Salicylanilides*

The action of membrane-active compounds depends solely on the concentration at which they are used. Membrane-active substances initially diffuse through the outer membrane of the cell and adsorb onto the cytoplasmic membrane. The greater the concentration of active compound in the cell's environment then the stronger the degree of adsorption. The mode of action of membrane-active compounds consists of the following sequential steps:

- Adsorption onto, and diffusion through, the cell's outer membrane
- Non-specific adsorption onto the cytoplasmic membrane
- Interference with the function of the membrane's key proteins, leading to disruption of the membrane function (the precise nature of this disruption varies from one membrane-active substance to another)
- Membrane disintegration and loss of semi-permeable character
- Escape of cytoplasmic constituents (*e.g.* organic molecules, inorganic ions)
- Inhibition of adenosine triphosphate (ATP) synthesis and substrate transport process
- Cell death

Examples of membrane-active compounds are shown in Figures 7 (*acids*, *alcohols* and *phenols*) and 8 (*quaternary ammonium salts*, *carbanilides*, *salicylanilides* and *guanidines*). Organic acids are commonly used as preservatives in cosmetic formulations. Examples include 'simple' molecules like salicylic acid **12** and sorbic acid **13** (Figure 7). Other membrane-active acids include benzoic, cinnamic, propionic, formic and usnic acids. Activity studies have revealed that weak acids only in the undissociated form are active against cell membranes. The antimicrobial effectiveness of acids is therefore pH dependent. It has also been shown that the binding of undissociated acid at the cytoplasmic membrane is a reversible process. The action of long-chain, fatty acids can cause structural changes in cell membranes which eventually lead to the inhibition of key cell processes like, for example, ATP synthesis and electron transport. In bacteria, for example, the adenosine triphosphate pool is diminished when oxygen supply to the cell is obstructed. The electron transport chain process is dependent on electron-donating molecules. If these molecules are not made available then the cell's oxygen supply is blocked. The shorter-chain, lipophilic acids inhibit amino acid uptake and, consequently, decouple the substrate transport and electron transport processes.

Like the organic acids, alcohols and phenols are also membrane-active substances. Examples of membrane-active alcohols include 3-phenoxy-1-propanol **14** and the isomeric dichlorobenzyl alcohols **15** and **16** (Figure 7). Membrane-active phenols include compounds like *p*-hydroxybenzoic esters **17**, 2,4-dinitrophenol **18**, 2-benzyl-4-chlorophenol **19**, tetrabromo-*o*-cresol **20** and *o*-phenylphenol **21** (Figure 7). In the case of phenols, it has been found that antimicrobial activity is dependent on the *pK* value. Studies have also shown that the adsorption of phenols onto the cytoplasmic membrane is strongly influenced by the hydrophobic nature of the molecule (in general, increased hydrophobicity leads to increased activity). At low concentrations, phenols have been found to disrupt cell-membrane synthesis. As a consequence of this, the membrane loses its structural integrity. Increased permeability of the membrane results, followed by the escape of key cytoplasmic components leading to the eventual death of the cell. At higher concentrations, phenols are capable of denaturing proteins. 2,4-Dinitrophenol **18** and halogenated phenols like tetrabromo-*o*-cresol **20** have been found to decouple oxidative phosphorylation of the electron

Acids

12

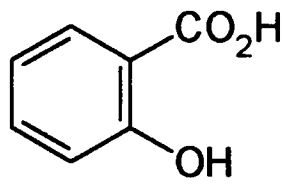

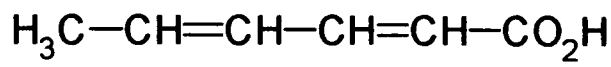

13

Alcohols

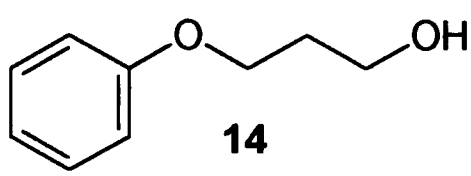

14

15

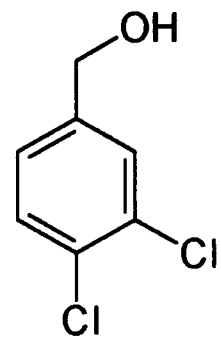

16

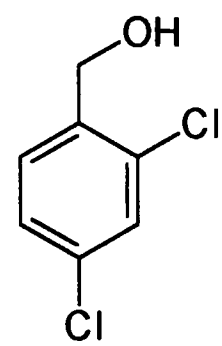

Phenols

17

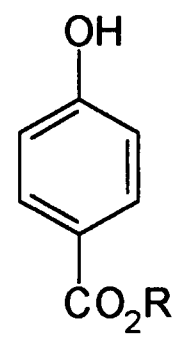

18

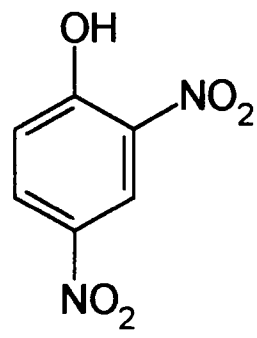

19

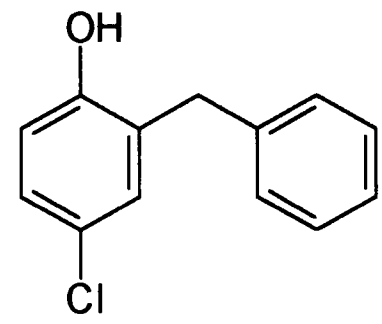

20

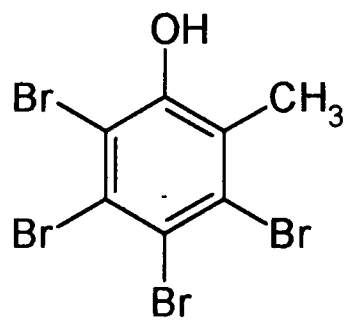

21

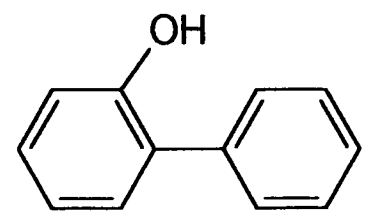

Fig. 7 Classes of membrane-active antimicrobial compounds: *acids*, *alcohols* and *phenols*.

Quaternary Ammonium Salts ('Quats')

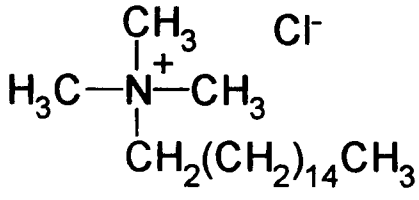

22

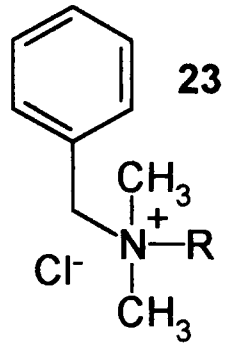

23

R = C_8H_{17} – $C_{18}H_{37}$

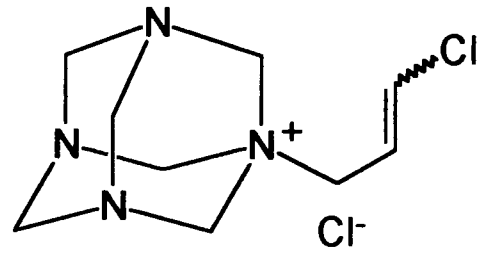

24

Carbanilides and Salicylanilides

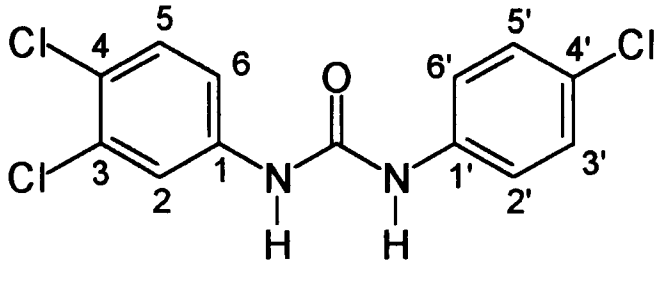

25

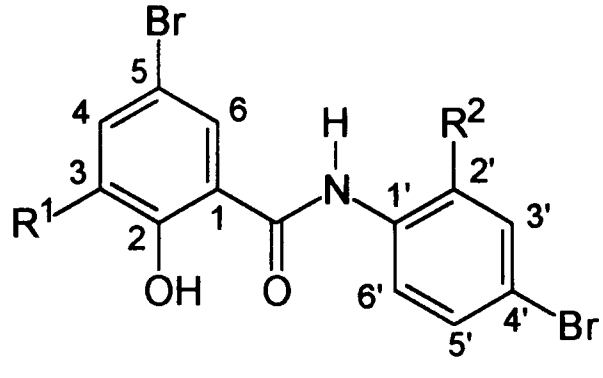

26 R^1 = Br, R^2 = H
27 R^1 = H, R^2 = Br

Guanidines

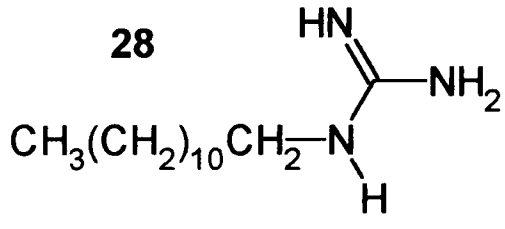

28

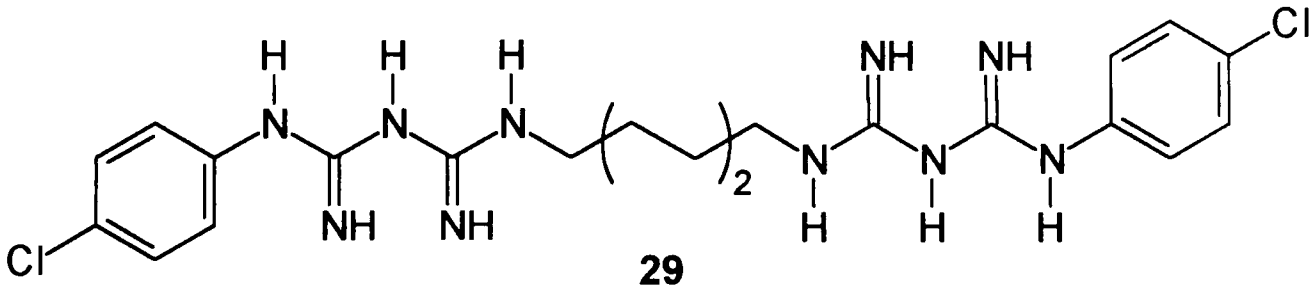

29

Fig. 8 Classes of membrane-active antimicrobial compounds: *quaternary ammonium salts*, *carbanilides* & *salicylanilides*, and *guanidines*.

transport process. 2,4-Dinitrophenol **18**, in particular, is known to increase the permeability for protons in artificial lipid membranes and in mitochondria.

One of the better-known sub-classes of membrane-active phenols are the *p*-hydroxybenzoic esters, or *parabens* for short. A key structural feature of parabens compounds is the possession of a hydrophobic alkyl chain ('R' in compound **17**, Figure 7). It has been shown that the antimicrobial activity of parabens compounds increases with an increase in chain length. However, the activity is found to drop off after an optimum chain size is reached. In addition, chain size affects the water-solubility of parabens compounds, the water-solubility decreasing with an increase in chain length. The investigation of structure–activity relationships in parabens compounds is therefore of key importance for determining the optimum structure required for maximum antimicrobial effectiveness.

One of the most extensively studied membrane-active substances are the quaternary ammonium salts, or *quats* for short. Quats and commonly used as disinfectants and as cosmetic preservatives. In addition, quat compounds are frequently used in oral hygiene ('mouthwash') formulations. Examples of membrane-active quaternary ammonium salts are shown in Figure 8 and include cetyltrimethylammonium chloride **22**, benzalkonium chloride **23** (commonly used as a disinfectant in hospitals[24]), and the structurally more exotic 1-(3-chloroallyl)-3,5,7-triaza-1-azoniaadamantane chloride **24**. The key structural features of quaternary ammonium salts appears to be the possession of a hydrophilic cationic component, *i.e.* the positively-charged nitrogen atom, and a hydrophobic alkyl chain. Because of the positive charge, quats can be effectively adsorbed onto the negatively charged outer membranes of cells. Like phenols (see above), quat compounds also disrupt the synthesis of cell-membranes, leading to increased membrane permeability and the subsequent loss of cytoplasmic constituents.

Other classes of membrane-active compounds shown in Figure 8 include the carbanilides and salicylanilides. An example of a membrane-active carbanilide is the urea derivative triclocarban (3,4,4'-trichlorocarbanilide) **25**. The membrane-active salicylanilide tribromsalan[25,26] (3,4',5-tribromosalicylanilide) **26** is commonly used in antiseptic formulations for soaps and detergents.[27] The isomeric variant **27** is also found to exhibit antimicrobial activity.[28] Compounds **26** and **27** are just two specific examples of a more general class of membrane-active compounds known as *halosalicylanilides*. The halogen

atom need not be bromine, as in compounds **26** and **27**, since the chlorosalicylanilides also display antimicrobial activity. 'Mixed' halosalicylanilides, containing both chlorine and bromine atoms, are also known and display antimicrobial properties. The mode of action of carbanilides and salicylanilides is similar to that of membrane-active phenols. For example, like 2,4-dinitrophenol **18** (Figure 7), triclocarban **25** is known to decouple oxidative phosphorylation of the electron transport process.

The final class of membrane-active compounds shown in Figure 8 is the guanidines, examples of which include dodecylguanidine **28** and chlorohexidine **29**. It has been proposed that the mode of action of guanidines is based on their interaction with the acid phospholipids of the cytoplasmic membrane. As a consequence of this, the functioning of key proteins in the cell is impaired, in particular the disfunctioning of the enzyme adenosine triphosphatase (ATPase). An important structural feature of the biguanide chlorohexidine **29**[29] appears to be the possession of a hexamethylene bridge, $(CH_2)_6$ (also found to be a structural necessity in polymeric biguanides). A loss in antimicrobial effectiveness results with biguanides that contain short ($<C_6$) or long methylene bridges ($>C_6$). This observation indicates that the structural integrity of cytoplasmic membrane phospholipids is only significantly effected when the interacting biguanide units are optimally spaced or connected.

1.3.3 Electrophilic Agents

The principle structural classes of electrophilic agents are as follows:

- *Aldehyde-releasing compounds*
- *Activated-halogen compounds*
- *Isothiazolinones*
- *Mercury compounds*

Electrophilic agents behave as strongly electrophilic species and react selectively with nucleophilic components of the cell. As a result, key enzymes and substrates vital to the cell's functioning are inactivated. Electrophilic agents therefore require the presence of a reactive functional group. In addition, the agent must possess the required structural factors (relating to size, shape, hydro-phobic/philic balance, conformation, stereochemistry, *etc.*) to enable the reactive functional group to correctly locate and position at the active site in order that it might function effectively. Examples of electrophilic agents are shown in Figure 9.

Aldehyde-releasing Compounds

30

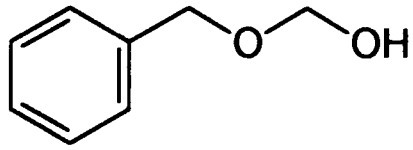

31

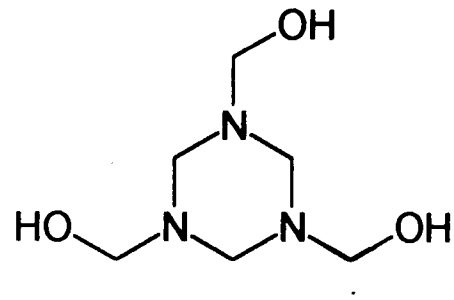

32

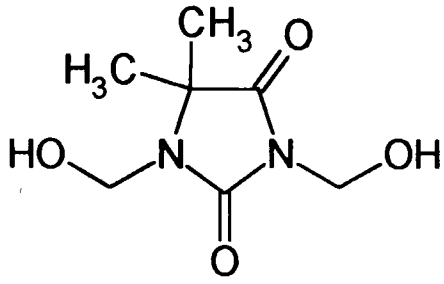

33

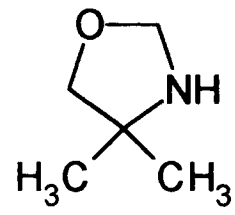

Activated Halogen Compounds

34

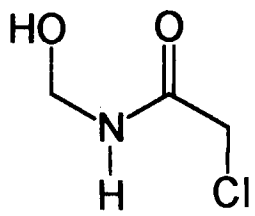

35

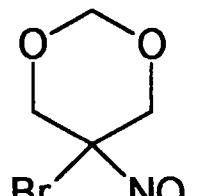

36

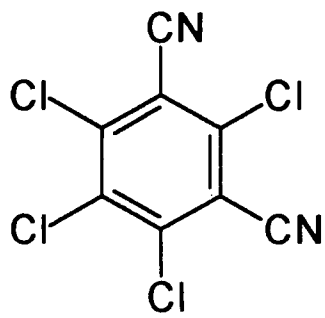

37

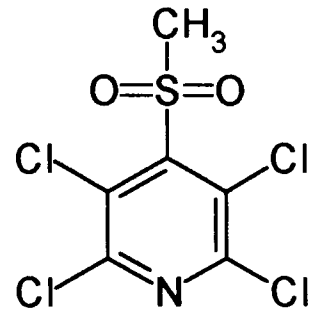

Isothiazolinones

38

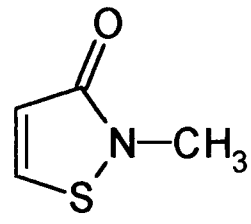

Mercury Compounds

39

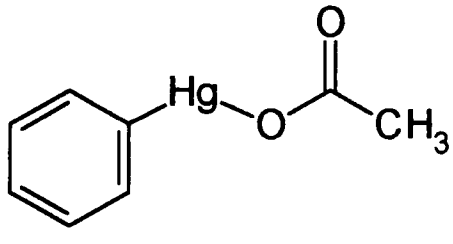

40

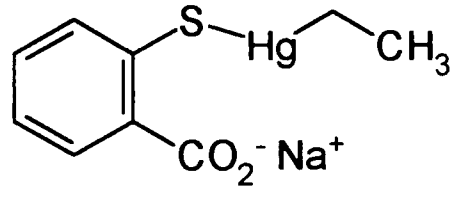

Fig. 9 Classes of electrophilic antimicrobial compounds: *aldehyde-releasing compounds*, *activated halogen compounds*, *isothiazolinones* and *mercury compounds*.

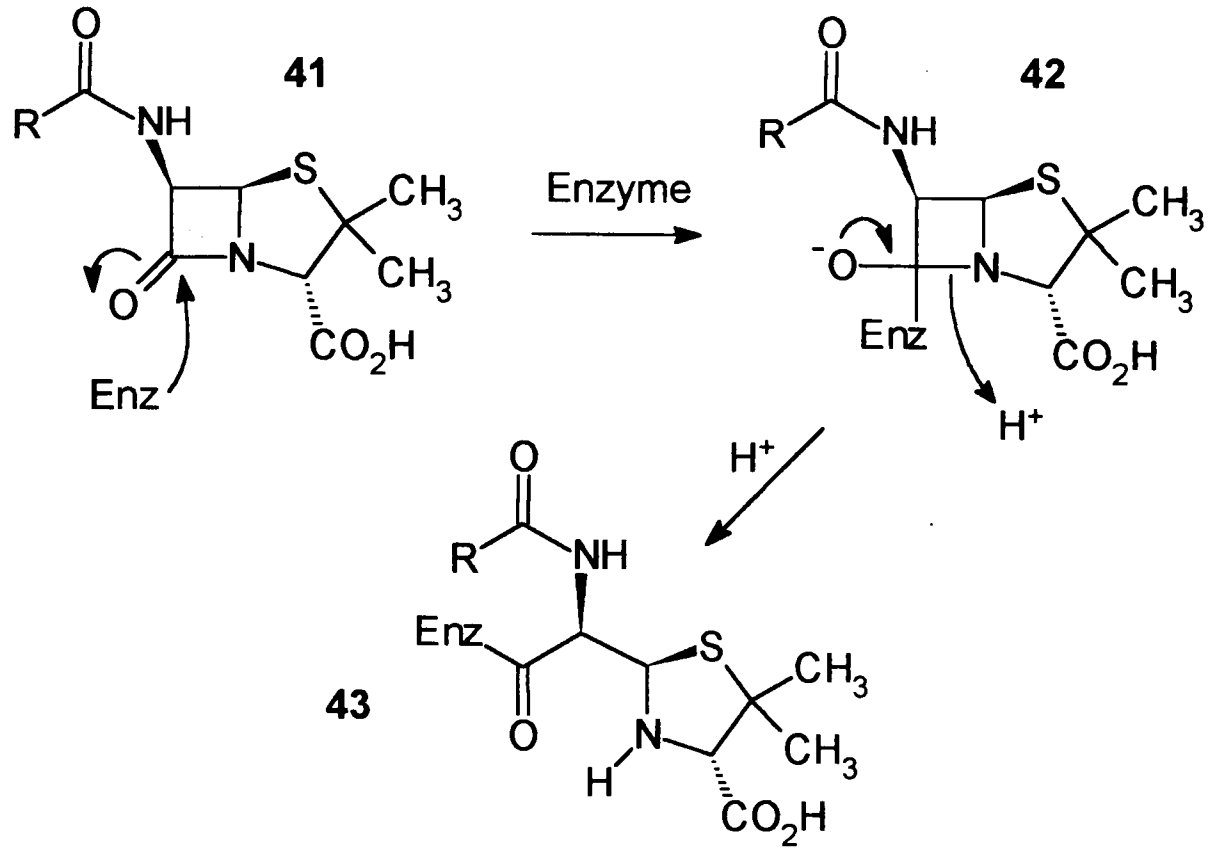

Fig. 10 The mode of action of penicillin antibiotics.

In biochemistry, it is commonly the case that the reaction between substrate and host molecule is sterically demanding. If the agent is to react selectively with the substrate molecule then specific steric requirements must be met. A good example of selective reactivity is the mode of action of penicillin antibiotics of the general type **41** (Figure 10). The β-lactam antibiotics bear a strong structural resemblance to certain molecular fragments that ultimately form the peptidoglycan component of cell walls. Enzymes, such as carboxypeptidase and transpeptidase ('Enz' in Figure 10), responsible for cell wall synthesis mistake the β-lactams for their true substrates. The reaction product is the stable β-lactam–enzyme adduct **43**. The enzyme is therefore deactivated and, as a result, cell wall synthesis is inhibited.

Electrophilic agents are commonly used as preservatives. Selective reactivity is less important here and, consequently, electrophilic preservatives need not meet strict steric requirements. Probably the best-known preservative is formaldehyde, $H_2C{=}O$. The formaldehyde molecule is small and highly electrophilic in nature. It is relatively reactive and, consequently, it has a low selectivity in chemical reactions. The formaldehyde molecule therefore has little, or no, bias towards the active sites of different substrate molecules. Formaldehyde reacts with nucleophilic cell components such as thiol groups and the amino

groups of amino acids and proteins, resulting in the formation of methylene bridges. An example of a formaldehyde reaction involving the amino acid histidine **44** is shown in Figure 11. Reaction of **44** with a molecule of protonated formaldehyde affords, after

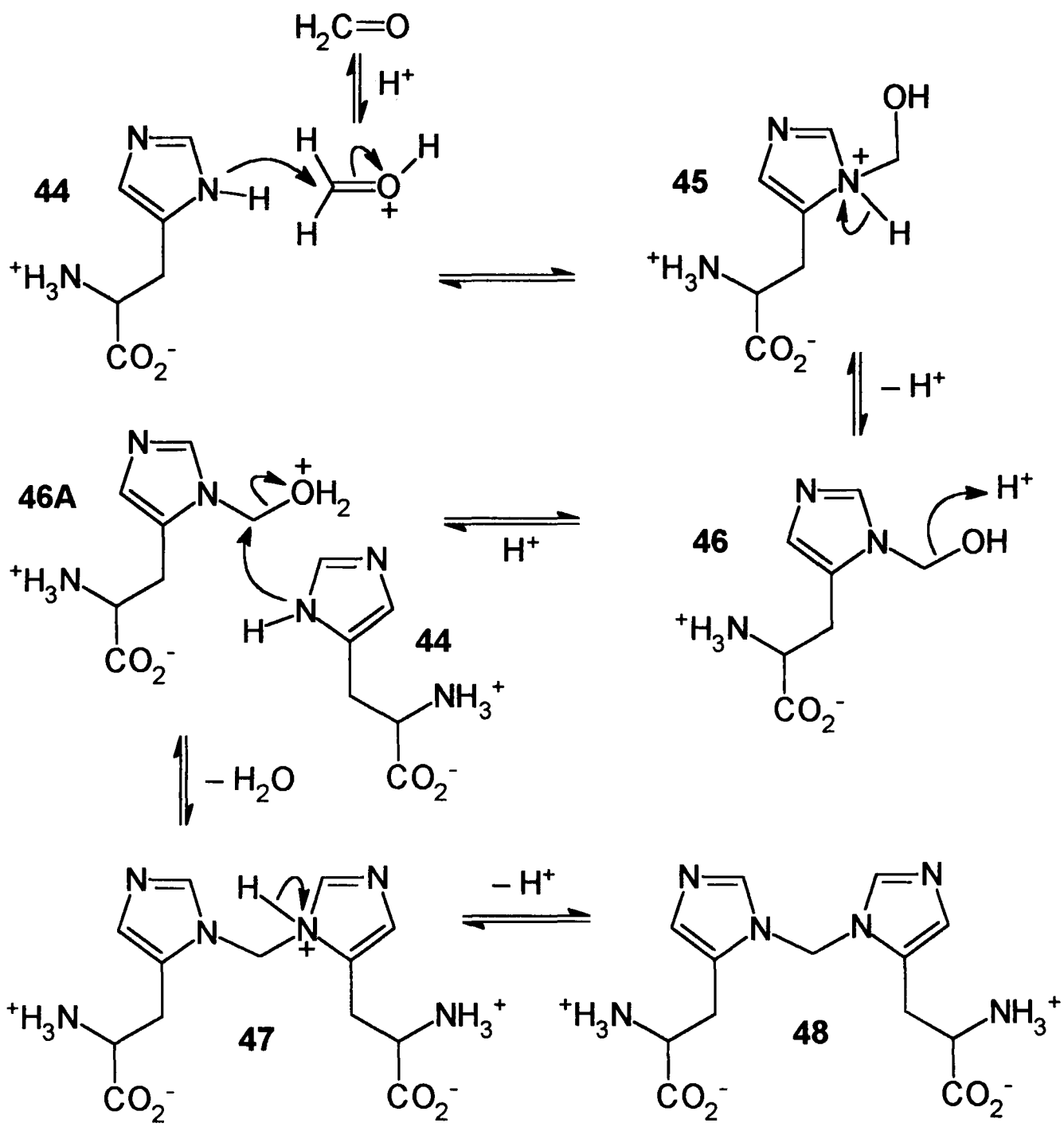

Fig. 11 An example of a formaldehyde reaction involving the amino acid histidine **44**; note the formation of the methylene bridge in **48**.

deprotonation, the *N*-hydroxymethyl compound **46**. The latter can then react with a molecule of histidine (or, alternatively, a nucleophile of a different type) to eventually produce the methylene-bridged histidine 'dimer' **48**. The methylene bridge thus produced can be hydrolyzed. Consequently, the reactions of formaldehyde with amino and thiol groups are

reversible. The overall effect of formaldehyde reactions in biochemical systems is the de-activation of protein enzymes leading, eventually, to perturbations of the tertiary structure.

Although formaldehyde is still used as a preservative, it sometimes proves more beneficial to employ formaldehyde- or aldehyde-releasing compounds. Examples of aldehyde-releasing compounds are shown in Figure 9 and include benzylalcohol hemiformal **30**, 1,3,5-tris(hydroxymethyl)-1,3,5-hexahydrotriazine **31**, 1,3-bis(hydroxymethyl)-5,5-dimethyl-2,4-imidazolidinedion **32** and 4,4-dimethyl-1,3-oxazolidine **33**. Aldehyde-releasing compounds contain formaldehyde in the guise of acetals, hemiacetals (cyclic or acyclic), aminals and mixed acetals containing N and O. Such compounds release formaldehyde into the proton-rich areas surrounding the cytoplasmic membrane of respiring cells. The advantage of aldehyde-releasing compounds is that they do not posses the high volatility associated with that of 'free' formaldehyde. Cosmetic formulations commonly

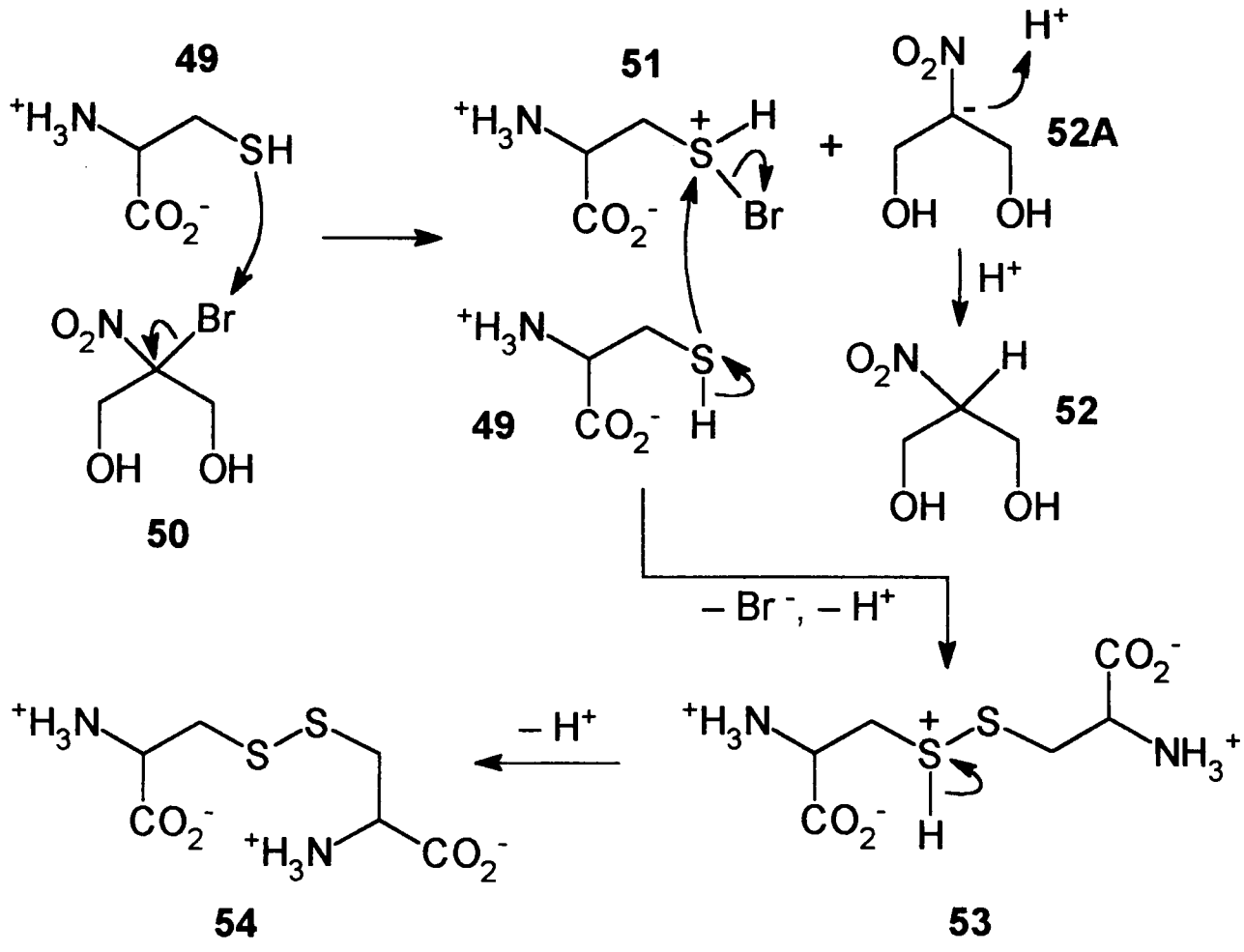

Fig. 12 Formation of cystine **54** resulting from the reaction of the amino acid cysteine **49** with 2-bromo-2-nitropropanediol **50**.

employ aldehyde-releasing compounds since the organic matter in some formulations has the tendency to deactivate 'free' formaldehyde. Commonly, aldehyde-releasing com-

pounds contain an additional electrophilic functionality (commonly a halogen atom) in order to give the compound a broader spectrum of action. This is illustrated in Figure 12 by the reaction of 2-bromo-2-nitropropane-1,3-diol **50** with the amino acid cysteine **49**. The C–Br bond in **50** is strongly polarized by the effect of the powerfully electron-withdrawing nitro group. 'Soft' nucleophiles like the sulfur atom of the thiol group in cysteine appear to act on the δ^+ bromine atom to afford the S–brominated cysteine **51**. Reaction of **51** with a molecule of cysteine produces, after deprotonation, the disulfide cystine **54**. The mechanism shown in Figure 12 has been proposed to account for the observed formation of disulfides (such as **54**) in biochemical systems. Co-enzyme A has also been found to react with **50** in a similar manner to that of cysteine. 'Hard' nucleophiles, on the other hand, appear to act on the nitro group of **50**. This is evidenced by the formation of nitrosamines (RR'N–N=O) in the presence of trace amounts of secondary amines.

Another class of electrophilic agents shown in Figure 9 is the activated halogen compounds, examples of which include 2-chloro-*N*-hydroxymethylacetamide **34**, 5-bromo-5-nitrodioxan **35**, 1,3-dicyano-tetrachlorobenzene **36** and 4-methylsulfonyl-tetrachloropyridine **37**. Antimicrobial substances containing activated halogen are commonly used in formulations for technical preservation and as antislime agents. The structural requirement for activated halogen compounds is the possession of an electron-withdrawing group in close proximity to the halogen atom (chlorine, bromine or iodine; fluorine is less common). Commonly used electron-withdrawing groups in activated halogen compounds include amido, cyano, sulfonyl and nitro. Antimicrobial activity in activated halogen compounds is not only induced by the proximity of electron-withdrawing groups. Vinyl groups directly attached to the halogen atom are also capable of exerting an activating influence ('vinylogous activation'). Vinyl compounds with activated halogen commonly have the halogen atom attached at position β to the electron-withdrawing group (*e.g.* compounds **36** and **37** in Figure 9). As a result, the C–halogen bond is considerably weakened. This has the effect of making the halogen-bearing carbon atom susceptible to nucleophilic attack in the form of addition–elimination reactions.

Isothiazolinones ('*kathons*') are a class of electrophilic agents that contain a 5-membered heterocyclic ring, an example of which is 2-methyl-isothiazolinone **38** (Figure 9). The antimicrobial activity of isothiazolinones is principally due to the reactivity of the

sulfur–nitrogen bond (this reactivity is similarly observed in the antimicrobial sulfenamide compounds, RR'N–S–$CFCl_2$). The mode of action of isothiazolinones involves nucleophilic attack at the sulfur atom by sulfur-containing nucleophiles (*e.g.* thiols and thiol acids), resulting in the opening of the isothiazolinone ring. Isothiazolinones are particularly reactive towards the thiol groups in enzymes and in amino acids. Consequently, isothiazolinones act as enzyme and amino acid 'blockers'. The mode of action of isothiazolinones is illustrated by the example shown in Figure 13. The thiol **55** acts on the sulfur atom of *N*-protonated 2-methyl-isothiazolinone **38A**. Ring-opening of the latter produces, after deprotonation, the disulfide **57** as the stable reaction product.[30]

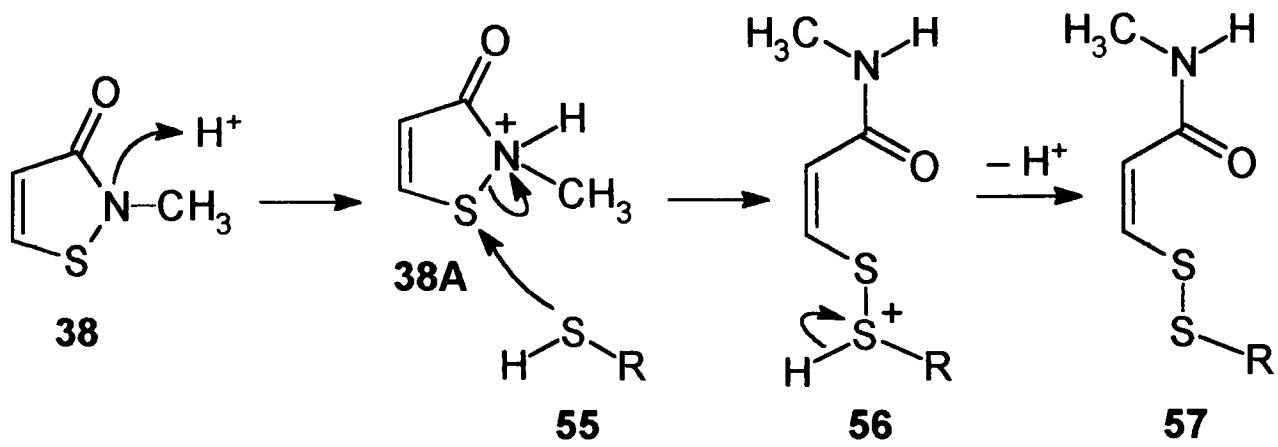

Fig. 13 Formation of the disulfide **57** resulting from ring-opening of the isothiazolinone **38**; R = alkyl, aryl, C(O)R', or C(S)SR'.

The final class of electrophilic agents shown in Figure 9 is the mercury compounds, examples of which include phenylmercuric acetate **39** and thimerosal **40**. Mercury compounds behave as 'soft' acids and react selectively with enzymes, membrane substrates, cell wall proteins and ribosomes. The products resulting from these reactions are extremely stable compounds. Owing to their toxic nature, mercury compounds are not widely used as antimicrobial agents. They are sometimes utilized, however, in preservative formulations in the cosmetics industry.

1.4 Vinyl Monomers, their Polymerization and their Polymers

1.4.1 Introduction

Polymers and polymeric materials are a prominent feature throughout this thesis. As a result, it was felt that a brief overview was necessary of the basic principles of polymer chemistry. Further information on polymer science can be found in textbooks by Cowie,[31] Allcock & Lampe,[32] Elias[33] and Billmeyer.[34]

A *polymer*, or *macromolecule*, is a large, high molecular weight molecule in which a certain structure is systematically repeated throughout the molecule. The repeated structure is called a *repeat unit*, or *monomer unit* (*monomer residue*). Polymers are distinct from non-polymeric materials in the followings ways:

- Molecular weights are very large (> ~10,000).
- Molecular weight may not be unique – different samples of the same polymer may differ in molecular weight.
- In any one polymer sample the molecules may not be all the same size – there may be a *distribution* of sizes.

Molecular size is an important feature since it gives the polymer characteristic physical properties (*e.g.* toughness in resins, tensile strength in fibres). The molecular weights of polymers can be determined from colligative properties (*e.g.* vapour pressure of solvent, depression of freezing point, osmotic pressure), viscosity measurements and light scattering measurements.

There are two main types of polymerization reaction – *addition polymerization* and *step-growth polymerization*. Whereas addition polymerization is limited to some alkene derivatives, many different types of molecule can undergo step-growth polymerization. This overview will be concerned with the characteristics of addition polymerization only.

Addition polymerization is restricted to certain alkenes. Not all alkenes will polymerize but most of those which do are monosubstituted or 1,1-disubstituted ethenes:

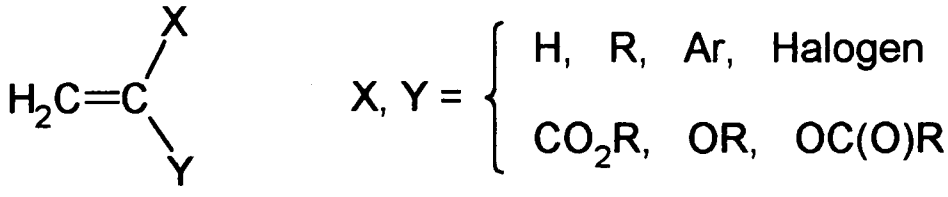

'X' or 'Y' can be a hydrogen atom, an alkyl or aryl group, or a halogen atom. Vinyl esters and vinyl ethers can be polymerized also. Examples of vinyl monomers commonly used in industry are shown below:

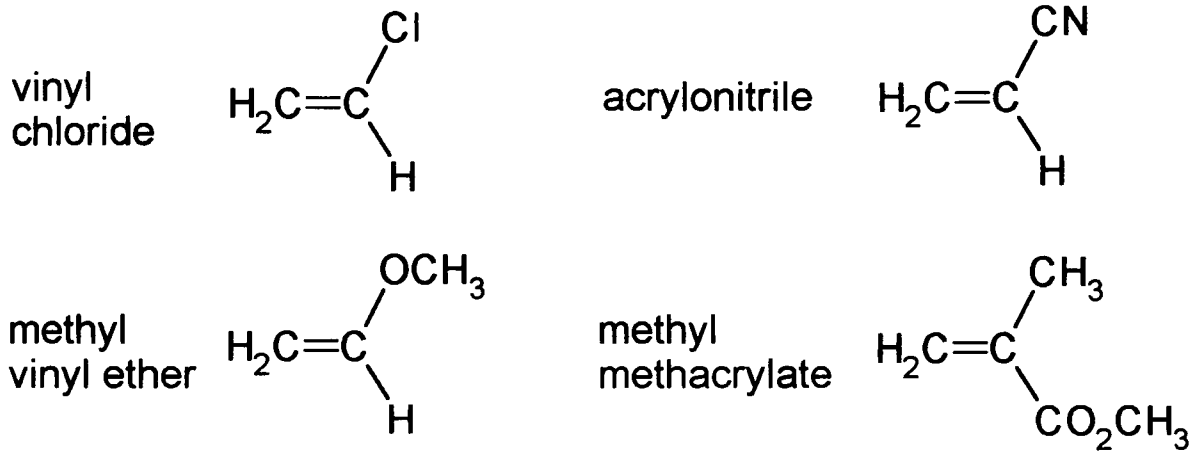

Symmetrically substituted ethenes and tetrasubstituted ethenes (below, top) do not, in general, polymerize. Exceptions, which will polymerize, are ethene and tetrafluoroethene ($H_2C{=}CH_2$ and $F_2C{=}CF_2$ respectively). Dienes can also be polymerized; examples include butadiene and isoprene (below, bottom).

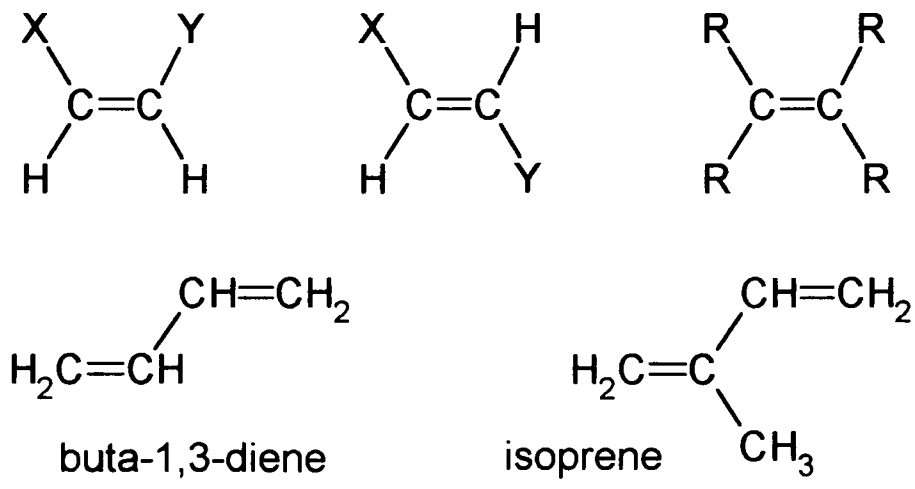

The addition polymerization of ethene derivatives involves the following overall reaction, where one of the bonds in the original double bond is used to allow monomer molecules to link together to form a long chain (a *linear macromolecule*):

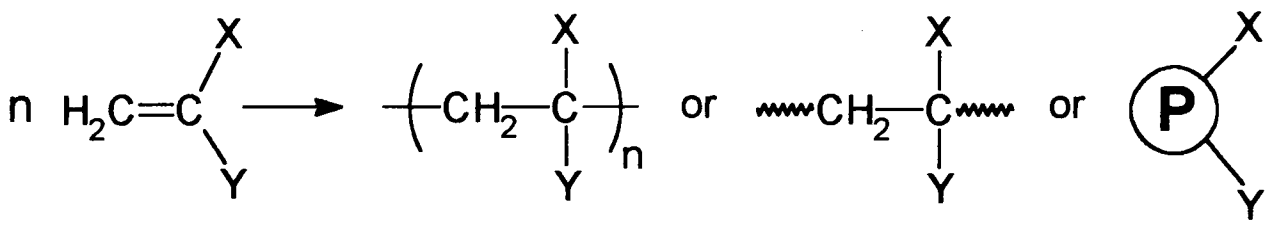

The size of a polymer is determined by the number of repeat units, *n*. A molecule with a small number of repeat units is called an *oligomer*. On the right hand side of the arrow (above) are shown the common ways in which polymers are represented. When only one type of monomer is polymerized the resultant macromolecule is sometimes referred to as a *homo-polymer* (or just 'polymer'). If two, or more, monomers are polymerized together the product is a *co-polymer*.

Polymers, in general, can be *linear* or *branched* in structure, or can form a two- or three-dimensional *network*:

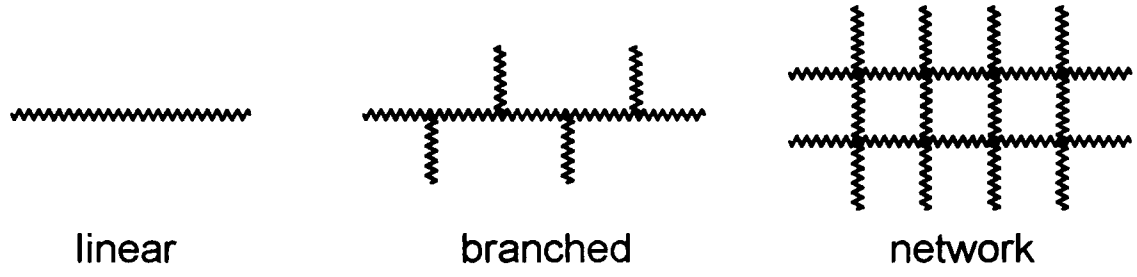

The mechanism of addition polymerization is a *chain reaction*, involving reactive intermediates known as *chain carriers*. The chain carriers can be free radicals, carbocations or carbanions.

1.4.2 Free Radical Addition Polymerization of Vinyl Monomers

The commonest, and most important, type of polymerization reaction is the free radical addition polymerization of vinyl monomers (however, not all monomers of the substituted ethene type can be polymerized by a free radical mechanism). In free radical addition polymerization, the intermediate chain carrier is:

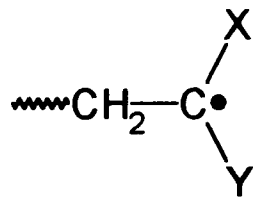

The free radical addition route is favoured by vinyl monomers that contain electron-withdrawing groups [*e.g.* X = CN, CO_2R, Ph, C(O)R, Cl]. If X is an electron-releasing group, the free radical route may be possible, provided that Y is an electron-withdrawing group:

e.g. methyl methacrylate

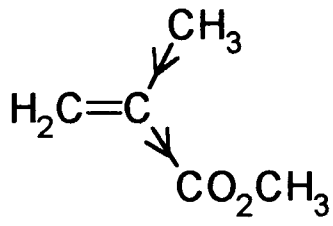

The free radical route is not normally possible if only electron-releasing substituents are present: *e.g.* X = H, and Y = R or OR; X = R, and Y = R or OR.

A chain reaction mechanism consists of three steps: *initiation*, *propagation* and *termination*. The first step, initiation, involves the formation of a reactive intermediate – the chain carrier. In the propagation step the chain carrier reacts with starting material and is, itself, regenerated. In the final step, termination, the chain carrier reacts so as to lose its activity. There are many propagation steps to each initiation or termination step, and the whole process from initiation to termination is extremely rapid. There are many types of chain reaction – addition polymerization is an example which involves a special type of propagation step in which the chain carrier increases in size as propagation proceeds. The mechanism of free radical addition polymerization will now be described in more detail.

Initiation

The initiation process involves two steps. In the first step, the *initiator* breaks down or decomposes to form the *primary radical*:

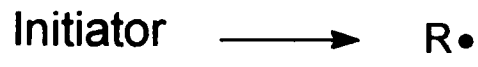

The formation of the primary radical is a relatively slow process since energy is required to break chemical bonds. The second step is comparatively faster and involves the reaction of the primary radical with a monomer molecule to form the chain carrier:

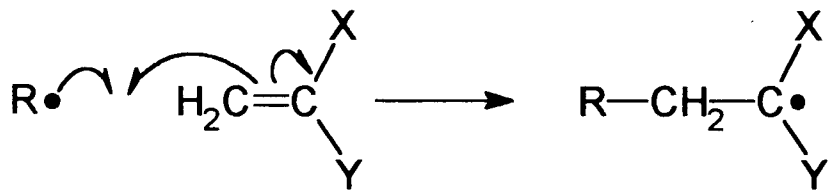

Initiator decomposition can be achieved either thermally or photochemically. An advantage of the latter method is that it allows reactions to be conducted at low temperatures (*e.g.* T = 0 °C). Common initiators used in organic polymerization systems are shown below and include (from top to bottom) benzoyl peroxide, azobis-*iso*-butyronitrile ('AIBN') and dicumyl peroxide:

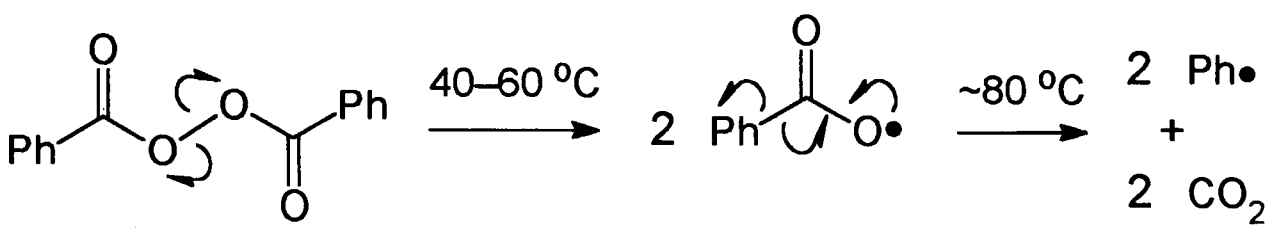

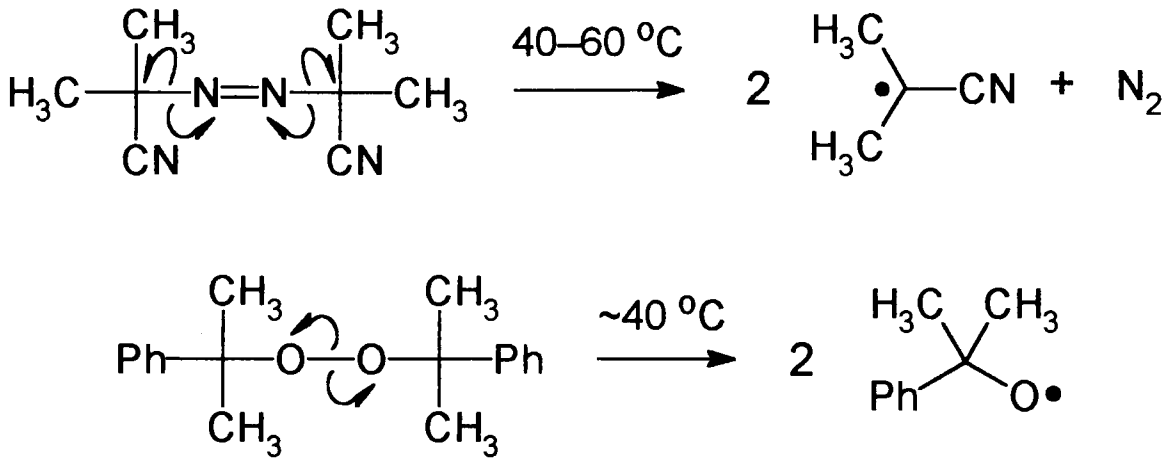

In aqueous polymerization systems, *redox initiators* are commonly employed, examples of which include hydrogen peroxide and potassium persulfate. In the presence of iron (II), hydrogen peroxide is reduced to hydroxide ion and a hydroxy radical, the latter of which acts as the initiator:

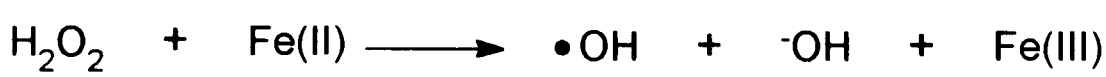

The initiator formed from persulfate ion is a sulfate ion radical:

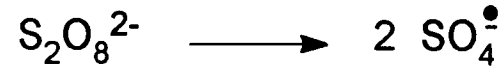

Polymerization reactions can also be initiated without an initiator present. In the case of *thermal initiation*, heating the monomer (*sans* initiator) produces a diradical which can, in turn, begin the propagation cycle. An example is the thermal initiation of styrene:

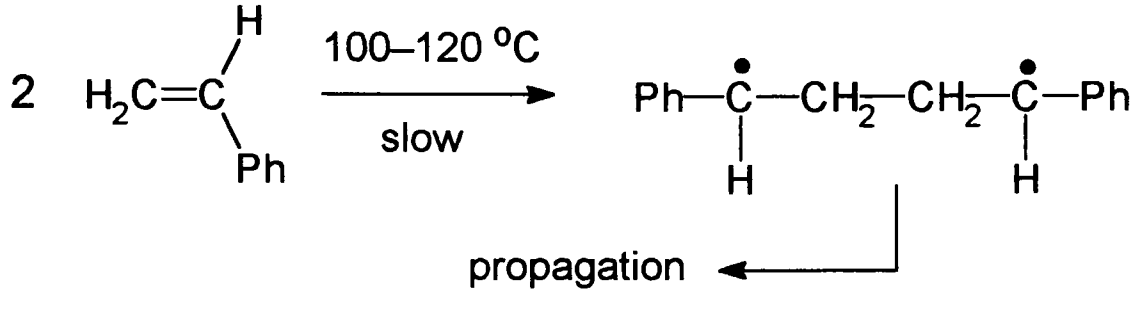

Kinetically, thermal initiation appears to be a second order process. Alternatively, polymerization reactions can be initiated photochemically. In the case of *photochemical initiation*, the monomer is irradiated with UV light. This results in the formation of free radicals which can start off the propagation cycle. An advantage of photochemical initiation is that the rate of polymerization is proportional to the intensity of absorbed light – the polymerization reaction can therefore be controlled.

Propagation

The propagation process involves the reaction of the chain carrier with a monomer molecule. The chain carrier is regenerated but is now one monomer unit longer in length:

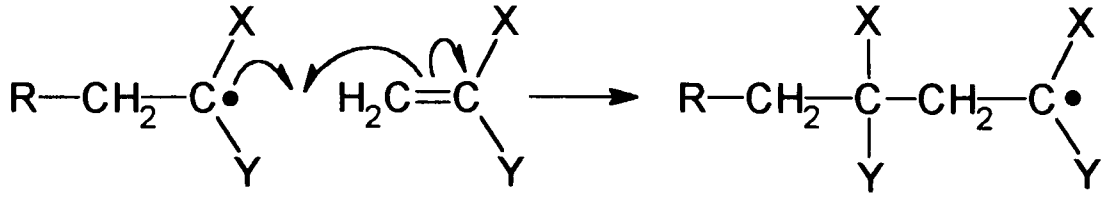

Although the chain carrier has increased in size it still has the same free radical end structure. The propagation process can continue for possibly hundreds of steps to

give a very long, linear chain that always contains a reactive free radical at one end of the chain:

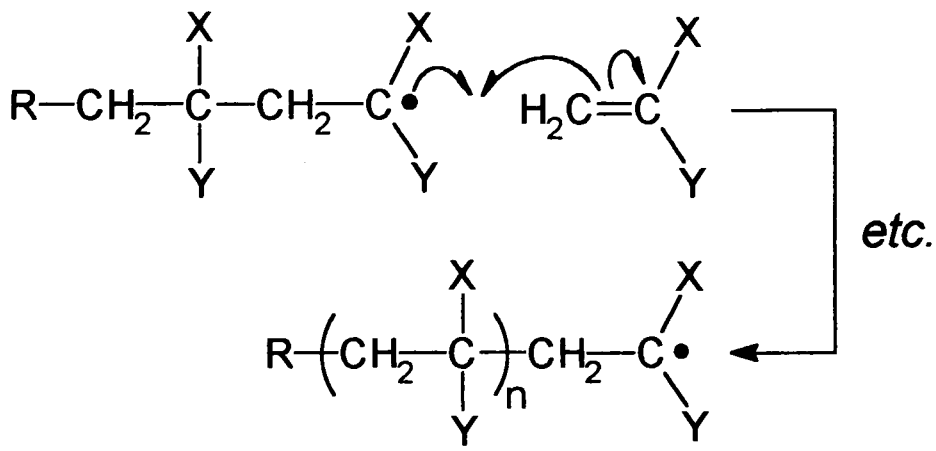

The propagation process is very fast since it involves the reaction of a radical and a molecule (⇒ low activation energy, E_{act} ~1–2 kJ). All chain carrier radicals have the same reactivity, regardless of chain length. There are three addition possibilities for the chain carrier and monomer: (i) *head to tail* addition, (ii) *head to head* (or *tail to tail*) addition, and (iii) *random* addition.

head to tail addition

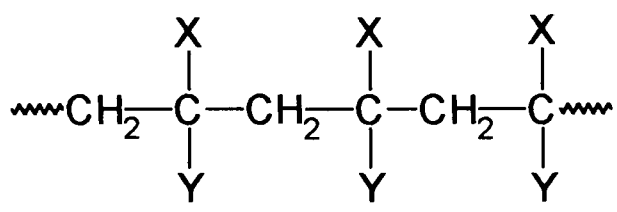

head to head or tail to tail addition

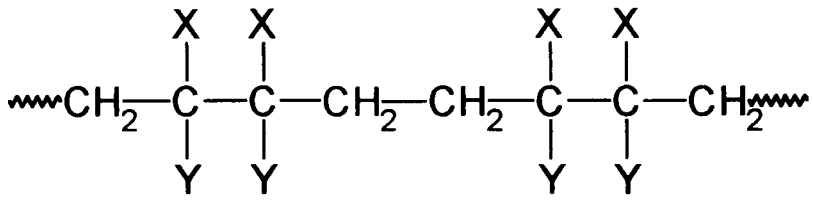

As a result of steric and radical stabilization factors polymers are almost entirely formed as a result of head to tail addition.

Termination

The termination process involves the reaction of two radicals. Since the energy of activation for radical–radical reactions is zero, termination reactions are very fast. There are three types of termination reaction: (i) *combination*, (ii) *disproportionation*, and (iii) *primary radical capture*. Termination by combination involves the reaction of a pair of growing chain carriers:

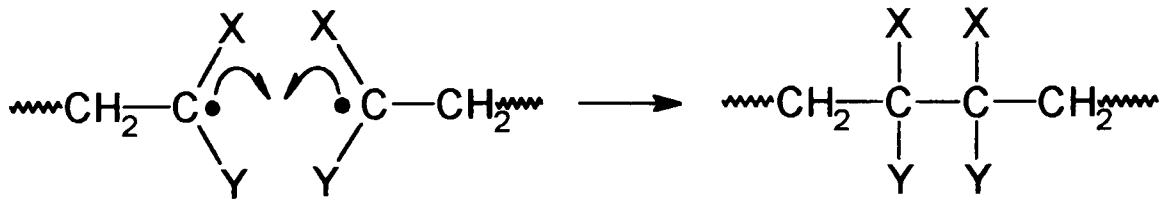

Thus the growth of these chains is stopped and the polymer molecule is the reaction product. The second type of termination reaction is disproportionation. In this case, one chain carrier abstracts a hydrogen atom from another chain carrier:

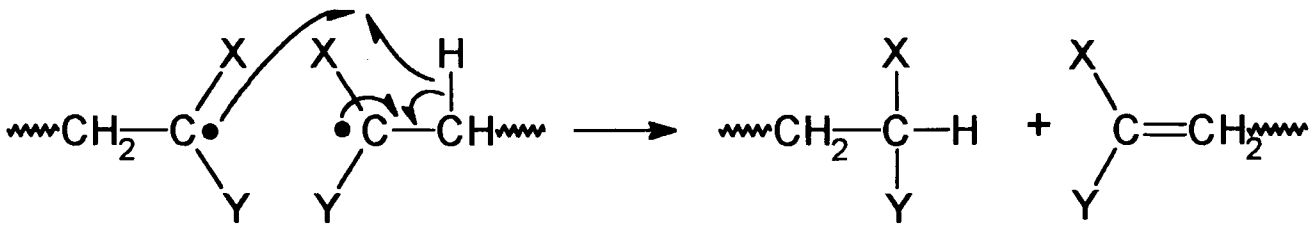

The product of this reaction is two polymer molecules, one molecule of which ends up with a vinyl terminus. Hydrogen atoms can also be abstracted from alkyl X and Y residues. For example, if X or Y = CH_3 the following termination product is possible:

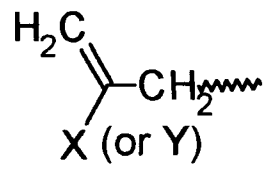

Hydrogen atom abstraction from alkyl residues on, or attached to, the polymer chain have identical rates of termination. The third type of termination reaction is primary radical capture. As the name implies, this involves the reaction of a chain carrier with a primary radical:

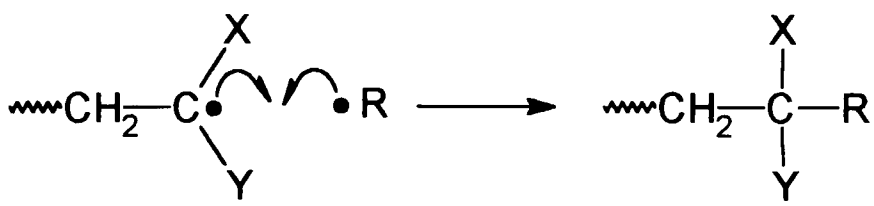

Since very small initiator concentrations are generally used in polymerization reactions, termination by primary radical capture is seldom important and is usually ignored. Only at high initiator concentrations (>1% by weight) does the effect of primary radical capture become significant.

Although the growth of chains is stopped by termination processes, other chains will be initiated and will propagate and terminate until the monomer is used up. For a particular chain, the whole process from initiation through many propagation steps to termination may occupy only a few seconds. The polymerization reaction, however, will take much longer since only a relatively small number of initiating radicals are produced at any instant.

Transfer

As well as initiation, propagation and termination there is an additional process called *transfer* in free radical polymerization. There are three types of transfer reaction: (i) *transfer to monomer*, (ii) *transfer to solvent*, and (iii) *transfer to polymer*. In each case, one chain carrier is stopped and a new chain carrier starts to grow. In the transfer to monomer process a chain carrier abstracts a hydrogen atom from a monomer molecule:

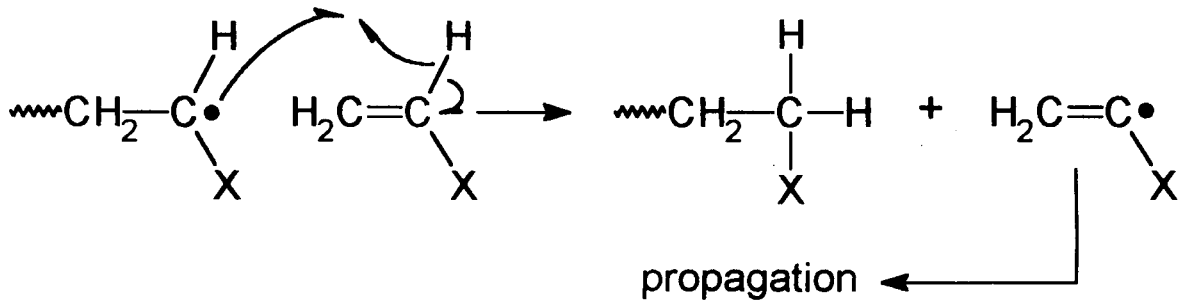

The growth of the chain carrier is therefore stopped but the monomer radical can start off a new propagation cycle. The transfer to solvent process is common in polymerization reactions carried out in solution. In this case, a chain carrier abstracts an atom (usually hydrogen) from the solvent:

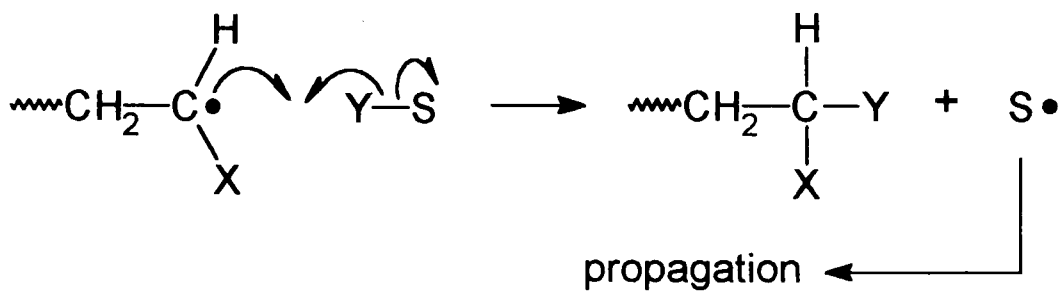

The radical S• thus formed can begin a new propagation cycle. However, if the radical S• is not very reactive the solvent will act as an *inhibitor* to the polymerization reaction. For example, the polymerization of styrene (H_2C=CHPh) is inhibited in the

solvents chloroform ($S\bullet = Cl_3C\bullet$) and toluene ($S\bullet = C_6H_5CH_2\bullet$). The transfer to solvent process affects chain size and consequently the physical properties of the resultant polymer. In this way, the solvent can be used to control chain size. In the transfer to polymer process a chain carrier abstracts a hydrogen atom from a polymer molecule:

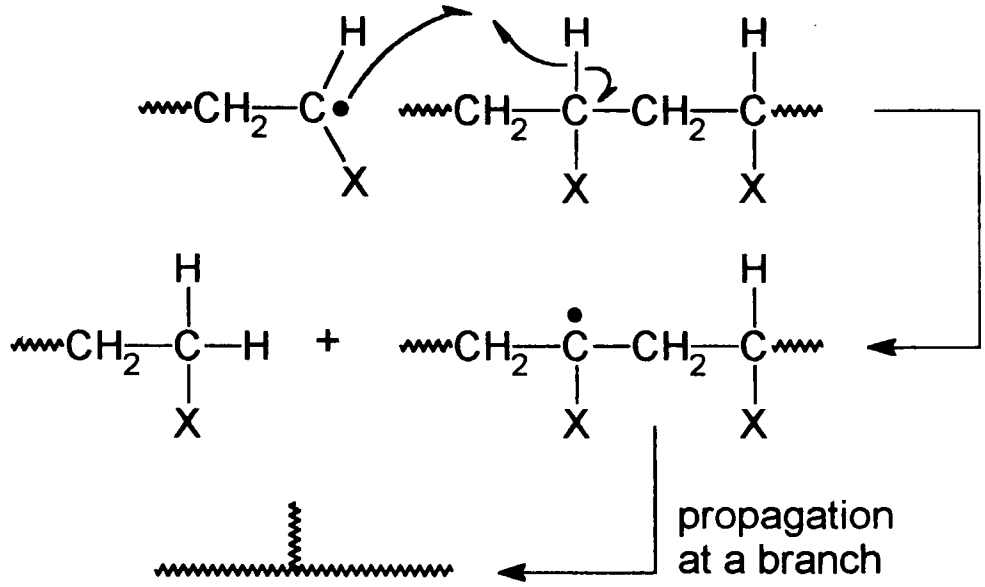

This reaction results in the formation of a radical centre at a point along the length of the polymer chain. A new propagation cycle can begin at this radical centre resulting in the formation of a *branch*. Usually, this is undesirable since the resultant increase in viscosity of the polymer mixture (the so-called *Tromsdorff-Norrish Effect*) can lead to gelation or even a thermal explosion. The transfer to polymer process only becomes important at high conversion.

Reaction Conditions for Free Radical Polymerization

Free radical polymerization reactions can be performed in solid, liquid and (although rare) gas phases. Reaction temperatures usually fall in the range 0–100 °C (atmospheric pressure). Common polymerization systems include the following:

- *Bulk* – This is the purest system and involves the polymerization of 'neat' monomer in the absence of a solvent.
- *Solution* – In this system, the monomer and initiator (0.001–1.0% by weight) are dissolved in an organic solvent and polymerized. A disadvantage of this system is the problem encountered with *solvent transfer* (see *Transfer*, above).

- *Suspension* – In this system, a solvent (usually water) is employed in which the monomer is immiscible. The resulting monomer–solvent suspension is rapidly stirred in a special polymerization reaction vessel. The polymer is produced in the form of small *beads* (or *pearls*) which can range from μm to mm in diameter.
- *Emulsion* – This is the most complex system. Monomer and water (commonly, in 1:1 or 1:2 amounts) and a water-soluble initiator (*e.g.* $K_2S_2O_8$) are emulsified using a *surfactant* (0.1–5.0% concentration range); in addition, emulsion systems commonly use either a stabilizer (to prevent coagulation) or a thickening agent. The emulsion produces *micelles*, comprised of between 50–100 surfactant molecules. Polymerization of the monomer occurs inside the miscelles to eventually produce the polymer in the form of a very fine powder.

1.4.3 Kinetics of Free Radical Addition Polymerization

It is not the intention of this overview to delve too deeply into the kinetics of polymerization reactions. All that will be given is the simple derivation of the expression for the overall rate of a free radical addition polymerization reaction.

In the reactions and rate equations listed below the following notation is used:

Radical processes		*Rate expressions*	
I	initiator	f	initiator efficiency
M	monomer	[I]	initiator concentration
M•	monomer radical	I_{ABS}	intensity of absorbed light
P_i•	chain carrier of i repeat units	k	overall rate constant
P_j	polymer of j repeat units	k_x	rate constant for process x
R•	primary radical	[M]	monomer concentration
S•	solvent radical	[P•]	total radical concentration
SY	solvent	[SY]	solvent concentration

The basic rate equations for the radical processes (ignoring primary radical capture) in a free radical addition polymerization reaction are as follows:

Initiator decomposition	$I \longrightarrow 2\,R\bullet$	
(k_d = decomposition rate constant)	$\text{Rate} = 2fk_d[I]$	(1)
Thermal initiation	$2\,M \longrightarrow R\bullet$	
(k_i = initiation rate constant)	$\text{Rate} = k_i[M]^2$	(2)
Photochemical initiation	$M \longrightarrow R\bullet$	
	$\text{Rate} \propto I_{ABS}$	(3)
Propagation	$P_i\bullet + M \longrightarrow P_{i+1}\bullet$	
(k_p = propagation rate constant)	$\text{Rate} = k_p[P\bullet][M]$	(4)
Termination by combination	$P_i\bullet + P_j\bullet \longrightarrow P_{i+j}$	
Termination by disproportionation	$P_i\bullet + P_j\bullet \longrightarrow P_i + P_j$	
(k_t = termination rate constant)	$\text{Rate} = 2k_t[P\bullet]^2$	(5)
Transfer to monomer	$P_i\bullet + M \longrightarrow P_i\text{–}H + M\bullet$	
(k_m = trans. to monomer rate constant)	$\text{Rate} = k_m[P\bullet][M]$	(6)
Transfer to solvent	$P_i\bullet + SY \longrightarrow P_i\text{–}Y + S\bullet$	
(k_s = trans. to solvent rate constant)	$\text{Rate} = k_s[P\bullet][SY]$	(7)

Assume that a steady state of radicals P• is present in the polymerization reaction. Mathematically, this can be expressed as:

$$d\,[P\bullet]/dt = 0 \tag{8}$$

In the initiation process polymer radicals are formed and in the termination process they are killed off. Eqn. (8) therefore gives:

$$d\,[P\bullet]/dt = 0 = (\text{Rate of initiation} - \text{Rate of termination}) \tag{9}$$

In other words, in the steady state, the rate of initiation is equal to the rate of termination. Therefore, from eqns. (1) and (5):

$$2fk_d[I] = 2k_t[P\bullet]^2 \tag{10}$$

$$\Rightarrow [P\bullet] = (fk_d[I]/k_t)^{½} \quad (11)$$

Now, the rate of the reaction is equal to the rate of polymerization. Since only propagation is important in consuming monomer the rate of polymerization is equal to the rate of propagation. Therefore, from eqn. (4):

$$\text{Rate of polymerization} = -d\,[M]/dt = k_p[P\bullet][M] \quad (12)$$

Substituting the expression for [P•] from eqn. (11) into eqn. (12) therefore gives:

$$\begin{aligned} -d\,[M]/dt &= k_p(fk_d[I]/k_t)^{½}\,[M] \\ &= k[M][I]^{½} \end{aligned} \quad (13)$$

In order to simplify matters the proportionality constants f, k_p, k_d and k_t have been absorbed into the overall rate constant $k = k_p(fk_d/k_t)^{½}$. Eqn. (13) therefore shows that the rate a free radical polymerization reaction is proportional to the product of the monomer concentration and the square root of the initiator concentration.

1.5 Antimicrobial Polymers and Surfaces

The antimicrobial compounds discussed in section 1.3, *Classes of Antimicrobial Agents and their Modes of Action*, were low molecular weight species. However, soluble polymeric antimicrobial agents and surface-immobilized antimicrobial agents exist also. The present section, which concludes the introductory chapter, will describe the merits and advantages of antimicrobial polymers and surfaces.

1.5.1 Low Molecular Weight AMAs *vs.* Polymeric AMAs

Consider an antimicrobial agent that exists in both low molecular weight and soluble polymeric forms. For example, the low molecular weight species could be either a polymerizable monomer or a non-polymerizable 'model' compound (*i.e.* an 'isolated' molecule). Now consider the interaction of these antimicrobial species with the outer surface of a cell wall or membrane.

The adsorption/desorption process involving a cell and the low molecular weight antimicrobial species is represented schematically in the top diagram of Figure 14a. The low molecular weight compound has less mass, and therefore less inertia, than its polymeric analogue. Consequently, the low molecular weight compound will adsorb onto, and desorb from, the cell surface relatively quickly. The movement of the low molecular weight molecules as they repetitively adsorb and desorb in the neighbourhood of the cell surface is not unlike that of Brownian motion.

Now consider the adsorption/desorption process involving a cell and the soluble polymeric antimicrobial species (Figure 14a, bottom diagram). The polymeric compound has more mass, and therefore more inertia, than its low molecular weight analogue. More importantly, the polymeric species behaves as a large, local concentration of the antimicrobial functionality. The polymer has a globular structure (in the form of a *random coil*) that is much smaller than a whole cell (note that the relative sizes of polymer and cell are not to scale in Figure 14a), but is very much larger than an isolated antimicrobial molecule (*i.e.* the low molecular weight species). Consequently, the adsorption of the polymeric species (in the absence of very specific binding effects) onto the cell surface is likely to be a rather slow, co-operative phenomenon.

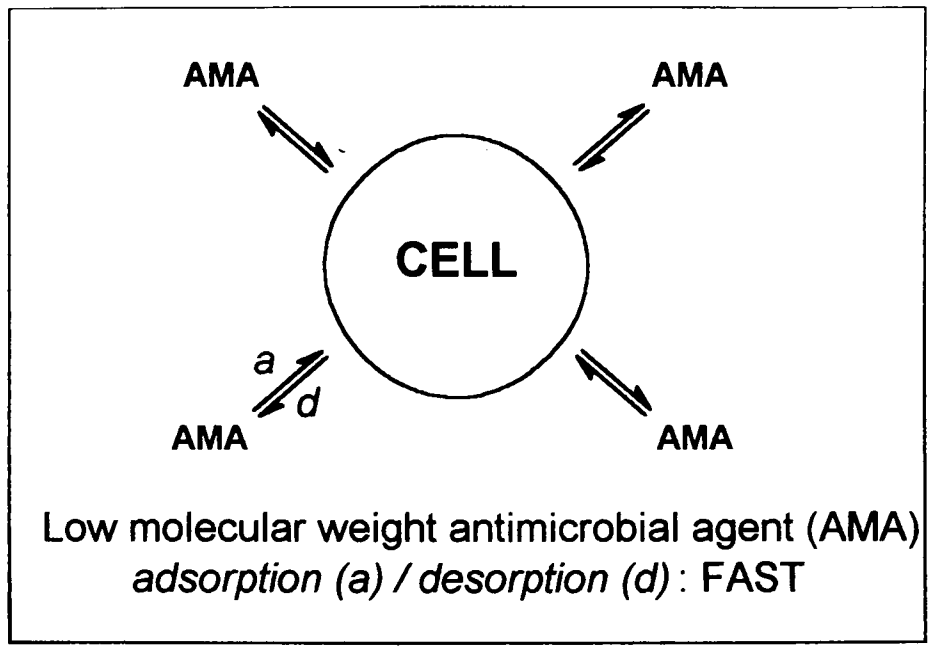

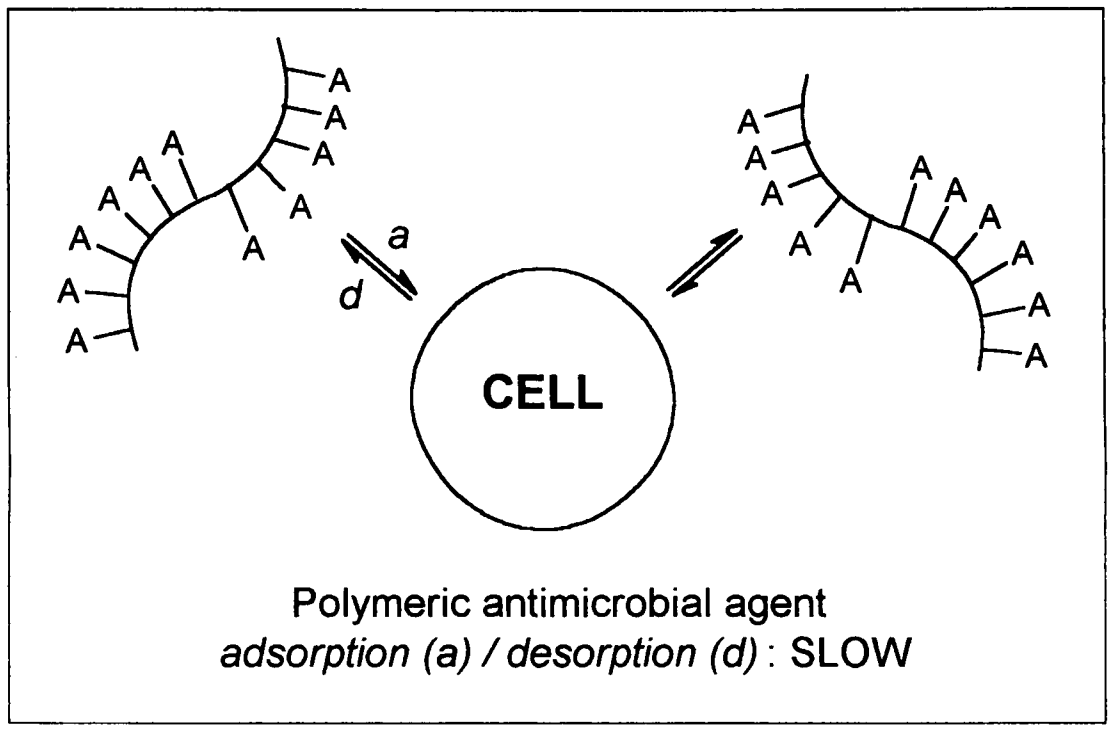

Fig. 14a Schematic representation of the kinetics of the adsorption/desorption process between a cell and low molecular weight (*top diagram*) and polymeric (*bottom diagram*) antimicrobial species. Diagrams are not to scale.

Another way of saying this is that the polymer will *progressively adsorb* onto the cell surface. This adsorption process is illustrated schematically in Figure 14b. A single segment ('A' in Figure 14b) on one end of the polymer chain will adsorb initially onto the cell surface. The adsorption of this first segment will facilitate, and accelerate, the adsorption of a second segment. The second segment will then facilitate the adsorption of a third segment, and so on. The overall result is that a series of polymer

segments will progressively adsorb onto the cell surface to produce a 'train' of polymer segments. It is also possible, at the same time, for the other end of the polymer to adsorb onto another part of the cell surface. This will result in the formation of a second 'train' and a 'loop' of unadsorbed polymer segments in the middle section of the polymer chain (this 'loop' of segments may, or may not, get adsorbed onto the cell surface). Importantly, the overall adsorption process for the polymeric species is *slower* than that involving the low molecular weight species. Crucially, the desorption process is likewise very slow for similar reasons.

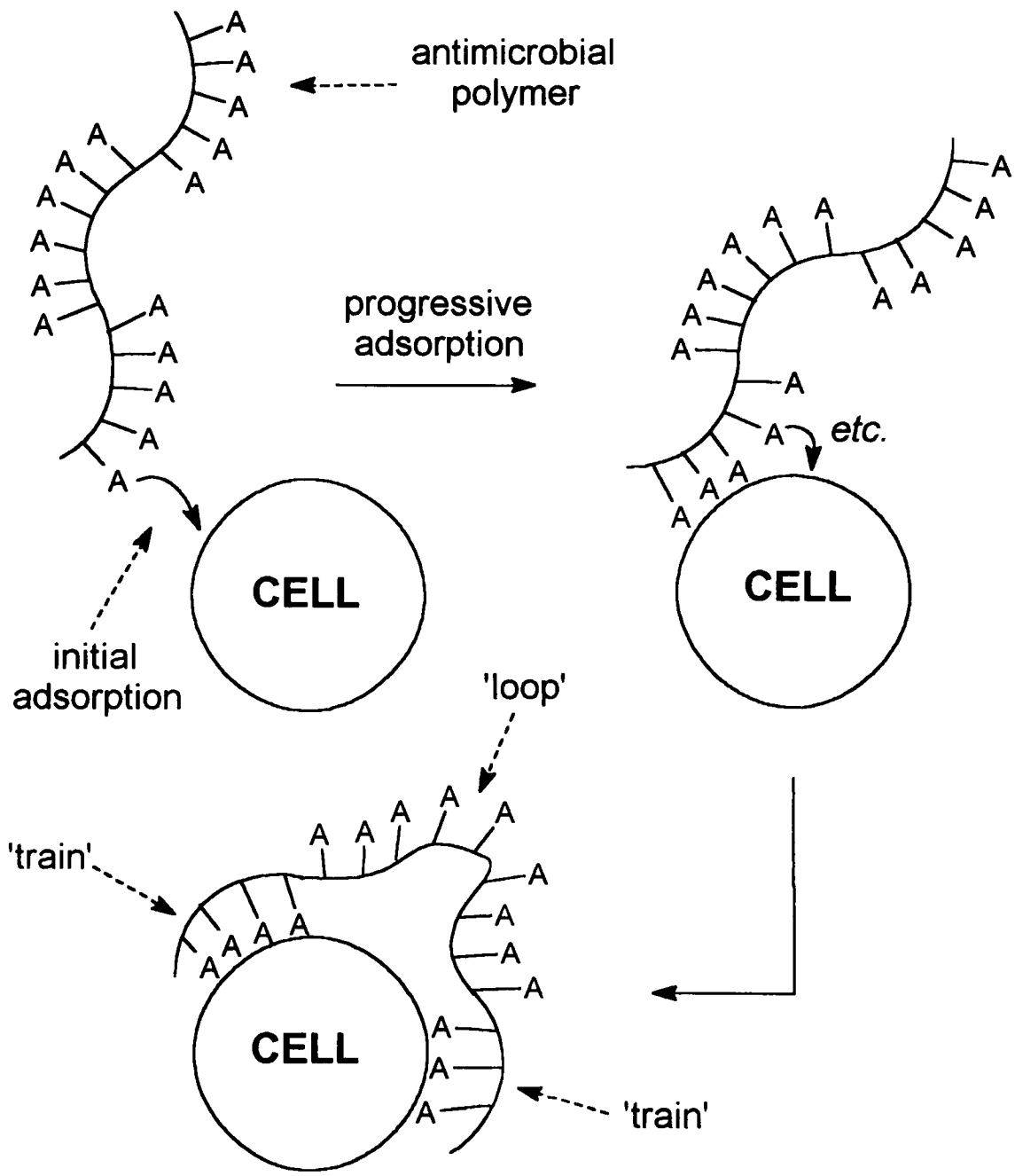

Fig. 14b Progressive adsorption of an antimicrobial polymer onto the outer surface of a cell wall (or membrane). Diagram is not to scale.

The above discussion therefore shows that the polymeric antimicrobial species is in contact with the cell surface for a longer period of time than the low molecular weight species. Consequently, the polymeric species has more opportunity to exert its antimicrobial influence on the cell. This kinetic factor associated with the polymeric species might, alone, be sufficient to enhance antimicrobial effects.

1.5.2 Polymeric Antimicrobial Agents

Now consider the design and synthesis of soluble antimicrobial polymers. There are two main approaches towards the synthesis of soluble polymeric antimicrobial agents. One approach involves the chemical modification of existing polymers. For example, a compound containing both an antimicrobial functionality and a pendant functional 'handle' could be covalently bound to a reactive functional group on a polymer. It is important to note, however, that if the functional 'handle' forms part of the anti-microbial functionality then the activity of the resultant polymer might be affected. An easier, and more versatile, approach towards the synthesis of antimicrobial polymers involves the preparation of polymerizable antimicrobial agents. In order to prepare a polymerizable species the antimicrobial compound is required to contain a function-ality that can be converted into a polymerizable group, such as a vinyl group. Examples of particularly useful functionalities include hydroxy and amino groups. These groups can be reacted with acid chlorides such as, for example, acryloyl chloride (H_2C=CHCOCl) or methacryloyl chloride (H_2C=CMeCOCl) to produce polymerizable functionalities.

Once the polymerizable antimicrobial agent has been prepared it is then required to convert it into a polymer or a co-polymer. Design concepts for different antimicrobial polymers and co-polymers are shown in Figure 15: (a)–(e). Polymer-ization of an antimicrobial monomer produces the homo-polymer (a). Sometimes, it is desirable to alter the hydrophobic/hydrophilic properties of an antimicrobial species. One method of accomplishing this is to attach an antimicrobial functionality to one end of a 'spacer' group. For example, the 'spacer 'group might be a hydrocarbon chain, $(CH_2)_n$, or a poly(ether) chain such as a *PEG* [poly(ethylene glycol), $HO(CH_2$-$CH_2O)_nH$]. The result of the polymerization of a monomeric antimicrobial species

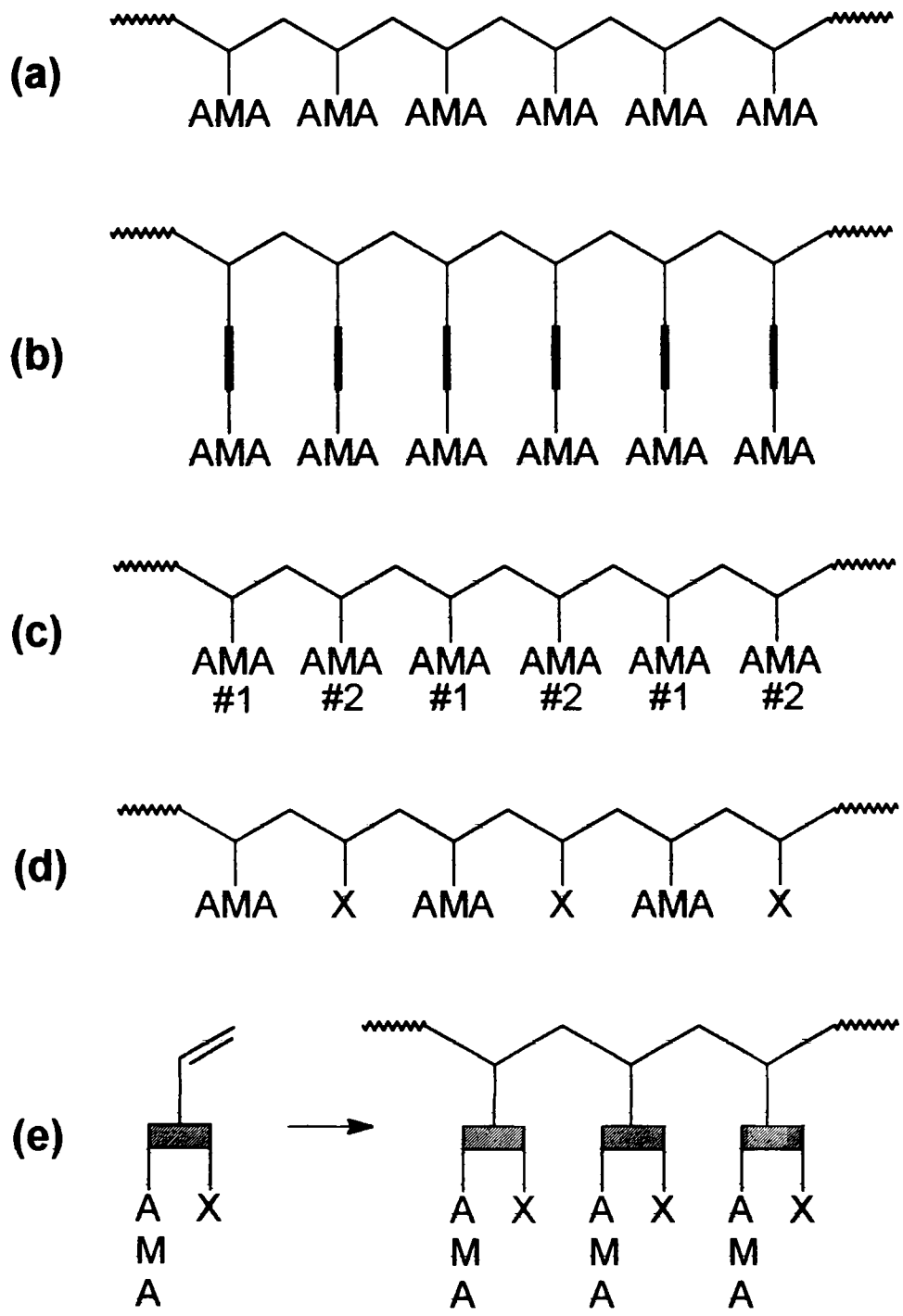

Fig. 15 Design concepts for antimicrobial polymers: (a) 'simple' homo-polymer; (b) homo-polymer with active group at one end of a 'spacer' group [**bold line**]; (c) co-polymer containing two different antimicrobial groups; (d) co-polymer with a non-active 'X' functionality (*e.g.* X = hydrophilic group); (e) homo-polymer with a non-active 'X' functionality.

containing a 'spacer' function is shown in (b). Note that the 'spacer' acts to distance the antimicrobial functionality (AMA) from the polymer chain. A novel effect is to co-polymerize two different monomeric antimicrobial agents. The resultant co-polymer is shown in (c). It is unlikely that the co-monomers will have identical reactivity ratios and so the simplistic alternating AMA#1–AMA#2 structure shown in (c) will probably

not result. If the co-monomers have unique reactivity ratios then a 'block' co-polymer is likely be formed. Alternatively, an antimicrobial monomer can be co-polymerized with a biologically inactive co-monomer. The resultant co-polymer is shown in (d). The 'X' group in (d) is derived from a non-active co-monomer and can be used to alter the physical properties of the polymer. For example, the homo-polymer (a) might contain an antimicrobial functionality that makes the polymer water-insoluble. Co-polymerization of the antimicrobial monomer with a co-monomer containing a hydrophilic 'X' functionality might result in the formation of a co-polymer (d) with improved water-solubility. An alternative approach to the polymer (d) is shown in (e). In this case, the antimicrobial monomer (shown on left) contains a pendant 'X' functionality. Polymerization of the monomer thus produces a homo-polymer with equal numbers of 'AMA' and 'X' groups.

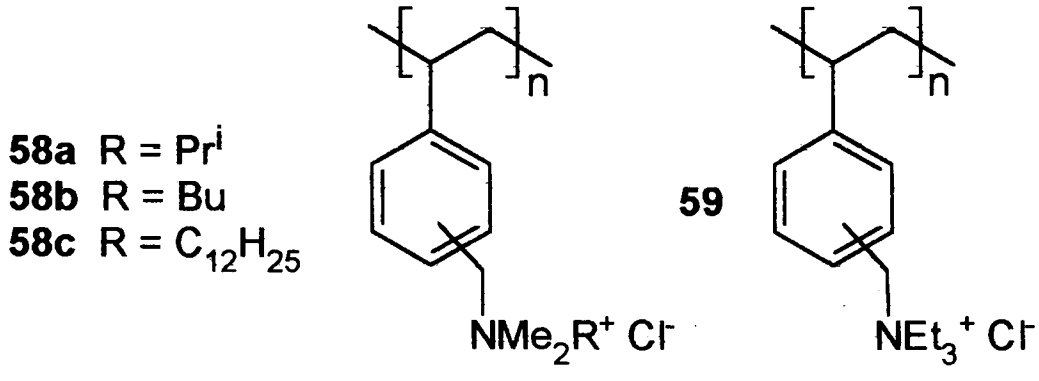

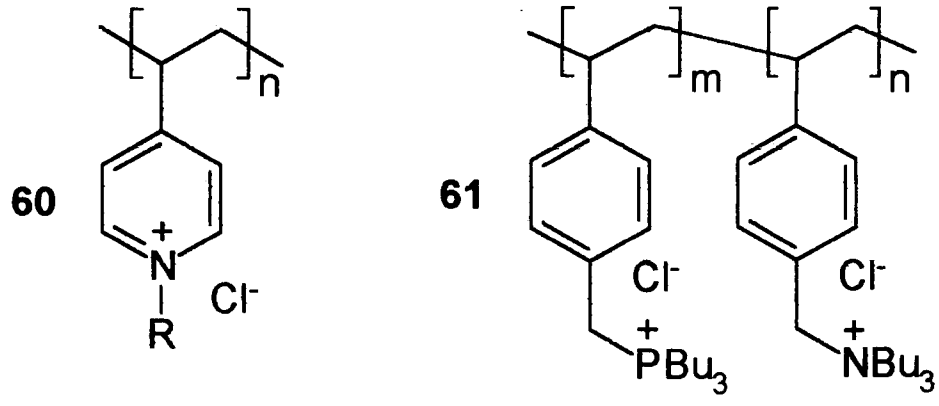

Fig. 16 Examples of antimicrobial polymers.

One of the best known classes of soluble antimicrobial polymer are the *cationic biocides*. Key structural features of these polymeric species include the possession of a positively charged atom and a hydrophobic group. A commonly studied sub-class of cationic biocide are the *polymeric quaternary ammonium salts* (or *polyquats* for short). Some examples of polyquats are shown in Figure 16. The series of antibacterial polymeric trialkylquaternary ammonium salts **58a–c** have been prepared

by Tazuke and co-workers.[35] The monomeric species were prepared from *m*/*p*-vinylbenzyl chloride ($H_2C{=}CHC_6H_4CH_2Cl$) and tertiary amines (Me_2RN). The polymers **58a–c** displayed antibacterial activity against both gram-positive bacteria (*Bacillius subtilis* and *Staphylococcus aureus*) and gram-negative bacteria (*Escherichia coli*, *Aerobacter aerogenes* and *Pseudomonas aeruginosa*) but tested more active, in general, against the former. In addition, the most active member of the series proved to be the long-chain, dodecyl polymer **58c**. The enhanced activity of this species was attributed to its increased hydrophobicity over that of the shorter-chain analogues **58a** and **58b**. The polymeric triethylquaternary ammonium salt **59** was also prepared and, likewise, displayed antibacterial activity.

Another example of a polymeric cationic species is the antimicrobial pyridinium polymer **60** (R = alkyl or benzyl group) prepared by Kawabata.[36] Quaternization of the pyridine ring was achieved by reaction of the nitrogen atom with an alkyl or benzyl chloride (RCl or $ArCH_2Cl$).

A final example of a cationic polymer is the antibacterial co-polymer **61** prepared by Endo.[37] The co-polymer **61** is composed of two different cationic antimicrobial functionalities, *viz.* a trialkylphosphonium salt ('m' unit) and a trialkylquaternary ammonium salt ('n' unit) [*c.f.* Figure 15 (c)]. The monomeric species were prepared from the reaction of *p*-vinylbenzyl chloride with either tributylphosphine (Bu_3P) or tributylamine (Bu_3N). The co-polymer **61** displayed significant antibacterial activity against the gram-positive bacterium *Staphylococcus aureus*. In addition, a series of co-polymers **61** were prepared in which the ratio of the quaternary ammonium and phosphonium salt co-monomers was varied. Antibacterial activity was found to increase monotonically with an increase in the number of phosphonium salt units.

1.5.3 Antimicrobial Surfaces

Antimicrobial *surfaces* are generally composed of a polymeric film, or surface, onto which is immobilized (either covalently or physically) an antimicrobial functionality. Antimicrobial surfaces can be exposed to either air or water. Consequently, they are designed with either 'dry' or 'wet' applications in mind. The particular choice of polymeric support and antimicrobial species with therefore vary from one application to

the next. Antimicrobial surfaces are commonly employed as self-sterilizing plastics (*e.g.* for medical use), antifouling marine coatings and paint coatings (see examples cited later).

There are two main approaches towards the preparation of antimicrobial surfaces. One approach involves the co-polymerization of an antimicrobial monomer with an excess of a biologically inactive co-monomer. The latter effectively serves as a polymeric 'support' for the antimicrobial species. The co-polymer thus produced is then dissolved in an organic solvent and cast as a polymeric film. Alternatively, the co-polymer can be surface cast in melt form. The second approach towards the preparation of surface-active antimicrobial agents is, in principle, synthetically more demanding. It involves the chemical modification of existing polymeric surfaces. In this approach, a pendant functional group on an antimicrobial compound is covalently bound to a reactive site (*e.g.* –COCl, $-CH_2Cl$) on a polymeric surface. Alternatively, a polymer containing an antimicrobial functionality can be 'grafted' onto a polymeric surface.

Design concepts for different antimicrobial surfaces are shown in Figure 17: (a)–(c). This figure is very similar to that of Figure 15 and shows common ways in which an antimicrobial functionality could be attached to a polymeric surface. In (a), the antimicrobial functionality (AMA) is covalently bound directly to the polymeric surface. In (b), a 'spacer' group is used to separate the active functionality from the surface [*c.f.* Figure 15 (b)]. The active group shares the surface with a non-active 'X' functionality in (c) [*c.f.* Figure 15 (d)]. Concepts (b) and (c) in Figure 17 might prove useful designs towards the preparation of an antimicrobial surface for a 'wet' application. Cells are hydrophilic species and, consequently, they may not venture in close proximity to a hydrophobic polymeric surface. The cell needs to be in contact with the active functionality (attached to the surface) in order for the latter to exert its antimicrobial effect. The use of a long hydrophilic spacer group in (b), or a hydrophilic 'X' functionality in (c), would therefore provide a hydrophilic periphery between the polymer surface and the outside environment. The polymer surface would therefore be considerably more 'cell-friendly' and might be sufficiently hydrophilic to 'fool' the cell into approaching it.

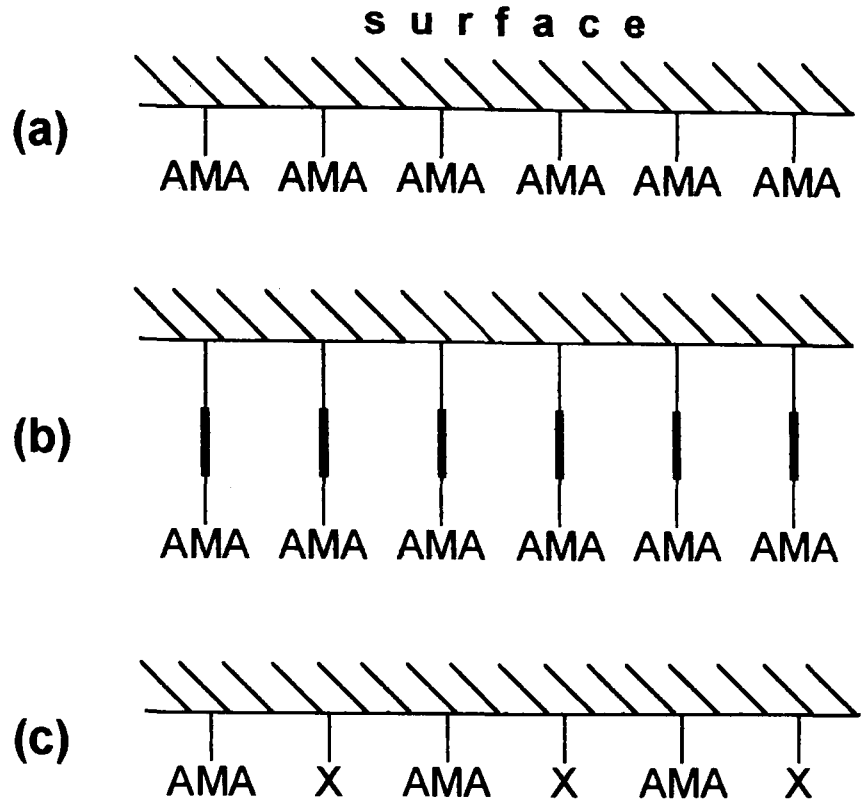

Fig. 17 Design concepts for antimicrobial surfaces: (a) active group attached directly to surface; (b) active group attached to surface via a 'spacer' group [**bold line**]; (c) active group + non-active 'X' functionality.

Examples of antimicrobial surfaces are shown in Figure 18. Pittman has prepared antifungal surfaces **62a** and **62b** containing pentachlorophenyl antimicrobial functionalities.[38] The surfaces **62a** and **62b** were prepared by co-polymerizing pentachlorophenyl acrylate ($H_2C{=}CHCO_2C_6Cl_5$) with vinyl acetate and ethyl acrylate respectively. The resultant co-polymers were then cast as films and tested for mildewcidal activity. Both surfaces inhibited the growth of fungal organisms such as *Aspergillus*, *Pseudomonas*, *Alternaria* and *Aureobasidium pullulans*. Surface-bound organotin biocides are also commonly employed as antifungal coatings. They are used principally as antifouling marine coatings[39–41] and mildew-resistant paint coatings.[42]

The bacterial contamination of polymers and polymeric substance poses a particular threat to mankind. Consequently, polymeric materials required for sterile applications (*e.g.* in medicine) are commonly decontaminated, or sterilized, prior to use. Research is now being directed towards the production of so-called 'self-sterilizing' materials, *i.e.* polymeric surfaces containing antibacterial agents. An example of such a 'self-sterilizing' material is the antibacterial surface **63a** prepared by Tazuke

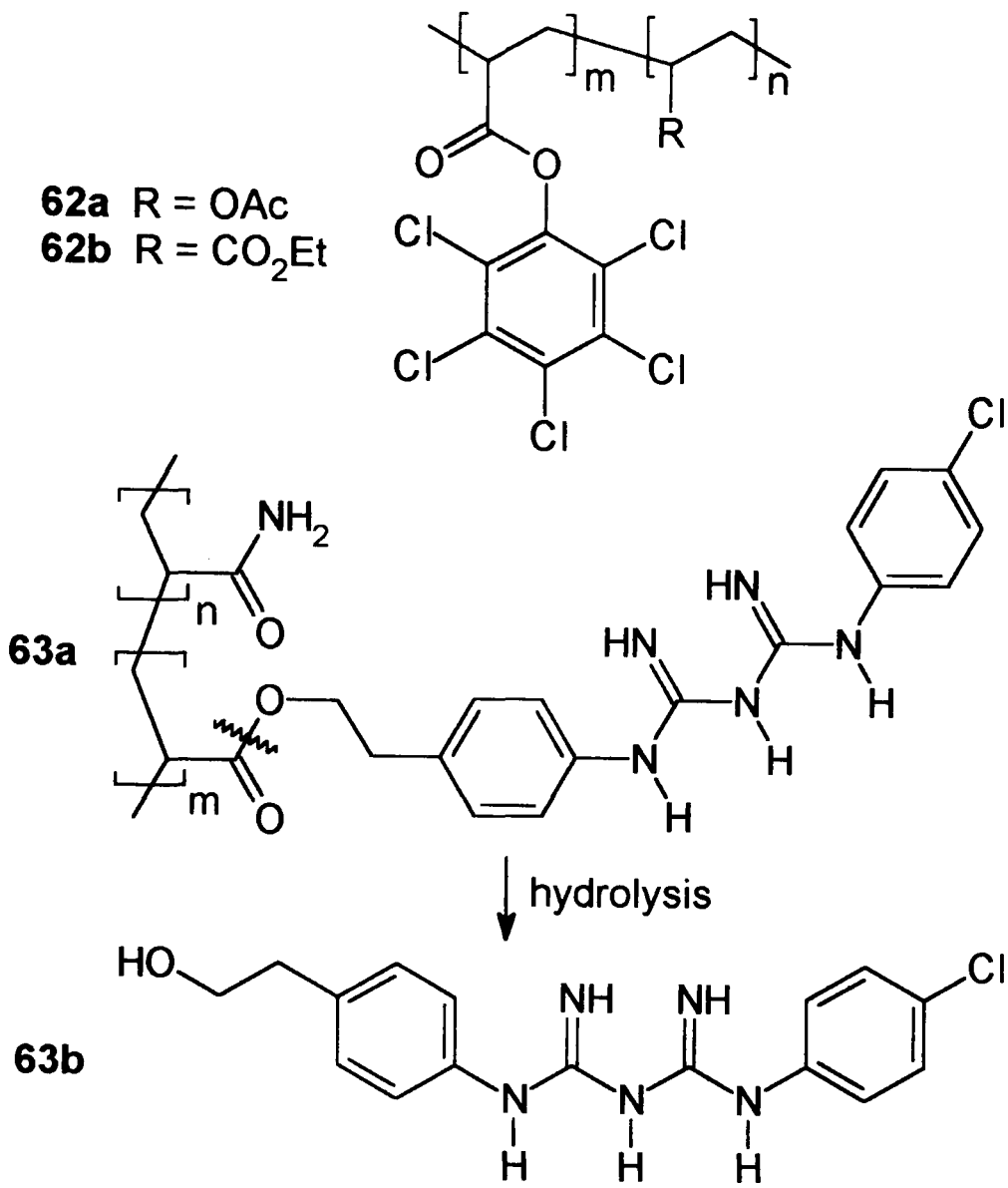

Fig. 18 Examples of antimicrobial surfaces.

and co-workers.[43] The surface **63a** is composed of a cross-linked poly(acrylamide) film containing a covalently-bound chlorophenylbiguanide functionality. The surface displayed antibacterial activity against bacterial organisms such as *Escherichia coli* and *Staphylococcus aureus*. Scanning electron microscopy revealed cell shrinkage and cell deformation. These morphological changes were ascribed to the release of the

hydroxyethyl-chlorophenylbiguanide species **63b**, resulting from hydrolysis of the ester linkage in **63a**.

Endo and co-workers have prepared the phosphonium salt-containing antibacterial films **64a** and **64b**.[44] These films were prepared in two steps. *p*-Vinylbenzyl chloride was firstly photografted onto a poly(propylene) film. The phosphonium salt functionality was then incorporated at the surface of the poly(propylene) film by the reaction of grafted vinylbenzyl chloride with tributylphosphine (PBu_3) and trioctylphosphine [$P(C_8H_{17})_3$]. This produced the films **64a** and **64b** respectively. The surfaces exhibited high antibacterial activity against *Staphylococcus aureus* and were particularly active against the gram-negative bacterium *Escherichia coli*. Morphological changes were monitored by scanning electron microscopy and revealed shrunken and deformed cells.

Three final examples of antimicrobial surfaces are the antibacterial *N*-halosulfonamide resins **65d–f** (Figure 19) prepared by Emerson.[44A–C] The macroreticular sulfonamide resins **65a–c** have been dubbed 'Haloscrub' resins owing to their ability to remove active chlorine from aqueous solutions of sodium hypochlorite (NaOCl).[44A,44D] The chlorine thus removed is covalently immobilized as N–Cl in the form of the *N*-halosulfonamide resins **65d–f**. Conversely, the resins **65d–f** release active chlorine into water in concentrations of sufficient strength to kill bacteria.[44E–G] *N*-halosulfonamide polymers such as **65d–f** therefore behave as water-disinfecting resins.

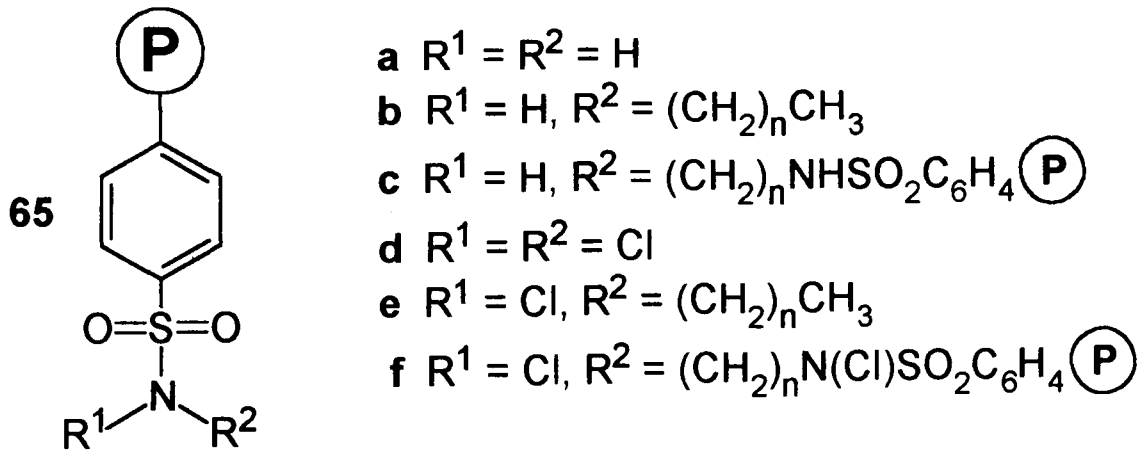

Fig. 19 Antibacterial *N*-halosulfonamides (**65d–f**).

2. EXPERIMENTAL

2.1 Analytical Methods and Instrumentation

Melting points were obtained on a Gallenkamp melting point apparatus in open capillaries and are uncorrected. IR spectra were recorded on a Mattson 1000 FTIR or 5000 FTIR spectrometer as KBr pellets (10 mm diameter) or thin films. The latter instrument used WinFIRST (v1.5) FTIR Software run on a Viglen 4DX33 PC. Spectra were recorded in transmittance mode (32 scans; resolution 2; signal gain 1) in the range 4000–400 cm^{-1}. Spectral smoothing was obtained by Savitzky-Golay weighted averaging (on twenty-one data points) using a cubic polynomial to determine the weighting factors. Peak picking was performed using the 'threshold' option with a three point weighted average peak selection filter. Printouts were obtained using a Hewlett Packard LaserJet 4L. UV spectra were recorded on a Philips PU 8720 using a 10 mm quartz-glass cuvette. Printouts were obtained using a Philips/Pye Unicam plotter. Mass spectra were determined on an AEIMS9 double focusing mass spectrometer using a GEC-905 computer-based data system. ^1H NMR spectra were recorded on a Brüker WM-250 spectrometer operating at 250 MHz in a Fourier transform mode. Unless otherwise stated all spectra were determined using deuteriochloroform as a solvent and all chemical shifts were quoted on the δ scale (*J* values are in Hz). Elemental analyses for C, H and N were determined using a Carlo Erba 1106 Analyser. Theoretical elemental microanalyses and molecular masses were calculated using the SoftShell Molecular Mass Calculator (v1.7).

2.2 Materials

A list of the chemicals and materials used in the experimental work is presented below; unless otherwise stated they were used as supplied. 'Bulk' grade solvents were generally used without purification but were distilled where appropriate.

Organic Chemicals	*Supplier*
Acrylamide	Aldrich
Acryloyl chloride (98%)	Aldrich
Amberlyst 15 resin (#55133: SO_3H, 4.3 meq g^{-1} dry)	BDH
2,2'-Azobis(2-methylpropionamidine) dihydrochloride	Polyscience
Azobis-*iso*-butyronitrile. Recrystallized.	Aldrich
2-Bromoethylamine hydrobromide (95%)	Aldrich
Chloroacetic acid (>99%)	Fisons
3-Chloropropylamine hydrochloride (98%)	Aldrich
3,3'-Dithiodipropionic acid (99%)	Aldrich
Dodecan-1-ol (98%)	BDH
Dowex 50-X8 resin (#55036: SO_3^- Na^+, 1.9 meq cm^{-3} wet)	BDH
Ethanethiol (ethyl mercaptan) (97%)	BDH
p-Hydroxybenzoic acid	BDH
2-Hydroxyethyl methacrylate (97%). Purified.	Aldrich
Iodoform	BDH
Isonicotinic acid (99%)	Aldrich
Nicotinic acid (niacin)	L. Light & Co.
o-Nitroaniline	BDH
Nonan-1-ol (99%)	Aldrich
Octan-1-ol (99%)	BDH
Pentan-1-ol (98%)	BDH
Pentan-2-ol (*sec*-pentanol) (99%)	BDH
Propan-1-ol	May & Baker
Propan-2-ol (*iso*-propanol) (99.5%)	Fisons

2-(4'-Thiazolyl)benzimidazole (98%)	Aldrich
N^1-(2-Thiazolyl)sulfanilamide (sulfathiazole) (98%)	Aldrich
p-Toluenethiol (*p*-thiocresol) (98%)	Aldrich
2-Thiolbenzoic acid (thiosalicylic acid) (98%)	Aldrich
Tri-*n*-butylphosphine (99%)	Aldrich
Triethylamine (99%)	Aldrich
Triethylphosphine (1.0 mol dm^{-3} solution in THF)	Aldrich
Tri-*n*-octylphosphine (~95%)	Fluka
Triphenylphosphine	BDH
m/p-Vinylbenzyl chloride (~ 70% *meta*, 30% *para* mixture)	Aldrich
m/p-Vinylbenzyl chloride (~ 60% *meta*, 40% *para* mixture)	Dow
p-Vinylbenzyl chloride (99%)	Kodak

Inorganic Chemicals	***Supplier***
Calcium chloride (anhydrous)	BDH
Hydrochloric acid (37%, sp gr 1.18)	BDH
Hydrogen peroxide (27.5% w/v solution in water)	Fisons
Iodine	Fisons
Magnesium sulfate (anhydrous)	BDH
Nitric acid	BDH
Potassium carbonate (anhydrous)	Aldrich
Potassium hydroxide	Fisons
Potassium persulfate	BDH
Ringer's solution tablets	BDH
Sodium chloride	BDH
Sodium hydrogen carbonate	BDH
Sodium hydroxide	Fisons
Sodium hypochlorite (aqueous solution, ≥ 5% active chlorine)	Aldrich
Sodium sulfate	BDH
Sodium sulfite (98%)	BDH

Sulfuric acid (95%, d 1.84 g cm^{-3})	BDH
Tetra-*n*-butylammonium chloride hydrate (98%)	Aldrich
Thionyl chloride	Fisons

2.3 *Syntheses*

2.3.1 Synthesis of Low Molecular Weight Compounds

Benzofuroxan **71** *(Scheme 3).*—This was prepared by the published method.[49] Sodium hypochlorite solution (5% active chlorine; 40 cm^3) was added at room temperature to a stirred solution of *o*-nitroaniline **70** (5.00 g, 36.2 mmol) in methanolic potassium hydroxide solution (2.1 g, 37.4 mmol, of KOH in 75 cm^3 of EtOH). During the hypochlorite addition a precipitate formed and the nitroaniline solution turned colour from a deep crimson-red to a brown-red; further addition of hypochlorite did not result in any significant colour change. The solution was then filtered to leave a yellow-orange precipitate (1.63 g), mp 65–67 °C. Addition of water to the filtrate afforded a further batch of identical precipitate (2.02 g). Recrystallization of the combined precipitates (3.65 g) from ethanol yielded sandy-brown crystals (2.91 g, 59%), benzofuroxan **71**, mp 67–68 °C (lit.,[49] 72 °C) (Found: C, 53.03; H, 3.12; N, 20.65. $C_6H_4N_2O_2$ requires C, 52.95; H, 2.96; N, 20.58%); MIC = 15.6 μg cm^{-3} (NAJ) and 62.5 μg cm^{-3} (MOJ); λ_{max} (ethanol)/nm 217 and 358; ν_{max}/cm^{-1} (KBr) 3428s, 3100w, 3080w, 1617s, 1586s, 1538s, 1485s, 1351w, 1015m, 892w and 747m; δ_H (250 MHz, $CDCl_3$) 7.29 (2 H, br s) and 7.48 (2 H, br s).

The compounds in Scheme 4 were prepared by the methods detailed by Sherrington.[58]

n-*Nonyl 4-hydroxybenzoate* **76** *(Scheme 4).*—*p*-Hydroxybenzoic acid **75** (25.03 g, 181 mmol), nonan-1-ol (31.5 cm^3; 26.05 g, 181 mmol) and concentrated sulfuric acid (1 cm^3) were dissolved in toluene (100 cm^3) and refluxed (Dean-Stark) for 17 h. The solution was then poured into a beaker of aqueous sodium hydrogen carbonate solution (16 g of $NaHCO_3$ in 300 cm^3 of H_2O) and crushed ice (300 cm^3). The resultant cream solution was transferred to a separating funnel along with toluene (200 cm^3), water (200 cm^3) and ethanol (100 cm^3). The lower, aqueous layer was run off and the organic layer washed with 4% aqueous sodium hydrogen carbonate solution (3 x 100 cm^3). The aqueous washings were then washed with ethyl acetate (3 x 200 cm^3). The combined toluene and ethyl acetate solutions were dried ($MgSO_4$), filtered and the volatiles removed *in vacuo*. Kugelrohr distillation (bp ~250 °C/0.01–0.001 mbar) afforded a white solid (18.2 g, 32%) which

revealed two spots on TLC, R_f [silica gel, 60% diethyl ether–petrol (40–60)] 0.23 and 0.56. Flash-column chromatography of the crude product on silica gel [eluent 60% diethyl ether–petrol (40–60)] afforded a white, waxy solid (11.8 g, 25% after distillation and chromatography), *n*-nonyl 4-hydroxybenzoate **76**, mp 38–39 °C (lit.,[60] 44 °C) (Found: C, 73.43; H, 9.79. $C_{16}H_{24}O_3$ requires C, 72.69; H, 9.15%); R_f [silica gel, 60% diethyl ether–petrol (40–60)] 0.56; MIC = 500 μg cm^{-3} (NAJ); ν_{max}/cm^{-1} (KBr) 3382s (O–H), 2928m, 2851w, 1683s (C=O), 1607m, 1590m, 1514w, 1279s, 1165m and 774w; δ_H (250 MHz, $CDCl_3$) 0.88 (3 H, t, *J* 6.4, CH_3), 1.15–1.55 [12 H, m, $(CH_2)_6CH_3$], 1.76 (2 H, qn, *J* 6.9, OCH_2CH_2), 4.30 (2 H, t, *J* 6.6, OCH_2), 6.66 (1 H, s, OH, exch.), 6.90 (2 H, d, *J* 8.5, Ar–H) and 7.96 (2 H, d, *J* 8.5, Ar–H).

n-*Nonyl 4-hydroxy-3-nitrobenzoate* **77** *(Scheme 4).*—*n*-Nonyl 4-hydroxybenzoate **76** (10.00 g, 37.8 mmol) was dissolved in dichloromethane (80 cm^3) and the solution cooled (ice–water bath). A mixture of concentrated nitric acid (70% w/v; 2.5 cm^3, 38 mmol) and concentrated sulfuric acid (sg 1.84; 1.7 cm^3, 38 mmol) was then added drop-wise, with stirring, and the mixture stirred for 18 h. The progress of the reaction was monitored by TLC: R_f [silica gel, 20% ethyl acetate–petrol (40–60)] 0.41 (brown; ester) and 0.66 (yellow; nitro-ester); after 18 h only the R_f 0.66 spot remained. Water (100 cm^3) was added to the reaction solution, and the aqueous layer washed with dichloromethane (2 x 80 cm^3). The combined organic layers were then washed with water (3 x 80 cm^3) until the aqueous washings were neutral. The organic solution was dried ($MgSO_4$), filtered and the solvent removed *in vacuo* to leave an orange solid (10.23 g). Flash-column chrom-atography of the crude product on silica gel [eluent 20% ethyl acetate–petrol (40–60)] afforded a waxy, yellow solid (9.94 g, 85%), *n*-nonyl 4-hydroxy-3-nitrobenzoate **77**, mp 44–46 °C (Found: C, 63.28; H, 8.03; N, 3.81. $C_{16}H_{23}NO_5$ requires C, 62.12; H, 7.49; N, 4.53%); R_f [silica gel, 20% ethyl acetate–petrol (40–60)] 0.66 (yellow); MIC = >1000 μg cm^{-3} (NAJ); ν_{max}/cm^{-1} (KBr) 3272m (O–H), 2915s, 2847m, 1728s (C=O), 1636s, 1548s (NO_2), 1337s (NO_2), 1277s, 1140m, 771m and 699s; δ_H (250 MHz, $CDCl_3$) 0.88 (3 H, t, *J* 6.5, CH_3), 1.1–1.5 [12 H, m, $(CH_2)_6CH_3$], 1.78 (2 H, qn, *J* 7.0, OCH_2CH_2), 4.34 (2 H, t, *J* 6.7, OCH_2), 7.23 (1 H, d, *J* 8.8, Ar–H, *ortho* to OH), 8.24 (1 H, dd, *J* 8.8 and 2.0,

Ar–H, *para* to NO_2), 8.82 (1 H, d, *J* 2.0, Ar–H, *ortho* to NO_2) and 10.90 (1 H, s, OH, exch.).

n-*Nonyl 3-amino-4-hydroxybenzoate* **78** *(Scheme 4).*—*n*-Nonyl 4-hydroxy-3-nitrobenzoate **77** (8.64 g, 27.9 mmol) was dissolved in ethanol (110 cm^3) and a small, spatula-full of 10% Pd/C catalyst added. The solution was shaken with hydrogen gas (3 atm; Cook Hydrogenator) at room temperature for 16 h. TLC [silica gel, 40% ethyl acetate–petrol (40–60)] after this time revealed three spots: R_f 0.46 (brown, intense; amino-ester), 0.72 (brown, faint) and 0.78 (yellow, faint; nitro-ester). The catalyst was removed by filtration and the solvent removed *in vacuo* to leave a brown solid (7.84 g). Flash-column chromatography of the crude product on silica gel [eluent 40% ethyl acetate–petrol (40–60)] afforded a tan solid (6.22 g, 80%), *n*-nonyl 3-amino-4-hydroxybenzoate **78**, mp 70–72 °C (Found: C, 71.81; H, 9.88; N, 4.75. $C_{16}H_{25}NO_3$ requires C, 68.78; H, 9.02; N, 5.01%); R_f [silica gel, 40% ethyl acetate–petrol (40–60)] 0.46 (brown); MIC = 7.8 μg cm^{-3} (NAJ); ν_{max}/cm^{-1} (KBr) 3480 (N–H), 3392s (O–H), 3320s (N–H), 2915s, 2847m, 1677s (C=O), 1608s (N–H), 1522m, 1387m, 1306s, 1208m, 1132m, 881w and 781m; δ_H (250 MHz, $CDCl_3$) 0.88 (3 H, t, *J* 6.5, CH_3), 1.1–1.6 [12 H, m, $(CH_2)_6CH_3$], 1.74 (2 H, qn, *J* 6.9, OCH_2CH_2), 4.27 (2 H, t, *J* 6.6, OCH_2), 4.83 (3 H, br s, OH + NH_2, exch.), 6.76 (1 H, d, *J* 8.2, Ar–H, *ortho* to OH), 7.42 (1 H, dd, *J* 8.2 and 1.9, Ar–H, *para* to NO_2) and 7.45 (1 H, d, *J* 1.9, Ar–H, *ortho* to NH_2).

Attempts to prepare the compounds in Scheme 5 used the methods detailed by Lewis *et al.*[61]

3,3'-Dithiodipropionyl dichloride **90** *(Scheme 5).*—Dithiodipropionic acid **89** (49.35 g, 0.235 mol), freshly distilled thionyl chloride (110 cm^3; 179.4 g, 1.51 mol) and pyridine (one drop) were stirred at room temperature for 4 d. Unreacted thionyl chloride was removed *in vacuo* to leave an amber solution (57.67 g, 99%), 3,3'-dithiodipropionyl dichloride **90**; ν_{max}/cm^{-1} (film) 3572w, 2922m, 1796s (C=O), 1404s, 1328m, 1157m, 1035s, 954s, 873s, 682s and 658s.

N,N'-*Bis-(2-bromoethyl)-3,3'-dithiodipropionamide* **92b** *(Scheme 5).*—2-Bromoethylamine hydrobromide **91b** (3.32 g, 16.2 mmol) was added to a stirred solution of 25% aqueous sodium hydroxide solution (7.4 cm^3, 46 mmol) and the flask contents cooled (ice–water bath). A dropping funnel was attached and charged with a solution of 3,3'-dithiodipropionyl dichloride **90** (1.00 g, 4.0 mmol) in toluene (20 cm^3). The toluene solution was added drop-wise, with continued stirring and cooling, over 30 min. The cooling bath was removed and the solution stirred at room temperature for a further 1.5 h. The solution was filtered and the precipitate washed with water until the washings were neutral. This left, after drying, an off-white solid (1.82 g), mp 128–131 °C. Recrystallization from toluene afforded a white solid, *N,N'*-bis-(2-bromoethyl)-3,3'-dithiodipropionamide **92b**, mp 137–138 °C (Found: C, 29.52; H, 3.47; Br, 38.85; N, 6.65; S, 16.18. $C_{10}H_{18}Br_2N_2O_2S_2$ requires C, 28.45; H, 4.30; Br, 37.85; N, 6.64; S, 15.19%); ν_{max}/cm^{-1} (KBr) 3288s, 3090w, 2919w, 1648s (C=O), 1564s, 1421w, 1396m, 1251m, 1187m, 945w and 738m; δ_H (250 MHz, C_5D_5N) 2.85 (2 H, t, *J* 7.0, CH_2CO), 3.19 (2 H, t, *J* 7.0, CH_2S), 3.66 (2 H, t, *J* 6.0, CH_2Br), 3.82 (2 H, q, *J* 6.4, CH_2N) and 9.31 (1 H, br s, NH).

Attempted synthesis of N,N'-*bis-(3-chloropropyl)-3,3'-dithiodipropionamide* **92a** *(Scheme 5).*—3-Chloropropylamine hydrochloride **91a** (11.31 g, 87.0 mmol), 25% aqueous sodium hydroxide solution (40 cm^3, 0.25 mol) and 3,3'-dithiodipropionyl dichloride **90** (5.37 g, 21.7 mmol) in toluene (100 cm^3) were stirred at room temperature for 4 h in a similar manner to that of **92b**. The solution was filtered and washed with water to leave, after drying, a tan solid (7.42 g, 95%), mp 103–105 °C. Recrystallization from acetone–water afforded an off-white solid, *N*-(3-chloropropyl)-3-mercaptopropionamide **94**, mp 106–107 °C. ^1H NMR spectroscopy and mass spectroscopy suggested that the thiol **94** had been formed and not, in fact, the disulfide **92a**; (Found: C, 39.99; H, 6.37; Cl, 19.90; N, 7.60; S, 17.47. $C_6H_{12}ClNOS$ requires C, 39.66; H, 6.66; Cl, 19.51; N, 7.71; S, 17.65%); R_f [alumina, CH_2Cl_2] 0.11; MIC = >1000 μg cm^{-3} (NAJ); ν_{max}/cm^{-1} (KBr) 3281s, 3064w, 2953w, 2911m, 1630s (C=O), 1536s, 1396m, 1251m, 1183m, 1064m, 911m and 706m; δ_H (250 MHz, $CDCl_3$) 1.70 (1 H, br s, SH, exch.), 2.02 (2 H, qn, *J* 6.4, CH_2CH_2Cl), 2.60 (2 H, t, *J* 6.8, CH_2CO), 3.00 (2 H, t, *J* 6.8, CH_2S), 3.45 (2 H, q, *J* 6.4, CH_2N), 3.61 (2 H,

t, *J* 6.4, CH_2Cl) and 6.23 (1 H, br s, NH, exch.); (Found: M^+, 183.0306, 15.8%. $C_6H_{12}Cl^{36.97}NOS$ requires *M*, 183.0299).

Attempted synthesis of 4(or 5)-chloro-2-(2-bromoethyl)-4-isothiazolin-3-one **93b** *(Scheme 5).*—Freshly distilled sulfuryl chloride (0.5 cm^3; 0.835 g, 6.2 mmol) was added over ~10 min, with cooling (ice–water bath), to a stirred slurry of *N,N'*-bis-(2-bromoethyl)-3,3'-dithiodipropionamide **92b** (300 mg, 0.71 mmol) in 1,2-dichloroethane (16 cm^3). The solution was allowed to warm to room temperature and stirred for 5d. The progress of the reaction was monitored by TLC: R_f [alumina, CH_2Cl_2] 0.44, 0.59; with time, the R_f 0.44 spot disappeared to be replaced by the R_f 0.59 spot. The volatiles were removed *in vacuo* to leave an oily residue (380 mg) which was then partitioned in diethyl ether–water. The ether layer was separated, dried ($MgSO_4$) and the ether removed *in vacuo* to afford a viscous, orange oil (290 mg). ^1H NMR spectroscopy (250 MHz, $CDCl_3$) revealed a complex set of peaks in the range δ 3.5–4.3 ppm, with no indications of the expected product, the bromoethylisothiazolinone **93b**.

Attempted synthesis of 4(or 5)-chloro-2-(3-chloropropyl)-4-isothiazolin-3-one **93a** *(Scheme 5).*—Sulfuryl chloride (4.4 cm^3; 7.35 g, 54 mmol) and *N*-(3-chloropropyl)-3-mercaptopropionamide **94** (3.00 g, 16.6 mmol) in 1,2-dichloroethane (50 cm^3) were stirred at room temperature for 5 d in a similar manner to that of **93b**. The volatiles were removed *in vacuo* to leave an oily residue which was then partitioned in diethyl ether–water. The ether layer was separated, dried ($MgSO_4$) and the ether removed *in vacuo* to afford a yellow-orange oil (1.7 g); R_f [alumina, CH_2Cl_2] 0.39, 0.55. ^1H NMR spectroscopy (250 MHz, $CDCl_3$) revealed a complex set of peaks in the range δ 1.9–4.1 ppm, with no indications of the expected product, the chloropropylisothiazolinone **93a**.

2-Dithiobenzoyl **98** and benzokathon **99** (Scheme 6) were prepared by the published methods.[64]

3H-1,2-Benzodithiol-3-one (2-dithiobenzoyl) **98** *(Scheme 6).*—[Note: Due to the potent stenches of ethanethiol and 2-dithiobenzoyl all experimental work was carried out in a well-ventilated fumehood] A dropping funnel was charged with a solution of ethanethiol

(6 cm^3; 5.03 g, 80.9 mmol) in concentrated sulfuric acid (25 cm^3). This was then added to a solution of thiosalicylic acid **97** (5.01 g, 32.5 mmol) in concentrated sulfuric acid (50 cm^3) at room temperature. The solution was stirred at room temperature for 30 min. A reflux condenser (connected to a liquid nitrogen trap) was attached and the solution heated (oil bath), with continued stirring, at 50 °C for 2.5 h. The flask contents were then poured into a beaker of crushed ice (500 cm^3) and the solution filtered to leave a fine, brown precipitate which was washed with water. The precipitate was transferred to a round-bottomed flask (1 L) and purified by volatilization in a current of steam. The distillate (~800 cm^3 of a cloudy-white solution) was then extracted with diethyl ether (2 x 400 cm^3, followed by 1 x 200 cm^3) and the ether washings dried ($MgSO_4$), filtered and the ether removed *in vacuo* to afford the crude product (870 mg). Recrystallization from ethanol afforded orange-yellow crystals (498 mg, 9%), 3*H*-1,2-benzodithiol-3-one (dithiobenzoyl) **98**, mp 70–73 °C (lit.,[65] 78–80 °C) (Found: C, 49.78; H, 2.33; S, 37.98. $C_7H_4OS_2$ requires C, 49.97; H, 2.40; S, 38.11%); MIC = 125 μg cm^{-3} (NAJ); ν_{max}/cm^{-1} (KBr) 3432s, 3075w, 2922w, 1662s (C=O), 1642s, 1576m, 1440m, 1266m, 1066m, 890s, 764m, 724m, 667w and 625w; δ_H (250 MHz, $CDCl_3$) 7.42 (1 H, m), 7.64 (2 H, m) and 7.97 (1 H, d, *J* 7.8).

1,2-Benzisothiazole-3-one (benzokathon) **99** *(Scheme 6).*—Dry ammonia gas was bubbled slowly through a solution of 3*H*-1,2-benzodithiol-3-one **98** (1 g, 5.94 mmol) in ethanol (50 cm^3) and the ethanol solution stirred at room temperature for 6 h. The ammonia gas was turned off, the flask stoppered and the solution stirred at room temperature for a further 16 h. The course of the reaction was monitored by TLC: R_f [silica gel, chloroform] 0.0 (immobile; benzokathon), 0.67 (3*H*-1,2-benzodithiol-3-one) and 0.80; after 22 h the immobile spot was very intense and the R_f 0.80 spot very faint. The reaction solution was concentrated (rotary evaporator), water (50 cm^3) added and the solution filtered to leave a flesh solid (2.35 g). The solid was heated for 10–15 min with 50% aqueous sodium hydroxide solution (20 cm^3) and the solution filtered to afford the sodium salt of benzo-kathon (1.0 g), mp 300 (softened)–315 (melt) °C. The benzokathon salt was dissolved in water (8 cm^3) and acidified with concentrated hydrochloric acid until neutral. The resultant precipitate was washed with water and dried. Recrystallization from ethanol yielded tan *platelets* (380 mg, 42%), 1,2-benzisothiazole-3-one (benzokathon) **99**, mp 156–157 °C

(lit.,[64] 158 °C) (Found: C, 55.54; H, 3.23; N, 9.27; S, 21.43. C_7H_5NOS requires C, 55.63; H, 3.34; N, 9.27; S, 21.17%); MIC = 250 μg cm^{-3} (NAJ), 250 μg cm^{-3} (SOJ) and 1000 μg cm^{-3} (MOJ); ν_{max}/cm^{-1} (KBr) 3462s, 3055m, 2925m, 2704m, 1645s (C=O), 1448m, 1321m, 739m and 606m; δ_H (250 MHz, $CDCl_3$) 7.45 (1 H, m), 7.66 (2 H, m), 8.08 (1 H, d, *J* 7.9) and 11.05 (1 H, br s, NH); δ_H (250 MHz, CD_3OD) 7.41 (1 H, t, *J* 7.5), 7.63 (1 H, td, *J* 7.6 and 1.1), 7.77 (1 H, d, *J* 8.2) and 7.95 (1 H, d, *J* 8.0).

The compounds **123** and **124** (Scheme 10) were prepared by the method detailed by Kenney *et al.*,[74] while **125** and **126** were prepared using the method of Ammo *et al.*[72]

p-*Tolylmercaptoacetic acid* **123** *(Scheme 10).*—Chloroacetic acid (5.21 g, 55.1 mmol) was added to a solution of *p*-thiocresol **122** (6.21 g, 50.0 mmol) in aqueous sodium hydroxide solution (4.22 g, 105 mmol, in 130 cm^3 water) and the mixture refluxed for 2 h. The solution was allowed to cool and then acidified with concentrated hydrochloric acid. The white precipitate (8.77 g, 96% crude), mp 69–71 °C, that formed was filtered off and washed with water. Recrystallization from hot ethanol gave colourless crystals (4.08 g, 45%), *p*-tolylmercaptoacetic acid **123**, mp 92–93 °C (lit.,[74] 88.5–90 °C) (Found: C, 59.17; H, 5.24; S, 17.55. $C_9H_{10}O_2S$ requires C, 59.32; H, 5.53; S, 17.59%); MIC = 250 μg cm^{-3} (NAJ) and 500 μg cm^{-3} (MOJ); λ_{max} (chloroform)/nm 294; ν_{max}/cm^{-1} (KBr) 3017s, 2920s, 2688m, 2591m, 2472m, 1702s (C=O), 1427s, 1305s, 1204s, 891s, 801s and 669m; δ_H (250 MHz, $CDCl_3$) 2.34 (3 H, s, CH_3), 3.63 (2 H, s, CH_2), 7.14 (2 H, d, *J* 8.0, Ar–H), 7.35 (2 H, d, *J* 8.0, Ar–H) and 10.61 (1 H, br s, CO_2H).

p-*Tolylsulfonylacetic acid* **124** *(Scheme 10).*—Hydrogen peroxide solution [27.5% w/v (minimum) solution in water: 1.43 cm^3; 393 mg, 11.6 mmol] was added at room temperature to a solution of *p*-tolylmercaptoacetic acid **123** (1.00 g, 5.49 mmol) in glacial acetic acid (10 cm^3). The solution was stoppered and stirred for 6 h. On concentration (rotary evaporator) a white solid formed, mp 110 °C. Recystallization from water gave a white solid (340 mg, 29%), *p*-tolylsulfonylacetic acid **124**, mp 110–115 °C (lit.,[74] 114–115 °C) (Found: C, 50.55; H, 4.95; S, 14.79. $C_9H_{10}O_4S$ requires C, 50.46; H, 4.70; S, 14.96%); MIC = >1000 μg cm^{-3} (NAJ) and >1000 μg cm^{-3} (MOJ); λ_{max} (chloroform)/nm 290;

ν_{max}/cm^{-1} (KBr) 3021s, 2953s, 2648m, 2517m, 1717s (C=O), 1649s, 1424s, 1324s (SO_2), 1163s (SO_2), 808s, 639m and 518s; δ_H (250 MHz, $CDCl_3$) 2.47 (3 H, s, CH_3), 4.14 (2 H, s, CH_2), 7.39 (2 H, d, *J* 8.2, Ar–H), 7.84 (2 H, d, *J* 8.2, Ar–H) and 8.35 (1 H, br s, CO_2H, exch.).

*Diiodomethyl-*p*-tolylsulfone (Amical)* **125** *(Scheme 10).*—*p*-Tolylsulfonylacetic acid **124** (650 mg, 3.03 mmol) was dissolved in 7% aqueous sodium hydroxide solution (30 cm^3) and the flask contents cooled (ice–water bath). Iodine (3.08 g, 12.1 mmol) was added and the solution stirred at 0–5 °C for 2 h. The solution was then filtered and the precipitate washed with water. The crude product was stirred in a solution of 25% aqueous sodium thiosulfate (30 cm^3) for 1.5 h in order to remove unreacted iodine (iodine reduced to iodide). The solid was filtered, washed with water and dried overnight ($CaCl_2$) to afford a tan powder (1.05 g, 82%), diiodomethyl-*p*-tolylsulfone **125**, mp 134–135 °C (lit.,[72] 148–148.5 °C). ^1H NMR spectroscopy revealed the product to be 89% pure, with an 11% impurity of the mono-iodo analogue **126**; (Found: C, 22.98; H, 1.82; I, 59.53; S, 7.67. $C_8H_8I_2O_2S$ requires C, 22.77; H, 1.91; I, 60.14; S, 7.60%); R_f [silica gel, CH_2Cl_2] 0.51; MIC = <1 μg cm^{-3} (NAJ) and 1.95 μg cm^{-3} (MOJ); λ_{max} (chloroform)/nm 244; ν_{max} (KBr)/cm^{-1} 2972m, 1593m, 1323s (SO_2), 1147s (SO_2), 1078m, 815m, 738s, 672m, 542s and 513m; δ_H (250 MHz, $CDCl_3$) 2.50 (3 H, s, CH_3), 5.96 (1 H, s, CHI_2), 7.40 (2 H, d, *J* 8.2, Ar–H) and 7.94 (2 H, d, *J* 8.2, Ar–H).

The above experiment was repeated using *p*-tolylsulfonylacetic acid **124** (650 mg, 3.03 mmol), aqueous sodium hydroxide solution (7%; 30 cm^3) and iodine (2.31 g, 9.10 mmol) to afford a light tan powder (795 mg) of mp 101–103 °C. ^1H NMR spectroscopy (250 MHz, $CDCl_3$) revealed a mixture comprised of diiodomethyl-*p*-tolylsulfone **125** (59%) and iodomethyl-*p*-tolylsulfone **126** (41%); R_f [silica gel, CH_2Cl_2] 0.40 (faint; **126**) and 0.51 (intense; **125**). The experiment was repeated, once again, using *p*-tolylsulfonyl-acetic acid **124** (650 mg, 3.03 mmol), aqueous sodium hydroxide solution (7%; 30 cm^3) and iodine (1.67 g, 6.58 mmol) to afford an off-white powder (775 mg) of mp 112–114 °C. ^1H NMR spectroscopy (250 MHz, $CDCl_3$) revealed a mixture comprised of iodo-methyl-*p*-tolylsulfone **126** (90%) and diiodomethyl-*p*-tolylsulfone **125** (10%); R_f [silica gel, CH_2Cl_2] 0.40 (intense; **126**) and 0.51 (faint; **125**).

Iodomethyl-p-tolylsulfone **126** *(Scheme 10).*—*p*-Tolylsulfonylacetic acid **124** (650 mg, 3.03 mmol), aqueous sodium hydroxide solution (7%, 30 cm^3) and iodine (785 mg, 3.09 mmol) were reacted, and the product worked up, in a similar manner to that of **125**. The reaction afforded a white solid (349 g, 39%), iodomethyl-*p*-tolylsulfone **126**, mp 125–127 °C. ^1H NMR spectroscopy revealed the product to be ~100% pure, with only a trace impurity of the di-iodo analogue **125**; (Found: C, 32.20 ; H, 3.17; I, 43.00; S, 10.67. $C_8H_9IO_2S$ requires C, 32.45; H, 3.06; I, 42.86; S, 10.83%); R_f [silica gel, CH_2Cl_2] 0.43; MIC = 3.9 μg cm^{-3} (NAJ) and 125 μg cm^{-3} (MOJ); λ_{max} (chloroform)/nm 244; ν_{max} (KBr)/ cm^{-1} 3025w, 2957w, 1598m, 1313s (SO_2), 1159s (SO_2), 1140s, 1083m, 817m, 744s, 665m, 548s and 496m; δ_H (250 MHz, $CDCl_3$) 2.49 (3 H, s, CH_3), 4.45 (2 H, s, CH_2I), 7.40 (2 H, d, *J* 8.3, Ar–H) and 7.86 (2 H, d, *J* 8.3, Ar–H).

Methyl nicotinate **146a** *(Scheme 13).*—This was prepared using a standard literature method.[89] Concentrated sulfuric acid (13.5 cm^3; 23.6 g, 241 mmol) was added drop-wise, with cooling, to a slurry of niacin **143** (10.00 g, 81.2 mmol) in methanol **145a** (50 cm^3; 39.5 g, 1.23 mol). The solution was then refluxed for 20 h. The reaction mixture was poured onto crushed ice (50 g) and concentrated aqueous ammonia solution (50 cm^3) added until the solution was alkaline (pH 9). The solution was extracted with diethyl ether (5 x 50 cm^3) and the ether extracts dried ($MgSO_4$), filtered and the solvent removed *in vacuo* to leave an off-white solid (9.26 g). The crude ester was distilled (Kugelrohr) to give a white solid (9.03 g, 81%), methyl nicotinate **146a**, bp ~165 °C/10 mbar (water-pump), mp 38–40 °C (lit.,[65] 42–43 °C) (Found: C, 61.36; H, 5.35; N, 10.21. $C_7H_7NO_2$ requires C, 61.31; H, 5.14; N, 10.21%); MIC = >1000 μg cm^{-3} (NAJ) and >1000 μg cm^{-3} (MOJ); λ_{max} (ethanol)/nm 218 and 263; ν_{max} (melt)/cm^{-1} 3437w, 3004w, 2953m, 1725s (C=O), 1591m, 1420m, 1283s, 1115s, 1025m, 742s and 703m; δ_H (250 MHz, $CDCl_3$) 3.94 (3 H, s, CH_3), 7.38 [1 H, ddd, *J* 8.0, 4.9 and 0.8, Ar–H(5)], 8.28 [1 H, dt, *J* 8.0 and 1.6, Ar–H(6)], 8.76 [1 H, dd, *J* 4.9 and 1.7, Ar–H(4)] and 9.21 [1 H, d, *J* 2.1, Ar–H(2)].

Methyl isonicotinate **147a** *(Scheme 13).*—Isonicotinic acid **144** (6.15 g, 50.0 mmol), methanol **145a** (30 cm^3; 19.8 g, 618 mmol) and concentrated sulfuric acid (8.3 cm^3; 14.5 g, 148 mmol) were reacted, and the product worked up, in a similar manner to that of

146a. Kugelrohr distillation gave a colourless oil (2.37 g, 35%), methyl isonicotinate **147a**, bp ~50 °C/0.05 mbar (Found: C, 59.56; H, 5.33; N, 10.15. $C_7H_7NO_2$ requires C, 61.31; H, 5.14; N, 10.21%); MIC = >1000 μg cm^{-3} (NAJ) and >1000 μg cm^{-3} (MOJ); λ_{max} (ethanol)/nm 213 and 274; ν_{max} (film)/cm^{-1} 3625w, 3446w, 3033m, 2954m, 1733s (C=O), 1562m, 1437m, 1286s, 1120s, 965m, 758m and 708m; δ_H (250 MHz, $CDCl_3$) 3.95 (3 H, s, CH_3), 7.84 [2 H, dd, *J* 4.4 and 1.6, Ar–H(3,5)] and 8.77 [2 H, dd, *J* 4.4 and 1.6, Ar–H(2,6)].

Ethyl nicotinate **146b** *(Scheme 13)*.—Niacin **143** (10.00 g, 81.2 mmol), ethanol **145b** (50 cm^3; 39.5 g, 856 mmol) and concentrated sulfuric acid (13.5 cm^3; 23.6 g, 241 mmol) were reacted, and the product worked up, in a similar manner to that of **146a**. Kugelrohr distillation gave a colourless oil (9.49 g, 77%), ethyl nicotinate **146b**, bp ~165 °C/10 mbar (water-pump) (Found: C, 63.39; H, 6.15; N, 9.30. $C_8H_9NO_2$ requires C, 63.56; H, 6.00; N, 9.27%); MIC = >1000 μg cm^{-3} (NAJ) and >1000 μg cm^{-3} (MOJ); λ_{max} (ethanol)/nm 222 and 263; ν_{max} (film)/cm^{-1} 3610w, 3429w, 2983m, 1721s (C=O), 1591m, 1421m, 1283s, 1112s, 1025m, 742s and 703m; δ_H (250 MHz, $CDCl_3$) 1.40 (3 H, t, *J* 7.1, CH_3), 4.40 (2 H, q, *J* 7.1, CH_2), 7.38 [1 H, ddd, *J* 8.0, 4.9 and 0.7, Ar–H(5)], 8.29 [1 H, dt, *J* 8.0 and 2.0, Ar–H(6)], 8.76 [1 H, dd, *J* 4.9 and 1.7, Ar–H(4)] and 9.21 [1 H, d, *J* 2.1, Ar–H(2)].

Ethyl isonicotinate **147b** *(Scheme 13)*.—Isonicotinic acid **144** (6.15 g, 50.0 mmol), ethanol **145b** (50 cm^3; 39.5 g, 856 mmol) and concentrated sulfuric acid (8.3 cm^3; 14.5 g, 148 mmol) were reacted, and the product worked up, in a similar manner to that of **146a**. Kugelrohr distillation gave a colourless oil (5.04 g, 67%), ethyl isonicotinate **147b**, bp ~75 °C/0.05 mbar (Found: C, 62.28; H, 5.35; N, 9.09. $C_8H_9NO_2$ requires C, 63.56; H, 6.00; N, 9.27%); MIC = >1000 μg cm^{-3} (NAJ) and >1000 μg cm^{-3} (MOJ); λ_{max} (ethanol)/nm 215 and 274; ν_{max} (film)/cm^{-1} 3616w, 3435w, 2983m, 1729s (C=O), 1564m, 1410m, 1283s, 1119s, 1021m, 758m and 708m; δ_H (250 MHz, $CDCl_3$) 1.41 (3 H, t, *J* 7.1, CH_3), 4.42 (2 H, q, *J* 7.1, CH_2), 7.85 [2 H, dd, *J* 4.5 and 1.6, Ar–H(3,5)] and 8.77 [2 H, dd, *J* 4.5 and 1.6, Ar–H(2,6)].

n-*Propyl nicotinate* **146c** *(Scheme 13)*.—Niacin **143** (10.00 g, 81.2 mmol), propan-1-ol **145c** (60 cm^3; 48.2 g, 803 mmol) and concentrated sulfuric acid (13.5 cm^3; 23.6 g, 241 mmol) were reacted, and the product worked up, in a similar manner to that of **146a**. Kugelrohr distillation gave a colourless oil (9.65 g, 72%), *n*-propyl nicotinate **146c**, bp ~125 °C/0.1–0.5 mbar (Found: C, 64.42; H, 6.63; N, 8.24. $C_9H_{11}NO_2$ requires C, 65.44; H, 6.71; N, 8.48%); MIC = 1000 [15.6] μg cm^{-3} (NAJ) and 500 μg cm^{-3} (MOJ); λ_{max} (ethanol)/nm 219 and 264; ν_{max} (film)/cm^{-1} 3612w, 3431w, 2969m, 1723s (C=O), 1591m, 1419m, 1284, 1113s, 1024m, 741m and 703m; δ_H (250 MHz, $CDCl_3$) 1.01 (3 H, t, *J* 7.4, CH_3), 1.78 (2 H, sx, *J* 7.1, CH_2CH_3), 4.29 (2 H, t, *J* 6.7, OCH_2), 7.37 [1 H, ddd, *J* 8.0, 4.9 and 0.9, Ar–H(5)], 8.27 [1 H, dt, *J* 8.2 and 2.0, Ar–H(6)], 8.74 [1 H, dd, *J* 4.8 and 1.8, Ar–H(4)] and 9.20 [1 H, dd, *J* 2.2 and 0.8, Ar–H(2)].

n-*Propyl isonicotinate* **147c** *(Scheme 13)*.—Isonicotinic acid **144** (6.15 g, 50.0 mmol), propan-1-ol **145c** (40 cm^3; 32.1 g, 535 mmol) and concentrated sulfuric acid (8.3 cm^3; 14.5 g, 148 mmol) were reacted, and the product worked up, in a similar manner to that of **146a**. Kugelrohr distillation gave a colourless oil (5.77 g, 70%), *n*-propyl isonicotinate **147c**, bp ~85 °C/0.01–0.05 mbar (Found: C, 64.55; H, 6.29; N, 7.94. $C_9H_{11}NO_2$ requires C, 65.44; H, 6.71; N, 8.48%); MIC = 1000 [125] μg cm^{-3} (NAJ) and 500 μg cm^{-3} (MOJ); λ_{max} (ethanol)/nm 213 and 274; ν_{max} (film)/cm^{-1} 3614w, 3437w, 2970m, 1729s (C=O), 1562m, 1408m, 1280s, 1120s, 938m, 758m and 708m; δ_H (250 MHz, $CDCl_3$) 1.01 (3 H, t, *J* 7.4, CH_3), 1.79 (2 H, sx, *J* 7.1, CH_2CH_3), 4.30 (2 H, t, *J* 6.7, OCH_2), 7.83 [2 H, dd, *J* 4.4 and 1.6, Ar–H(3,5)] and 8.76 [2 H, dd, *J* 4.4 and 1.6, Ar–H(2,6)].

iso-*Propyl nicotinate* **146d** *(Scheme 13)*.—Niacin **143** (10.00 g, 81.2 mmol), propan-2-ol **145d** (50 cm^3; 39.2 g, 653 mmol) and concentrated sulfuric acid (13.5 cm^3; 23.6 g, 241 mmol) were reacted, and the product worked up, in a similar manner to that of **146a**. Kugelrohr distillation gave a colourless oil (7.65 g, 57%), *iso*-propyl nicotinate **146d**, bp ~100 °C/0.05–0.10 mbar (Found: C, 65.33; H, 6.95; N, 8.53. $C_9H_{11}NO_2$ requires C, 65.44; H, 6.71; N, 8.48%); MIC = >1000 μg cm^{-3} (NAJ) and >1000 μg cm^{-3} (MOJ); λ_{max} (ethanol)/nm 218 and 263; ν_{max} (film)/cm^{-1} 3607w, 3427w, 2982m, 1723s (C=O), 1591m, 1419m, 1286s, 1103s, 1025m, 742m and 703m; δ_H (250 MHz, $CDCl_3$) 1.39 (6 H, d, *J* 6.2,

2 x CH_3), 5.28 (1 H, sp, *J* 6.2, OCH), 7.38 [1 H, ddd, *J* 7.9, 4.9 and 0.9, Ar–H(5)], 8.29 [1 H, dt, *J* 7.8 and 2.0, Ar–H(6)], 8.76 [1 H, dd, *J* 4.9 and 1.7, Ar–H(4)] and 9.21 [1 H, q, *J* 1.0, Ar–H(2)].

iso-*Propyl isonicotinate* **147d** *(Scheme 13).*—Isonicotinic acid **144** (6.15 g, 50.0 mmol), propan-2-ol **145d** (40 cm^3; 31.4 g, 523 mmol) and concentrated sulfuric acid (8.3 cm^3; 14.5 g, 148 mmol) were reacted, and the product worked up, in a similar manner to that of **146a**. Kugelrohr distillation gave a colourless oil (5.40 g, 65%), *iso*-propyl isonicotinate **147d**, bp ~60 °C/0.05 mbar (Found: C, 66.21; H, 5.82; N, 8.58. $C_9H_{11}NO_2$ requires C, 65.44; H, 6.71; N, 8.48%); MIC = 1000 [62.5] μg cm^{-3} (NAJ) and 500 μg cm^{-3} (MOJ); λ_{max} (ethanol)/nm 213 and 275; ν_{max} (film)/cm^{-1} 3615w, 3434w, 2982m, 1723s (C=O), 1561m, 1409m, 1281s, 1104s, 919m, 759m and 709m; δ_H (250 MHz, $CDCl_3$) 1.39 (6 H, d, *J* 6.2, 2 x CH_3), 5.28 (1 H, sp, *J* 6.2, OCH), 7.85 [2 H, dd, *J* 4.4 and 1.6, Ar–H(3,5)] and 8.77 [2 H, dd, *J* 4.4 and 1.6, Ar–H(2,6)].

n-*Pentyl nicotinate* **146e** *(Scheme 13).*—This was prepared by the published method.[90] Thionyl chloride (7.3 cm^3; 12.0 g, 101 mmol) was added drop-wise over 16 min, with stirring and cooling, to a slurry of niacin **143** (12.31 g, 100 mmol) in pyridine (16 cm^3). The solution was then heated at 100 °C for 1 h. Pentan-1-ol **145e** (11.9 cm^3; 9.69 g, 110 mmol) was added drop-wise over 13 min and the mixture heated at 100 °C for a further 3 h. The mixture was poured into water (150 cm^3) and aqueous sodium hydroxide solution added to render the solution alkaline (pH 11). The insoluble top layer was then dissolved in diethyl ether (50 cm^3) and washed, respectively, with dilute sodium carbonate solution (50 cm^3) and water (2 x 50 cm^3). The original aqueous layer was extracted with diethyl ether (2 x 50 cm^3) and the combined ether solutions dried ($MgSO_4$), filtered and the solvent removed *in vacuo* to leave a reddish-brown oil (13.97 g). Kugelrohr distillation of the crude ester gave a yellow oil (11.58 g, 60%), *n*-pentyl nicotinate **146e**, bp ~170 °C/ 0.1–0.2 mbar (Found: C, 65.35; H, 8.18; N, 6.38. $C_{11}H_{15}NO_2$ requires C, 68.37; H, 7.82; N, 7.25%); MIC = 250 μg cm^{-3} (NAJ) and 250 μg cm^{-3} (MOJ); λ_{max} (ethanol)/nm 218 and 263; ν_{max} (film)/cm^{-1} 3430w, 2958m, 1726s (C=O), 1591m, 1419m, 1283s, 1113s, 1025m, 741m and 703m; δ_H (250 MHz, $CDCl_3$) 0.93 (3 H, t, *J* 6.9, CH_3), 1.42 [4 H, m,

(CH_2)$_2CH_3$], 1.78 (2 H, qn, *J* 6.7, OCH_2CH_2), 4.35 (2 H, t, *J* 6.7, OCH_2), 7.39 [1 H, dd, *J* 7.8 and 4.9, Ar–H(5)], 8.30 [1 H, dt, *J* 8.0 and 1.9, Ar–H(6)], 8.77 [1 H, dd, *J* 4.9 and 1.7, Ar–H(4)] and 9.23 [1 H, d, *J* 1.8, Ar–H(2)].

sec-*Pentyl nicotinate* **146f** *(Scheme 13).*—Niacin **143** (12.31 g, 100 mmol), thionyl chloride (7.3 cm^3; 12.0 g, 101 mmol), pyridine (16.0 cm^3; 15.6 g, 198 mmol) and pentan-2-ol **145f** (12.0 cm^3; 9.68 g, 110 mmol) were reacted, and the product worked up, in a similar manner to that of **146e**. Kugelrohr distillation gave a yellow oil (4.23 g, 22%), *sec*-pentyl nicotinate **146f**, bp ~125 °C/0.01–0.05 mbar (Found: C, 68.49; H, 8.10; N, 7.22. $C_{11}H_{15}NO_2$ requires C, 68.37; H, 7.82; N, 7.25%); MIC = 500 μg cm^{-3} (NAJ) and 500 μg cm^{-3} (MOJ); λ_{max} (ethanol)/nm 218 and 263. ν_{max} (film)/cm^{-1} 3421w, 2960m, 1723s (C=O), 1591m, 1419m, 1287s, 1110s, 1024m, 742m and 703m; δ_H (250 MHz, $CDCl_3$) 0.94 (3 H, t, *J* 7.3, CH_2CH_3), 1.35 (3 H, d, *J* 6.3, $CHCH_3$), 1.3–1.8 (4 H, m, CH_2CH_2), 5.19 (1 H, sx, *J* 6.3, OCH), 7.37 [1 H, ddd, *J* 7.9, 4.9 and 0.8, Ar–H(5)], 8.28 [1 H, dt, *J* 7.9 and 1.9, Ar–H(6)], 8.75 [1 H, dd; *J* 4.8 and 1.7, Ar–H(4)] and 9.21 [1 H, t, *J* 1.1, Ar–H(2)].

n-*Octyl nicotinate* **146g** *(Scheme 13).*—Niacin **143** (12.31 g, 100 mmol), thionyl chloride (7.3 cm^3; 12.0 g, 101 mmol), pyridine (16.0 cm^3; 15.6 g, 198 mmol) and octan-1-ol **145g** (17.4 cm^3; 14.3 g, 110 mmol) were reacted, and the product worked up, in a similar manner to that of **146e**. Kugelrohr distillation gave a yellow oil (16.69 g, 71%), *n*-octyl nicotinate **146g**, bp ~200 °C/0.1–0.2 mbar (Found: C, 70.06; H, 10.22; N, 5.25. $C_{14}H_{21}NO_2$ requires C, 71.46; H, 8.99; N, 5.95%); MIC = 31.25 μg cm^{-3} (NAJ) and 500 μg cm^{-3} (MOJ); λ_{max} (ethanol)/nm 219 and 263; ν_{max} (film)/cm^{-1} 3433w, 2927s, 1726s (C=O), 1591m, 1419m, 1283s, 1114s, 1024m, 741m and 703m; δ_H (250 MHz, $CDCl_3$) 0.87 (3 H, t, *J* 7.0, CH_3), 1.28 [10 H, m, (CH_2)$_5CH_3$], 1.78 (2 H, qn, *J* 6.7, OCH_2CH_2), 4.35 (2 H, t, *J* 6.7, OCH_2), 7.39 [1 H, ddd, *J* 8.0, 4.9 and 0.8, Ar–H(5)], 8.30 [1 H, dt, *J* 8.0 and 2.0, Ar–H(6)], 8.77 [1 H, dd, *J* 4.8 and 1.7, Ar–H(4)] and 9.23 [1 H, d, *J* 2.1, Ar–H(2)].

n-*Octyl isonicotinate* **147g** *(Scheme 13)*.—Isonicotinic acid **144** (9.21 g, 74.8 mmol), thionyl chloride (5.5 cm^3; 9.0 g, 75.4 mmol), pyridine (12.0 cm^3; 11.7 g, 148 mmol) and octan-1-ol **145g** (13.0 cm^3; 10.7 g, 82.2 mmol) were reacted, and the product worked up, in a similar manner to that of **146e**. Kugelrohr distillation gave a yellow oil (11.63 g, 66%), *n*-octyl isonicotinate **147g**, bp ~150 °C/0.001–0.01 mbar (Found: C, 70.38; H, 9.65; N, 5.61. $C_{14}H_{21}NO_2$ requires C, 71.46; H, 8.99; N, 5.95%); MIC data N/A; λ_{max} (ethanol)/nm 216 and 274; ν_{max} (film)/cm^{-1} 3437w, 2927s, 1730s (C=O), 1563w, 1408m, 1281s, 1120m, 950w, 758m and 708m; δ_H (250 MHz, $CDCl_3$) 0.88 (3 H, t, *J* 6.7, CH_3), 1.28 [10 H, m, $(CH_2)_5CH_3$], 1.78 (2 H, qn, *J* 7.0, OCH_2CH_2), 4.35 (2 H, t, *J* 6.7, OCH_2), 7.84 [2 H, dt, *J* 4.5 and 0.8, Ar–H(3,5)] and 8.77 [2 H, dt, *J* 4.5 and 0.8, Ar–H(2,6)].

n-*Nonyl nicotinate* **146h** *(Scheme 13)*.—Niacin **143** (12.32 g, 100 mmol), thionyl chloride (7.3 cm^3; 12.0 g, 101 mmol), pyridine (16.0 cm^3; 15.6 g, 198 mmol) and nonan-1-ol **145h** (19.2 cm^3; 15.9 g, 110 mmol) were reacted, and the product worked up, in a similar manner to that of **146e**. Kugelrohr distillation gave a yellow oil (21.56 g, 86%), *n*-nonyl nicotinate **146h**, bp ~215 °C/0.05–0.1 mbar (Found: C, 71.02; H, 9.20; N, 4.79. $C_{15}H_{23}NO_2$ requires C, 72.25; H, 9.30; N, 5.62%); MIC = 250 μg cm^{-3} (NAJ); λ_{max} (ethanol)/nm 218 and 263; ν_{max} (film)/cm^{-1} 3433w, 2926s, 1726s (C=O), 1591m, 1467m, 1283s, 1114s, 1025m, 741m and 703m; δ_H (250 MHz, $CDCl_3$) 0.88 (3 H, t, *J* 6.6, CH_3), 1.28 [12 H, m, $(CH_2)_6CH_3$], 1.78 (2 H, qn, *J* 6.7, OCH_2CH_2), 4.35 (2 H, t, *J* 6.7, OCH_2), 7.40 [1 H, ddd, *J* 7.9, 4.9 and 0.8, Ar–H(5)], 8.30 [1 H, dt, *J* 8.0 and 2.0, Ar–H(6)], 8.78 [1 H, dd, *J* 4.9 and 1.7, Ar–H(4)] and 9.23 [1 H, d, *J* 1.4, Ar–H(2)].

n-*Dodecyl nicotinate* **146i** *(Scheme 13)*.—Niacin **143** (12.31 g, 100 mmol), thionyl chloride (7.3 cm^3; 12.0 g, 101 mmol), pyridine (16.0 cm^3; 15.6 g, 198 mmol) and dodecan-1-ol **145i** (24.5 cm^3; 20.4 g, 110 mmol) were reacted, and the product worked up, in a similar manner to that of **146e**. Kugelrohr distillation gave a white solid (24.7 g, 85%), *n*-dodecyl nicotinate **146i**, bp ~200 °C/0.01–0.05 mbar (Found: C, 74.19; H, 10.30; N, 4.55. $C_{18}H_{29}NO_2$ requires C, 74.18; H, 10.03; N, 4.81%); MIC = 1000 μg cm^{-3} (NAJ) and >1000 μg cm^{-3} (MOJ); λ_{max} (ethanol)/nm 219 and 263; ν_{max} (melt)/cm^{-1} 3429w, 2924s, 1726s (C=O), 1591m, 1468m, 1284m, 1116s, 1025m, 741m and 703m; δ_H (250 MHz,

$CDCl_3$) 0.86 (3 H, t, *J* 6.6, CH_3), 1.25 [18 H, m, $(CH_2)_9CH_3$], 1.77 [2 H, qn, *J* 7.0, OCH_2CH_2), 4.34 (2 H, t, *J* 6.7, OCH_2), 7.38 [1 H, ddd, *J* 7.9, 4.9 and 0.8, Ar–H(5)], 8.28 [1 H, dt, *J* 7.9 and 2.0, Ar–H(6)], 8.76 [1 H, dd, *J* 4.9 and 1.7, Ar–H(4)] and 9.21 [1 H, dd, *J* 2.1 and 0.8, Ar–H(2)].

n-*Dodecyl isonicotinate* **147i** *(Scheme 13).*—Isonicotinic acid **144** (9.21 g, 74.8 mmol), thionyl chloride (5.5 cm^3; 9.0 g, 75.4 mmol), pyridine (12.0 cm^3; 11.7 g, 148 mmol) and dodecan-1-ol **145i** (19.0 cm^3; 15.6 g, 83.6 mmol) were reacted, and the product worked up, in a similar manner to that of **146e**. Kugelrohr distillation gave a yellow oil–solid mixture (16.52 g, 76%), *n*-dodecyl isonicotinate **147i**, bp ~200 °C/0.01 mbar (Found: C, 70.97; H, 9.83; N, 2.65. $C_{18}H_{29}NO_2$ requires C, 74.18; H, 10.03; N, 4.81%); MIC data N/A; λ_{max} (ethanol)/nm 215 and 274; ν_{max} (film)/cm^{-1} 2925s, 1733s (C=O), 1563w, 1467s, 1280s, 1212m, 1120m, 941m, 758m and 708m; δ_H (250 MHz, $CDCl_3$) 0.88 (3 H, t, *J* 6.6, CH_3), 1.26 [18 H, m, $(CH_2)_9CH_3$], 1.78 [2 H, qn, *J* 7.3, OCH_2CH_2), 4.35 (2 H, t, *J* 6.7, OCH_2), 7.85 [2 H, dd, *J* 4.4 and 1.6, Ar–H(3,5)] and 8.78 [2 H, dd, *J* 4.4 and 1.6, Ar–H(2,6)].

2.3.2 Synthesis of Vinyl Monomers

N-*Acryloyl-2-(4'-thiazolyl)benzimidazole* **67** *(Scheme 1).*—This was prepared by the published method.[47] Acryloyl chloride (0.74 cm^3; 0.82 g, 9.11 mmol) in sodium-dried benzene (20 cm^3) was added drop-wise over 17 min to a stirred solution of 2-(4'-thiazolyl)benzimidazole **66** (2.45 g, 12.2 mmol) and triethylamine (1.8 cm^3; 1.31 g, 12.9 mmol) in dry benzene (100 cm^3) at 11–13 °C. The reaction solution was then stirred at room temperature for 19 h. The benzene solution was filtered (to remove $Et_3N^+Cl^-$) and washed with 5% aqueous sodium hydrogen carbonate solution (3 x 50 cm^3) and water (4 x 50 cm^3) respectively. The benzene layer was dried (Na_2SO_4) and the solvent removed *in vacuo* to afford a yellow solid (1.51 g, 65%), *N*-acryloyl-2-(4'-thiazolyl)benzimidazole **67**, mp 120–121 °C (lit.,[47] 139.5–140.5 °C). Several attempts were made to recrystallize the crude product but met with failure – **67** did not appear to be stable to heating and, as a result, decomposed during the recrystallization procedure (Found: C, 60.89; H, 3.71; N, 16.52; S, 12.26. $C_{13}H_9N_3OS$ requires C, 61.16; H, 3.55; N, 16.46; S, 12.56%); MIC =

500 μg cm^{-3} (NAJ) and >1000 μg cm^{-3} (MOJ); λ_{max} (ethanol)/nm 222, 267 and 300; ν_{max}/ cm^{-1} (KBr) 3087w, 1701s (C=O), 1613m, 1475m, 1403s, 1317s, 1280s, 1159s, 993s and 768m; δ_H (250 MHz, $CDCl_3$) 5.83 (1 H, dd, *J* 10.0 and 1.4, CH=CHH_{cis}), 6.29 (1 H, dd, *J* 17.0 and 10.0, C*H*=CH_2), 6.46 (1 H, dd, *J* 17.0 and 1.4, CH=CHH_{trans}), 7.42 (2 H, m, benzene ring), 7.83 (1 H, m, benzene ring), 7.93 (1 H, m, benzene ring), 8.20 (1 H, d, *J* 2.1, thiazole ring) and 8.89 (1 H, d, *J* 2.1, thiazole ring).

Attempted synthesis of N^1*-acryloyl-*N^1*-(2-thiazolyl)sulfanilamide* **69** *(Scheme 2).*— N^1-(2-Thiazolyl)sulfanilamide **68** (1.00 g, 3.92 mmol), acryloyl chloride (0.24 cm^3; 0.27 g, 2.95 mmol) and triethylamine (0.58 cm^3; 0.42 g, 4.16 mmol) in sodium-dried benzene (37 cm^3) were reacted in a similar manner to that of **67**. The solution was stirred at room temperature for 24 h. The usual work-up afforded a brown oil (80 mg). In addition, a benzene-insoluble orange-brown solid (1.30 g) was obtained when the reaction solution was filtered, prior to work up. ^{1}H NMR spectroscopy (250 MHz, C_5D_5N) revealed the solid to be a mixture of starting material **68** and $Et_3N^+Cl^-$. The spectrum of the oil (250 MHz, $CDCl_3$) was rather complex and 'noisy' but revealed little, if any, sign of the desired product **69**. A second attempt was made at the synthesis of **69** but failed. The above experimental procedure was repeated (at the same scale) with the exception that the reaction was heated (oil-bath) at 60 °C for 24 h. The usual work-up afforded, in the same way as before, a brown oil (60 mg) and a benzene-insoluble solid (1.52 g).

A note on the microanalytical treatment of the phosphonium salts **105** *and* **111** *(Scheme 7).* —These were prepared by the published method.[67] Both ^{1}H NMR spectroscopy and IR spectroscopy revealed these phosphonium salts were hydrated to varying degrees. In order to determine the degree of hydration for each sample the microanalytical results were treated thus: the percentages found for the elements C, H, Cl and P were added together and subtracted from 100%. This gave the percentage of oxygen in the sample. As the only source of oxygen came from absorbed water this corresponded to the percentage of oxygen due to hydration. If it is assumed that the formula for the hydrated phosphonium salt is $[C_aH_bClP]\cdot xH_2O$ then the degree of hydration *x* can readily be determined from the equation: $x = \%O\,MW/[1600 - (18.016\%O)]$, where *%O* is the experimentally determined percentage of oxygen, and *MW* is the molecular weight of the unhydrated salt

(corresponding to the formula, C_aH_bClP). This calculation assumed the sample was free of impurities.

Two different samples of vinylbenzyl chloride were used for the transformations shown in Scheme 7: a *m/p*-mixture **108** (Dow Chemicals; assay: 60% *meta*-isomer, 40% *para*-isomer), and the pure *p*-isomer **109** (Kodak). ^{1}H NMR spectroscopic data on each sample is as follows.—**108**: δ_H(250 MHz, $CDCl_3$) 4.62 (2 H, s, CH_2Cl, *m*- and *p*-isomers), 5.32 (1 H, d, *J* 10.9, CH=CHH_{cis}, *p*-isomer), 5.33 (1 H, d, *J* 10.9, CH=CHH_{cis}, *m*-isomer), 5.81 (1 H, d, *J* 17.6, CH=CHH_{trans}, *p*-isomer), 5.82 (1 H, d, *J* 17.6, CH=CHH_{trans}, *m*-isomer), 6.76 (1 H, dd, *J* 17.6 and 10.9, C*H*=CH_2, *m*- and *p*-isomers) and 7.3–7.6 (4 H, m, Ar–H, *m*- and *p*-isomers); **109**: δ_H(250 MHz, $CDCl_3$) 4.61 (2 H, s, CH_2Cl), 5.33 (1 H, dd, *J* 10.2 and 0.7, CH=CHH_{cis}), 5.82 (1 H, dd, *J* 17.6 and 0.7, CH=CHH_{trans}), 6.76 (1 H, dd, *J* 17.6 and 10.2, C*H*=CH_2), 7.38 (2 H, d, *J* 8.3, Ar–H) and 7.45 (2 H, d, *J* 8.3, Ar–H).

Triethyl-3(and 4)-(vinylbenzyl)phosphonium chloride **105a** *(Scheme 7).*—*m/p*-Vinylbenzyl chloride **108** (4.65 cm^3; 4.99 g, 32.7 mmol) was added drop-wise at room temperature to a stirred solution of triethylphosphine **110a** (27 cm^3 of a 1.0 mol dm^{-3} solution in THF; 3.19 g, 27.0 mmol). A nitrogen balloon was attached and the reaction flask covered with aluminium foil. The solution was stirred at room temperature for 3 d. The solution was then filtered and the precipitate washed with *n*-hexane. Recrystallization from *tert*-butyl alcohol, followed by *in vacuo* drying (T = 45 °C), afforded a white powder (3.69 g, 42%), triethyl-3(and 4)-(vinylbenzyl)phosphonium chloride **105a**, mp 160 °C (lit.,[67] 169–171 °C) (Found: C, 65.36; H, 8.27; Cl, 13.02; P, 11.45. $[C_{15}H_{24}ClP]\bullet 0.33H_2O$ requires C, 65.10; H, 8.98; Cl, 12.81; P, 11.19%); MIC = 1000 μg cm^{-3} (NAJ) and >1000 μg cm^{-3} (SOJ); ν_{max}/cm^{-1} (KBr) 3430s, 2962m, 2911s, 1591w, 1442m, 1408m, 1268m, 1047m, 906s, 860s, 817s and 766m; δ_H(250 MHz, $CDCl_3$) 1.17 (9 H, t, *J* 7.7, 3 x CH_3, *m*- or *p*-isomer), 1.25 (9 H, t, *J* 7.7, 3 x CH_3, *m*- or *p*-isomer), 2.23 (br s, abs. H_2O, exch.), 2.4–2.6 (6 H, m, 3 x C$H_2$$CH_3$, *m*- and *p*-isomers), 4.24 (2 H, d, $J_{H,P}$ 15.4, Ar–CH_2–P, *m*- and *p*-isomers), 5.28 (1 H, d, *J* 10.9, CH=CHH_{cis}, *m*- and *p*-isomers), 5.73 (1 H, d, *J* 17.7, CH=CHH_{trans}, *p*-isomer), 5.78 (1 H, d, *J* 17.5, CH=CHH_{trans}, *m*-isomer), 6.66 (1 H, dd, *J*

17.6 and 10.8, C*H*=CH_2, *m*- and *p*-isomers) and 7.2–7.5 (4 H, m, Ar–H, *m*- and *p*-isomers).

Tri-n-*butyl-3(and 4)-(vinylbenzyl)phosphonium chloride* **105b** *(Scheme 7).*—*m*/*p*-Vinylbenzyl chloride **108** (5.0 g, 32.7 mmol) and tri-*n*-butylphosphine **110b** (6.8 cm^3; 5.52 g, 27.3 mmol) in toluene (13 cm^3) were reacted in a similar manner to that of **105a**. The solution was filtered and the precipitate washed with toluene. Recrystallization from toluene afforded a white solid (5.90 g, 61%), tri-*n*-butyl-3(and 4)-(vinylbenzyl)phosphonium chloride **105b**, mp 136 °C (lit.,[67] 135–137 °C) (Found: C, 67.96; H, 10.05; Cl, 9.72; P, 8.20. $[C_{21}H_{36}ClP]\bullet 0.95H_2O$ requires C, 67.80; H, 10.27; Cl, 9.53; P, 8.33%); MIC = >1000 μg cm^{-3} (NAJ) and >1000 μg cm^{-3} (SOJ); ν_{max}/cm^{-1} (KBr) 3417s, 2958s, 2925s, 2871s, 1601w, 1458m, 1414m, 1097m, 993w, 912m, 812w and 719w; δ_H(250 MHz, $CDCl_3$) 0.90 (9 H, t, *J* 6.7, 3 x CH_3, *m*- and *p*-isomers), 1.44 [12 H, m, 3 x $CH_2(CH_2)_2CH_3$, *m*- and *p*-isomers], 2.26 (s, abs. H_2O, exch.), 2.40 [6 H, br m, 3 x $CH_2(CH_2)_2CH_3$, *m*- and *p*-isomers], 4.27 (2 H, d, $J_{H,P}$ 15.3, Ar–CH_2–P, *m*- and *p*-isomers), 5.29 (1 H, d, *J* 10.9, CH=CH_{cis}, *m*- and *p*-isomers), 5.74 (1 H, d, *J* 17.6, CH=CH_{trans}, *p*-isomer), 5.77 (1 H, d, *J* 17.5, CH=CH_{trans}, *m*-isomer), 6.67 (1 H, dd, *J* 17.6 and 10.9, C*H*=CH_2, *m*- and *p*-isomers) and 7.3–7.5 (4 H, m, Ar–H, *m*- and *p*-isomers).

Tri-n-*butyl-4-(vinylbenzyl)phosphonium chloride* **111b** *(Scheme 7).*—*p*-Vinylbenzyl chloride **109** (5.0 g, 32.7 mmol) and tri-*n*-butylphosphine **110b** (6.8 cm^3; 5.5 g, 27.3 mmol) in *n*-hexane (13 cm^3) were reacted in a similar manner to that of **105b**. Recrystallization from toluene afforded a white solid, tri-*n*-butyl-4-(vinylbenzyl)phosphonium chloride **111b**, mp 123 °C (Found: C, 64.56; H, 9.62; Cl, 9.61; P, 8.40. $[C_{21}H_{36}ClP]\bullet 1.9H_2O$ requires C, 64.82; H, 10.31; Cl, 9.11; P, 7.96%); MIC = >1000 μg cm^{-3} (NAJ); ν_{max}/cm^{-1} (KBr) 3414s, 1632w, 1465s, 1414s, 1106s, 990m, 913s, 862s and 744m; δ_H(250 MHz, $CDCl_3$) 0.88 (9 H, br t, *J* 6.5, 3 x CH_3), 1.42 [12 H, m, 3 x $CH_2(CH_2)_2CH_3$], 2.35 [6 H, br m, 3 x $CH_2(CH_2)_2CH_3$], ~2.35 (overlapped former peak, abs. H_2O, exch.), 4.27 (2 H, d, $J_{H,P}$ 15.4, Ar–CH_2–P), 5.26 (1 H, d, *J* 10.9, CH=CH_{cis}), 5.72 (1 H, d, *J* 17.5, CH=CH_{trans}), 6.65 (1 H, dd, *J* 17.5 and 10.9, C*H*=CH_2), 7.34 (2 H, d, *J* 8.4, Ar–H) and 7.39 (2 H, d, *J* 8.4, Ar–H).

Tri-n-*octyl-3(and 4)-(vinylbenzyl)phosphonium chloride* **105c** *(Scheme 7).*—*m*/*p*-Vinylbenzyl chloride **108** (5.0 g, 32.7 mmol) and tri-*n*-octylphosphine **110c** (12.2 cm^3; 10.1 g, 27.3 mmol) in *n*-hexane (13 cm^3) were reacted in a similar manner to that of **105b**. The crude product was triturated with *n*-hexane to afford a colourless gum, tri-*n*-octyl-3(and 4)-(vinylbenzyl)phosphonium chloride **105c**; MIC = 62.5 μg cm^{-3} (NAJ); ν_{max}/cm^{-1} (nujol) 1404w, 1251w, 1166m, 1013m, 911m, 851m and 800m; δ_H (250 MHz, $CDCl_3$) 0.85 (9 H, t, *J* 6.5, 3 x CH_3, *m*- and *p*-isomers), 1.0–1.9 [36 H, m, 3 x $CH_2(CH_2)_6CH_3$, *m*- and *p*-isomers], 2.37 [6 H, br m, 3 x $CH_2(CH_2)_6CH_3$, *m*- and *p*-isomers], ~3.0 (br s, abs. H_2O, exch.), ~4.25 (2 H, d, $J_{H,P}$ ~15.2, Ar–CH_2–P, *m*-isomer), 4.26 (2 H, d, $J_{H,P}$ 15.2, Ar–CH_2–P, *p*-isomer), ~5.28 (1 H, d, *J* ~10.7, CH=CH_{cis}, *p*-isomer), 5.29 (1 H, d, *J* 10.7, CH=CH_{cis}, *m*-isomer), 5.74 (1 H, d, *J* 16.8, CH=CH_{trans}, *p*-isomer), 5.78 (1 H, d, *J* 17.6, CH=CH_{trans}, *m*-isomer), 6.66 (1 H, dd, *J* 17.9 and 11.0, C*H*=CH_2, *m*- and *p*-isomers) and 7.2–7.5 (4 H, m, Ar–H, *m*- and *p*-isomers).

Tri-n-*octyl-4-(vinylbenzyl)phosphonium chloride* **111c** *(Scheme 7).*—*p*-Vinylbenzyl chloride **109** (5.0 g, 32.7 mmol) and tri-*n*-octylphosphine **110c** (12.2 cm^3; 10.1 g, 27.3 mmol) in *n*-hexane (13 cm^3) were reacted in a similar manner to that of **105b**. The crude product was triturated with *n*-hexane to afford a colourless gum, tri-*n*-octyl-4-(vinylbenzyl)phosphonium chloride **111c**; ν_{max}/cm^{-1} (nujol) 3294s, 1506w, 1404w, 1106w, 1038w, 979w, 898m and 855m; δ_H (250 MHz, $CDCl_3$) 0.85 (9 H, t, *J* 6.3, 3 x CH_3), 1.0–1.8 [36 H, m, 3 x $CH_2(CH_2)_6CH_3$], 2.37 [6 H, br m, 3 x $CH_2(CH_2)_6CH_3$], 4.27 (2 H, d, $J_{H,P}$ 15.4, Ar–CH_2–P), 5.27 (1 H, d, *J* 10.9, CH=CH_{cis}), 5.74 (1 H, d, *J* 17.6, CH=CH_{trans}), 6.66 (1 H, dd, *J* 17.6 and 10.9, C*H*=CH_2) and 7.34 (4 H, s, Ar–H).

Triphenyl-3(and 4)-(vinylbenzyl)phosphonium chloride **105d** *(Scheme 7).*—*m*/*p*-Vinylbenzyl chloride **108** (5.0 g, 32.7 mmol) and triphenylphosphine **110d** (7.15 g, 27.3 mmol) in toluene (13 cm^3) were reacted in a similar manner to that of **105b** to afford a white solid (2.74 g, 24%), triphenyl-3(and 4)-(vinylbenzyl)phosphonium chloride **105d**, mp 252 °C (lit.,[67] 256 °C) (Found: C, 78.01; H, 6.08; Cl, 8.53; P, 7.54. $[C_{27}H_{24}ClP]\bullet 0.0H_2O$ requires C, 78.16; H, 5.83; Cl, 8.54; P, 7.47%); MIC = >1000 [31.25] μg cm^{-3} (NAJ) and >1000 μg cm^{-3} (SOJ); ν_{max}/cm^{-1} (KBr) 3397s, 3054m, 2991m, 2861s, 2785m, 1592m, 1482s,

1443s (P–Ph), 1192s, 1113s, 1000s, 904m, 818m, 749s and 692s; δ_H (250 MHz, $CDCl_3$) 2.04 (s, abs. H_2O, exch.), 5.10 (1 H, d, *J* 11.0, CH=CHH_{cis}, *m*-isomer), 5.22 (1 H, d, *J* 10.8, CH=CHH_{cis}, *p*-isomer), 5.40 (1 H, d, *J* 17.4, CH=CHH_{trans}, *m*-isomer), 5.47 (2 H, d, $J_{H,P}$ 14.5, Ar–CH_2–P, *m*- and *p*-isomers), 5.66 (1 H, d, *J* 17.5, CH=CHH_{trans}, *p*-isomer), 6.43 (1 H, dd, *J* 17.4 and 11.0, C*H*=CH_2, *m*-isomer), 6.59 (1 H, dd, *J* 17.5 and 10.8, C*H*=CH_2, *p*-isomer) and 6.9–7.9 (19 H, m, Ar–H, *m*- and *p*-isomers).

Triphenyl-4-(vinylbenzyl)phosphonium chloride **111d** *(Scheme 7).*—*p*-Vinylbenzyl chloride **109** (5.0 g, 32.7 mmol) and triphenylphosphine **110d** (7.15 g, 27.3 mmol) in toluene (13 cm^3) were reacted in a similar manner to that of **105b** to afford a white solid (2.35 g, 21%), triphenyl-4-(vinylbenzyl)phosphonium chloride **111d**, mp 160 °C (Found: C, 74.46; H, 5.37; Cl, 9.36; P, 6.40. $[C_{27}H_{24}ClP]\bullet 1.2H_2O$ requires C, 74.28; H, 6.09; Cl, 8.12; P, 7.09%); MIC = >1000 [62.5] μg cm^{-3} (NAJ); ν_{max}/cm^{-1} (KBr) 3362w, 3055m, 3000m, 2902s, 2800s, 1651m, 1523s, 1447s (P–Ph), 1115s, 979s, 936s, 847s, 732s and 677s; δ_H (250 MHz, $CDCl_3$) 2.21 (s, abs. H_2O, exch.), 5.21 (1 H, d, *J* 10.9, CH=CHH_{cis}), 5.44 (2 H, d, $J_{H,P}$ 14.7, Ar–CH_2–P), 5.65 (1 H, d, *J* 17.6, CH=CHH_{trans}), 6.58 (1 H, dd, *J* 17.6 and 10.9, C*H*=CH_2), 6.9–8.0 (19 H, m, Ar–H).

1-(4-Vinylbenzyl)-3-carbmethoxypyridinium chloride **148a** *(Scheme 13).*—*p*-Vinylbenzyl chloride **109** (3.0 cm^3; 3.2 g, 21.1 mmol) and methyl nicotinate **146a** (549 mg, 4.0 mmol) were stirred at 70 °C for 21 h in a sealed, round-bottomed flask. Diethyl ether (20 cm^3) was added and the resultant precipitate filtered and washed repeatedly with diethyl ether to afford a pink solid (862 mg, 74%), 1-(4-vinylbenzyl)-3-carbmethoxypyridinium chloride **148a**, mp 135–137 °C (Found: C, 66.11; H, 5.41; Cl, 12.40; N, 4.72. $C_{16}H_{16}ClNO_2$ requires C, 66.32; H, 5.57; Cl, 12.24; N, 4.83%); MIC = 1000 μg cm^{-3} (NAJ) and >1000 μg cm^{-3} (MOJ); λ_{max} (ethanol)/nm 204 and 253; ν_{max} (KBr)/cm^{-1} 3445w, 3046m, 2951m, 1729s (C=O), 1639m, 1438m, 1298s, 1158s, 927m, 745m and 605w; δ_H (250 MHz, $CDCl_3$) 2.55 (s, abs. H_2O, exch., integration corresponded to ~ $[C_{16}H_{16}ClNO_2]\bullet 0.4H_2O$), 3.98 (3 H, s, CH_3), 5.29 (1 H, d, *J* 10.9, CH=CHH_{cis}), 5.73 (1 H, d, *J* 17.6, CH=CHH_{trans}), 6.53 (2 H, s, NCH_2), 6.64 (1 H, dd, *J* 17.6 and 10.9, C*H*=CH_2), 7.36 [2 H, d, *J* 8.1, Ar(vbz)–H], 7.68 [2 H, d, *J* 8.1, Ar(vbz)–H], 8.24 [1 H, t, *J* 7.1, Ar(py)–(5)],

8.83 [1 H, d, *J* 8.0, Ar(py)–H(4)], 9.74 [1 H, s, Ar(py)–H(2)] and 10.35 [1 H, d, *J* 5.8, Ar(py)–H(6)].

1-(4-Vinylbenzyl)-4-carbmethoxypyridinium chloride **149a** *(Scheme 13).*—*p*-Vinylbenzyl chloride **109** (3.0 cm^3; 3.2 g, 21.1 mmol) and methyl isonicotinate **147a** (550 mg, 4.0 mmol) were reacted, and the product worked up, in a similar manner to that of **148a** to afford a yellow solid (710 mg, 61%), 1-(4-vinylbenzyl)-4-carbmethoxypyridinium chloride **149a**, mp 142 °C (Found: C, 64.46; H, 6.06; Cl, 12.02; N, 4.55. $C_{16}H_{16}ClNO_2$ requires C, 66.32; H, 5.57; Cl, 12.24; N, 4.83%); MIC = >1000 μg cm^{-3} (NAJ) and >1000 μg cm^{-3} (MOJ); λ_{max} (ethanol)/nm 206 and 253; ν_{max} (KBr)/cm^{-1} 3410s, 3027m, 2974m, 1733s (C=O), 1642m, 1467m, 1297s, 1120m, 802m and 687m; δ_H (250 MHz, $CDCl_3$) 2.78 (s, abs. H_2O, exch., integration corresponded to ~ $[C_{16}H_{16}ClNO_2]\bullet 0.7H_2O$), 3.96 (3 H, s, CH_3), 5.25 (1 H, d, *J* 10.9, CH=CHH_{cis}), 5.69 (1 H, d, *J* 17.6, CH=CHH_{trans}), 6.48 (2 H, s, NCH_2), 6.59 (1 H, dd, *J* 17.6 and 10.9, C*H*=CH_2), 7.31 [2 H, d, *J* 8.2, Ar(vbz)–H], 7.71 [2 H, d, *J* 8.2, Ar(vbz)–H], 8.35 [2 H, d, *J* 6.7, Ar(py)–(3,5)] and 10.00 [2 H, d, *J* 6.7, Ar(py)–H(2,6)].

1-(4-Vinylbenzyl)-3-carbethoxypyridinium chloride **148b** *(Scheme 13).*—*p*-Vinylbenzyl chloride **109** (3.0 cm^3; 3.2 g, 21.1 mmol) and ethyl nicotinate **146b** (0.55 cm^3; 609 mg, 4.0 mmol) were reacted, and the product worked up, in a similar manner to that of **148a** to afford an orange-brown solid (874 mg, 72%), 1-(4-vinylbenzyl)-3-carbethoxypyridinium chloride **148b**, mp 46–48 °C (Found: C, 64.98; H, 6.76; Cl, 13.41; N, 3.27. $C_{17}H_{18}ClNO_2$ requires C, 67.21; H, 5.97; Cl, 11.67; N, 4.61%); MIC = 1000 μg cm^{-3} (NAJ) and 1000 μg cm^{-3} (MOJ); λ_{max} (ethanol)/nm 206 and 254; ν_{max} (melt)/cm^{-1} 3385s, 3006s, 1739s (C=O), 1633m, 1473m, 1297s, 1174s, 914m, 749m and 692w; δ_H (250 MHz, $CDCl_3$) 1.40 (3 H, t, *J* 7.1, CH_3) 2.66 (s, abs. H_2O, exch., integration corresponded to ~ $[C_{17}H_{18}ClNO_2]\bullet 1.1H_2O$), 4.43 (2 H, q, *J* 7.1, OCH_2), 5.29 (1 H, d, *J* 10.9, CH=CHH_{cis}), 5.73 (1 H, d, *J* 17.6, CH=CHH_{trans}), 6.46 (2 H, s, NCH_2), 6.64 (1 H, dd, *J* 17.6 and 10.9, C*H*=CH_2), 7.37 [2 H, d, *J* 8.2, Ar(vbz)–H], 7.66 [2 H, d, *J* 8.2, Ar(vbz)–H], 8.27 [1 H, t, *J* 7.1, Ar(py)–(5)], 8.81 [1 H, d, *J* 8.1, Ar(py)–H(4)], 9.61 [1 H, s, Ar(py)–H(2)] and 10.27 [1 H, d, *J* 6.1, Ar(py)–H(6)].

1-(4-Vinylbenzyl)-4-carbethoxypyridinium chloride **149b** *(Scheme 13).*—*p*-Vinylbenzyl chloride **109** (3.0 cm^3; 3.2 g, 21.1 mmol) and ethyl isonicotinate **147b** (600 mg, 4.0 mmol) were reacted, and the product worked up, in a similar manner to that of **148a** to afford a yellow solid (1.12 g, 93%), 1-(4-vinylbenzyl)-4-carbethoxypyridinium chloride **149b**, mp 73–78 °C (Found: C, 65.90; H, 6.70; Cl, 12.60.; N, 3.99. $C_{17}H_{18}ClNO_2$ requires C, 67.21; H, 5.97; Cl, 11.67; N, 4.61%); MIC = >1000 μg cm^{-3} (NAJ) and >1000 μg cm^{-3} (MOJ); λ_{max} (ethanol)/nm 206 and 253; ν_{max} (KBr)/cm^{-1} 3406s, 3026m, 2975m, 1729s (C=O), 1642m, 1466m, 1286s, 1118s, 1005m, 756m and 688m; δ_H (250 MHz, $CDCl_3$) 1.35 (3 H, t, *J* 7.1, CH_3), 2.98 (s, abs. H_2O, exch., integration corresponded to ~ $[C_{17}H_{18}ClNO_2]$• $0.7H_2O$), 4.39 (2 H, q, *J* 7.1, OCH_2), 5.22 (1 H, d, *J* 10.9, CH=CHH_{cis}), 5.66 (1 H, d, *J* 17.6, CH=CHH_{trans}), 6.46 (2 H, s, NCH_2), 6.56 (1 H, dd, *J* 17.6 and 10.9, C*H*=CH_2), 7.28 [2 H, d, *J* 8.1, Ar(vbz)–H], 7.73 [2 H, d, *J* 8.1, Ar(vbz)–H], 8.35 [2 H, d, *J* 6.5, Ar(py)–(3,5)] and 10.07 [2 H, d, *J* 6.5, Ar(py)–H(2,6)].

*1-(4-Vinylbenzyl)-3-(carb-*n*-propoxy)pyridinium chloride* **148c** *(Scheme 13).*—*p*-Vinylbenzyl chloride **109** (5.6 cm^3; 6.0 g, 39.4 mmol) and *n*-propyl nicotinate **146c** (1.65 g, 10.0 mmol) were reacted, and the product worked up, in a similar manner to that of **148a** to afford a brown gum (3.15 g, 99%), 1-(4-vinylbenzyl)-3-(carb-*n*-propoxy)pyridinium chloride **148c** (Found: C, 62.69; H, 6.53; Cl, 12.84; N, 3.89. $C_{18}H_{20}ClNO_2$ requires C, 68.03; H, 6.34; Cl, 11.16; N, 4.41%); MIC = >1000 [125] μg cm^{-3} (NAJ) and 1000 μg cm^{-3} (MOJ); λ_{max} (ethanol)/nm 205 and 254; ν_{max} (film)/cm^{-1} 3385s, 2970m, 1733s (C=O), 1636m, 1470m, 1295s, 1169s, 915m, 749m and 693w; δ_H (250 MHz, $CDCl_3$) 0.98 (3 H, t, *J* 7.4, CH_3), 1.79 (2 H, sx, *J* 7.1, CH_2CH_3), 3.37 (br s, abs. H_2O, exch., integration corresponded to ~ $[C_{18}H_{20}ClNO_2]$•$0.5H_2O$), 4.31 (2 H, t, *J* 6.8, OCH_2), 5.28 (1 H, d, *J* 10.9, CH=CHH_{cis}), 5.73 (1 H, d, *J* 17.6, CH=CHH_{trans}), 6.54 (2 H, s, NCH_2), 6.64 (1 H, dd, *J* 17.6 and 10.9, C*H*=CH_2), 7.36 [2 H, d, *J* 8.0, Ar(vbz)–H], 7.73 [2 H, d, *J* 8.0, Ar(vbz)–H], 8.33 [1 H, t, *J* 7.0, Ar(py)–(5)], 8.83 [1 H, d, *J* 8.0, Ar(py)–H(4)], 9.80 [1 H, s, Ar(py)–H(2)] and 10.31 [1 H, d, *J* 5.7, Ar(py)–H(6)].

*1-(4-Vinylbenzyl)-4-(carb-*n*-propoxy)pyridinium chloride* **149c** *(Scheme 13).*—*p*-Vinylbenzyl chloride **109** (5.6 cm^3; 6.0 g, 39.4 mmol) and *n*-propyl isonicotinate **147c** (1.65 g,

10.0 mmol) were reacted, and the product worked up, in a similar manner to that of **148a** to afford a flesh solid (2.52 g, 79%), 1-(4-vinylbenzyl)-4-(carb-*n*-propoxy)pyridinium chloride **149c**, mp 129–131 °C (Found: C, 66.72; H, 6.62; Cl, 12.00; N, 3.81. $C_{18}H_{20}ClNO_2$ requires C, 68.03; H, 6.34; Cl, 11.16; N, 4.41%); MIC = >1000 [125] μg cm^{-3} (NAJ) and 1000 μg cm^{-3} (MOJ); λ_{max} (ethanol)/nm 206 and 254; ν_{max} (KBr)/cm^{-1} 3424s, 2968m, 2926m, 1733s (C=O), 1639m, 1462m, 1288s, 1120m, 801w, 756w and 688w.; δ_H (250 MHz, $CDCl_3$) 0.98 (3 H, t, *J* 7.4, CH_3), 1.77 (2 H, sx, *J* 7.1, CH_2CH_3), 2.53 (br s, abs. H_2O, exch., integration corresponded to ~ $[C_{18}H_{20}ClNO_2]\bullet 0.6H_2O$), 4.32 (2 H, t, *J* 6.7, OCH_2), 5.26 (1 H, d, *J* 10.9, CH=CHH_{cis}), 5.70 (1 H, d, *J* 17.6, CH=CHH_{trans}), 6.51 (2 H, s, NCH_2), 6.60 (1 H, dd, *J* 17.6 and 10.9, C*H*=CH_2), 7.32 [2 H, d, *J* 8.1, Ar(vbz)–H], 7.73 [2 H, d, *J* 8.1, Ar(vbz)–H], 8.36 [2 H, d, *J* 6.5, Ar(py)–(3,5)] and 10.07 [2 H, d, *J* 6.5, Ar(py)–H(2,6)].

1-(4-Vinylbenzyl)-3-(carb-iso-*propoxy)pyridinium chloride* **148d** *(Scheme 13).*—*p*-Vinylbenzyl chloride **109** (7.1 cm^3; 7.6 g, 50.0 mmol) and *iso*-propyl nicotinate **146d** (1.65 g, 10.0 mmol) were reacted, and the product worked up, in a similar manner to that of **148a** to afford a brown glass (3.66 g, ~100%), 1-(4-vinylbenzyl)-3-(carb-*iso*-propoxy)pyridinium chloride **148d** (Found: C, 64.56; H, 6.02; Cl, 15.55; N, 3.02. $C_{18}H_{20}ClNO_2$ requires C, 68.03; H, 6.34; Cl, 11.16; N, 4.41%.). MIC = 1000 μg cm^{-3} (NAJ) and 1000 μg cm^{-3} (MOJ); λ_{max} (ethanol)/nm 206 and 254; ν_{max} (melt)/cm^{-1} 3405s, 2984m, 1729s (C=O), 1636m, 1469m, 1297s, 1171s, 1103s, 926m and 750w; δ_H (250 MHz, $CDCl_3$) 1.38 (6 H, d, *J* 6.3, 2 x CH_3), 2.76 (br s, abs. H_2O, exch., integration corresponded to ~ $[C_{18}H_{20}ClNO_2]\bullet 0.5H_2O$), 5.26 (1 H, sp, *J* 6.2, OCH), 5.29 (1 H, d, *J* 10.8, CH=CHH_{cis}), 5.74 (1 H, d, *J* 17.6, CH=CHH_{trans}), 6.48 (2 H, s, NCH_2), 6.64 (1 H, dd, *J* 17.5 and 11.0, C*H*=CH_2), 7.38 [2 H, d, *J* 8.1, Ar(vbz)–H], 7.66 [2 H, d, *J* 8.1, Ar(vbz)–H], 8.27 [1 H, t, *J* 7.0, Ar(py)–(5)], 8.81 [1 H, d, *J* 8.0, Ar(py)–H(4)], 9.57 [1 H, s, Ar(py)–H(2)] and 10.37 [1 H, d, *J* 6.0, Ar(py)–H(6)].

1-(4-Vinylbenzyl)-4-(carb-iso-*propoxy)pyridinium chloride* **149d** *(Scheme 13).*—*p*-Vinylbenzyl chloride **109** (5.6 cm^3; 6.0 g, 39.4 mmol) and *iso*-propyl isonicotinate **147d** (1.65 g, 10.0 mmol) were reacted, and the product worked up, in a similar manner to that of **148a**

to afford a yellow solid (3.35 g, ~100%), 1-(4-vinylbenzyl)-4-(carb-*iso*-propoxy)pyridinium chloride **149d**, mp 117–125 °C (Found: C, 66.66; H, 6.37; Cl, 12.12; N, 3.74. $C_{18}H_{20}ClNO_2$ requires C, 68.03; H, 6.34; Cl, 11.16; N, 4.41%); MIC = >1000 [125] μg cm^{-3} (NAJ) and 1000 μg cm^{-3} (MOJ); λ_{max} (ethanol)/nm 206 and 253; ν_{max} (KBr)/cm^{-1} 3433s, 3029m, 2979m, 1728s (C=O), 1642m, 1468m, 1292s, 1105m, 916m, 825m and 687m; δ_H (250 MHz, $CDCl_3$) 1.33 (6 H, d, *J* 6.2, 2 x CH_3), 2.97 (s, abs. H_2O, exch., integration corresponded to ~ $[C_{18}H_{20}ClNO_2]\bullet 1.0H_2O$), 5.21 (1 H, sp, *J* 6.2, OCH), 5.22 (1 H, d, *J* 10.9, CH=CHH_{cis}), 5.66 (1 H, d, *J* 17.6, CH=CHH_{trans}), 6.44 (2 H, s, NCH_2), 6.56 (1 H, dd, *J* 17.6 and 10.9, C*H*=CH_2), 7.28 [2 H, d, *J* 8.1, Ar(vbz)–H], 7.70 [2 H, d, *J* 8.1, Ar(vbz)–H], 8.34 [2 H, d, *J* 6.6, Ar(py)–(3,5)] and 10.00 [2 H, d, *J* 6.6, Ar(py)–H(2,6)].

1-(4-Vinylbenzyl)-3-(carb-n-*pentoxy)pyridinium chloride* **148e** *(Scheme 13).*—*p*-Vinylbenzyl chloride **109** (3.0 cm^3; 3.2 g, 21.1 mmol) and *n*-pentyl nicotinate **146e** (0.75 cm^3; 766 mg, 4.0 mmol) were reacted, and the product worked up, in a similar manner to that of **148a** to afford a sandy solid (817 mg, 60%), 1-(4-vinylbenzyl)-3-(carb-*n*-pentoxy)-pyridinium chloride **148e**, mp 93–97 °C (Found: C, 65.77; H, 7.13; Cl, 9.92; N, 3.60. $C_{20}H_{24}ClNO_2$ requires C, 69.45; H, 6.99; Cl, 10.25; N, 4.05%); MIC = 500 μg cm^{-3} (NAJ) and 1000 μg cm^{-3} (MOJ); λ_{max} (ethanol)/nm 205 and 253; ν_{max} (KBr)/cm^{-1} 3386s, 3023s, 2930m, 1729s (C=O), 1631m, 1465m, 1392m, 1308s, 1125m, 927m, 750m and 695m; δ_H (250 MHz, $CDCl_3$) 0.90 (3 H, s, CH_3), 1.34 [4 H, s, (CH_2)$_2CH_3$], 1.76 (2 H, s, OCH_2CH_2), ~2.5 (s, abs. H_2O, integration corresponded to ~ $[C_{20}H_{24}ClNO_2]\bullet 1.3H_2O$), 4.36 (2 H, t, *J* 6.1, OCH_2), 5.30 (1 H, d, *J* 10.7, CH=CHH_{cis}), 5.74 (1 H, d, *J* 17.3, CH=CHH_{trans}), 6.45 (2 H, s, NCH_2), 6.65 (1 H, dd, *J* 17.4 and 11.0, C*H*=CH_2), 7.39 [2 H, d, *J* 7.1, Ar(vbz)–H], 7.64 [2 H, d, *J* 7.4, Ar(vbz)–H], 8.29 [1 H, s, Ar(py)–(5)], 8.81 [1 H, d, *J* 7.1, Ar(py)–H(4)], 9.46 [1 H, s, Ar(py)–H(2)] and 10.35 [1 H, s, Ar(py)–H(6)].

1-(4-Vinylbenzyl)-3-(carb-sec-*pentoxy)pyridinium chloride* **148f** *(Scheme 13).*—*p*-Vinylbenzyl chloride **109** (3.0 cm^3; 3.2 g, 21.1 mmol) and *sec*-pentyl nicotinate **146f** (0.77 g, 4.0 mmol) were reacted, and the product worked up, in a similar manner to that of **148a** to afford a red-brown gum (1.51 g, ~100%), 1-(4-vinylbenzyl)-3-(carb-*sec*-pentoxy)pyrid-

inium chloride **148f** (Found: C, 64.87; H, 7.51; Cl, 11.58; N, 3.34. $C_{20}H_{24}ClNO_2$ requires C, 69.45; H, 6.99; Cl, 10.25; N, 4.05%); MIC = 1000 μg cm^{-3} (NAJ) and 1000 μg cm^{-3} (MOJ); λ_{max} (ethanol)/nm 207 and 254; ν_{max} (film)/cm^{-1} 3385s, 2959s, 1729s (C=O), 1633m, 1468m, 1295s, 1169s, 913m, 750m and 679w; δ_H (250 MHz, $CDCl_3$) 0.90 (3 H, t, *J* 7.3, CH_2CH_3), 1.34 (5 H, d, *J* 6.3, $CHCH_3$ + CH_2CH_3), 1.5–1.9 (2 H, m, $CHCH_2$), 2.74 (br s, abs. H_2O, exch., integration corresponded to ~ $[C_{20}H_{24}ClNO_2]\bullet 1.2H_2O$), 5.16 (1 H, sx, *J* 6.3, OCH), 5.29 (1 H, d, *J* 10.9, $CH{=}CH_{cis}$), 5.74 (1 H, d, *J* 17.6, $CH{=}CH_{trans}$), 6.43 (2 H, s, NCH_2), 6.65 (1 H, dd, *J* 17.6 and 10.9, $CH{=}CH_2$), 7.39 [2 H, d, *J* 8.1, Ar(vbz)–H], 7.64 [2 H, d, *J* 8.1, Ar(vbz)–H], 8.31 [1 H, t, *J* 7.0, Ar(py)–(5)], 8.81 [1 H, d, *J* 7.9 Ar(py)–H(4)], 9.44 [1 H, s, Ar(py)–H(2)] and 10.33 [1 H, d, *J* 5.7, Ar(py)–H(6)].

*1-(4-Vinylbenzyl)-3-(carb-*n*-octoxy)pyridinium chloride* **148g** *(Scheme 13).*—*p*-Vinylbenzyl chloride **109** (3.0 cm^3; 3.2 g, 21.1 mmol) and *n*-octyl nicotinate **146g** (0.95 cm^3; 938 mg, 4.0 mmol) were reacted, and the product worked up, in a similar manner to that of **148a** to afford an off-white solid (1.06 g, 69%), 1-(4-vinylbenzyl)-3-(carb-*n*-octoxy)pyridinium chloride **148g**, mp 60 (softened)–100 (decomp.) °C (Found: C, 68.50; H, 8.09; Cl, 8.89; N, 3.31. $C_{23}H_{30}ClNO_2$ requires C, 71.21; H, 7.79; Cl, 9.14; N, 3.61%); MIC = 62.5 μg cm^{-3} (NAJ) and >1000 μg cm^{-3} (MOJ); λ_{max} (ethanol)/nm 205 and 253; ν_{max} (KBr)/cm^{-1} 3439s, 3031m, 2932s, 1726s (C=O), 1630m, 1466m, 1309s, 1117m, 910m, 751m and 694m; δ_H (250 MHz, $CDCl_3$) 0.87 (3 H, t, *J* 6.4, CH_3), 1.26 [10 H, m, $(CH_2)_5CH_3$], 1.76 (2 H, qn, *J* 6.9, OCH_2CH_2), 2.46 (s, abs. H_2O, exch., integration corresponded to ~ $[C_{23}H_{30}ClNO_2]\bullet 1.4H_2O$), 4.36 (2 H, t, *J* 6.8, OCH_2), 5.30 (1 H, d, *J* 10.9, $CH{=}CH_{cis}$), 5.75 (1 H, d, *J* 17.6, $CH{=}CH_{trans}$), 6.45 (2 H, s, NCH_2), 6.66 (1 H, dd, *J* 17.6 and 10.9, $CH{=}CH_2$), 7.39 [2 H, d, *J* 8.0, Ar(vbz)–H], 7.65 [2 H, d, *J* 8.0, Ar(vbz)–H], 8.30 [1 H, t, *J* 6.8, Ar(py)–(5)], 8.81 [1 H, d, *J* 7.6, Ar(py)–H(4)], 9.46 [1 H, s, Ar(py)–H(2)] and 10.36 [1 H, d, *J* 5.2, Ar(py)–H(6)].

*1-(4-Vinylbenzyl)-4-(carb-*n*-octoxy)pyridinium chloride* **149g** *(Scheme 13).*—*p*-Vinylbenzyl chloride **109** (3.5 cm^3; 3.8 g, 24.6 mmol) and *n*-octyl isonicotinate **147g** (1.45 g, 6.16 mmol) were reacted, and the product worked up, in a similar manner to that of **148a** to

afford a yellow solid (1.64 g, 68%), 1-(4-vinylbenzyl)-4-(carb-*n*-octoxy)pyridinium chloride **149g**, mp 79 (softened)–87 (melt) °C (Found: C, 66.14; H, 7.79; Cl, 9.61; N, 3.31. $C_{23}H_{30}ClNO_2$ requires C, 71.21; H, 7.79; Cl, 9.14; N, 3.61%); MIC = 62.5 μg cm^{-3} (NAJ) and 250 μg cm^{-3} (MOJ); λ_{max} (ethanol)/nm 208 and 253; ν_{max} (KBr)/cm^{-1} 3417s, 3027m, 2925s, 1729s (C=O), 1641m, 1466m, 1287s, 1120s, 912m, 805m and 687m; δ_H (250 MHz, $CDCl_3$) 0.86 (3 H, t, *J* 6.6, CH_3), 1.26 [10 H, m, $(CH_2)_5CH_3$], 1.73 (2 H, qn, *J* 6.8, OCH_2CH_2), 2.53 (s, abs. H_2O, exch., integration corresponded to ~ $[C_{23}H_{30}ClNO_2]$• $0.4H_2O$), 4.35 (2 H, t, *J* 6.7, OCH_2), 5.26 (1 H, d, *J* 10.9, CH=CHH_{cis}), 5.69 (1 H, d, *J* 17.6, CH=CHH_{trans}), 6.52 (2 H, s, NCH_2), 6.60 (1 H, dd, *J* 17.6 and 10.9, C*H*=CH_2), 7.31 [2 H, d, *J* 8.0, Ar(vbz)–H], 7.72 [2 H, d, *J* 8.0, Ar(vbz)–H], 8.35 [2 H, d, *J* 6.2, Ar(py)–(3,5)] and 10.07 [2 H, d, *J* 6.2, Ar(py)–H(2,6)].

1-(4-Vinylbenzyl)-3-(carb-n-*nonoxy)pyridinium chloride* **148h** *(Scheme 13).*—*p*-Vinylbenzyl chloride **109** (3.0 cm^3; 3.2 g, 21.1 mmol) and *n*-nonyl nicotinate **146h** (1.0 cm^3; 985 mg, 4.0 mmol) were reacted, and the product worked up, in a similar manner to that of **148a** to afford a cream solid (1.05 g, 66%), 1-(4-vinylbenzyl)-3-(carb-*n*-nonoxy)pyridinium chloride **148h**, mp 111–112 °C (Found: C, 71.15; H, 7.33; Cl, 9.20; N, 3.04. $C_{24}H_{32}ClNO_2$ requires C, 71.71; H, 8.02; Cl, 8.82; N, 3.48%); MIC = 62.5 μg cm^{-3} (NAJ); ν_{max} (KBr)/cm^{-1} 3471w, 3043m, 2922s, 1747s (C=O), 1630m, 1475m, 1297s, 1114m, 904m, 747m and 690m; δ_H (250 MHz, $CDCl_3$) 0.87 (3 H, t, *J* 6.5, CH_3), 1.26 [12 H, m, $(CH_2)_6CH_3$], 1.75 (2 H, qn, *J* 6.9, OCH_2CH_2), 2.48 (s, abs. H_2O, exch., integration corres-ponded to ~ $[C_{24}H_{32}ClNO_2]$•$1.3H_2O$), 4.36 (2 H, t, *J* 6.9, OCH_2), 5.30 (1 H, d, *J* 10.9, CH=CHH_{cis}), 5.75 (1 H, d, *J* 17.6, CH=CHH_{trans}), 6.45 (2 H, s, NCH_2), 6.65 (1 H, dd, *J* 17.6 and 10.9, C*H*=CH_2), 7.39 [2 H, d, *J* 8.1, Ar(vbz)–H], 7.65 [2 H, d, *J* 8.2, Ar(vbz)–H], 8.30 [1 H, t, *J* 7.0, Ar(py)–(5)], 8.81 [1 H, d, *J* 8.0, Ar(py)–H(4)], 9.46 [1 H, s, Ar(py)–H(2)] and 10.36 [1 H, d, *J* 5.9, Ar(py)–H(6)].

1-(4-Vinylbenzyl)-3-(carb-n-*dodecoxy)pyridinium chloride* **148i** *(Scheme 13).*—*p*-Vinylbenzyl chloride **109** (3.0 cm^3; 3.2 g, 21.1 mmol) and *n*-dodecyl nicotinate **146i** (1.16 g, 4.0 mmol) were reacted, and the product worked up, in a similar manner to that of **148a** to afford a cream solid (1.28 g, 72%), 1-(4-vinylbenzyl)-3-(carb-*n*-dodecoxy)pyridinium

chloride **148i**, mp 55 °C (Found: C, 69.95; H, 9.43; Cl, 8.01; N, 3.08. $C_{27}H_{38}ClNO_2$ requires C, 73.03; H, 8.63; Cl, 7.98; N, 3.15%); MIC = 62.5 μg cm^{-3} (NAJ) and 500 μg cm^{-3} (MOJ); λ_{max} (ethanol)/nm 206 and 253; ν_{max} (KBr)/cm^{-1} 3435m, 3043m, 2921s, 1746s (C=O), 1630m, 1475m, 1297s, 1115m, 903m, 747m and 690m; δ_H (250 MHz, $CDCl_3$) 0.87 (3 H, t, *J* 6.6, CH_3), 1.25 [18 H, m, $(CH_2)_9CH_3$], 1.76 (2 H, qn, *J* 6.7, OCH_2CH_2), 2.23 (s, abs. H_2O, exch., integration corresponded to ~ $[C_{27}H_{38}ClNO_2]$•1.6H_2O), 4.37 (2 H, t, *J* 6.8, OCH_2), 5.31 (1 H, dd, *J* 10.9 and 0.5, CH=CHH_{cis}), 5.76 (1 H, dd, *J* 17.6 and 0.5, CH=CHH_{trans}), 6.46 (2 H, s, NCH_2), 6.67 (1 H, dd, *J* 17.6 and 10.9, C*H*=CH_2), 7.41 [2 H, d, *J* 8.1, Ar(vbz)–H], 7.65 [2 H, d, *J* 8.2, Ar(vbz)–H], 8.29 [1 H, t, *J* 7.0, Ar(py)–(5)], 8.82 [1 H, d, *J* 8.0, Ar(py)–H(4)], 9.43 [1 H, s, Ar(py)–H(2)] and 10.42 [1 H, d, *J* 5.7, Ar(py)–H(6)].

1-(4-Vinylbenzyl)-4-(carb-n-*dodecoxy)pyridinium chloride* **149i** *(Scheme 13).*—*p*-Vinylbenzyl chloride **109** (3.5 cm^3; 3.8 g, 24.6 mmol) and *n*-dodecyl isonicotinate **147i** (1.79 g, 6.14 mmol) were reacted, and the product worked up, in a similar manner to that of **148a** to afford a cream solid (570 mg, 21%), 1-(4-vinylbenzyl)-4-(carb-*n*-dodecoxy)pyridinium chloride **149i**, mp 123 °C (Found: Cl, 7.79. $C_{27}H_{38}ClNO_2$ requires Cl, 7.98%; results for C, H, N analysis would not duplicate); MIC = 62.5 μg cm^{-3} (NAJ) and 500 μg cm^{-3} (MOJ); λ_{max} (ethanol)/nm 206 and 253; ν_{max} (KBr)/cm^{-1} 3408s, 3029m, 2917s, 1733s (C=O), 1642w, 1468m, 1292s, 1124m, 805m, 755m and 688m; δ_H (250 MHz, $CDCl_3$) 0.87 (3 H, t, *J* 6.6, CH_3), 1.25 [18 H, m, $(CH_2)_9CH_3$], 1.75 (2 H, qn, *J* 7.0, OCH_2CH_2), 2.08 (s, abs. H_2O, exch., integration corresponded to ~ $[C_{27}H_{38}ClNO_2]$•0.8H_2O), 4.37 (2 H, t, *J* 6.7, OCH_2), 5.29 (1 H, d, *J* 10.9, CH=CHH_{cis}), 5.72 (1 H, d, *J* 17.6, CH=CHH_{trans}), 6.54 (2 H, s, NCH_2), 6.63 (1 H, dd, *J* 17.6 and 10.9, C*H*=CH_2), 7.35 [2 H, d, *J* 8.2, Ar(vbz)–H], 7.70 [2 H, d, *J* 8.2, Ar(vbz)–H], 8.37 [2 H, d, *J* 6.6, Ar(py)–(3,5)] and 10.01 [2 H, d, *J* 6.6, Ar(py)–H(2,6)].

The sample of *m/p*-vinylbenzyl chloride **108** used for the transformation shown in Scheme 15 was purchased from Aldrich and consisted of a mixture of 70% *meta*-isomer and 30% *para*-isomer. The ^{1}H NMR spectrum of **108** was similar to that of the spectrum of *m/p*-vinylbenzyl chloride (60% *meta*-, 40% *para*-isomer) obtained from Dow Chemicals. The

exception was that in the Aldrich spectrum the signals due to the *meta*-isomer were more prominent.

*1-[3(and 4)-Vinylbenzyl]-3-(carb-*n*-octoxy)pyridinium chloride* **151** *(Scheme 15).*— *m/p*-Vinylbenzyl chloride **108** (10.0 cm^3; 10.7 g, 70.4 mmol) and *n*-octyl nicotinate **146g** (prepared as in Scheme 13; 4.00 g, 17.0 mmol) were stirred, neat, at 66 °C (oil bath) for 18 h. The solution was allowed to cool and diethyl ether (40 cm^3) added – a gummy material formed. Repeated trituration with diethyl ether afforded a flesh, 'glassy' gum (4.15 g, 63%), 1-[3(and 4)-vinylbenzyl]-3-(carb-*n*-octoxy)pyridinium chloride **151**. Repeated attempts were made to reconstitute the gum **151** into a powdery solid but these met with failure (Found: C, 66.92; H, 6.07; Cl, 18.20; N, 1.13. $C_{23}H_{30}ClNO_2$ requires C, 71.21; H, 7.79; Cl, 9.14; N, 3.61%); MIC data N/A; ν_{max} (film)/cm^{-1} 3439s, 3018s, 2926s, 1731s (C=O), 1633m, 1471m, 1304s, 1171m, 910m and 743m; δ_H (250 MHz, $CDCl_3$) 0.85 (3 H, t, *J* 6.6, CH_3, *m*- and *p*-isomers), 1.24 [10 H, m, $(CH_2)_5CH_3$, *m*- and *p*-isomers], 1.72 (2 H, qn, *J* 6.8, OCH_2CH_2, *m*- and *p*-isomers), 3.25 (s, abs. H_2O, exch., integration corresponded to ~ $[C_{23}H_{30}ClNO_2]\bullet 1.5H_2O$), 4.31 (2 H, t, *J* 6.8, OCH_2, *m*- and *p*-isomers), 5.25 (1 H, d, *J* 11.0, CH=CH_{cis}, *m*-isomer), 5.26 (1 H, d, *J* 11.0, CH=CH_{cis}, *p*-isomer), 5.71 (1 H, d, *J* 18.1, CH=CH_{trans}, *p*-isomer), 5.78 (1 H, d, *J* 17.7, CH=CH_{trans}, *m*-isomer), 6.39 (2 H, s, NCH_2, *m*- and *p*-isomers), 6.61 (1 H, dd, *J* 17.5 and 10.9, C*H*=CH_2, *p*-isomer), 6.63 (1 H, dd, *J* 17.6 and 10.9, C*H*=CH_2, *m*-isomer), 7.2–7.8 (4 H, m, Ar–H, *m*- and *p*-isomers), 8.32 [1 H, t, *J* 6.9, Ar(py)–(5), *m*- and *p*-isomers], 8.78 [1 H, d, *J* 7.8, Ar(py)–H(4), *m*- and *p*-isomers], 9.47 [1 H, s, Ar(py)–H(2), *m*- and *p*-isomers] and 10.19 [1 H, d, *J* 5.2, Ar(py)–H(6), *m*- and *p*-isomers].

2.3.3 Polymerization and Co-polymerization of Vinyl Monomers

*Poly[tri-*n*-butyl-3(and 4)-(vinylbenzyl)phosphonium chloride]* **112b** *(Scheme 8).*—This was prepared by the published method.[67] Tri-*n*-butyl-3(and 4)-(vinylbenzyl)phosphonium chloride **105b** (500 mg, 1.4 mmol) and 2,2'-azobis(2-methylpropionamidine) dihydrochloride (9 mg) were dissolved in distilled water (5 cm^3; monomer concentration = 0.28 mol dm^{-3}, initiator concentration = 1.8 g dm^{-3}) in a *quik-fit* test-tube. The solution was then degassed using three freeze-pump-thaw cycles under high vacuum. The test-tube was

evacuated, sealed and heated at 60 °C (oil bath) for 5.5 h. The solvent was removed *in vacuo* to leave a colourless gum. Addition of diethyl ether produced a sticky, white residue. The ether was decanted and the residue dissolved in the minimum amount of methanol. The methanol solution was then pipetted into a beaker of cold diethyl ether, whilst stirring vigorously with a glass rod. The polymer was scraped off the glass rod and dried *in vacuo* (T = 55 °C) to afford a white solid (330 mg, 66%), poly[tri-*n*-butyl-3(and 4)-(vinylbenzyl)phosphonium chloride] **112b** (Found: C, 61.83; H, 9.33; Cl, 7.55; P, 7.38. $[C_{21}H_{36}ClP]_n$ requires C, 71.06; H, 10.22; Cl, 9.99; P, 8.73%); MIC = >1000 [125] μg cm^{-3} (NAJ); δ_H (250 MHz, CD_3OD) 0.94 (9 H, br s, 3 x CH_3), 1.47 [12 H, br s, 3 x $CH_2(CH_2)_2CH_3$], 2.20 [6 H, br s, 3 x $CH_2(CH_2)_2CH_3$], ~3.8 (2 H, v br s, Ar–CH_2–P), ~6.5 [br s, Ar–H] and 7.11 (br s, Ar–H).

*Poly[1-(4-vinylbenzyl)-3-(carb-*n*-octoxy)pyridinium chloride]* **150** *(Scheme 14).*—1-(4-Vinylbenzyl)-3-(carb-*n*-octoxy)pyridinium chloride **148g** (prepared as in Scheme 13; 499 mg, 1.29 mmol) and azobis-*iso*-butyronitrile (10.4 mg, 0.0633 mmol) were dissolved in tetrahydrofuran (3 cm^3; monomer concentration = 0.43 mol dm^{-3}, initiator concentration = 0.021 mol dm^{-3}) in a round-bottomed polymerization flask (50 cm^3) with magnetic stirrer bar. The solution was then degassed using five freeze-pump-thaw cycles under high vacuum. The flask was evacuated, sealed and the solution stirred at 60 °C (oil bath) for 18 h. The solvent was removed *in vacuo* to afford a brown gum (812 mg). The gum was dissolved in the minimum amount of tetrahydrofuran and pipetted into a beaker of diethyl ether, the latter cooled with an acetone–dry ice bath. The fine precipitate that formed was repeatedly triturated with diethyl ether. On exposure to the air, however, the precipitate reconstituted back into a gum. Agitation of the gum with a glass rod eventually afforded a tan powder (136 mg, 27% conversion), poly[1-(4-vinylbenzyl)-3-(carb-*n*-octoxy)pyridinium chloride] **150**, mp 127–135 °C (volume contraction occurred at ~100 °C) (Found: C, 63.60; H, 7.65; Cl, 4.63; N, 2.74. $[C_{23}H_{30}ClNO_2]_n$ requires C, 71.21; H, 7.79; Cl, 9.14; N, 3.61%); MIC = >1000 [31.25] μg cm^{-3} (NAJ) and >1000 μg cm^{-3} (MOJ); ν_{max} (KBr)/cm^{-1} 3420s, 2926s, 2855m, 1724s (C=O), 1638s, 1463m, 1387w, 1292s, 1170s, 1066w, 945w, 819w, 553w. The ^1H NMR spectrum (250 MHz, $CDCl_3$) consisted of a series of broad signals characteristic of those found in polymer spectra. Key spectral features were

as follows: δ 0.86 (CH_3), 1.27 [$(CH_2)_5CH_3$], 1.77 (OCH_2CH_2), 5.5–7.7 (v br, Ar–H), 8.05 (Ar–H) and 9.0–10.0 (ex br, Ar–H) ppm. Additional signals occurred at δ 2.05, 2.67 (v br), 3.29, 3.60, 4.23 and 4.36 ppm. The δ 4.23 or 4.36 ppm peak might be indicative of OCH_2. The peaks in the range δ 2.05–3.60 ppm are probably due to the methine and methylene protons of the polymer backbone.

*Attempted synthesis of poly{1-[3(and 4)-vinylbenzyl]-3-(carb-*n*-octoxy)pyridinium chloride}* **152** *(Scheme 15; Route ii).*—A solution of potassium persulfate (10.0 mg, 0.037 mmol) in deionized water (1 cm^3) was added to a solution of 1-[3(and 4)-vinylbenzyl]-3-(carb-*n*-octoxy)pyridinium chloride **151** (502 mg, 1.29 mmol) in deionized water (5 cm^3) (total solution volume 6 cm^3; monomer concentration = 0.22 mol dm^{-3}, initiator concentration = 0.0062 mol dm^{-3}) in a polymerization flask with magnetic stirrer bar. Upon addition of the persulfate the monomer solution turned milky white. Despite this observation the solution was degassed and stirred at 66 °C (oil bath) for 19 h. After the solvent was decanted it was discovered that a gel-like residue had stuck fast to the bottom of the polymerization flask. The gelatinous material was examined and found to be completely insoluble in a wide variety of common bench solvents (including water). A series of swelling tests were conducted: using a Pasteur pipette, solvent was dropped onto a dry sample of the gel material on a glass slide; swelling effects were then looked for using a microscope. The gel swelled in *N*,*N*-dimethylformamide, dimethylsulfoxide, ethanol, methanol and tetrahydrofuran (slight swelling), but did not swell in acetone, benzene, dichloromethane, diethyl ether, ethyl acetate, *n*-hexane, toluene and water. As a result of the above observations it was concluded that the gel was polymer **152** in the form of either a very high molecular weight species, or a cross-linked gel (Found: C, 66.96; H, 7.62; Cl, 7.38; N, 2.75. $[C_{23}H_{30}ClNO_2]_n$ requires C, 71.21; H, 7.79; Cl, 9.14; N, 3.61%).

*Poly{1-[3(and 4)-vinylbenzyl]-3-(carb-*n*-octoxy)pyridinium chloride}* **152** *(Scheme 15; Route iii).*—1-[3(and 4)-Vinylbenzyl]-3-(carb-*n*-octoxy)pyridinium chloride **151** (500 mg, 1.29 mmol) and azobis-*iso*-butyronitrile (10.0 mg, 0.061 mmol) were dissolved in tetrahydrofuran (4 cm^3; monomer concentration = 0.32 mol dm^{-3}, initiator concentration = 0.015 mol dm^{-3}) in a polymerization flask with magnetic stirrer bar. The solution was then

degassed and stirred at 78 °C (oil bath) for 20 h. The solvent was removed *in vacuo* to afford a viscous, brown oil (1.01 g). The oil was dissolved in dichloromethane (3 cm^3) and pipetted into a beaker of acetone (30 cm^3), the latter cooled with an acetone–dry ice bath. The liquid was decanted to leave a gum-like residue. Agitation of the gum with a glass rod eventually afforded a sandy powder (36 mg, 7% conversion), poly{1-[3(and 4)-vinylbenzyl]-3-(carb-*n*-octoxy)pyridinium chloride} **152**, mp >340 °C (Found: C, 63.81; H, 7.39; Cl, 5.22; N, 2.53. $[C_{23}H_{30}ClNO_2]_n$ requires C, 71.21; H, 7.79; Cl, 9.14; N, 3.61%); MIC data N/A; ν_{max}(KBr)/cm^{-1} 3427s, 2926s, 2855m, 1727s (C=O), 1638m, 1462m, 1393w, 1293s, 1168s, 1059w, 795w, 707w and 563w. The ^1H NMR spectrum (250 MHz, $CDCl_3$) consisted of a series of broad signals characteristic of those found in polymer spectra. Key spectral features were as follows: δ 0.87 (CH_3), 1.27 [$(CH_2)_5CH_3$], 1.78 (OCH_2CH_2), 5.8–6.5 (ex br, NCH_2), 6.5–7.8 (v br, Ar–H), 7.8–8.6 (v br, Ar–H), ~8.9 (br, Ar–H) and 9.0–10.5 (ex br, Ar–H) ppm. Additional signals occurred at δ (approx.) 1.9, 2.4, 3.3 (v br), 3.6, 4.2 and 4.35 ppm. The δ 4.2 or 4.35 ppm peak might be indicative of OCH_2. The peaks in the range δ 1.9–3.6 ppm are probably due to the methine and methylene protons of the polymer backbone.

Purification of 2-hydroxyethyl methacrylate co-monomer.—A literature purification method[45] was followed. 2-Hydroxyethyl methacrylate (50 cm^3; 54 g, 0.4 mol) was dissolved in water (200 cm^3) and washed with *n*-hexane (3 x 200 cm^3) [to remove dimethacrylate impurity]. The aqueous layer was then treated with aqueous sodium hydrogen carbonate solution (0.1 mol dm^{-3}, 100 cm^3) [to remove methacrylic acid] followed by saturated aqueous sodium chloride solution (50 cm^3). The monomer was extracted from the aqueous layer with diethyl ether (3 x 150 cm^3). The ether extracts were dried ($MgSO_4$), filtered and the ether removed *in vacuo*. The 2-hydroxyethyl methacrylate was distilled under reduced pressure (bp 56 °C/0.4 mbar) into an ice-cooled flask and stored in a refrigerator.

*General Procedure for the Co-polymerization of 1-[3(and 4)-Vinylbenzyl]-3-(carb-*n*-octoxy)pyridinium chloride* **151** *(Scheme 15)*.—1-[3(and 4)-Vinylbenzyl]-3-(carb-*n*-octoxy)-pyridinium chloride **151** (388 mg, 1.00 mmol), co-monomer (acrylamide, or 2-hydroxy-

ethyl methacrylate; 1.00 mmol, 1:1 molar ratio with **151**) and azobis-*iso*-butyronitrile (9.2 mg, 0.056 mmol) were dissolved in tetrahydrofuran [4 cm^3; monomer concentrations = 0.25 mol dm^{-3} (**151**), 0.25 mol dm^{-3} (co-monomer), initiator concentration = 0.014 mol dm^{-3}] in a polymerization flask with magnetic stirrer bar. The solution was then degassed and stirred at 64 °C (oil bath) for 19 h. The solvent was removed *in vacuo*, the residue weighed and then dissolved in the minimum amount of tetrahydrofuran. This solution was pipetted into a beaker of ice-cold water (~50 cm^3). The gum-like residue that formed was agitated with a glass rod till powdery in constitution.

Acrylamide Co-polymer **153***: Crude*—viscous, brown oil (1.0 g). *Purified*—tan powder (127 mg, 28% conversion) (Found: C, 63.47; H, 7.52; Cl, 4.33; N, 4.09%); MIC data N/A; ν_{max} (KBr)/cm^{-1} 3429s, 3209m (N–H), 2927s, 2855m, 1724s (ester C=O), 1666s (AAm C=O), 1453m, 1293s, 1170s, 801m, 706w and 566m. The ^{1}H NMR spectrum (250 MHz, $CDCl_3$) consisted of a series of broad signals characteristic of those found in polymer spectra. Key spectral features were as follows: δ 0.87 (CH_3), 1.27 [(CH_2)$_5CH_3$], 1.73 (OCH_2CH_2), 5.5–7.8 (v br, Ar–H), 7.8–8.6 (v br, Ar–H), ~8.8 (br, Ar–H) and 9.0–10.5 (ex br, Ar–H) ppm. Additional signals occurred at δ 1.56, 2.26, 2.49, 3.34, 3.63, 3.86, 4.22, 4.35 and 5.10 ppm. The δ 4.22 or 4.35 ppm peak might be indicative of OCH_2. The peaks in the range δ 1.56–3.86 ppm are probably due to the methine and methylene protons of the polymer backbone. The NH_2 protons could not be clearly identified in the spectrum. In theory, $RCONH_2$ can occur anywhere in the range δ 5–12 ppm.

2-Hydroxyethyl Methacrylate Co-polymer **154***: Crude*—brown oil (1.13 g). *Purified*—sandy-brown powder (41 mg, 8% conversion), mp 78 (softened)–110 (melt) °C (volume contraction occurred at ~60 °C) (Found: C, 63.86; H, 7.68; Cl, 3.38; N, 2.22 %); MIC data N/A; ν_{max} (KBr)/cm^{-1} 3372s, 2928s, 2855s, 1724s (C=O), 1663s, 1454s, 1292s, 1168s, 772w, 707w and 517m. The ^{1}H NMR spectrum (250 MHz, $CDCl_3$) consisted of a series of broad signals characteristic of those found in polymer spectra. Key spectral features were as follows: δ 0.88 (with sh, CH_3), 1.28 [(CH_2)$_5CH_3$], 1.73 (OCH_2CH_2 of C_8 chain), 5.6–7.8 (v br, Ar–H), 7.8–8.6 (v br, Ar–H), 8.6–9.0 (v br, Ar–H) and 9.0–10.0 (ex br, Ar–H) ppm. Additional signals occurred at δ 1.57, ~3.8, 4.13, 4.22,

4.36 and ~5.1 ppm. The δ 4.22 or 4.36 ppm peak might be indicative of OCH_2 (C_8 chain). The peaks in the range δ 1.57–4.13 ppm are probably due to the HEMA fragment, $(CH_2)_2$, and the methine and methylene protons of the polymer backbone.

2.3.4 Chemical Modification of Sulfonic Acid Resin Beads

Notes on experimental work concerning chemical modification of Amberlyst and Dowex resins with the aim of producing a 'polymeric Amical' resin:

Amberlyst and Dowex ion exchange resins.—Amberlyst 15 and Dowex 50-X8 are both strongly acidic cation exchange resins of the sulfonic acid type (SO_3^- H^+). Whereas the former is a 'rigid', non-swelling, macroreticular resin the latter is a 'soft', swellable, gel-type resin. The technical specifications on Amberlyst 15 and Dowex 50-X8 resins are summarized in Table 14. Both resins were conditioned before use according to a standard literature technique.[78] Although the Amberlyst 15 resin was supplied in the required ionic form it was conditioned still the same to ensure that all SO_3^- groups were in protonated form. The Dowex 50-X8 resin was supplied in the form of its sodium salt (SO_3^- Na^+) and therefore required conditioning to the sulfonic acid form. For experimental purposes both resin types were required in dry form.

Theoretical elemental microanalyses of the resins **138**, **139**, **141** and **142** *(Scheme 12).*—The general structure of Amberlyst and Dowex sulfonic acid resins can be represented as: $-[CH_2CH(C_6H_4SO_3H)]_\alpha-[CH_2CH(C_6H_5)]_{1-\alpha}-$. Note that this representation does not take into account benzene rings involved in cross-linking. The factor α determines the percentage of benzene rings that have sulfonic acid groups. Elemental microanalyses were carried out on individual dry samples of Amberlyst 15 and Dowex 50-X8 (H^+ form) resins. This allowed the factor α to be calculated for each resin type (refer to *Calculation of Degree of Sulfonation of Sulfonic Acid Resins* in section 3.3.5 for further details). The calculations were based on experimentally determined sulfur contents (%) [carbon and hydrogen (%) values are too unreliable, in general]. In addition to allowing α to be calculated, the sulfur percentage obtained from elemental microanalysis enabled a check to be made on the value of the exchange capacity of each resin. For the Amberlyst 15 resin %S = 13.90%, corresponding to an α value of 0.69 (*i.e.* 69% of the benzene rings

have sulfonic acid groups), and an exchange capacity of 4.3 meq g^{-1} (*c.f.* literature value of 4.3 meq g^{-1}). For the Dowex 50-X8 resin %S = 12.95%, corresponding to an α value of 0.62 (*i.e.* 62% of the benzene rings have sulfonic acid groups), and an exchange capacity of 4.0 meq g^{-1} (*c.f.* experimentally determined value of 3.9 meq g^{-1}). With α values calculated for each resin type this allowed the calculation of theoretical elemental microanalyses for the chemically modified resins **139**, **141** and **142**. These calculations were based on the functionalized fragment: $-[CH_2CH(C_6H_4X)]_\alpha-[CH_2CH(C_6H_5)]_{1-\alpha}-$ (*e.g.* **138**, X = SO_3H). The theoretical elemental microanalyses calculated for both the Amberlyst and Dowex versions of the resins **139**, **141** and **142** are presented below and summarized in Table 16. In addition, analyses have been calculated (for comparative purposes) for the mono- and tri-iodo analogues, respectively **142b** and **142c**, of the diiodomethyl-*p*-benzenesulfone resin **142a**. The theoretical %C and %H values (based on the experimental %S values) are also given for the Amberlyst 15 and Dowex 50-X8 sulfonic acid resins.

Amberlyst 15 sulfonic acid resin **138** (based on 13.90% S: requires C, 60.28; H, 5.07%); *Dowex 50-X8 sulfonic acid resin* **138** (based on 12.95% S: requires C, 62.48; H, 5.25%); p-*benzenesulfonyl chloride resin* **139** (Amberlyst version requires C, 55.82; H, 4.29; Cl, 14.21; S, 12.85%; Dowex version requires C, 58.15; H, 4.51; Cl, 13.30; S, 12.03%); p-*benzenesulfonylacetic acid resin* **141** (Amberlyst version requires C, 59.80; H, 5.03; S, 11.74%; Dowex version requires C, 61.70; H, 5.19; S, 11.05%); *diiodomethyl*-p-*benzenesulfone resin* **142a** (Amberlyst version requires C, 31.46; H, 2.44; I, 52.78; S, 6.67%; Dowex version requires C, 33.54; H, 2.62; I, 50.98; S, 6.44%); *monoiodomethyl*-p-*benzenesulfone resin* **142b** (Amberlyst version requires C, 42.62; H, 3.58; I, 35.75; S, 9.03%; Dowex version requires C, 44.89; H, 3.78; I, 34.12; S, 8.62%); *triiodomethyl*-p-*benzenesulfone resin* **142c** (Amberlyst version requires C, 24.93; H, 1.76; I, 62.75; S, 5.28%; Dowex version requires C, 26.77; H, 1.93; I, 61.03; S, 5.14%).

5% Aqueous hydrochloric acid solution (used as resin regenerating solution).—Concentrated hydrochloric acid (37%, sp gr 1.18; 67.5 cm^3) was made up to 500 cm^3 with deionized water in a half-litre measuring cylinder. This produced a 5% aqueous solution of hydrochloric acid corresponding to a molarity of: (5/100) x (1000/36.46) = 1.37 mol dm^{-3}.

Conditioning of Amberlyst 15 resin.—Dry Amberlyst 15 resin [BDH #55133] (dry exchange capacity 4.3 meq g^{-1}; 50 cm^3, 30.17 g, 129.7 meq) was transferred into a 500 x 25 mm ion exchange column fitted with a sintered-glass filter bed (porosity 1). To ensure efficient packing the resin bed was back-washed with tap water to about twice the bed volume (~100 cm^3). Excess water was run off to slightly above the top level of the bed and the column pre-washed with deionized water (2 x 50 cm^3). For strongly acidic cation exchange resins (like Amberlyst 15) it is recommended to use a volume of regenerating solution equivalent to four times the theoretical capacity of the resin bed. In the present case the volume of 5% aqueous hydrochloric acid (the recommended regenerant used) this corresponded to was 378 cm^3 (refer to *Sulfonic Acid Ion Exchange Resins – Technical Specifications and Conditioning* in section 3.3.5 for further details). As a result the resin bed was treated with a solution of 5% aqueous hydrochloric acid (380 cm^3) at an average flow rate of 0.07 bed volumes per minute (BV min^{-1}). The column was then thoroughly washed with deionized water (10 x 50 cm^3); the flow rate of the first wash was 0.07 BV min^{-1}, and all subsequent washes thereafter at 0.15 BV min^{-1}. The column was drained of water and remaining traces of water removed by washing the resin bed with acetone (5 x 50 cm^3) at a flow rate of 0.37 BV min^{-1}. After the column was drained of acetone the resin bed was briefly purged with a jet of compressed air. Finally, the conditioned Amberlyst 15 resin was transferred to a clean, dry powder round and dried *in vacuo* (~40 °C) for 24 h to yield opaque, 'cement' grey beads. The resin beads were stored over anhydrous calcium chloride in a desiccator (Found: C, 50.60; H, 5.82; S, 13.90%); plate assay: 0.5–1 mm inhibition zone; liquid assay: no growth; supernatant test: 10^3 cfu cm^{-3}; ν_{max}/cm^{-1} (KBr) 3412s, 2928m, 1648s, 1601m, 1493w, 1451w, 1412w, 1215s, 1169s, 1127s, 1035s, 1007s, 834m, 675s and 580s.

Conditioning of Dowex 50-X8 resin to sulfonic acid form ($SO_3^- H^+$).—'Wet' Dowex 50-X8 resin in the form of its sodium salt [BDH #55036] (wet exchange capacity 1.9 meq cm^{-3}; 50 cm^3, 42.2 g, 95 meq) was conditioned in a similar manner to that described previously for the Amberlyst 15 resin. The theoretical volume of regenerant solution required corresponded to 277 cm^3 of 5% aqueous hydrochloric acid. The actual volume used was 280 cm^3. The conditioned Dowex 50-X8 resin was dried and stored in the manner described for the Amberlyst 15 resin to yield 'glassy', red-brown beads (24.41 g). Quantitative

recovery enabled calculation of the resin's dry exchange capacity: (95 meq/24.41 g) = 3.9 meq g^{-1} (Found: C, 46.41; H, 5.63; S, 12.95%); plate assay: 1–2 mm inhibition zone; liquid assay: no growth; supernatant test: ≤ 10^2 cfu cm^{-3}; ν_{max}/cm^{-1} (KBr) 3450s, 2928m, 1710s, 1645s, 1600m, 1494w, 1450w, 1412m, 1221s, 1156s, 1127s, 1034s, 1005s, 833m, 673s and 579s.

General Procedure for the Synthesis of p-*Benzenesulfonyl chloride resins* **139**, *chemically modified from Amberlyst 15 or Dowex 50-X8 resins* **138** *(Scheme 12).*—Dry sulfonic acid resin **138** (21.5 meq) was gently refluxed with thionyl chloride (50 cm^3; 81.5 g, 685 mmol) for 5 h. Excess thionyl chloride was removed *in vacuo* and the beads swirled in calcium chloride-dried dichloromethane (5 x 10 cm^3). The beads were then dried (drying pistol) for 4 h and stored over anhydrous calcium chloride (desiccator).

Amberlyst 15 resin **139**: 'cement' grey beads (Found: C, 50.47; H, 4.59; Cl, 6.33; S, 13.91%); plate assay: 2 mm inhibition zone; liquid assay: no growth; supernatant test: ≤ 10^2 cfu cm^{-3}; ν_{max}/cm^{-1} (KBr) 3209s, 2930s, 1705s, 1645s, 1599m, 1484w, 1449w, 1410w, 1369m (SO_2), 1169s, 1130s, 1034m, 1004m, 835w, 674m and 580s.

Dowex 50-X8 resin **139**: 'black' (in reality very dark brown) beads (Found: C, 49.17; H, 4.44; Cl, 8.61; S, 14.81%); plate assay: 2–3 mm inhibition zone; liquid assay: no growth; supernatant test: ≤ 10^2 cfu cm^{-3}; ν_{max}/cm^{-1} (KBr) 3454s, 2929s, 1709s, 1644s, 1598m, 1493w, 1450w, 1413m, 1351m (SO_2), 1173s, 1126s, 1034s, 1005s, 917m, 834m, 673m and 581s.

General Procedure for the Synthesis of p-*Benzenesulfonylacetic acid resins* **141**, *chemically modified from Amberlyst 15 or Dowex 50-X8 resins* **139** *(Scheme 12; Route II).*—This procedure (and those detailed for routes III and IV, below) was adapted from a literature method[77] that detailed the conversion of low molecular weight sulfonyl chlorides into sulfonylacetic acids via an aqueous sulfite reductive route. A three-necked round-bottomed flask, fitted with condenser and thermometer, was charged with a solution of sodium sulfite (5.30 g, 42.0 mmol) in deionized water (13 cm^3). Dry resin **139** (18.2 meq) was added in one go and the flask contents heated (oil bath), unstirred, at 60 °C for 2 h. During the course of the reaction the solution pH was monitored and kept at

pH ~8 by the addition of 30% aqueous sodium hydroxide solution. The solution was then acidified with chloroacetic acid (1.99 g, 21.1 mmol) and heated, unstirred, for a further 3¼ h at 80–95 °C. The flask contents were cooled (ice–water) and acidified to pH ~1 with 37% aqueous hydrochloric acid. The solution was filtered and the beads collected and swirled in deionized water (10 x 25 cm^3) and acetone (5 x 25 cm^3) respectively. Finally, the resin beads were dried (drying pistol) for 3 h and stored over anhydrous calcium chloride (desiccator).

Amberlyst 15 resin **141** *(Route II):* light grey beads (Found: C, 47.28; H, 4.63; S, 13.32%); plate assay: no inhibition; liquid assay: complete growth; supernatant test: complete growth; ν_{max}/cm^{-1} (KBr) 3459s, 2928m, 1717m (C=O), 1637s, 1493w, 1450w, 1411w, 1307w (SO_2), 1187s, 1127s, 1038s, 1010s, 833m, 678s and 581s.

Attempted synthesis of Dowex 50-X8 resin **141** *(Route II):* brown beads (Found: C, 45.27; H, 4.35; S, 14.05%); plate assay: no inhibition; liquid assay: no growth; supernatant test: 4.0 x 10^4 cfu cm^{-3}; ν_{max}/cm^{-1} (KBr) 3463s, 2926m, 1637s, 1496w, 1450w, 1411w, 1186s, 1128s, 1039s, 1009s, 834m, 677s and 580s (*n.b.* near-identical to spectrum of Dowex 50-X8, $SO_3^- Na^+$ form).

General Procedure for the Synthesis of p-*Benzenesulfonylacetic acid resins* **141**, *chemically modified from Amberlyst 15 or Dowex 50-X8 resins* **139** *(Scheme 12; Route III).*— A three-necked round-bottomed flask, fitted with propeller stirrer and condenser, was charged with an organic phase of chloroacetic acid (1.16 g, 12.3 mmol) in dichloromethane (25 cm^3) and an aqueous phase of sodium sulfite (2.70 g, 21.4 mmol) and tetra-*n*-butylammonium chloride hydrate (300 mg, 1.1 mmol; 5.0 mol % w.r.t. Na_2SO_3) in deionized water (25 cm^3). Dry resin **139** (10.7 meq) was added in one go and the flask contents stirred with heating (oil bath) until the dichloromethane gently refluxed (~40 °C). The flask contents were stirred and refluxed for 6 h. During the course of the reaction the solution pH was monitored and kept at pH ~8 by the addition of 30% aqueous sodium hydroxide solution. The flask contents were cooled (ice–water) and acidified to pH ~2 with 37% aqueous hydrochloric acid. The solution was filtered and the beads collected and swirled in deionized water (10 x 10 cm^3) and

acetone (5 x 10 cm^3) respectively. Finally, the resin beads were dried (drying pistol) for 5 h and stored over anhydrous calcium chloride (desiccator).

- *Amberlyst 15 resin* **141** *(Route III):* light grey beads (Found: C, 48.86; H, 4.71; S, 11.41%); plate assay: no inhibition; liquid assay: ~10^4 cfu cm^{-3}; supernatant test: complete growth; ν_{max}/cm^{-1} (KBr) 3471s, 2929m, 1709w (C=O), 1638s, 1492w, 1450w, 1411w, 1361w (SO_2), 1184s, 1127s, 1038s, 1009s, 834m, 677s and 581s.

Dowex 50-X8 resin **141** *(Route III):* dark brown beads (Found: C, 51.16; H, 5.32; S, 12.90%); plate assay: possible inhibition no zone (*i.e.* direct contact inhibition); liquid assay: ~10^4–10^5 cfu cm^{-3}; supernatant test: 2.0 x 10^3 cfu cm^{-3}; ν_{max}/cm^{-1} (KBr) 3452s, 2927m, 1709w (C=O), 1638s, 1493w, 1451w, 1411w, 1350w (SO_2), 1179s, 1127s, 1038s, 1009s, 917w, 833w, 675s and 581s.

General Procedure for the Synthesis of p*-Benzenesulfonylacetic acid resins* **141**, *chemically modified from Amberlyst 15 or Dowex 50-X8 resins* **139** *(Scheme 12; Route IV).*— A three-necked round-bottomed flask, fitted with propeller stirrer and condenser, was charged with dichloromethane (20 cm^3) and an aqueous phase of sodium sulfite (2.50 g, 19.8 mmol) and tetra-*n*-butylammonium chloride hydrate (275 mg, 1.0 mmol; 5.0 mol % w.r.t. Na_2SO_3) in deionized water (30 cm^3). Dry resin **139** (9.9 meq) was added in one go and the flask contents stirred with heating (oil bath) until the dichloromethane gently refluxed (~40 °C). The flask contents were stirred and refluxed for 1 h. An organic phase of chloroacetic acid (1.07 g, 11.3 mmol) in dichloromethane (20 cm^3) was added and the flask contents stirred for a further 5 h at 40 °C. The flask contents were cooled (ice–water) and acidified to pH ~2 with 37% aqueous hydrochloric acid. The solution was filtered and the beads collected and swirled in deionized water (10 x 10 cm^3) and acetone (5 x 10 cm^3) respectively. Finally, the resin beads were dried (drying pistol) for 3 h and stored over anhydrous calcium chloride (desiccator).

Amberlyst 15 resin **141** *(Route IV):* light grey beads (Found: C, 48.85; H, 4.73; S, 13.10%); plate assay: no inhibition; liquid assay: ~10^4 cfu cm^{-3}; supernatant test: complete growth; ν_{max}/cm^{-1} (KBr) 3465s, 2926m, 1709w (C=O), 1638s, 1493w, 1451w, 1411w, 1363w (SO_2), 1184s, 1127s, 1038s, 1009s, 834m, 679s and 580s.

Dowex 50-X8 resin **141** *(Route IV):* dark brown beads (Found: C, 51.00; H, 5.18; S, 13.49%); plate assay: 1 mm inhibition zone; liquid assay: no growth; supernatant test: 1.0 x 10^1 cfu cm^{-3}; ν_{max}/cm^{-1} (KBr) 3449s, 2931m, 1635s, 1492w, 1451w, 1412w, 1351m (SO_2), 1177s, 1127s, 1037s, 1008s, 917w, 834w, 675s and 581s.

*General Procedure for the Attempted Synthesis of Diiodomethyl-*p*-benzenesulfone resins* **142a**, *chemically modified from Amberlyst 15 or Dowex 50-X8 resins* **141** *(Scheme 12; resins* **141** *from Routes II–IV).*— A three-necked round-bottomed flask, fitted with a propeller stirrer, was charged with an organic phase of iodine (9.34 g, 36.8 mmol) in dichloromethane (250 cm^3) and an aqueous phase of sodium hydroxide (6.42 g, 161 mmol) and tetra-*n*-butylammonium chloride hydrate (2.23 g, 8.0 mmol; 5.0 mol % w.r.t. NaOH) in deionized water (125 cm^3). The resin product isolated from the attempted synthesis of the resin **141** (9.2 meq) was added in one go and the flask contents stirred at r.t. for 22 h. The solution was filtered and the beads collected. The Amberlyst-derived resin beads were swirled in deionized water (5 x 20 cm^3) and acetone (10 x 20 cm^3) respectively, while the Dowex-derived resin beads were swirled in 50% aqueous methanol (5 x 20 cm^3) and acetone (5 x 20 cm^3) respectively. Finally, the resin beads were dried (drying pistol) for 4–5 h and stored over anhydrous calcium chloride (desiccator). It was anticipated that, despite the washes, the resin samples might still contain trapped or unreacted molecular iodine. As a result all resin bead samples were extracted in a Soxhlet as follows.

Soxhlet extraction of crude resins **142a**.—A sample of resin **142a** (~1–2 g) was transferred into a *Whatman* cellulose extraction thimble (25 x 80 mm) and the thimble plugged with a piece of glass wool. The Amberlyst-derived resin beads were extracted in a Soxhlet with acetone for 24 h, collected and swirled in acetone (5 x 10 cm^3). The Dowex-derived resin beads, on the other hand, were extracted in a Soxhlet with methanol for 24 h, collected and swirled in methanol (3 x 10 cm^3) and acetone (3 x 10 cm^3) respectively. In addition, the Dowex-derived resin **142a** from the homogeneous reduction route (Scheme 12; Method II) was extracted in a Soxhlet with acetone (24 h) prior to its methanol extraction. After extraction all resin beads samples were

dried (drying pistol) for 4–5 h and stored over anhydrous calcium chloride (desiccator).

Attempted synthesis of Amberlyst 15 resin **142a** *(originated from Route II): Unpurified*—tan beads (Found: C, 44.80; H, 4.43; I, 4.31; S, 12.76%); plate assay: no inhibition; liquid assay: no growth; supernatant test: complete growth. *Acetone Soxhlet extraction*—light tan beads (Found: C, 45.41; H, 3.99; I, 4.85; S, 9.60%); plate assay: no inhibition; liquid assay: no growth; supernatant test: complete growth; ν_{max}/cm^{-1} (KBr) 3475s, 2928m, 1634s, 1493w, 1450w, 1411w, 1368w, 1187s, 1127s, 1039s, 1010s, 834m, 677s and 580s (*n.b.* very similar to spectrum of Dowex 50-X8, $SO_3^- Na^+$ form).

Attempted synthesis of Amberlyst 15 resin **142a** *(originated from Route III): Unpurified*—flesh beads (Found: C, 46.38; H, 4.55; I, 1.09; S, 12.51%); plate assay: 2–3 mm inhibition zone; liquid assay: 2×10^2 cfu cm^{-3}; supernatant test: inhibitory growth (cell number N/A). *Acetone Soxhlet extraction*—flesh beads (Found: C, 45.77; H, 4.37; I, 0.53; S, 12.89%); plate assay: no inhibition; liquid assay: 2×10^2 cfu cm^{-3}; supernatant test: complete growth; ν_{max}/cm^{-1} (KBr) 3449s, 2926m, 1635s, 1494w, 1450w, 1411w, 1352w, 1187s, 1128s, 1040s, 1010s, 834m, 678s and 581s (*n.b.* very similar to spectrum of Dowex 50-X8, $SO_3^- Na^+$ form).

Attempted synthesis of Amberlyst 15 resin **142a** *(originated from Route IV): Unpurified*—flesh beads (Found: C, 45.51; H, 4.45; I, 0.85; S, 12.76%); plate assay: 3 mm inhibition zone; liquid assay: 2×10^2 cfu cm^{-3}; supernatant test: complete growth. *Acetone Soxhlet extraction*—flesh beads (Found: C, 45.77; H, 4.41; I, 0.81; S, 13.19%); plate assay: 3–4 mm inhibition zone; liquid assay: complete growth; supernatant test: complete growth; ν_{max}/cm^{-1} (KBr) 3436s, 2926m, 1637s, 1493w, 1450w, 1411w, 1353w, 1187s, 1127s, 1039s, 1010s, 834m, 679s and 580s (*n.b.* very similar to spectrum of Dowex 50-X8, $SO_3^- Na^+$ form).

Attempted synthesis of Dowex 50-X8 resin **142a** *(originated from Route II): Unpurified*—brown beads (Found: C, 44.48; H, 4.23; I, 7.91; S, 13.14%); plate assay: 3–4 mm inhibition zone; liquid assay: no growth; supernatant test: 2.9×10^2 cfu cm^{-3}. *Acetone Soxhlet extraction*—brown beads (Found: C, 44.50; H, 4.02; I, 8.15; S, 12.82%); plate assay: 3–4 mm inhibition zone; liquid assay: no growth; supernatant test: 9×10^1 cfu cm^{-3}. *Acetone then methanol Soxhlet extraction*—brown beads (Found: C, 44.99; H, 4.31;

I, 0.91; S, 13.35%); plate assay: no inhibition; liquid assay: complete growth; supernatant test: complete growth; ν_{max}/cm^{-1} (KBr) 3453s, 2926m, 1638s, 1494w, 1451w, 1411w, 1349w, 1187s, 1128s, 1039s, 1009s, 834m, 676s and 579s (*n.b.* near-identical to spectrum of Dowex 50-X8, $SO_3^- Na^+$ form).

Attempted synthesis of Dowex 50-X8 resin **142a** *(originated from Route III): Unpurified*—dark brown beads (Found: C, 48.01; H, 4.68; I, 0.81; S, 13.56%); plate assay: 5 mm inhibition zone; liquid assay: 2 x 10^2 cfu cm^{-3}; supernatant test: complete growth. *Methanol Soxhlet extraction*—dark brown beads (Found: C, 46.92; H, 4.58; I, 0.55; S, 13.65%); plate assay: no inhibition; liquid assay: complete growth; supernatant test: complete growth; ν_{max}/cm^{-1} (KBr) 3443s, 2927m, 1638s, 1494w, 1451w, 1411w, 1349w, 1187s, 1128s, 1039s, 1009s, 834m, 676s and 581s (*n.b.* near-identical to spectrum of Dowex 50-X8, $SO_3^- Na^+$ form).

Attempted synthesis of Dowex 50-X8 resin **142a** *(originated from Route IV): Unpurified*—dark brown beads (Found: C, 48.01; H, 4.81; I, 1.63; S, 13.10%); plate assay: no inhibition; liquid assay: complete growth; supernatant test: complete growth. *Methanol Soxhlet extraction*—dark brown beads (Found: C, 47.07; H, 4.57; I, 0.81; S, 13.90%); plate assay: no inhibition; liquid assay: complete growth; supernatant test: complete growth; ν_{max}/cm^{-1} (KBr) 3449s, 2924m, 1635s, 1495w, 1450w, 1411w, 1357w, 1187s, 1128s, 1039s, 1009s, 834m, 676s and 580s (*n.b.* near-identical to spectrum of Dowex 50-X8, $SO_3^- Na^+$ form).

2.4 *Testing for Antimicrobial Activity*

2.4.1 Minimum Inhibitory Concentration

Introduction

The *Minimum Inhibitory Concentration* (MIC) is the minimum concentration of a chemical compound required to either inhibit or completely kill microbial growth. If the compound is active against microbial growth then it is referred to as an *antimicrobial agent* (AMA). The more active, or potent, the AMA, then the smaller the MIC value. It is common practice to express the MIC value in micrograms per cubic centimeter ($\mu g\ cm^{-3}$). A common method used to test for antimicrobial activity is the *microtitre plate technique*.[46] A microtitre plate experiment is, typically, relatively straightforward to set up and carry out. The test has the added advantage in that it requires only a relatively small weight (~40 mg) of chemical sample. The result of the test allows a 'quick' assessment to be made of a the sample's potential as an antimicrobial agent.

AMA #1	A											
	B											
	C											
	D											
AMA #2	E											
	F											
	G											
	H											
		1	2	3	4	5	6	7	8	9	10	11	12
[AMA]		10^3	500	250	125	62.5	31.2	15.6	7.8	3.9	1.9	1	0

Fig. 20 Schematic representation of a microtitre plate of the type used to assess antimicrobial activity. The plate consists of ninety-six wells arranged in twelve columns (1–12) and eight rows (A–H). Commonly, two AMAs can be tested per plate. Every well contains the test medium in addition to the following combinations of AMA/inoculum: *white wells* – AMA + inoculum; *light-gray wells* – AMA only (no inoculum); *dark-grey wells* – inoculum only (no AMA); *hatched wells* – test medium only (no AMA and no inoculum). AMA concentrations are in $\mu g\ cm^{-3}$. Refer to the text for further details.

A typical microtitre plate consists of an array of ninety-six U-shaped wells. The eight rows are labelled A–H, and the columns numbered 1–12 (Figure 20). Samples of the compounds prepared in this thesis were tested as follows: A solution of known concentration was first prepared of the chemical agent (or AMA) in the test medium. Three different test media were used for these experiments: Norwegian apple juice (NAJ), Mills orange juice (MOJ) and Sainsbury's orange juice (SOJ). The solution of chemical agent was then pipetted into the wells in columns 1–11, making serial dilutions (1/2) from one well to the next (moving from left to right). In this way each well contained a different concentration of AMA. The wells were then inoculated with the test organism (a yeast strain, *Saccharomyces cerevisiae* EL1). The experiment was carried out in triplicate (rows A–C). The wells in row D contained only AMA (no inoculum), and those in column 12 contained only inoculum (no AMA). Row D and column 12 served as 'control' wells. Column 12 represented 'normal', uninhibited, microbial growth, while row D was used to test for any 'reactionary' effects (*e.g.* precipitation) between the AMA and the test medium. The plate was then covered and incubated at room temperature for 2 days. Set up in this way the microtitre plate could be used to test two different AMA samples. Alternatively, a single AMA sample could be tested in two different media. At the end of the incubation period the plate was examined for microbial (*i.e.* yeast) growth – no microbial growth in the wells indicated *total kill*, and partial growth indicated *inhibition* (retarded growth). The MIC value (in $\mu g\ cm^{-3}$) was read as the *lowest concentration of agent which showed no growth*. All MIC values quoted in this thesis were determined using the microtitre plate technique as described above.

Determination of the MIC Value

In the wells in columns 1–11, one of four observations can be made. These observations are illustrated by the hypothetical examples shown in Figures 21 and 22. For AMA #1 (Figure 21), microbial growth is observed in every test well (columns 1–11, rows A–C). This does not necessarily mean that the agent has no antimicrobial activity. Rather, the agent concentration is too low to determine antimicrobial activity and, as a result, the MIC value is recorded as $>1000\ \mu g\ cm^{-3}$. If required, the MIC test could be repeated with a higher starting concentration (*e.g.* $2000\ \mu g\ cm^{-3}$) of AMA in the first well. This would

enable the exact MIC value to be determined. For AMA #2 (Figure 21), no microbial growth is observed in any of the wells except those in the control, column 12 (inoculum, but no AMA). The agent, therefore, is extremely inhibitory and the MIC value is recorded as <1 μg cm^{-3}. In order to determine the exact MIC value the test could be repeated with a lower starting concentration (*e.g.* 1 μg cm^{-3}) of AMA in the first well.

A	A	++	++	++	++	++	++	++	++	++	++	++	++
M	B	++	++	++	++	++	++	++	++	++	++	++	++
A	C	++	++	++	++	++	++	++	++	++	++	++	++
#1	D	–	–	–	–	–	–	–	–	–	–	–	–
A	E	–	–	–	–	–	–	–	–	–	–	–	++
M	F	–	–	–	–	–	–	–	–	–	–	–	++
A	G	–	–	–	–	–	–	–	–	–	–	–	++
#2	H	–	–	–	–	–	–	–	–	–	–	–	–
		1	**2**	**3**	**4**	**5**	**6**	**7**	**8**	**9**	**10**	**11**	**12**
[AMA]		10^3	500	250	125	62.5	31.2	15.6	7.8	3.9	1.9	1	0

Fig. 21 Schematic representation of the appearance of a microtitre plate for two hypothetical AMAs. Normal (*i.e.* uninhibited) microbial growth is indicated by '++' and no microbial growth by '–'. The MIC values are recorded as >1000 μg cm^{-3} for AMA #1 and <1 μg cm^{-3} for AMA #2.

A	A	–	–	–	+	+	+	+	+	+	++	++	++
M	B	–	–	–	+	+	+	+	+	+	++	++	++
A	C	–	–	–	+	+	+	+	+	+	++	++	++
#3	D	–	–	–	–	–	–	–	–	–	–	–	–
A	E	+	+	+	+	+	+	++	++	++	++	++	++
M	F	+	+	+	+	+	+	++	++	++	++	++	++
A	G	+	+	+	+	+	+	++	++	++	++	++	++
#4	H	–	–	–	–	–	–	–	–	–	–	–	–
		1	**2**	**3**	**4**	**5**	**6**	**7**	**8**	**9**	**10**	**11**	**12**
[AMA]		10^3	500	250	125	62.5	31.2	15.6	7.8	3.9	1.9	1	0

Fig. 22 Schematic representation of the appearance of a microtitre plate for two hypothetical AMAs. Normal (*i.e.* uninhibited) microbial growth is indicated by '++', inhibited microbial growth by '+' and no microbial growth by '–'. The MIC values are recorded as 250 μg cm^{-3} for AMA #3 and >1000 [31.2] μg cm^{-3} for AMA #4.

In the case of AMA #3 (Figure 22), the concentration range 1–1000 μg cm^{-3} is sufficient to determine the MIC value (*c.f* AMAs #1 and #2, Figure 21). Column 4 is the last column in which microbial growth is observed. The MIC value is recorded as the concentration of agent in the column (with no microbial growth) to the left of column 4, *viz.* column 3. The MIC value is therefore 250 μg cm^{-3}. For AMA #4 (Figure 22), the agent has an inhibitory effect on microbial growth in columns 1–6. In columns 7–11, normal (*i.e.* uninhibited) microbial growth is observed compared to the control, column 12 (inoculum, but no AMA). This means that the microbial cells in columns 1–6 were not killed outright – rather, their growth was slowed down or inhibited. The MIC value is therefore recorded as >1000 μg cm^{-3} but with an inhibitory effect on microbial growth down to ~31.2 μg cm^{-3}. The MIC values quoted in this thesis indicate total kill of microbial growth. Inhibitory effects, if any, are indicated in square brackets, *e.g.* AMA #4, MIC = >1000 [31.25] μg cm^{-3}.

Experimental

Materials and equipment.—Test organism (*Saccharomyces cerevisiae* EL1, isolated from unpasteurized Norwegian apple juice), test medium [either Norwegian apple juice (NAJ), diluted 1:1 with water, Sainsbury's orange juice (SOJ), or Mills orange juice (MOJ)], test agent or AMA (40.0 mg), ethanol, quarter strength Ringer's solution tablets (BDH), sterile microtitre plates (96 U-well, with lid), sterile micro-pipette tips, plastic pipettes (10 cm^3), plastic petri dishes, plastic sample bottles, multi-sampler pipette (8-pronged, 100 μl), micro-pipettes (1000 μl, 100 μl).

Preparation of inoculum solution.—The inoculum solution was prepared twenty-four hours prior to the MIC test. The test organism used was *Saccharomyces cerevisiae* EL1, originally isolated from unpasteurized Norwegian apple juice. Growth medium (10 cm^3) was inoculated with either a solution of yeast culture (100 μl) or with one colony from a yeast plate. The seed was then incubated at 30 °C for 24 h. The seed solution, containing ~10^7 cells cm^{-3}, was then gently mixed and a sample (100 μl) diluted with quarter strength Ringer's solution (900 μl). Two further serial dilutions (1/10) with Ringer's solution were

performed to give a solution with ~10^4 cells cm^{-3}. Finally, a sample of this solution (100 μl) was added to the test medium (10 cm^3). This produced an inoculum solution with ~10^2 cells cm^{-3}.

Preparation of agent solution and loading of microtitre plate.—An accurately weighed sample of the chemical agent (40.0 mg) under test was dissolved in ethanol (2 cm^3) and a sample of the resultant solution (1 cm^3) added to the test medium (9 cm^3). This produced an approximate 0.2% w/v solution of the agent in the test medium. A sterile microtitre plate (96 U-well, with lid) consisting of twelve columns 1–12 and eight rows A–H (Figure 20) was used to perform the MIC test. Each agent was tested in triplicate in rows A–C, columns 1–11. Row D and column twelve acted as 'control' wells. Set up in this way the plate could be used to test two agents per plate (or, alternatively, one agent could be tested in two different media). A sample of the test medium (100 μl) was transferred to each well in rows A–D, columns 2–12. A sample of the 0.2% w/v test medium–agent solution (200 μl) was then added to each well in column 1, rows A–D. Serial dilutions (1/2) were then performed by transferring a sample of the test medium–agent solution (100 μl) from well A1 to well A2, and then from well A2 to well A3, *etc.*, until well A11 was reached. The final transfer was discarded. The final well, A12, therefore contained only test medium and no agent. The above procedure was repeated for rows B–D (a multi-sampler pipette enables the serial dilutions for rows A–D to be performed simultaneously). A sample of the inoculum solution (100 μl), containing 10^2 cells cm^{-3} of *Saccharomyces cervisiae* EL1, was then added to every well in rows A–C, columns 1–12. During this procedure the wells were filled from right to left, in order of increasing concentration. This ensured that the effect of any material accidentally carried over from one well to the next would minimize the resultant error in concentration. Finally, a sample of the test medium (100 μl) was added to each well in row D, columns 1–12. Row D therefore contained no inoculum and served as a control to ensure that any precipitate-like matter observed in the inoculated wells was not due to agent that had 'reacted' with the test medium (which, otherwise, could give rise to false readings when the plate is examined for effects on microbial growth). The above loading procedure therefore produced agent concentrations of 1000 μg cm^{-3} in column 1 down to 1 μg cm^{-3} in column 11 (Figure 20).

The wells in column 12 contained no agent (0 $\mu g\ cm^{-3}$) and served as controls in which normal, uninhibited, yeast growth could be monitored. The plate was then incubated at room temperature for 48 h. After this time, the plate was examined and the MIC value read as the lowest concentration of agent that showed no yeast growth. Microbial growth was indicated by the deposition of tiny yeast 'spores' in the bottom of the wells.

2.4.2 Plate/Liquid Assay Techniques for the Testing of Resin Beads

Introduction

Section 2.4.1 described the microtitre plate technique for the determination of MIC values of antimicrobial agents in solution. This section details two other methodologies commonly used to assess antimicrobial activity – the *plate assay* and *liquid assay* techniques. In addition, the *supernatant test* is also described. The latter is, experimentally, similar to the liquid assay technique and serves as a convenient test for AMA 'leaching' (or 'leakage') from surfaces onto which the agent is immobilized, chemically or physically (*e.g.* a polymeric bead).

Whereas MIC tests are commonly used for testing soluble chemical agents the plate/liquid assay techniques are particularly useful for assessing the antimicrobial activity of intrinsically insoluble materials. A key research area described in this thesis concerned synthetic work on diiodomethylsulfones. One of the aims of this work was to synthesize a polymeric version of a 'simple' diiodomethylsulfone in the form of polymeric resin beads. The plate/liquid assay methods proved useful techniques for assessing the antimicrobial activity of bead samples. It is with the testing of these beads in mind that the plate and liquid assay techniques are described.

Plate Assay Technique

The plate assay technique can be considered a 'dry' test as the chemical agent is present in the dry state, and not in solution (*c.f.* MIC testing), when tested.

In a typical plate assay experiment a malt extract agar (MEA) plate is inoculated with the test organism (*e.g.* a yeast strain) and the test samples (*e.g.* resin beads) placed onto the agar surface in the form of well-spaced, circular groups (Figure 23a). The plate is then incubated at 25 °C for two days after which time it is examined for

inhibitory effects. 'Normal', uninhibited microbial growth is represented by a 'lawn' of growth of the micro-organism (*e.g.* a 'lawn' of yeast). Active beads would inhibit microbial growth and, as a result, an *inhibition zone* free of microbial growth would be created around the test sample area. Active samples are measured by the thicknesses (in millimetres) of their inhibition zones. A test plate comprised of chemically unique samples will typically exhibit inhibition zones of varying thickness (Figure 23b).

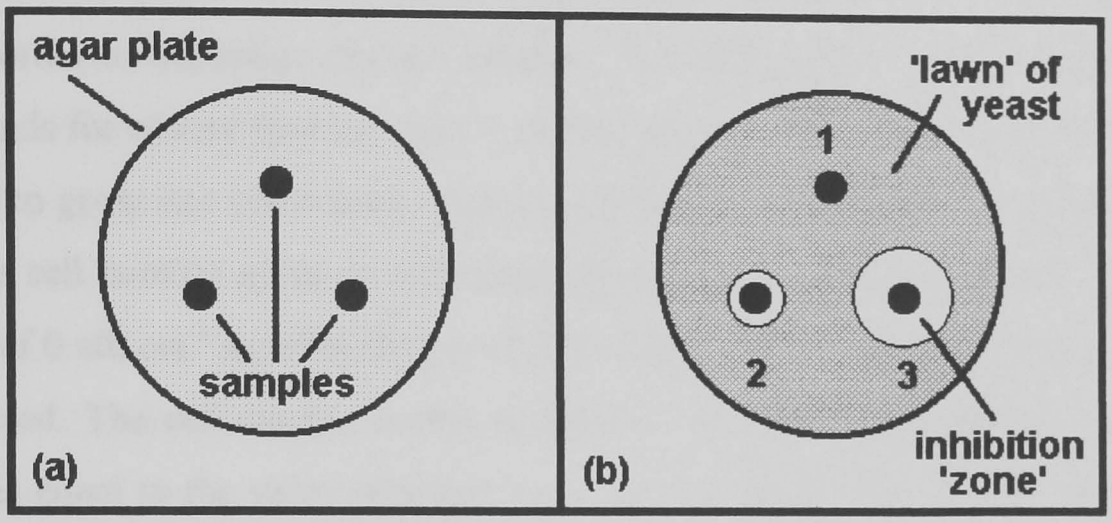

Fig. 23 Schematic representation of a hypothetical plate assay test performed on three chemically different resin bead samples. The samples are arranged on the surface of an agar plate previously inoculated with a yeast strain (a). After an incubation period the plate is examined for inhibitory effects (b). A 'lawn' of yeast has grown on the surface of the agar. Samples 2 and 3 show inhibitory effects with resultant 'zones' of inhibition around each sample (note that the zone is larger in the case of sample 3). Sample 1 shows no inhibitory effects.

Zones of inhibition around a sample indicate that the agent responsible for inhibiting microbial growth has 'leached' into the surrounding environment. In the case of resin beads, for example, this could mean that a chemical agent (formerly immobilized chemically onto the resin or physically incorporated into it) has diffused through the agar from the resin. If the agent is active then it will inhibit microbial growth around the area of the test sample – hence the production of an inhibition zone. In general, the larger the zone of inhibition the more active the test sample.

Liquid Assay Technique

The liquid assay technique is a 'wet' test since the chemical agent is present in the solution state when tested. The liquid assay (wet) and plate assay (dry) techniques therefore serve as complimentary tests for microbial growth.

In a typical liquid assay experiment the test medium (*e.g.* orange juice) is added to sterile vials containing the test samples. The samples are inoculated and incubated at 25 °C for one day. Samples of the test medium are then taken and plated out onto MEA plates. Viable count determinations are performed on each sample plate in order to determine the *cell number*. The cell number is in units of cfu cm^{-3}; 'cfu' stands for colony forming units – each single cell, when plated out onto agar, is assumed to grow into one colony, thus each colony is assumed to be formed from one cell. The cell number gives an indication of the extent of microbial growth. A cell number of 0 cfu cm^{-3} signifies that no microbial growth (*i.e.* total microbial kill) could be detected. The cell number corresponding to 'normal', *i.e.* uninhibited, microbial growth is equal to the value obtained for a 'control' plate. For example, in the anti-microbial tests carried out for this thesis a cell number on the order of $\sim 10^7$ cfu cm^{-3} was obtained for control plates. The cell number corresponding to inhibited microbial growth falls in the range between 0 and the 'control' value (*e.g.* $0 <$ cell number $< \sim 10^7$ cfu cm^{-3}).

A positive result (*i.e.* inhibition or total kill) observed in a liquid assay test can be explained in one of two ways: (i) the microbial cells have come into direct contact with the test material or surface (*e.g.* antimicrobial resin beads – the cells would diffuse into the bead, come into contact with the antimicrobially active part of the bead, there be killed, and diffuse out of the bead), or (ii) an antimicrobially active chemical agent has 'leached' from the test material/surface and passed into solution where it can proceed to kill cells. A positive liquid assay result cannot therefore, in general, be unambiguously interpreted. If, however, the liquid assay test is used in conjunction with other tests for antimicrobial activity (*e.g.* the plate assay and super-natant tests) then the ambiguity may be removed or at least partly explained.

Supernatant Test

The supernatant test is similar in experimental method to the liquid assay technique and provides a simple way to test for the 'leakage' of antimicrobially active agents from a test surface or material.

In a typical supernatant experiment the test medium is added to sterile vials containing test samples. The samples are incubated (*sans* inolculum) at 25 °C for one day. The test medium is removed from the samples and transferred to fresh vials which are, in turn, inoculated and incubated at 25 °C for two days. Samples are then plated out onto MEA plates and viable count determinations performed as described for the liquid assay technique.

Unlike a liquid assay test, a positive result obtained from a supernatant test is near conclusive evidence that an antimicrobial substance has 'leached' off the test surface/material into the surrounding liquid environment. 'Leaching' would have had to occur during the initial incubation period. The 'leached' substance would therefore be present in solution throughout the second incubation period. Since the samples used in the second incubation are inoculated the end result is the inhibition of microbial growth.

Presentation of Results of Antimicrobial Tests

The results of substances tested using the above-described antimicrobial techniques are presented in the analytical parts of the *Syntheses* section (see 2.3). The results are indicated in the following format: *plate assay:* result; *liquid assay:* result; *supernatant test:* result. For example, a typical entry might be: 'plate assay: 3–4 mm inhibition zone; liquid assay: no growth; supernatant test: 2.9×10^2 cfu cm^{-3}.' The results are formatted as described below.

Plate assay results.—Active samples have the inhibition zone thickness (in mm) indicated; the term *no inhibition* indicates samples that failed to display inhibition zones.

Liquid assay results.—The viable count method was used to determine cell numbers (cfu cm^{-3}) and hence the extent of microbial growth: no microbial growth ≡ 0 cfu cm^{-3}; inhibited microbial growth ≡ 0 < cell number < ~10^7 cfu cm^{-3}; 'normal', un-

inhibited microbial growth ≡ ≥ ~10^7 cfu cm^{-3} ('control' value). When no microbial growth could be detected (*i.e.* total microbial kill) this is indicated by the term *no growth*; inhibited microbial growth is indicated by the cell number (cfu cm^{-3}); the term *complete growth* indicates 'normal', uninhibited microbial growth (*i.e.* similar microbial growth compared to that observed on a 'control' plate).

Supernatant test results.—These results are indicated in the same manner as for the liquid assay results.

Experimental

Materials and equipment.—Test organism (*Saccharomyces cerevisiae* EL1 – isolated from unpasteurized Norwegian apple juice), test medium Mills orange juice (undiluted), resin bead samples (weighed to give 0.2 meq), malt extract agar plates, Eppendorf vials (polypropylene, 1.5 cm^3), sterile micro-pipette tips, micro-pipettes, ethanol.

Preparation of inoculum solutions.—These were prepared in an identical manner to the inoculum solutions used in the MIC tests (see 2.4.1, *Experimental*).

Plate assay.—MEA plates were inoculated with 10^6 cells cm^{-3} of *Saccharomyces cerevisiae* EL1 and left to dry for 5 min. Test samples of the resin beads (0.2 meq), were then carefully placed onto the agar/yeast surface and arranged in the form of crude circles (approximate diameter, 10–15 mm), keeping samples well spaced from each other. Note: the plates were sampled as quickly as possible to lessen the chances of contamination of the agar/yeast surface. The plate was covered and a careful note made of the identity and relative positions of each sample. Typically, between four and six resin bead samples were tested per plate. In addition, a 'control' plate was set up without bead samples. The plates were then incubated at 25 °C for 48 h. After this time each plate was examined for possible inhibitory effects. Active beads displayed inhibitory 'zones' around the sample area.

Liquid assay.—Resin bead samples (0.2 meq) were weighed into sterile Eppendorf vials (1.5 cm^3 capacity). Mills orange juice (1 cm^3) was added to each vial and each sample inoculated with 10^1 cells cm^{-3} of *Saccharomyces cerevisiae* EL1. In addition, a

'control' vial was set up without any bead sample. The samples were then incubated at 25 °C for 24 h. After this time a representative sample of orange juice was removed from each vial and plated out onto MEA plates. Viable count determinations were performed on each sample in order to determine the extent of microbial growth.

Supernatant test.—Resin bead samples (0.2 meq) were weighed into sterile Eppendorf vials (1.5 cm^3 capacity) and Mills orange juice (1 cm^3) added to each vial. In addition, a 'control' vial was set up without any bead sample. The samples were then incubated at 25 °C for 24 h. After this time the juice was removed from each sample and transferred to fresh sterile vials. These vials were then inoculated with 10^1 cells cm^{-3} of *Saccharomyces cerevisiae* EL1 and incubated at 25 °C for a further 48 h. After this time a sample of juice was removed from each vial and plated out onto MEA plates. Viable count determinations were performed on each sample in order to determine the extent of microbial growth.

3. RESULTS AND DISCUSSION

3.1 Towards the Synthesis of Polymerizable AMAs

3.1.1 Introduction

This thesis is concerned with the design, synthesis and microbiological testing of novel polymerizable and polymeric antimicrobial agents (AMAs). Rather than concentrate on a specific class of AMA it was decided, instead, to study several classes, with the intention of highlighting the diversity in molecular structure and modes of action of antimicrobial agents.

Collected and presented in the following sub-sections (3.1.2–3.1.5) are the avenues of research that proved to be the least fruitful. These studies were discontinued due to either time restrictions or failed syntheses. All but one of the antimicrobial compounds described below are non-polymerizable. Although several 'model' compounds were prepared and tested, time restrictions prevented the study of polymerizable analogues. Despite this, each sub-section concludes with suggestions and syntheses of potentially interesting polymerizable derivatives.

3.1.2 Thiazolyl Compounds

Cho *et al.* recently reported the synthesis of the thiazolyl vinyl monomer **67** from the thiazolylbenzimidazole compound **66** (Scheme 1).[47] Additionally, Cho prepared the homopolymer of **67** and the co-polymer of **67** with acrylic acid. The fungicidal activities of the model compounds and polymers were tested against *Aspergillus niger* and *Chaetomium globusum* and were found to decrease in the order: **66** > **67** > poly(**67**) > poly(**67**-*co*-acrylic acid).

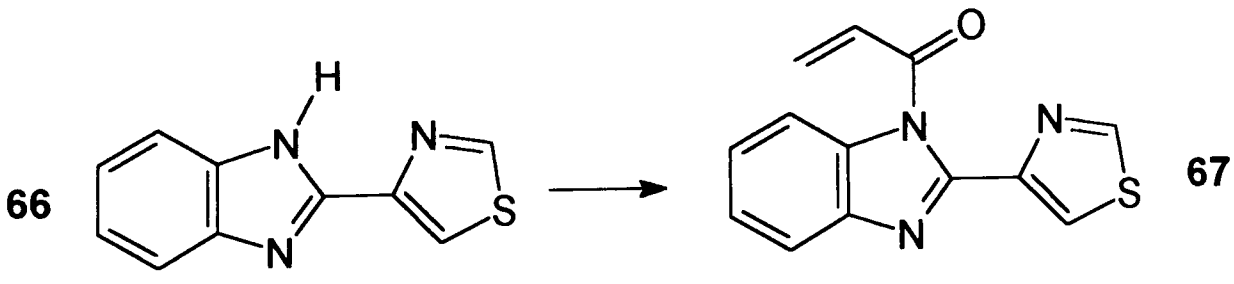

Scheme 1 *Reagents and conditions:* acryloyl chloride, C_6H_6 (dry), Et_3N, 11 °C→r.t., 19 h.

The potential of thiazolyl compounds as polymerizable and polymeric antimicrobial compounds seemed worthy of investigation. As a result, the thiazolyl monomer **67** was prepared and tested for antimicrobial activity against *Saccharomyces cerevisiae* EL1 in apple juice and orange juice. The monomer **67** was prepared according to the literature method.[47] A solution of 2-(4'-thiazolyl)benzimidazole **66** (Aldrich), acryloyl chloride and triethylamine in sodium-dried benzene was stirred at room temperature to afford *N*-acryloyl-2-(4'-thiazolyl)benzimidazole **67** (Scheme 1) as a yellow solid (65%), mp 120–121 °C (lit.,[47] 139.5–140.5 °C). Repeated attempts were made to recrystallize the crude product but these met with failure as decomposition resulted. The monomer **67** was characterized by elemental microanalysis and UV, FTIR and ^{1}H NMR spectroscopic techniques. The UV electronic spectrum (ethanol; 190–400 nm range) of **67** consisted of three bands at 222, 267 and 300 nm, while the FTIR spectrum (KBr pellet; 4000–400 cm^{-1} range) revealed a strong carbonyl absorption at 1701 cm^{-1}. The ^{1}H NMR spectrum (250 MHz, $CDCl_3$) of **67** revealed vinyl protons at δ 5.83 (*J* 10.0 and 1.4 Hz), 6.29 (*J* 17.0 and 10.0 Hz) and 6.46 (*J* 17.0 and 1.4 Hz) ppm. The aromatic signals appeared as multiplets at δ 7.42, 7.83 and 7.93 ppm, while the pair of thiazolyl protons appeared as an AB quartet (*J* 2.1 Hz) at δ 8.20 and 8.89 ppm. The monomer **67** was tested for antimicrobial activity against the yeast strain *Saccharomyces cerevisiae* EL1 (concentration test range: 1000–1 μg cm^{-3}). The resulting MIC values were 500 μg cm^{-3} in NAJ and >1000 μg cm^{-3} in MOJ.

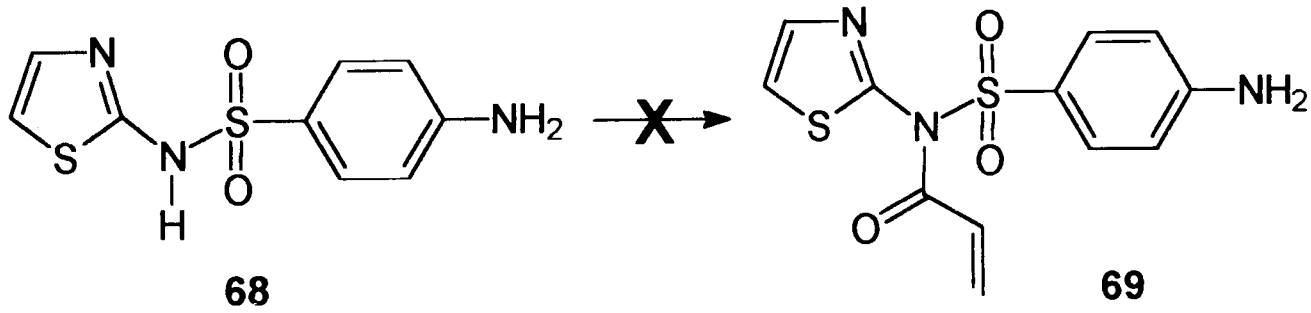

68 **69**

Scheme 2 *Reagents and conditions:* acryloyl chloride, C_6H_6 (dry), Et_3N, r.t., 24 h.

As can be seen from the above MIC results, the monomer **67** was not particularly active. Consequently, it was decided to use Cho's acrylation procedure on another thiazolyl compound, namely *N'*-(2-thiazolyl)sulfanilamide **68** (Scheme 2). A sample of **68**

(Aldrich) was reacted with acryloyl chloride in a similar manner to that of **66** (Scheme 1). Work-up afforded a benzene-insoluble solid and a trace amount of a brown, oily residue. ^{1}H NMR spectroscopy (250 MHz, C_5D_5N) revealed the solid to be a mixture of starting material **68** and triethylammonium chloride by-product. The ^{1}H NMR spectrum (250 MHz, $CDCl_3$) of the oil was very 'noisy' and complex but revealed little, if any, indication of the desired product, the thiazolylsulfanilamide monomer **69**. A second attempt was made at the synthesis of **69**. This time, the reaction mixture was heated at 60 °C. The reaction afforded, in the same way as before, unreacted starting material and a trace amount of an oily residue. ^{1}H NMR spectroscopy of the latter revealed no indication of the desired product **69**.

3.1.3 Benzofuroxan

Following on from the work of earlier studies[48] the antimicrobial activity of benzofuroxan **71** (Scheme 3) was investigated. Structurally, benzofuroxan (benzofurazan 1-oxide) consists of a benzene ring fused to an interesting five-membered heterocyclic ring system containing an *N*-oxide group.

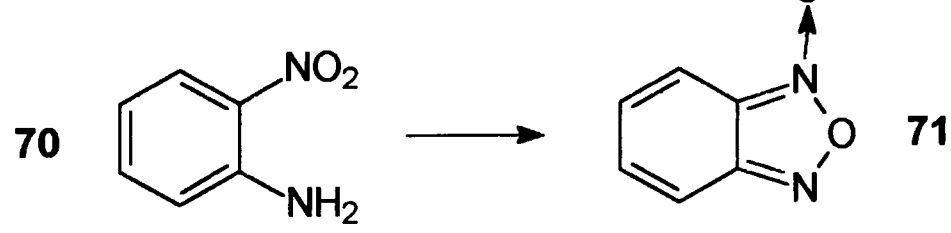

Scheme 3 *Reagents and conditions:* MeOH, KOH, NaOCl (aq), r.t.

Benzofuroxan **71** was prepared according to an early synthesis described by Green and Rowe.[49] Aqueous sodium hypochlorite solution was added to a solution of *ortho*-nitroaniline **70** in methanolic potassium hydroxide (Scheme 3); the oxidation reaction produces 'dinitrosobenzene', $C_6H_4(NO)_2$, which then isomerizes to the *N*-oxide, five-membered heterocyclic ring system of benzofuroxan.[50] Recrystallization of the crude product from ethanol afforded benzofuroxan **71** as sandy-brown crystals (59%), mp 67–68 °C (lit.,[49] 72 °C). The product was characterized by elemental microanalysis and UV, FTIR and ^{1}H NMR spectroscopic techniques. The UV electronic spectrum (ethanol; 190–500 nm range) of **71** consisted of two bands at 217 and 358 nm. The FTIR spectrum (KBr pellet;

4000–400 cm^{-1} range) of **71** revealed bands at 3100 (Ar–H), 3080 (Ar–H), 1617, 1586, 1538, 1485, 1015 and 747 (*ortho*-disubstituted benzene ring) cm^{-1}. The ^1H NMR spectrum (250 MHz, $CDCl_3$) of **71** consisted of a pair of broad singlets, of equal intensity, at δ 7.29 and 7.48 ppm. Benzofuroxan was tested for antimicrobial activity against the yeast strain *Saccharomyces cerevisiae* EL1 (concentration test range: 1000–1 μg cm^{-3}). The resulting MIC values were 15.6 μg cm^{-3} in NAJ and 62.5 μg cm^{-3} in MOJ.

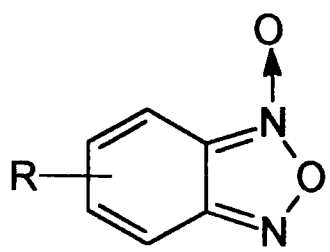

72a R = OH
72b R = $OC(O)CH=CH_2$
73a R = NH_2
73b R = $NHC(O)CH=CH_2$
74 R = $CH=CH_2$

Fig. 24 Suggested routes to polymerizable benzofuroxans.

As can be seen from the above MIC results, benzofuroxan **71** showed significant activity against *Saccharomyces cerevisiae*. Encouraged by these results, it was decided to undertake the synthesis of a polymerizable benzofuroxan. Unfortunately, time restrictions prevented this work. Shown in Figure 24, however, are suggested routes to some 'simple' polymerizable benzofuroxans (**72b**, **73b**). Green and Rowe's synthesis of benzofuroxan **71** (Scheme 3) relies on having an *ortho* arrangement of nitro and amino groups on a benzene ring. A precursor towards a polymerizable benzofuroxan would therefore be an *ortho*-nitroaniline that contained a functional handle. The benzofuroxan ring system could be formed using Green and Rowe's method, and the functional handle then used to attach a vinyl group. Potentially useful functional handles are hydroxyl and amino groups. Fortunately, the synthesis of hydroxybenzofuroxan **72a** and aminobenzofuroxan **73a** are given in the literature.[51] Reaction of **72a** and **73a** with acryloyl chloride should then give the acrylate monomer **72b** and the acrylamido monomer **73b** respectively (alternatively, the acrylation reaction could be performed prior to formation of the benzofuroxan ring system). A final candidate for a polymerizable benzofuroxan is vinylbenzofuroxan **74**. This could, in principle, be prepared from vinyl-*o*-nitroaniline using the method of Green and Rowe. However, vinyl *ortho*-nitroaniline could

not be found listed in any chemical catalogue and, as a consequence, it would have to be synthesized beforehand.

3.1.4 Parabens Compounds

p-Hydroxy benzoate esters ('parabens'), $HO–C_6H_4–CO_2R$, are potent antimicrobial agents but are relatively non-toxic to humans. Parabens compounds are commonly used as preservatives in the cosmetics, food and pharmaceutical industries.[52] The mode of action of parabens compounds is varied as they are known to affect the following:

- RNA, DNA and protein synthesis.[53]
- Deactivation of enzymes.[54]
- Disruption of cell membranes.[55,56]
- Inhibition of amino acid uptake.[57]

A recent study examined the antimicrobial activity of 3-substituted parabens esters, in particular the 3-amino parabens ester **78** (Scheme 4).[58] It was decided to investigate further the parabens ester **78**, with the aim of producing a polymerizable analogue.

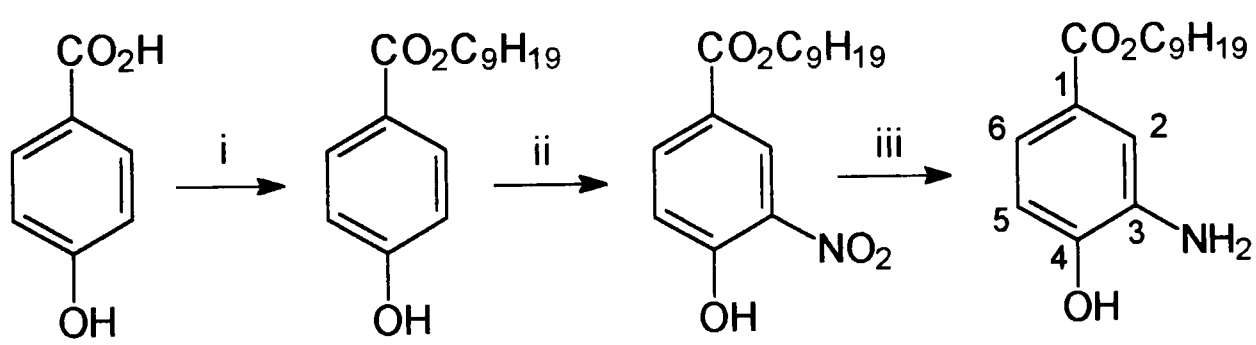

Scheme 4 *Reagents and conditions:* i, n-$C_9H_{19}OH$, conc. H_2SO_4, toluene, Dean-Stark, 17 h; ii, conc. H_2SO_4, conc. HNO_3, CH_2Cl_2, r.t., 18 h; iii, H_2, Pd/C, EtOH, r.t., 16 h.

The method detailed by Brown *et al.*[58] was used to prepare **78**. The three-step synthesis of **78** is shown in Scheme 4. A solution of *p*-hydroxybenzoic acid **75** and nonan-1-ol in toluene was refluxed in a Dean-Stark apparatus to afford the crude ester **76**. Purification by distillation and flash-column chromatography (silica gel)[59] gave the *n*-nonyl parabens ester **76** as a white solid (25%), mp 38–39 °C (lit.,[60] 44 °C). A solution of the ester **76**

in dichloromethane was then stirred with a mixture of concentrated sulfuric and concentrated nitric acid to afford the crude product **77**. Purification by flash-column chromatography (silica gel) gave the 3-nitro parabens ester **77** as a yellow solid (85%), mp 44–46 °C. Finally, the nitro parabens ester **77** was hydrogenated (palladium/carbon catalyst) using a Cook hydrogenation apparatus to afford the crude product **78**. Purification by flash-column chromatography (silica gel) gave the 3-amino parabens ester **78** as a tan solid (80%; 12% overall yield from *p*-hydroxybenzoic acid **75**), mp 70–72 °C.

Table 1 Synthesis of the 3-amino parabens compound **78** (Scheme 4).

Cpd.[a]	Yield (%)[b]	Mp (°C)	ν_{max} / cm^{-1} [c]	MIC[d]/μg cm^{-3}
76	25	38–39	3382 (O–H) & 1683 (C=O)	500
77	85	44–46	3272 (O–H), 1728 (C=O) 1548 (NO_2) & 1337 (NO_2)	>1000
78	80	70–72	3480 (N–H), 3392 (O–H), 3320 (N–H), 1677 (C=O) & 1608 (N–H)	7.8

[a]Compound. [b]After flash-column chromatography (silica gel). [c]KBr pellet. [d]Test organism, *Saccharomyces cerevisiae* EL1; test medium, Norwegian apple juice.

The series of compounds **76–78** were characterized by elemental microanalysis and FTIR and ^{1}H NMR spectroscopic techniques. The FTIR spectra (KBr pellet; 4000–400 cm^{-1} range) of **76**, **77** and **78** revealed strong carbonyl absorptions at 1683, 1728 and 1677 cm^{-1} respectively, and sharp hydroxyl bands at 3382, 3272 and 3392 cm^{-1} respectively. The nitro compound **77** revealed bands at 1548 and 1337 cm^{-1} due to the nitro group, while the amino compound **78** revealed N–H bands at 3480 (stretch), 3320 (stretch) and 1608 (bend) cm^{-1}. The ^{1}H NMR spectrum (250 MHz, $CDCl_3$) of **78** revealed signals at δ 0.88 (t), 1.1–1.6 (m), 1.74 (qn) and 4.27 (t) ppm due to the nonyl chain, and signals due to the aromatic protons at δ 6.76 (d), 7.42 (dd) and 7.45 (d) ppm. The signals due to the hydroxyl and amino groups overlapped and appeared as a broad singlet at δ 4.83 (exch.) ppm. The series of parabens esters **76–78** were tested for antimicrobial activity against the yeast strain *Saccharomyces cerevisiae* EL1 (concentration test range: 1000–1 μg cm^{-3}). The MIC values (recorded in NAJ) were as follows: **76**, MIC = 500

$\mu g\ cm^{-3}$; **77**, MIC = >1000 $\mu g\ cm^{-3}$; and **78**, MIC = 7.8 $\mu g\ cm^{-3}$. A summary of yields, melting points, FTIR spectral data and MIC values for the series of compounds **76–78** is presented in Table 1.

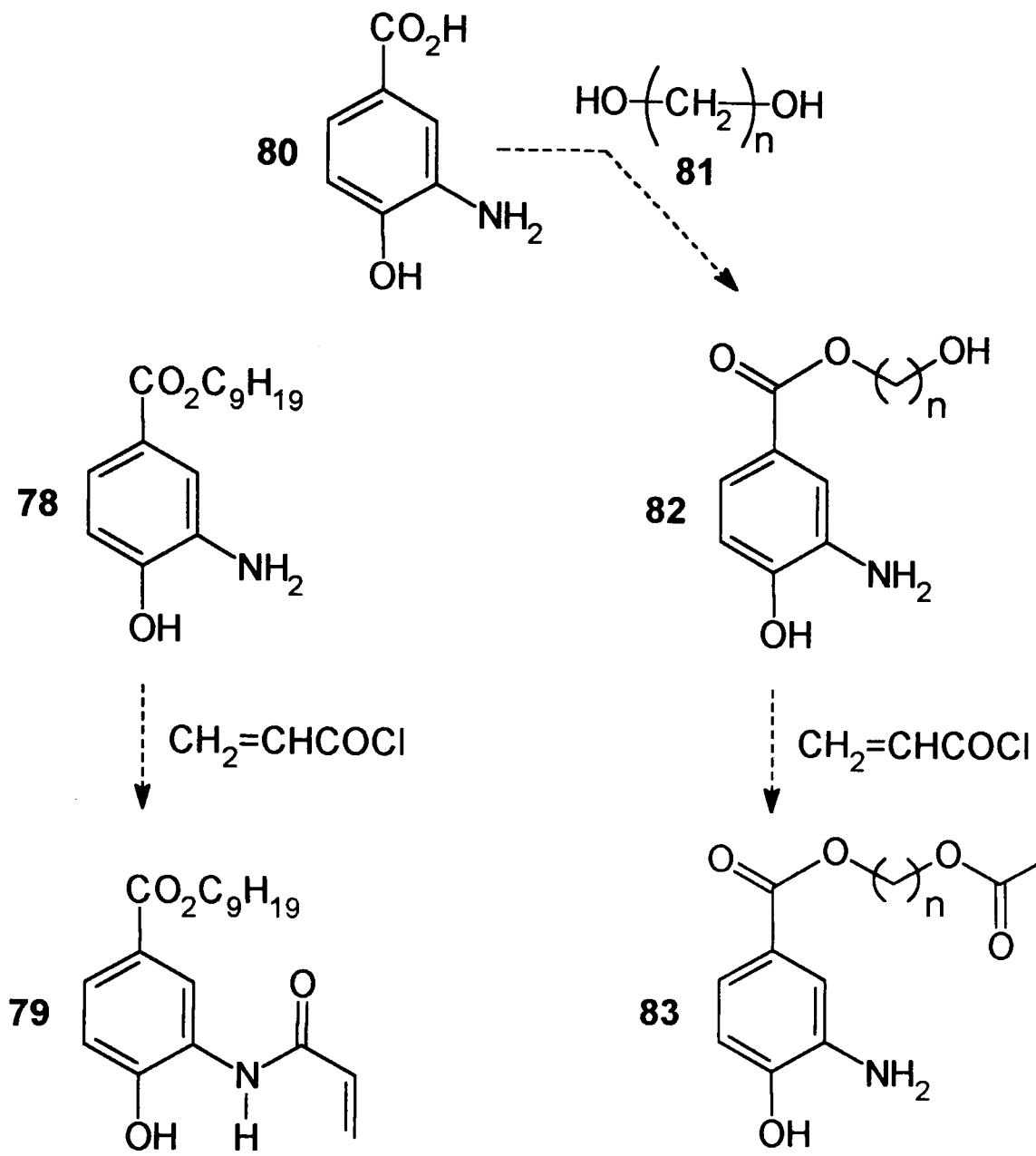

Fig. 25 Suggested routes to polymerizable amino parabens.

The microbiological tests revealed the amino parabens **78**, MIC = 7.8 $\mu g\ cm^{-3}$, was very active against *Saccharomyces cerevisiae*. Unfortunately, time restrictions prevented the investigation of polymerizable analogues of **78**. Shown in Figure 25, however, are suggested routes to two polymerizable amino parabens compounds. On paper, a 'simple' polymerizable version of **78** is the acrylamido parabens ester **79**. The latter could be prepared by the reaction of **78** with acryloyl chloride. Note that in order to avoid *O*-acrylation, the hydroxyl group of **78** would probably need to be pre-protected (for example, as a trimethylsilyl ether) beforehand. It must be borne in mind,

however, that functionalization of the amino group (as in **79**) may render the resultant molecule inactive. A second, more elaborate example of a polymerizable amino parabens compound is the acrylate **83** (Figure 25). 3-Amino-*p*-hydroxybenzoic acid **80** could be converted to the benzoate alcohol **82** using the di-alcohol **81**. The aliphatic hydroxyl group of **82** could then be acrylated with acryloyl chloride to give the acrylate **83**. In an alternative synthesis, a di-amine could be used in preference to the di-alcohol **81** for the conversion **80** → **82**. This would afford, after the acrylation step, an acrylamido monomer, **83** but with both the C(O)O groups replaced by C(O)NH. Note in the monomer **83** that the polymerizable unit forms part of the ester chain. The alkyl chain is a key feature in parabens compounds. As a result, structural modification of the chain may affect the antimicrobial activity of the resultant molecule (*c.f.* the acrylamido parabens compound **79**).

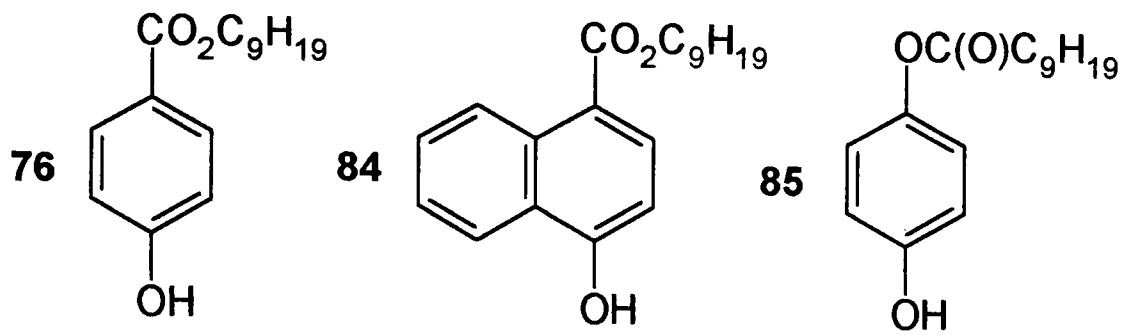

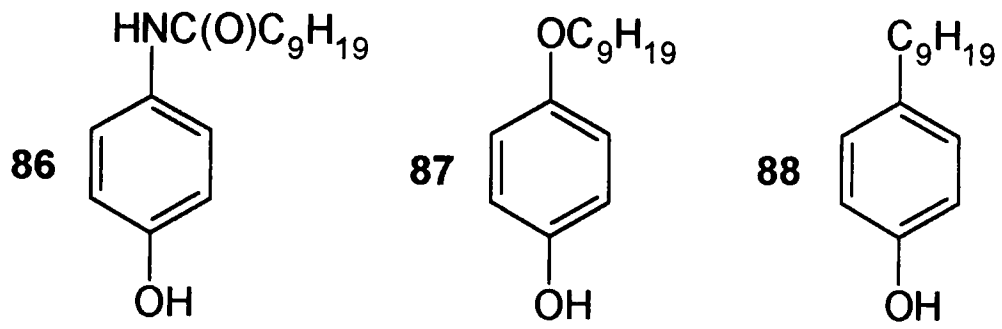

Fig. 26 Structural variants **84–88** of *n*-nonyl 4-hydroxybenzoate **76**.

It may be profitable to investigate further the relationship between antimicrobial activity and parabens structure. Shown in Figure 26 is the nonyl parabens compound **76** and a selection of structural variants, compounds **84–88**. Comparison of the antimicrobial activities of **76** and **84–88** may go some way to indicate the required optimum structure for maximum antimicrobial potency. For example, compound **84** might be used to assess the influence of further conjugation on antimicrobial activity. As a second example, con-

sider compound **85**. In this case, the 'sense' of the ester group is inverted with the result that the alkyl chain and benzene ring are now attached to electron-withdrawing and electron-donating groups respectively (*c.f.* structure **76**). Finally, consider compounds **86–88**. In these examples, the benzene ring and alkyl chain are linked *via* functional groups other than an ester group. The antimicrobial activities of **86–88** might be used to ascertain the necessity for the ester linkage in the parabens structure.

3.1.5 Isothiazolinones

Kathons

4-Isothiazolin-3-ones ('kathons') are potent antimicrobial agents and are principally used as preservatives in the cosmetics industry.[22] The synthesis of kathons **93** by one-step chlorination–cyclization of the respective dithiodipropionamides **92** (Scheme 5) has been described by Lewis *et al.*[61] From the comprehensive range of kathons prepared by Lewis, the chloropropyl kathon **93a** was found to be particularly interesting. The kathon **93a** has a primary alkyl chloride group which would serve as a useful functional handle for the preparation of polymerizable analogues. It was decided to prepare the kathon **93a** with the aim of producing a polymerizable isothiazolinone.

An attempt was made to synthesize the kathon **93a** using the method detailed by Lewis.[61] The three-step synthesis of **93a** is shown in Scheme 5. Dithiodipropionic acid **89** was stirred with thionyl chloride, at room temperature, to afford 3,3'-dithiodipropionyl dichloride **90** as an amber liquid (99%). The acid chloride **90** in toluene was then added to a solution of 3-chloropropylamine hydrochloride **91a** in aqueous sodium hydroxide in an attempt to prepare the dithiodipropionamide **92a**. Work-up afforded a tan solid, mp 103–105 °C. Recrystallization of the latter from acetone–water gave an off-white solid, mp 106–107 °C. The ^{1}H NMR spectrum (250 MHz, $CDCl_3$) of the recrystallized product revealed signals at δ 2.02 (qn), 2.60 (t), 3.00 (t), 3.45 (q) and 3.61 (t) ppm, and a broad singlet at δ 6.23 (exch.) ppm. Although these spectral features are consistent with the structure **92a**, the spectrum contained an additional signal in the form of a broad singlet at δ 1.70 (exch.) ppm. The chemical shift of this singlet falls in the range expected for thiol protons, *viz.* δ 1–2 ppm.[62] This evid-

ence suggested that the thiol **94**, and not the dithiodipropionamide **92a**, had been formed. Supporting evidence for the structure **94** came from high resolution mass spectroscopy. The parent ion of **92a**, corresponding to $C_{12}H_{22}Cl_2N_2O_2S_2$, would be expected at *m/z* 360.0500 ($Cl^{34.97}$) and *m/z* 364.04410 ($Cl^{36.97}$). No signals corresponding to these *m/z* values were found in the mass spectrum of the product isolated from the attempted reaction **90** → **92a**. However, there was a signal at *m/z* 183.0306 (15.8% abundance) which suggested the parent ion of **94** ($C_6H_{12}Cl^{36.97}NOS$ requires *M*, 183.0299). Unfortunately, no melting point data for the dithiodipropionamide **92a** was cited by Lewis.[61] As a result, no comparison could be made with the melting point of the thiol **94**. The FTIR spectrum (KBr pellet; 4000–400 cm^{-1} range) of **94** revealed a strong carbonyl absorption at 1630 cm^{-1}. The MIC value of **94** was >1000 μg cm^{-3} (recorded in NAJ against *Saccharomyces cerevisiae* EL1; concentration test range: 1000–1 μg cm^{-3}).

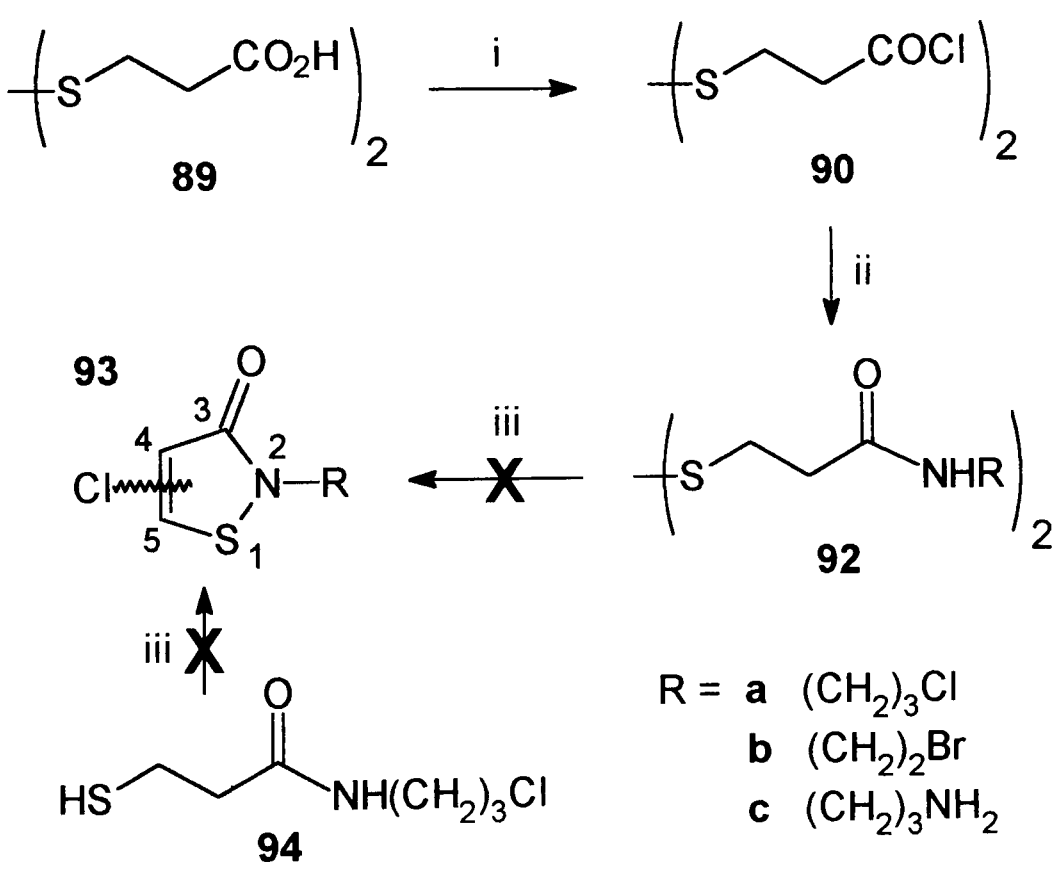

Scheme 5 *Reagents and conditions:* i, $SOCl_2$, py (catalytic), r.t., 4 d; ii, RNH_2(.HX) **91**, NaOH (aq), toluene, 0 °C→r.t., 1½–2 h; iii, SO_2Cl_2, CH_2Cl_2, 0 °C→r.t., 1–5 d.

The ring-closure of **94** to the chloropropyl kathon **93a** was attempted, despite the failure to prepare the dithiodipropionamide **92a**. A solution of **94** in 1,2-dichloro-

ethane was stirred with sulfuryl chloride, at room temperature, for several days. Work-up of the reaction mixture afforded a yellow-orange oil. The ^{1}H NMR spectrum (250 MHz, $CDCl_3$) of the oil consisted of a complex set of peaks in the range δ 1.9–4.1 ppm. However, there was little, if any, indication of the desired product, the chloropropyl kathon **93a**. The oil was distilled but ^{1}H NMR spectroscopy revealed it to be little-changed from the crude material. Repeated attempts were made to prepare **93a** but all met with failure. Attempts to prepare **93a** using a different chlorination–cyclization agent (thionyl chloride) and a different solvent (chloroform) also met with failure.

The Lewis paper[61] did not include the preparation of the bromoethyl kathon **93b** (Scheme 5) so it was decided to attempt its preparation next. In a similar manner to **93a**, the bromoethyl group of the kathon **93b** could be utilized as a functional handle in the preparation of polymerizable kathons. 3,3'-Dithiodipropionyl dichloride **90** and 2-bromoethylamine hydrobromide **91b** were reacted in a similar manner to that described for the attempted preparation of the dithiodipropionamide **92a**. Work-up afforded an off-white solid, mp 128–131 °C. Recrystallization of the latter from toluene gave a white solid, mp 137–138 °C. The ^{1}H NMR spectrum (250 MHz, C_5D_5N) of the recrystallized product revealed signals at δ 2.85 (t), 3.19 (t), 3.66 (t), 3.82 (q) ppm, and a broad singlet at δ 9.31 ppm. No sign of a thiol proton was evident from the spectrum. As a consequence, it was concluded that the dithiodipropionamide **92b** had been successfully prepared. The FTIR spectrum (KBr pellet; 4000–400 cm^{-1} range) of **92b** revealed a strong carbonyl absorption at 1648 cm^{-1}.

The ring-closure of **92b** to the bromoethyl kathon **93b** was attempted next. The dithiodipropionamide **92b** and sulfuryl chloride were reacted in a similar manner to that described for the attempted preparation of the kathon **93a**. Work-up of the reaction mixture afforded an orange oil. The ^{1}H NMR spectrum (250 MHz, $CDCl_3$) of the oil consisted of a complex set of peaks in the range δ 3.5–4.3 ppm. However, there was little, if any, indication of the desired product, the bromoethyl kathon **93b**.

It was additionally planned to synthesize the aminopropyl kathon **93c** (Scheme 5). This could be prepared from the ring-closure of the derived dithiodipropionamide

92c. Due, however, to time constraints and the failure to synthesize **93a** and **93b**, the preparation of the kathon **93c** was aborted.

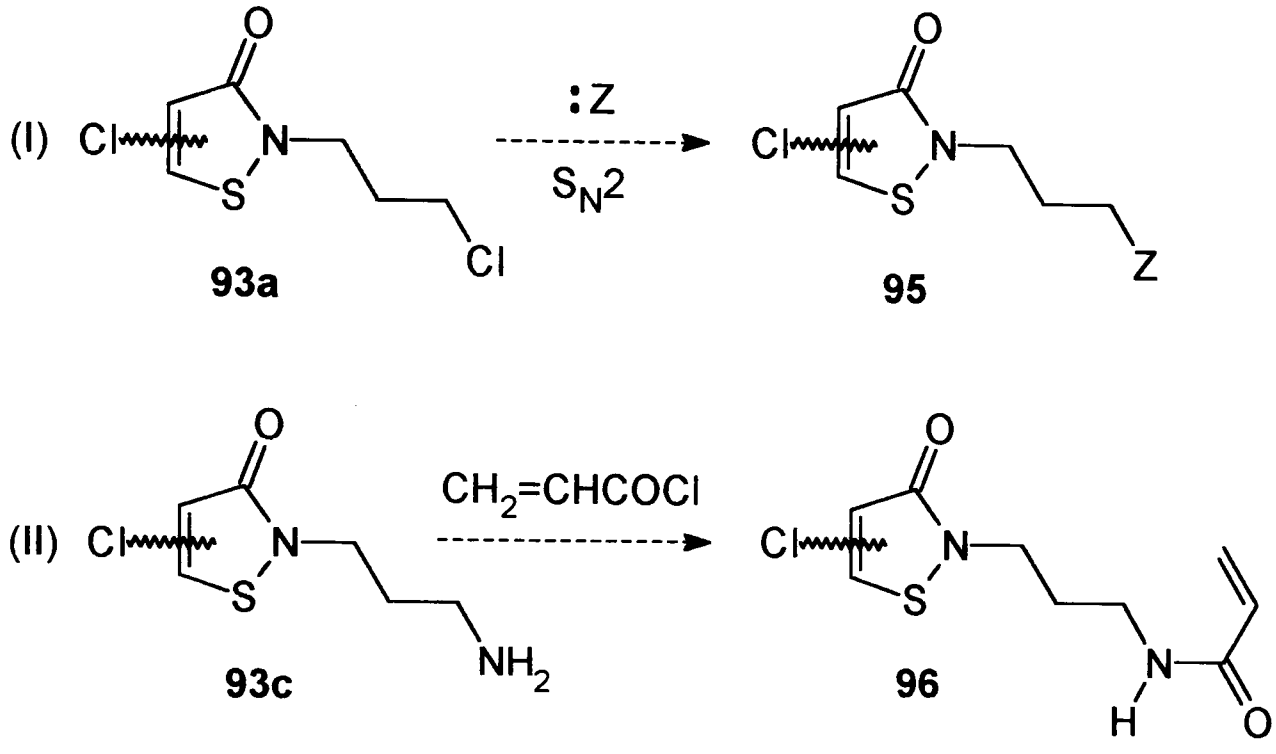

Fig. 27 Suggested routes to polymerizable kathons.

Due to failed syntheses, the investigation of polymerizable analogues of the kathons **93a** and **93b** was not possible. Shown in Figure 27, however, are suggested routes to the polymerizable kathons **95** and **96**. In Route I, 'Z' represents a molecule containing both a nucleophilic atom (*e.g.* N or O) and a polymerizable group (*e.g.* –CH=CH_2). The S_N2-like substitution of the chlorine atom of **93a** with the nucleophilic atom of 'Z' would give the polymerizable kathon **95**. In order to facilitate the S_N2 reaction, however, it may be necessary to replace the chlorine atom of **93a** with a better leaving group (*e.g.* OTos). The bromoethyl kathon **93b** (Scheme 5) could be reacted with 'Z' in a similar fashion to that of **93a**. In the second example shown in Figure 27 (Route II), the amino group of the aminopropyl kathon **93c** could be acrylated with acryloyl chloride to give the acrylamido kathon **96**. The hydroxy analogue of **93c** (NH_2 replaced by OH) could be acrylated in a similar fashion. Alternatively, **93c** could be reacted with methacryloyl chloride [CH_2=$C(CH_3)$COCl] or a methacrylate ester [CH_2=$C(CH_3)CO_2R$]. This would produce a monomer that could be more readily polymerized.

Benzokathon

Following on from the work of earlier studies[48] the antimicrobial activity of benzokathon **99** (Scheme 6) was investigated. Structurally, benzokathon (1,2-benzisothiazole-3-one, or 2-thiobenzimide)[63] consists of the basic isothiazolin-3-one ring system fused to a benzene ring. Oxidation of the sulfur atom of benzokathon produces the well-known sweetener *Saccharin*® (*o*-benzoic sulfimide), **99** but with –S– replaced by $-SO_2-$.

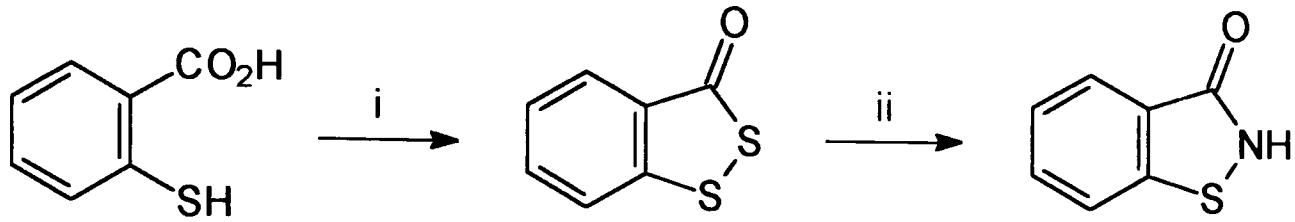

97 **98** **99**

Scheme 6 *Reagents and conditions:* i, EtSH, conc. H_2SO_4, 50 °C, 2½ h; ii, NH_3 (g), EtOH, r.t., 22 h.

Benzokathon **99** was prepared according to the synthesis described by M^{c}Kibben and M^{c}Clelland.[64] The two-step synthesis of **99** is shown in Scheme 6. A solution of thiosalicylic acid **97** and ethanethiol in concentrated sulfuric acid was heated at 50 °C for 2.5 h. Purification of the crude product by steam distillation and recrystallization from ethanol afforded 3*H*-1,2-benzodithiol-3-one (2-dithiobenzoyl) **98** as orange-yellow crystals (9%), mp 70–73 °C (lit.,[65] 78–80 °C). Gaseous ammonia was bubbled through an ethanolic solution of 2-dithiobenzoyl **98** at room temperature. The crude benzokathon obtained was converted to its sodium salt and precipitated from water with concentrated hydrochloric acid. Recrystallization from ethanol afforded benzo-kathon **99** as tan *platelets* (42%), mp 156–157 °C (lit.,[64] 158 °C). 2-Dithiobenzoyl **98** and benzokathon **99** were characterized by elemental microanalysis and FTIR and ^{1}H NMR spectroscopic techniques. The FTIR spectra (KBr pellet; 4000–400 cm^{-1} range) of **98** and **99** revealed strong carbonyl absorptions at 1662 and 1645 cm^{-1} respectively. The ^{1}H NMR spectra (250 MHz, $CDCl_3$) of 2-dithiobenzoyl **98** and benzokathon **99** were very similar to each other. Each spectrum revealed a second order splitting pattern for the four aromatic protons: **98**, δ 7.42 (1 H, m), 7.64 (2 H, m) and 7.97 (1 H, d) ppm; **99**, δ 7.45 (1 H, m), 7.66 (2 H, m) and 8.08 (1 H, d) ppm. The NH proton of **99** app-

eared as a broad singlet at δ 11.05 ppm. The ^{1}H NMR spectrum (250 MHz) of benzokathon was also recorded in d_4-methanol. Interestingly, the spectrum revealed a first order splitting pattern for the four aromatic protons (*c.f.* second order spectrum in $CDCl_3$): **99**, δ 7.41 (1 H, t), 7.63 (1 H, td), 7.77 (1 H, d) and 7.95 (1 H, d) ppm. 2-Dithiobenzoyl **98** and benzokathon **99** were tested for antimicrobial activity against the yeast strain *Saccharomyces cerevisiae* EL1 (concentration test range: 1000–1 μg cm^{-3}). The MIC values were as follows: **98**, MIC = 125 μg cm^{-3} (NAJ); **99**, MIC = 250 μg cm^{-3} (NAJ), 250 μg cm^{-3} (SOJ) and 1000 μg cm^{-3} (MOJ).

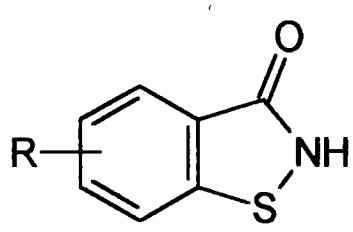

100a R = OH
100b R = OC(O)CH=CH$_2$
101a R = NH$_2$
101b R = NHC(O)CH=CH$_2$
102 R = CH=CH$_2$

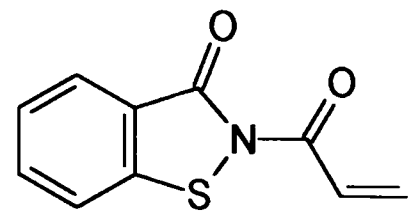

103

Fig. 28 Suggested routes to polymerizable benzokathons.

As can be seen from the above MIC results, benzokathon **99** showed moderate activity against *Saccharomyces cerevisiae* in NAJ and SOJ. Encouraged by these results, it was decided to undertake the synthesis of a polymerizable benzokathon. Unfortunately, time restrictions prevented this work. Shown in Figure 28, however, are suggested routes to some 'simple' polymerizable benzokathons. M^{c}Kibben and M^{c}Clelland's synthesis of benzokathon **99** (Scheme 6) relies on having an *ortho* arrangement of carboxylic acid and thiol groups on a benzene ring. A precursor towards a polymerizable benzokathon would therefore be a thiosalicylic acid that contained a functional handle. The benzokathon ring system could be formed using M^{c}Kibben and M^{c}Clelland's method, and the functional handle then used to attach a vinyl group. Potentially useful functional handles are hydroxyl and amino groups. Neither of the hydroxy- or amino-thiosalicylic acids is commercially available, however, so each would have to be synthesized beforehand. Reaction of hydroxybenzokathon **100a** and amino-benzokathon **101a** with acryloyl chloride should then give the acrylate monomer **100b** and the acrylamido monomer **101b** respectively (alternatively, the acrylation reaction could be performed prior to formation of the benzokathon ring system). Another candidate for a

polymerizable benzokathon is vinylbenzokathon **102**. This could, in principle, be prepared from vinylthiosalicylic acid using the method of McKibben and McClelland's. However, vinylthiosalicylic acid is not commercially available and, as a consequence, it would have to be synthesized beforehand. A final candidate for a polymerizable benzokathon is the acrylamido monomer **103**. The latter could be prepared from the reaction of benzokathon **99** (Scheme 6) with acryloyl chloride.

3.2 *Phosphonium Salts*

3.2.1 Introduction

Quaternary ammonium salts (quats) are, perhaps, the best known class of cationic biocides. The antimicrobial activity of low molecular weight and polymeric versions of quaternary ammonium compounds has been studied before (refer to section 3.4 for further details). The target site for low molecular weight cationic biocides is the cytoplasmic membrane. The mode of action involves diffusion through the cell wall to the cytoplasmic membrane, followed by disruption of the membrane leading to death of the cell. Another class of cationic biocide are the *phosphonium salts*. In comparison to quaternary ammonium compounds, very little research has been performed on the antibacterial activity of polymeric phosphonium salts.[66] Recently, however, a series of papers were published detailing studies by Endo and co-workers on the synthesis and antibacterial testing of a range of low molecular weight and polymeric trialkyl- and triaryl-phosphonium salts.[37,44,67–69]

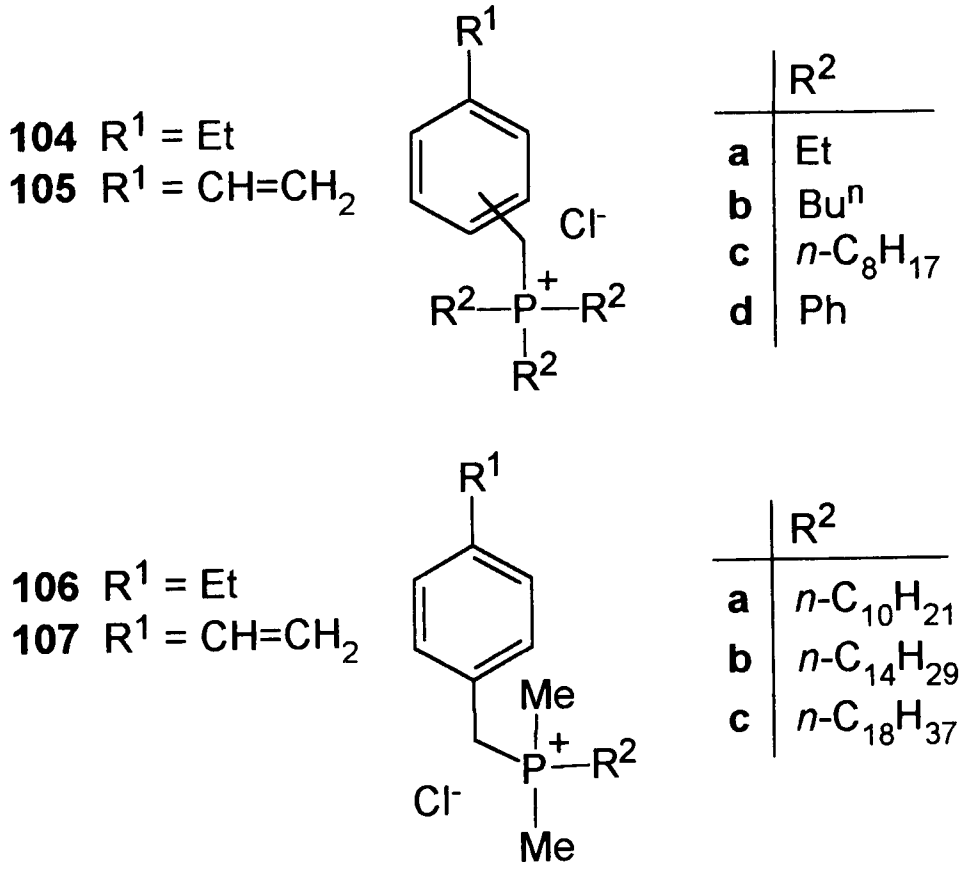

Fig. 29 Antibacterial phosphonium salts.

The phosphonium compounds studied by Endo include those shown in Figure 29. The phosphonium salts were tested against the bacterial organisms *Staphylococcus aureus* and *Escherichia coli* in order to determine their antibacterial effectiveness. It was found that polymeric versions of **105a–d** had higher antibacterial activities than the corresponding low molecular weight model compounds **104a–d** and **105a–d**. In addition, compounds with the longest alkyl chain (R^2 = *n*-C_8H_{17}) were more active than compounds with shorter chains.[67] The effects of counter anion structure, molecular weight and co-polymer composition on the activity of polymeric versions of **105b** were investigated.[68] Antibacterial activity was low for polymers with counter anions that formed a tight ion-pair, while it was high for polymers that tended to dissociate to form 'free' ions; activity decreased in the order: Cl^- > BF_4^- (tetrafluoroborate) > ClO_4^- (perchlorate) > PF_6^- (hexafluorophosphate). In addition, antibacterial activity was found to increase with homo-polymer molecular weight and also with the mole fraction of phosphonium salt monomer in the co-polymers. Polymeric phosphonium salts with particularly long alkyl chain were studied.[69] The antibacterial activity of polymeric versions of **107a–c** decreased with an increase in chain length. In contrast, the reverse trend in activity was observed for the low molecular weight compounds **106a–c** and **107a–c**. In this case, activity increased with an increase in chain length. In addition to the study of polymeric phosphonium salts, Endo has managed to successfully immobilize phosphonium salts (*para*-isomeric versions of **105b** and **105c**) onto the surface of poly(propylene) by photografting.[44] The resultant phosphonium salt films were found to exhibit high surface bactericidal activity. Finally, Endo has investigated co-polymers of the *para*-isomeric version of **105b** and the analogous quaternary ammonium monomer (*p*-**105b**, but with P^+ replaced with N^+).[37] Antibacterial activity was found to increase with the mole fraction of phosphonium salt monomer in the co-polymers. Mixtures of phosphonium salt homo-polymers and quaternary ammonium salt homo-polymers (prepared from the same monomers used in the co-polymerization studies) were also examined. Maximum antibacterial activity was achieved with an optimum mixture of the two homo-polymers.

Inspired by the above research it was decided to prepare a selection of Endo's phosphonium salt monomers and polymers and test them for antimicrobial activity against *Saccharomyces cerevisiae* EL1 in apple juice and orange juice.

3.2.2 Monomer and Polymer Synthesis

The polymerizable phosphonium salts **105a–d** (Scheme 7) were prepared by the method published by Endo.[67] A solution of *m/p*-vinylbenzyl chloride **108** in solvent (toluene, *n*-hexane, or tetrahydrofuran) was stirred, separately, with each of the phosphines **110a–d** to afford the following phosphonium salts: triethyl **105a** [mp 160 °C (*c.f.* lit.,[67] 169–171 °C); 42%], tri-*n*-butyl **105b** [mp 136 °C (*c.f.* lit.,[67] 135–137 °C); 61%], tri-*n*-octyl **105c** (gum), and triphenyl **105d** [mp 252 °C (*c.f.* lit.,[67] 256 °C); 24%]. Endo prepared the phosphonium salts **105a–d** from a sample of *m/p*-vinylbenzyl chloride **108** that was composed of 68% *meta*-isomer and 32% *para*-isomer. The sample of *m/p*-vinylbenzyl chloride **108** (Dow Chemicals) used in the present studies was confirmed by ^{1}H NMR spectroscopy (250 MHz, $CDCl_3$) to be composed of approximately 60% *meta*-isomer and 40% *para*-isomer. As a result, Endo's phosphonium salt series **105a–d** are slightly more enriched (by ~8%) with *meta*-isomer in comparison to the series **105a–d** prepared for the present studies. This means that the melting points for each series should be slightly different. For comparative purposes, the melting points of **105a–d** from the Endo preparation are indicated parenthetically in the melting point data listed above.

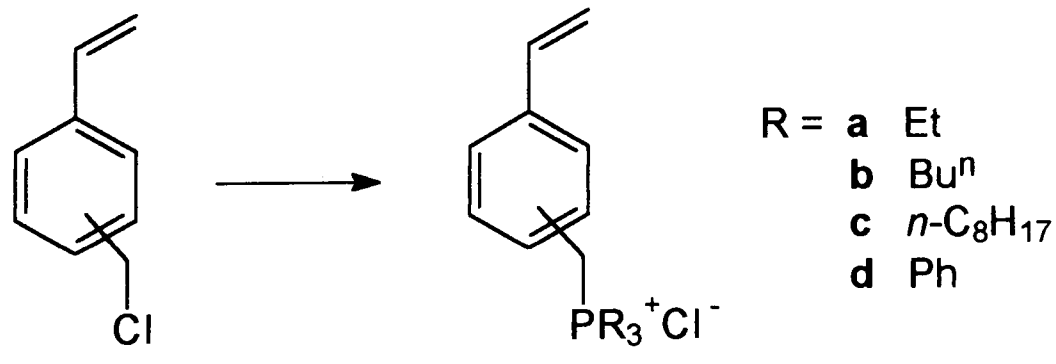

108 *m/p*-mixture
109 *p*-isomer

105 *m/p*-mixture
111 *p*-isomer

Scheme 7 *Reagents and conditions:* PR_3 **110**, solvent (toluene, *n*-hexane or THF), r.t. , 2–5 d (N_2).

Endo published microbiological data for *m/p*-isomeric mixtures of **105a–d** only. Consequently, it was decided to prepare the corresponding *para*-isomeric phosphonium salts in order to determine if substitution of the vinyl group had an effect on antimicrobial activity. The *para*-isomeric phosphonium salt monomers **111b–d** were prepared in a similar manner to that of **105a–d** with the exception that pure *p*-vinylbenzyl chloride **109** (Kodak) was used instead of **108**: tri-*n*-butyl **111b** (mp 123 °C), tri-*n*-octyl **111c** (gum), and triphenyl **111d** (mp 160 °C; 21%). The triethyl salt **111a** was not prepared. A summary of yields and melting points for the series of phosphonium salts **105** and **111** is presented in Table 2.

Table 2 Synthesis of polymerizable phosphonium salts **105** and **111** (Scheme 7).

	105 (*m/p*-isomeric mixture)		**111** (*p*-isomer)	
R	Yield (%)[a]	Mp (°C)	Yield (%)[a]	Mp (°C)
a Et	42	160	Not synthesized	
b Bu^n	61	136	—	123
c *n*-C_8H_{17}	—	gum	—	gum
d Ph	24	252	21	160

[a]Isolated yield.

The series of phosphonium salts **105** and **111** were characterized by elemental microanalysis, FTIR and ^{1}H NMR spectroscopic techniques. IR and ^{1}H NMR spectroscopy revealed that the majority of the phosphonium salts were hydrated to varying degrees. The degree of hydration was calculated from elemental microanalytical data (see section 2.3.2 for further details) and ranged from 0.33–1.9 molecules of water per phosphonium salt molecule. Selected ^{1}H NMR spectral data for the series of phosphonium salts **105** and **111** is presented in Tables 3 and 4 respectively.

The series of phosphonium salts **105** and **111** were tested for antimicrobial activity. The MIC values were determined in NAJ and SOJ media against the yeast strain *Saccharomyces cerevisiae* EL1; the concentration test range was 1000–1 μg cm^{-3}. The data obtained from the MIC tests is summarized in Table 5. It came as a disappointment to find that all but one of the phosphonium salts tested were inactive. All had MIC values ≥1000 μg cm^{-3} except for that of the tri-*n*-octyl monomer **105c**, MIC = 62.5

Table 3 Partial ^{1}H NMR (δ/ppm; *J*/Hz) spectral data[a] for the polymerizable phosphonium salts **105** (Scheme 7). *N.b.* '*m*' – *meta*-isomer; '*p*' – *para*-isomer.

	R			
	a Et	**b** Bu^n	**c** n-C_8H_{17}	**d** Ph
Me	1.17 (t, *J* 7.7, *m* or *p*) 1.25 (t, *J* 7.7, *m* or *p*)	0.90 (t, *J* 6.7, *m* & *p*)	0.85 (t, *J* 6.5, *m* & *p*)	—
$ArCH_2PCH_2$	2.4–2.6 (m, *m* & *p*)	2.40 (br m, *m* & *p*)	2.37 (br m, *m* &.*p*)	—
$ArCH_2P$	4.24 (d, $J_{H,P}$ 15.4, *m* & *p*)	4.27 (d, $J_{H,P}$ 15.3, *m* & *p*)	4.25 (d, $J_{H,P}$ 15.2, *m*) 4.26 (d, $J_{H,P}$ 15.2, *p*)	5.47 (d, $J_{H,P}$ 14.5, *m* & *p*)
$CH=CHH_{cis}$	5.28 (d, *J* 10.9, *m* & *p*)	5.29 (d, *J* 10.9, *m* & *p*)	5.28 (d, *J* 10.7, *p*) 5.29 (d, *J* 10.7, *m*)	5.10 (d, *J* 11.0, *m*) 5.22 (d, *J* 10.8, *p*)
$CH=CHH_{trans}$	5.73 (d, *J* 17.7, *p*) 5.78 (d, *J* 17.5, *m*)	5.74 (d, *J* 17.6, *p*) 5.77 (d, *J* 17.5, *m*)	5.74 (d, *J* 16.8, *p*) 5.78 (d, *J* 17.6, *m*)	5.40 (d, *J* 17.4, *m*) 5.66 (d, *J* 17.5, *p*)
$CH=CH_2$	6.66 (dd, *J* 17.6 and 10.8, *m* & *p*)	6.67 (dd, *J* 17.6 and 10.9, *m* & *p*)	6.66 (dd, *J* 17.9 and 11.0, *m* & *p*)	6.43 (dd, *J* 17.4 and 11.0, *m*) 6.59 (dd, *J* 17.5 and 10.8, *p*)

[a]Recorded at 250 MHz in $CDCl_3$.

Table 4 Partial ^{1}H NMR (δ/ppm; *J*/Hz) spectral data[a] for the polymerizable phosphonium salts **111** (Scheme 7).[b]

	R		
	b Bu^n	**c** n-C_8H_{17}	**d** Ph
Me	0.88 (br t, *J* 6.5)	0.85 (t, *J* 6.3)	—
$ArCH_2PCH_2$	2.35 (br m)	2.37 (br m)	—
$ArCH_2P$	4.27 (d, $J_{H,P}$ 15.4)	4.27 (d, $J_{H,P}$ 15.4)	5.44 (d, $J_{H,P}$ 14.7)
$CH=CHH_{cis}$	5.26 (d, *J* 10.9)	5.27 (d, *J* 10.9)	5.21 (d, *J* 10.9)
$CH=CHH_{trans}$	5.72 (d, *J* 17.5)	5.74 (d, *J* 17.6)	5.65 (d, *J* 17.6)
$CH=CH_2$	6.65 (dd, *J* 17.5 & 10.9)	6.66 (dd, *J* 17.6 & 10.9)	6.58 (dd, *J* 17.6 & 10.9)

[a]Recorded at 250 MHz in $CDCl_3$. [b]The tri-*n*-butyl salt **111a** was not prepared.

$\mu g\ cm^{-3}$ in NAJ (despite MIC values of >1000 $\mu g\ cm^{-3}$, **105d** and **111d** were the only compounds to show inhibitory effects: **105d** down to 31.25 $\mu g\ cm^{-3}$, and **111d** down to 62.5 $\mu g\ cm^{-3}$). Endo tested his phosphonium salt series **105a–d** against *Staphylococcus aureus* and *Escherichia coli* and found that the most active member of the series was the tri-*n*-octyl monomer **105c**.[67] The above MIC results therefore support Endo's finding.

Overall, Endo showed the phosphonium salt series **105a–d** to be more microbiologically active than the in-house synthesized phosphonium salt series. It is important to point out, however, that Endo's compounds were tested against *bacteria* (*viz. Staphylococcus aureus* and *Escherichia coli*), whereas the in-house compounds were tested against a *yeast* organism (*viz. Saccharomyces cerevisiae*). Bacteria and yeasts are different classes of micro-organism and consequently they have completely different structures (refer to section 1.2.1, *The Structure of Micro-organisms*, for further details). The microbiological activity of a given chemical species might therefore be expected to vary from one type of organism to another.

Table 5 MIC data[a] for the polymerizable phosphonium salts **105** and **111** (Scheme 7). *N.b.* '—' – not prepared.

	NAJ[b]: MIC/$\mu g\ cm^{-3}$		SOJ[c]: MIC/$\mu g\ cm^{-3}$	
R	**105**	**111**	**105**	**111**
a Et	1000	—	>1000	—
b Bu^n	>1000	>1000	>1000	N/A
c *n*-C_8H_{17}	62.5	N/A	N/A	N/A
d Ph	>1000[d]	>1000[e]	>1000	N/A

[a]Test organism, *Saccharomyces cerevisiae* EL1. [b]Norwegian apple juice. [c]Sainsbury's orange juice. [d,e]Inhibitory effect down to: [d]31.25, [e]62.5 $\mu g\ cm^{-3}$.

As mentioned in the introduction, it is generally found that polymeric phosphonium salts have higher antibacterial activities than the corresponding low molecular weight compounds. A cationic polymer has a higher positive charge density than the corresponding monomer and, as a result, the former can more effectively adsorb onto cell surfaces.[67] The tri-*n*-butyl phosphonium salt monomer **105b** was selected for polymerization. This would allow a comparison to be made between the activities of the monomer and polymer. The monomer **105b** was homo-polymerized

(Scheme 8) according to the published method.[67] Monomer **105b** and initiator, 2,2'-azobis(2-methylpropionamidine) dihydrochloride, were dissolved in water and the solution degassed (freeze-pump-thaw method) and then heated at 60 °C for 5.5 h. The crude product was dissolved in methanol and precipitated into diethyl ether to afford the homo-polymer **112b** as a white solid (66% conversion). ^{1}H NMR spectroscopy (250 MHz, CD_3OD) of **112b** revealed a series of broad signals, characteristic of those found in typical polymer spectra. Notably prominent signals were those due to the *n*-butyl chain: δ 0.94 (3 x CH_3), 1.47 [3 x $CH_2(CH_2)_2CH_3$] and 2.20 [3 x $CH_2(CH_2)_2$-CH_3] ppm. The Ar–CH_2–P signal appeared as a very broad singlet at δ 3.8 ppm, while the aromatic protons were found at δ 6.5 and 7.11 (each, a broad singlet) ppm. The polymer **112b** was soluble in water and had an MIC of >1000 μg cm^{-3} in NAJ but exhibited an inhibitory effect down to 125 μg cm^{-3} (*c.f.* monomer **105b**, MIC = >1000 μg cm^3 in NAJ; no inhibitory effect observed).

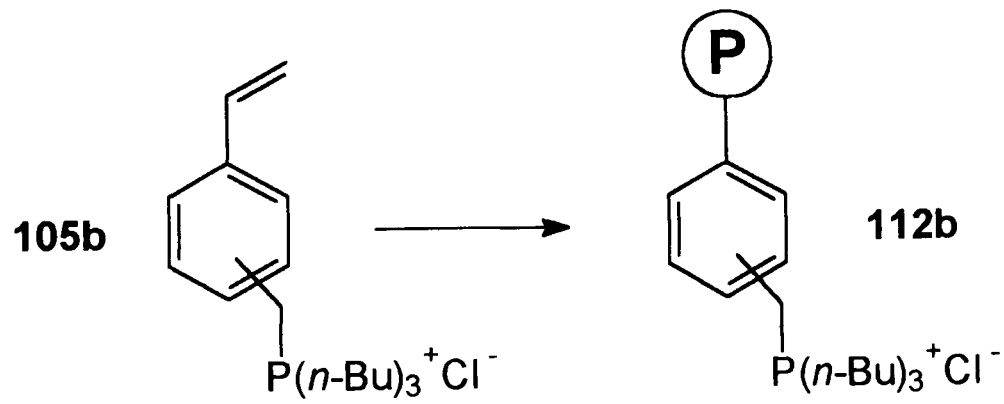

Scheme 8 *Reagents and conditions:* 2,2'-azobis(2-methylpropionamidine)•2HCl, H_2O, 60 °C, 5½ h.

In conclusion, the most active monomer tested from the series **105a–d** was the tri-*n*-octyl phosphonium salt **105c**. This result supports the general finding that cationic biocides with long alkyl chains are more active than those with shorter chains. The tri-*n*-butyl homo-polymer **112b** was found to inhibit yeast growth more than the corresponding monomer **105b**. This result is in agreement with the finding that polymeric cationic biocides generally tend to be more active than the corresponding low molecular weight compounds.

3.2.3 Other Polymerizable and Polymeric Phosphonium Salts

The phosphonium salt monomer **105** (Scheme 7) essentially consists of a hydrophilic functionality (the phosphonium salt, $-PR_3^+Cl^-$) and a hydrophobic functionality (the vinylbenzyl group, $-C_6H_4CH=CH_2$). The polymerizable phosphonium salts **113–116** (Figure 30) are considerably more hydrophilic in nature than **105** and may prove worthy of study in the future. The methacrylate monomer **113** and the methacrylamide monomer **114** are both derived from methacrylic acid. In each of these examples, the vinyl and phosphonium salt groups are separated by a dimethylene bridge. Further structural variation on **113** and **114** might include a longer hydrocarbon bridge or, alternatively, a more hydrophilic bridge (*e.g.* an ether bridge). The final two polymerizable phosphonium salts shown in Figure 30 are based on vinyl ethers. Compound **115** is similar to that of **113** and **114** as it has a dimethylene bridge separating the phosphonium salt and vinyl groups. The vinyl ether **116** contains an ethoxy group as part of the bridge and therefore serves as a more hydrophilic variant of **115**.

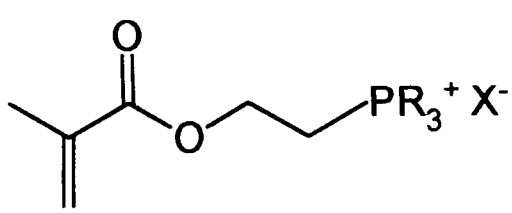

113

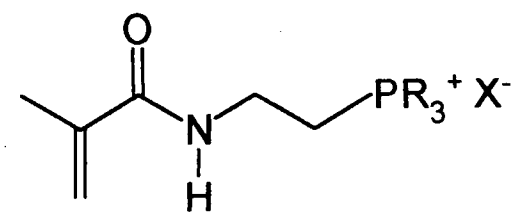

114

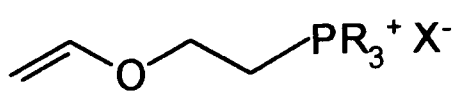

115

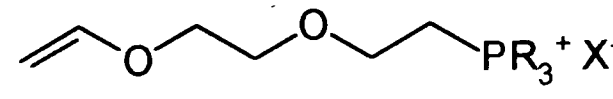

116

Fig. 30 Candidates for polymerizable phosphonium salts.

In his co-polymer studies[68] Endo employed styrene, acrylamide and *N*-vinyl-2-pyrrolidone as co-monomers with the tri-*n*-butyl phosphonium salt monomer **105b** (Scheme 7). Two additional co-monomers worthy of study are 2-hydroxyethyl methacrylate (HEMA) **117** and dodecyl methacrylate **118** (Figure 31). A co-polymer comprised of the monomers **105** and **117** would be considerably hydrophilic in nature; this enhanced hydrophilicity may prove to be an important contributory factor to the

polymer's bactericidal effectiveness. Alternatively, **105** might be co-polymerized with the hydrophobic monomer **118**. As mentioned previously, an important feature of cationic biocides is the possession of a long alkyl chain. A co-polymer of **105** and **118** would effectively possess two different antimicrobial functionalities, a trialkylphosphonium salt and a dodecyl group. It would prove interesting to correlate co-polymer composition with antibacterial activity. Such a study would reveal the optimum 'balance' required of the two functionalities for maximum antibacterial activity.

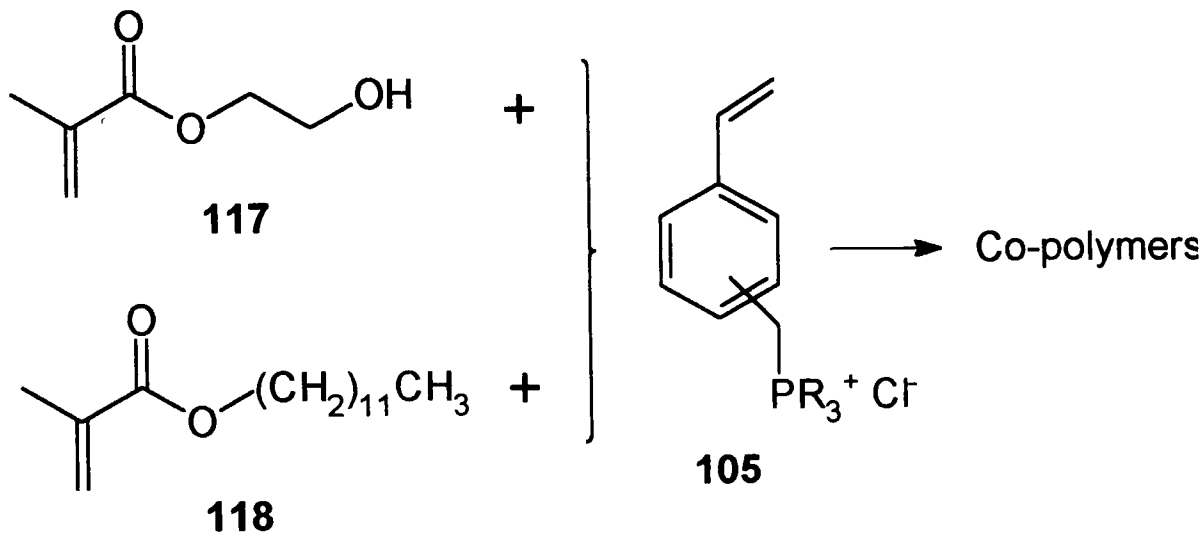

Fig. 31 Phosphonium salt co-polymers – suggested co-monomers.

3.3 *Diiodomethyl Sulfones*

3.3.1 Introduction

As discussed in the introductory chapter an important class of antimicrobial agents are the *activated halogen compounds*. The key structural feature of these molecules can be represented as X–C–E, where X is a halogen atom (X = Cl, Br or I) and E is an electron-withdrawing group (*e.g.* $CONH_2$, CO_2R, CN, NO_2). The antimicrobial efficacy of these compounds is induced by the activation of the halogen atom by electron-withdrawing groups in direct proximity to it.

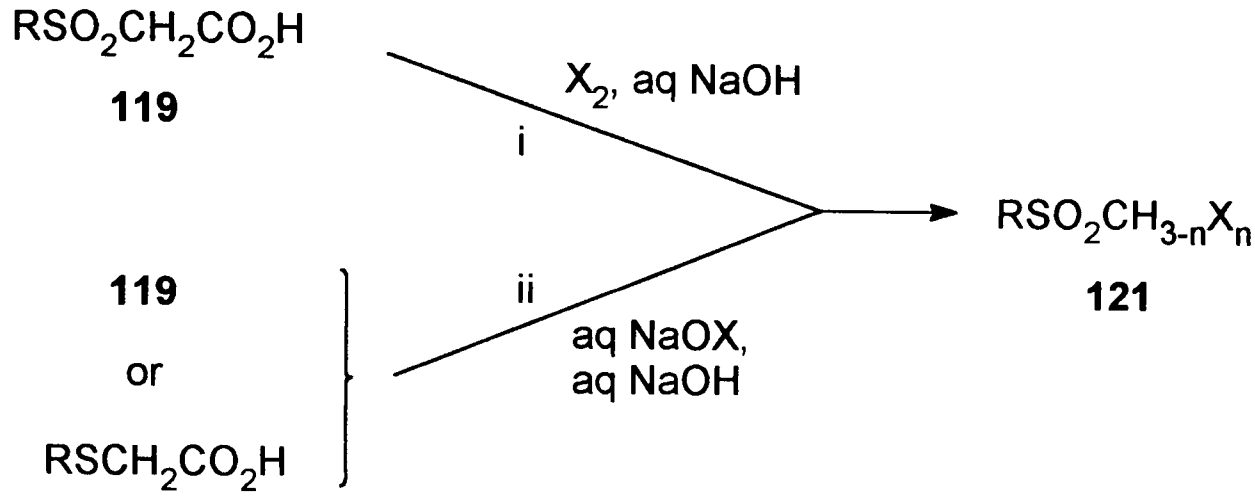

Scheme 9 Preparation of halomethyl sulfones (R = alkyl, aryl or Ph; n = 1–3).

When E = SO_2R (R = alkyl, aryl or Ph) the subsequent compounds are referred to as *halomethyl sulfones*, and have the general formula $RSO_2CH_{3-n}X_n$, where n = 1–3. Two synthetic procedures commonly used to prepare halomethyl sulfones are shown in Scheme 9. In the first of these (Route i), the substituted sulfonylacetic acid **119** is treated with an aqueous solution of sodium hydroxide and a halogen at neutral pH.[70] Halogenation followed by decarboxylation yields the halomethyl sulfone **121**. In the second procedure (Route ii), **119** (or its ester) is halogenated with sodium hypohalite in an alkaline aqueous solution to produce **121**.[71] Alternatively, the aryl thioacetic acid **120** (R = Ar) can be halogenated with sodium hypohalite.[71] In this case, oxidation of the sulfur to the sulfonyl group occurs in addition to halogenation and

decarboxylation. The number of halogen atoms in the halomethyl sulfone **121** depends on the relative stoichiometric proportions of sulfonylacetic acid **119** (or **120**) and halogen (or hypohalite) used in the reaction – a proportionately larger quantity of the latter will result in a greater degree of halogenation.

The halomethyl sulfones **121** produced in this way are commonly used as protective coatings for foams, latex and textiles against the degradative effects of fungi and bacteria.[70] The *diiodomethyl sulfones* (X = I, n = 2) are especially useful as antifungal and antibacterial coatings.[70–72] The present studies are concerned, in particular, with *diiodomethyl*-p-*tolylsulfone*, $MeC_6H_4SO_2CHI_2$.

3.3.2 Diiodomethyl-*p*-tolylsulfone (Amical)

Diiodomethyl-*p*-tolylsulfone **125** (Scheme 10) commonly goes under the trade name *Amical*. Apart from being used as an antifugal and antibacterial coating (as previously cited) Amical is also used as a pesticide against ants, termites and cockroaches.[73] It was decided to investigate further Amical's antimicrobial activity. A sample of Amical was first prepared and tested and then potentially interesting polymerizable and polymeric Amical analogues were considered.

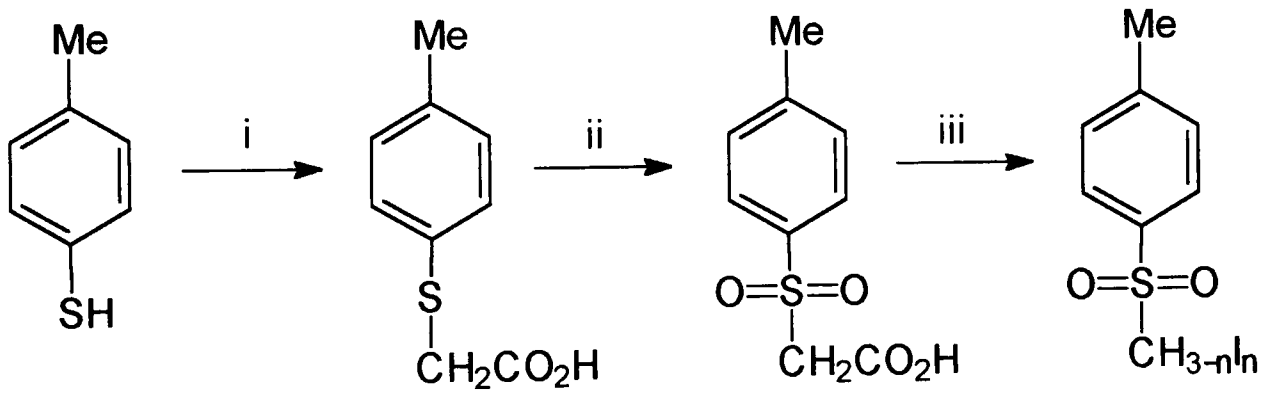

122 **123** **124** **125** n = 2 **126** n = 1

Scheme 10 *Reagents and conditions:* i, $ClCH_2CO_2H$, NaOH (aq), Δ, 2 h; ii, H_2O_2 (aq), AcOH, r.t., 6 h; iii, NaOH (aq), I_2, 0–5 °C, 2 h.

A sample of Amical was prepared according to the synthetic route shown in Scheme 10. The synthesis used a combination of two literature methods: the method of Kenney *et al.*[74] was followed to prepare the sulfonylacetic acid **124**, and then the

method of Ammo *et al.*[72] was used to convert **124** into Amical **125**. A solution of *p*-thiocresol **122** in aqueous sodium hydroxide solution was refluxed with chloroacetic acid to give *p*-tolylmercaptoacetic acid **123** (45% yield), mp 92–93 °C (lit.,[74] 88.5–90 °C), MIC = 250 μg cm^{-3} (NAJ) and >500 μg cm^{-3} (MOJ). Oxidation of a solution of **123** in acetic acid with aqueous hydrogen peroxide solution yielded *p*-tolylsulfonyl-acetic acid **124** (29% yield), mp 110–115 °C (lit.,[74] 114–115 °C), MIC = >1000 μg cm^{-3} (NAJ) and >1000 μg cm^{-3} (MOJ). Finally, a solution of **124** in aqueous sodium hydroxide was stirred with a 3 molar excess of iodine (w.r.t. *p*-tolylsulfonylacetic acid **124**) to afford diiodomethyl-*p*-tolylsulfone (Amical) **125** (82% yield) as a dark-tan powder, mp 134–135 °C (lit.,[72] 148–148.5), MIC = <1 μg cm^{-3} (NAJ) and 1.95 μg cm^{-3} (MOJ). ^{1}H NMR spectroscopy was used to calculate the percentage purity of the product. The results revealed that the reaction product was composed of 89% Amical **125** and 11% of the mono-iodo Amical analogue, iodomethyl-*p*-tolylsulfone **126**. The percentages were calculated by integration of the CHI_2 and CH_2I signals: **125** $MeC_6H_4SO_2CHI_2$ (singlet, δ 5.96 ppm), **126** $MeC_6H_4SO_2CH_2I$ (singlet, δ 4.45 ppm).

Table 6 Compositions and melting points of mixtures of Amical **125** and its mono-iodo analogue **126** and how they vary with the molar excess of iodine used in the synthesis (Scheme 10, Route iii).

	Composition[a]			
Molar excess I_2[b]	**125** (%)	**126** (%)	Appearance	Mp (°C)
0	trace	~100	white powder	125–127
1.2	10	90	off-white powder	112–114
2.0	59	41	light tan powder	101–103
3.0	89	11	dark tan powder	134–135

[a]Determined by ^{1}H NMR spectroscopy (250 MHz, $CDCl_3$). [b]W.r.t. *p*-tolylsulfonylacetic acid **124** (Scheme 10).

The iodonation reaction (Scheme 10, Route iii) was repeated using molar excesses of iodine (w.r.t **124**) in the range 0–3. Obtained from these experiments were various mixtures of Amical **125** and the mono-iodo Amical analogue **126**. A summary of the compositions and melting points of these **125/126** mixtures is presented in Table 6. When a 0 molar excess of iodine was used the mono-iodo Amical analogue, iodomethyl-*p*-tolylsulfone **126** (39% yield) was produced as a white powder, mp 125–

127 °C, MIC = 3.9 μg cm^{-3} (NAJ) and 125 μg cm^{-3} (MOJ). ^{1}H NMR spectroscopy revealed that **126** was ~100% pure, with only a trace impurity of Amical **125**. Similarly, iodine molar excesses of 1.2 and 2.0 yielded **125/126** mixtures of 10%/90% (mp 112–114 °C) and 59%/41% (mp 101–103 °C) respectively. For comparative purposes a sample of Amical was purchased from Angus Chemicals. The finely divided tan powder (trade name, Amical 48), mp 142–145 °C (lit.,[75] 157 °C), MIC = <1 μg cm^{-3} (NAJ) and 3.9 μg cm^{-3} (MOJ), was shown by ^{1}H NMR spectroscopy to be ~94% pure, with a ~6% impurity of the mono-iodo Amical analogue **126**. A summary of yields, melting points and MIC values of a selection of the compounds discussed above is presented in Table 7.

Table 7 Synthesis of Amical **125** and the mono-iodo Amical analogue **126** (Scheme 10) plus comparative data for Amical 48.

				MIC[a]/μg cm^{-3}	
Compound	Yield (%)[b]	Mp (°C)	Lit. mp (°C)	NAJ[c]	MOJ[d]
123	45	92–93	88.5–90[74]	250	>500
124	29	110–115	114–115[74]	>1000	>1000
125[e]	82	134–135	148–148.5[72]	<1	1.95
126[f]	39	125–127	—	3.9	125
Amical 48[g]	—	142–145	157[75]	<1	3.9

[a]Test organism, *Saccharomyces cerevisiae* EL1. [b]Isolated yield. [c]Norwegian apple juice. [d]Mills orange juice. [e]11% Impurity of **126**. [f]Trace impurity of **125**. [g]Angus Chemicals (composition: 94% **125**, 6% **126**).

As can be seen from the MIC data shown in Table 7 both the Amical precursors **123** and **124** are relatively inactive. However, both Amical **125** and the mono-iodo Amical analogue **126** are quite potent antimicrobial agents (especially in NAJ). In addition, the MIC values obtained for the Angus Chemicals Amical agreed quite favourably with the values obtained for the in-house synthesized Amical.

3.3.3 Polymerizable Aromatic Diiodomethyl Sulfones

Due to the favourable MIC results obtained for Amical **125** it was decided to try to synthesize a series of polymerizable Amical analogues and then attempt their polymerization. Unfortunately, time restrictions prevented this work. However, suggested

routes to three 'simple' polymerizable aromatic diiodomethyl sulfones are shown in Figure 32. The synthesis of Amical **125** (Scheme 10, Route iii) relies on having a molecule with an aromatic sulfonylacetic acid group ($ArSO_2CH_2CO_2H$). The latter can, in turn, be prepared from an aromatic thiol (ArSH) via the aromatic sulfide ($ArSCH_2CO_2H$). A potential precursor towards a polymerizable diiodomethyl sulfone would therefore be a di-substituted thiophenol with a functional handle, the latter of which could be used to add on a vinyl group. Molecules fitting these criteria are *p*-hydroxythiophenol **127a** and *p*-aminothiophenol **128a**, both commercially available materials. Thus **127a** and **128a** could be used as starting materials towards the synthesis of the acrylate **127b** and the acrylamide **128b** respectively. However, due to the di-functional nature of both precursors it would have to be decided on the best time to introduce the acrylation step into the overall reaction scheme, *i.e.* before, during, or after the conversion $SH \rightarrow SO_2CHI_2$ (Scheme 10). A final candidate for a polymerizable aromatic diiodomethyl sulfone is the vinyl compound **129b**. This could be prepared from *p*-vinylthiophenol **129a**. However, the latter is not a commercially available material and would therefore have to be synthesized beforehand.

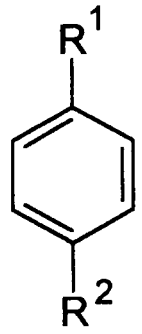

127a $R^1 = OH$, $R^2 = SH$
127b $R^1 = OC(O)CH=CH_2$, $R^2 = SO_2CHI_2$
128a $R^1 = NH_2$, $R^2 = SH$
128b $R^1 = NHC(O)CH=CH_2$, $R^2 = SO_2CHI_2$
129a $R^1 = CH=CH_2$, $R^2 = SH$
129b $R^1 = CH=CH_2$, $R^2 = SO_2CHI_2$

Fig. 32 Suggested routes to polymerizable diiodomethyl sulfones.

3.3.4 UV Spectrophotometric Studies of Amical Decomposition

Introduction

Samples of Amical **125** (Scheme 10) were submitted for ^1H NMR spectral analysis. The NMR laboratory returned the samples as solutions in the solvent used for the NMR experiment, in this case deuteriochloroform. It was observed that the deuteriochloroform solutions were all violet in colour. Although not directly relevant to the

research detailed in this thesis this observation was found sufficiently interesting to merit further investigation.

It is a well-known observation that if iodine is dissolved in organic solvents the resultant solutions are tinted characteristic colours. For example, a solution of iodine in ethanol is pale brown in colour, whereas a chloroform solution of iodine is violet in colour (*c.f.* observation in previous paragraph). In order to investigate the violet colour of the NMR solutions a series of UV spectrophotometric experiments were carried out. A solution was freshly prepared of Amical (Angus Chemicals) in chloroform. The UV spectrum was run immediately and revealed a single, intense, off-scale band centered at ~316 nm (Figure 33, broken line). The sample was removed from the UV instrument and left to stand in daylight, at room temperature. After only a few minutes the chloroform solution (originally colourless) had turned a pale violet colour, with the violet intensity gradually increasing with time. The solution was left to stand in daylight for 35 min after which time a second UV spectrum was taken. This time, in addition to the aforementioned 316 nm band, the spectrum revealed a broad, lower intensity band at 512 nm (Figure 33, solid line). It was suspected that the 512 nm band was due to iodine produced from the breakdown of Amical. In order to check this suspicion a solution was prepared of iodine in chloroform and the UV spectrum taken. The spectrum showed a sharp band at 241 nm and a broad, intense band at 512 nm (Figure 34). The above experiments therefore confirmed the original suspicion that Amical in chloroform breaks down (in a manner yet to be ascertained) to form molecular iodine, giving rise to a characteristic iodine peak in the UV spectrum at 512 nm. Note that the violet colour of the Amical solution cannot be attributed to an iodine impurity in the Amical sample. If this were true the chloroform would *immediately* turn violet on addition of the Amical – this is not observed. The following questions now arise: (i) is the Amical breakdown process affected by either light or concentration?; and (ii) how much Amical breaks down to form iodine? (all the sample or only a fraction of it?). In order to help attempt to answer these questions a further series of UV experiments were performed.

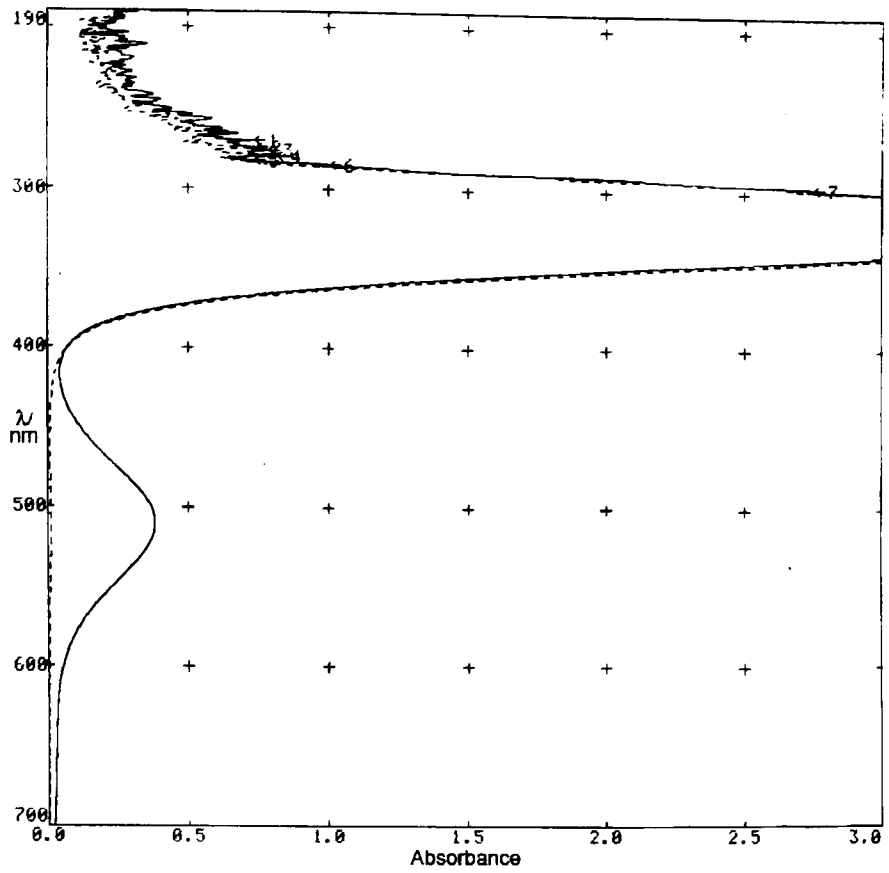

Fig. 33 UV Absorbance spectrum of a solution of Amical **125** (Scheme 10) in chloroform (0.0079 mol dm^{-3}) left in daylight. Note the appearance, with time, of the I_2 band at 512 nm: broken line, t = 0 min, A_{512} = 0.013; solid line, t = 35 min, A_{512} = 0.274.

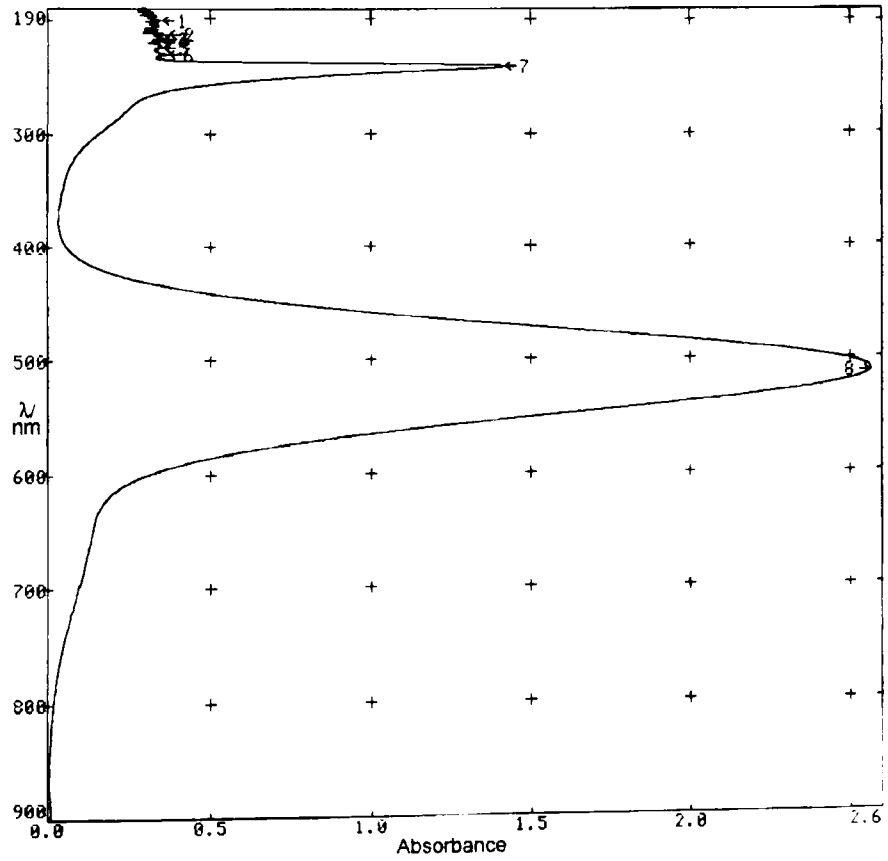

Fig. 34 UV Absorbance spectrum of a solution of I_2 (Fisons) in chloroform. Note the prominent band at 512 nm.

Effect of Light on Amical Breakdown

The first of these experiments examined the effect of light on Amical breakdown. An accurately weighed sample of Amical (10.0 mg) was placed into a 1 cm UV quartz-glass cuvette (fitted with stopper). The cuvette was then charged with chloroform (3.00 cm^3), measured from a graduated pipette. This produced an approx. 0.0079 mol dm^{-3} solution of Amical in chloroform. The cuvette was stoppered, quickly shaken and placed immediately in the UV spectrophotometer. Fixed wavelength (512 nm) absorbance measurements were then made at periodic intervals, over the course of one hour. During the period between measurements the cuvette was removed from the UV instrument and left to stand in daylight. In addition, the cuvette was briefly shaken prior to each absorbance measurement. The above experiment was repeated on a freshly prepared Amical solution of identical concentration (0.0079 mol dm^{-3}) to that used in the previous experiment. This time, however, the cuvette was left inside the UV instrument, in darkness, throughout the course of the absorbance measurements. A third experiment was performed on a fresh solution of Amical (0.0079 mol dm^{-3}). This time, in the period between absorbance measurements, the cuvette was placed under a UV light source (a hand-held 254 nm UV lamp of the type commonly used for viewing TLC plates). The results obtained from these experiments are shown in Table 8,[‡] with the data represented graphically in Figure 35. As can be seen from Figure 35 the rate of Amical breakdown to iodine increased in the order, darkness < daylight < UV light. In the case of the UV light irradiated sample the rate of iodine production levelled off after ~35 min but with the sample left in daylight iodine production was steady over the course of one hour. When the Amical sample was kept in darkness iodine formation was almost totally suppressed with only a very small, residual absorbance being measured. In conclusion, the above experiment shows that the breakdown of Amical to iodine occurs more readily in the presence of light. The breakdown mechanism therefore appears to be photochemical in nature.

[‡] Tables 8–13 are reproduced at the end of this section.

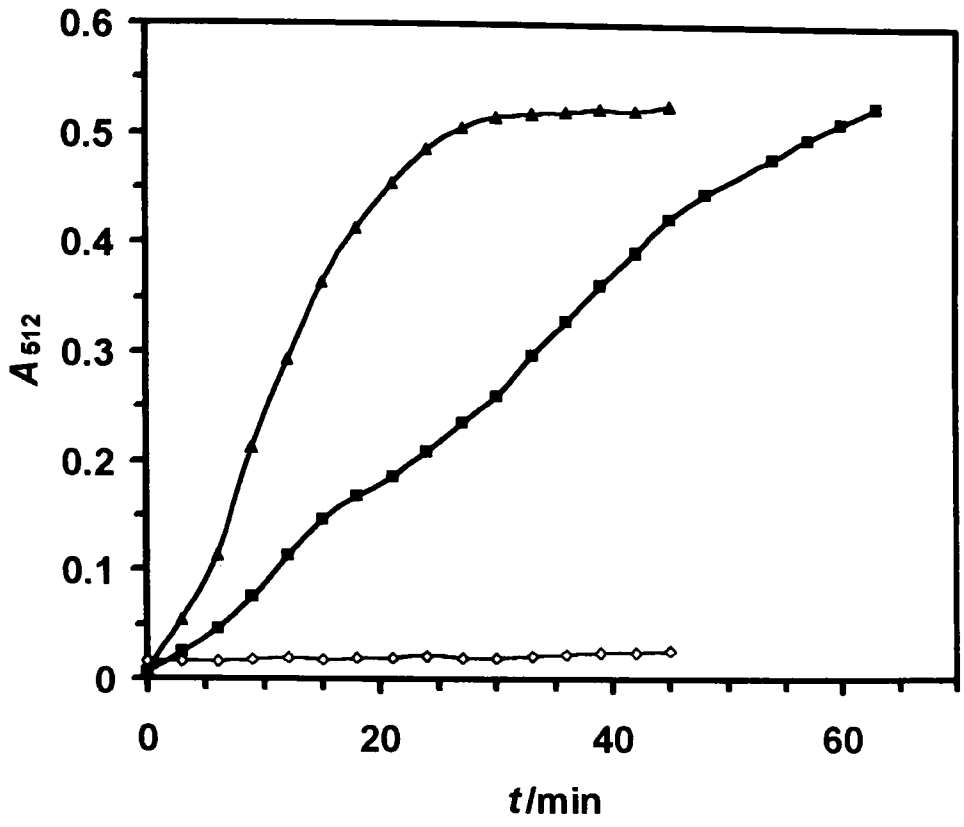

Fig. 35 Plot of I_2 absorbance (A_{512}) *vs.* time for 0.0079 mol dm^{-3} solutions of Amical **125** (Scheme 10) in $CHCl_3$ subjected to UV_{254} light (▲), daylight (■) and darkness (◊). Refer to Table 8 for the raw data.

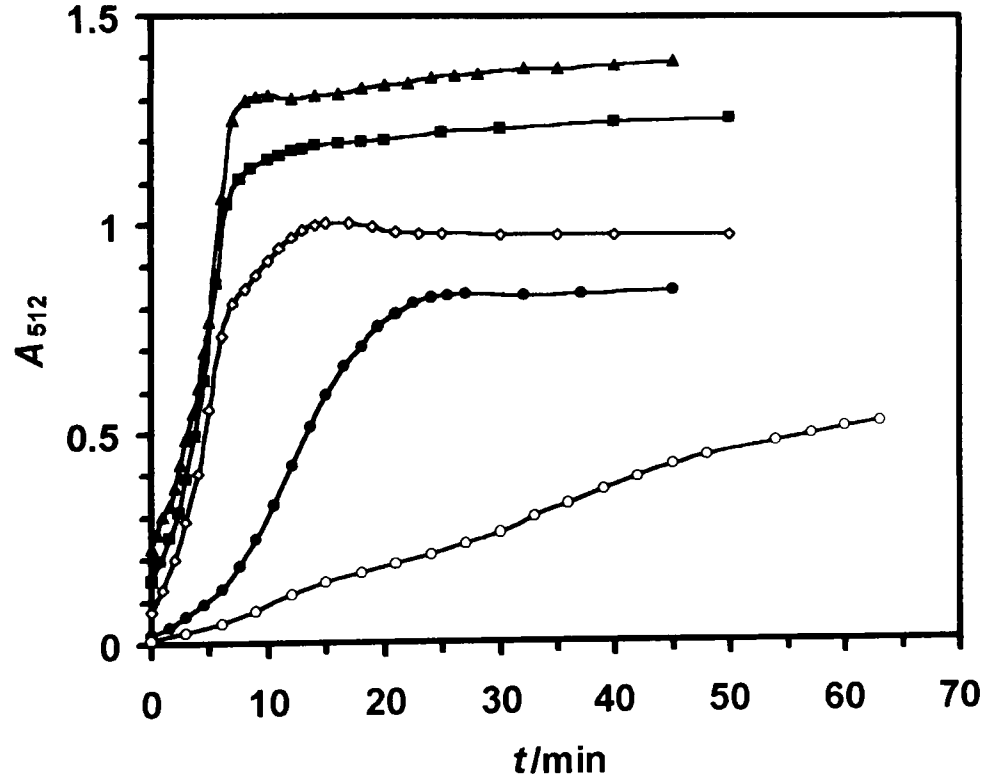

Fig. 36 Plot of I_2 absorbance (A_{512}) *vs.* time for differently concentrated solutions of Amical **125** (Scheme 10) in $CHCl_3$ subjected to daylight: [Amical]/mol dm^{-3} = 0.237 (▲), 0.158 (■), 0.079 (◊), 0.030 (●) and 0.0079 (○). Refer to Table 9 for the raw data.

Effect of Concentration on Amical Breakdown

The second series of experiments examined the effect of concentration on Amical breakdown to iodine. A solution of Amical in chloroform (0.030 mol dm^{-3}) was prepared rapidly in a graduated flask (25 cm^3). During the solution preparation the flask was covered with a towel in order to exclude light. A sample of the solution was transferred to a cuvette. A series of fixed wavelength (512 nm) absorbance measurements were then made at periodic intervals, over the course of about one hour. During the period between measurements the cuvette was removed from the UV instrument and left to stand in daylight. The above experiment was repeated on three further Amical solutions of concentrations 0.237, 0.158 and 0.079 mol dm^{-3}. The results obtained from these experiments (along with the 0.0079 mol dm^{-3} 'daylight' data obtained in a previous experiment – see Figure 35) are shown in Table 9, with the data represented graphically in Figure 36. As can be seen from Figure 36 the rate of Amical breakdown to iodine increased with increasing concentration. Additionally, the time at which the absorbance levelled off decreased with an increase in concentration. For example, in the case of the most concentrated solution (0.237 mol dm^{-3}) the absorbance began to level off after ~10 min. However, with the 0.030 mol dm^{-3} solution the absorbance didn't begin to level off until ~25 min. Finally, as commented on earlier, the absorbance of the 0.0079 mol dm^{-3} solution continued to increase steadily over the course of one hour. The final interesting feature to be noted from Figure 36 is the absorbance level-off values: the more concentrated the solution, the larger the absorbance level-off value. In conclusion, the above experiment shows that with an increase in Amical concentration: (i) the breakdown of Amical to iodine occurs more quickly; and (ii) iodine production reaches a larger plateau value in a faster time.

For UV spectra the Beer–Lambert law states:

$$A = \log (I_o/I) = \varepsilon c l \qquad (1)$$

where A is the solution absorbance, I_o and I are the intensities of the incident and transmitted light respectively, ε is the molar extinction coefficient (cm^{-1} mol^{-1} dm^3), c is the solution concentration (mol dm^{-3}), and l is the path length (cm) of the absorbing solution.

Applying eqn. (1) to the present UV studies it can be seen that iodine absorbance is a direct measure of iodine concentration. The above experiments have shown that Amical breaks down in solution to produce iodine as a by-product. Moreover, iodine production reaches a level-off, or plateau, value after a certain time (Figure 36). Iodine absorbance is therefore a direct measure of the concentration of Amical that has broken down to iodine. If the level-off iodine absorbance is measured for an Amical solution of known concentration then it would be possible to calculate the percentage decomposition of Amical to iodine. Repeating this procedure for a series of Amical solutions of different concentration would therefore enable a correlation to be made between the degree of Amical decomposition and concentration. Such a correlation was made for the concentraion curves shown in Figure 36 and is described as follows.

In order to determine iodine concentrations from the absorbance values an iodine absorbance–concentration calibration graph was calculated. A standard stock solution (0.0020 mol dm^{-3}) of iodine in chloroform was prepared. This solution was used, in turn, to prepare a series of standard solutions with concentrations of 0.0016, 0.0014, 0.0012, 0.001, 0.008, 0.006, 0.004, 0.002 and 0.0001 mol dm^{-3}. Fixed wavelength (512 nm) absorbance measurements were then determined for each solution. The results obtained from these experiments are shown in Table 10, with the data represented graphically in Figure 37. The molar extinction coefficient of iodine in chloroform can now be calculated using the Beer–Lambert law. For the present experiments the path length l = 1 cm and so eqn. (1) simplifies to A_{512} (I_2) = $\varepsilon[I_2]$. A plot of A_{512} versus $[I_2]$ should therefore produce a straight line, intersecting the origin, of slope ε (Figure 37). The slope of the line in Figure 37 is therefore the value of the extinction coefficient ε of iodine in chloroform. Linear regression analysis[76] was performed on the data points in Figure 37 and yielded a value of ε = 894 cm^{-1} mol^{-1} dm^3. Substituting the value of ε into eqn. (1) and rearranging gives,

$$[I_2] = A_{512}/894 \quad [CHCl_3, c = 1 \text{ cm}] \tag{2}$$

Given the absorbance A_{512} of an iodine solution in chloroform it is now possible to calculate the iodine concentration using eqn. (2). Such a calculation was performed for

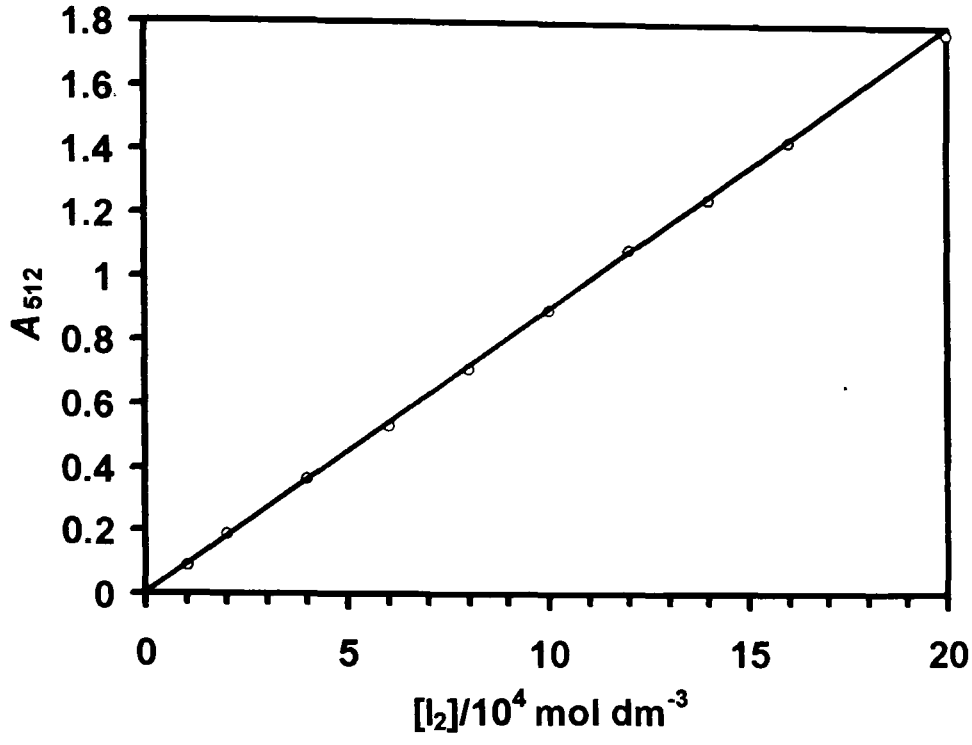

Fig. 37 Plot of I_2 absorbance (A_{512}) *vs.* concentration for solutions of I_2 in $CHCl_3$. Refer to Table 10 for the raw data.

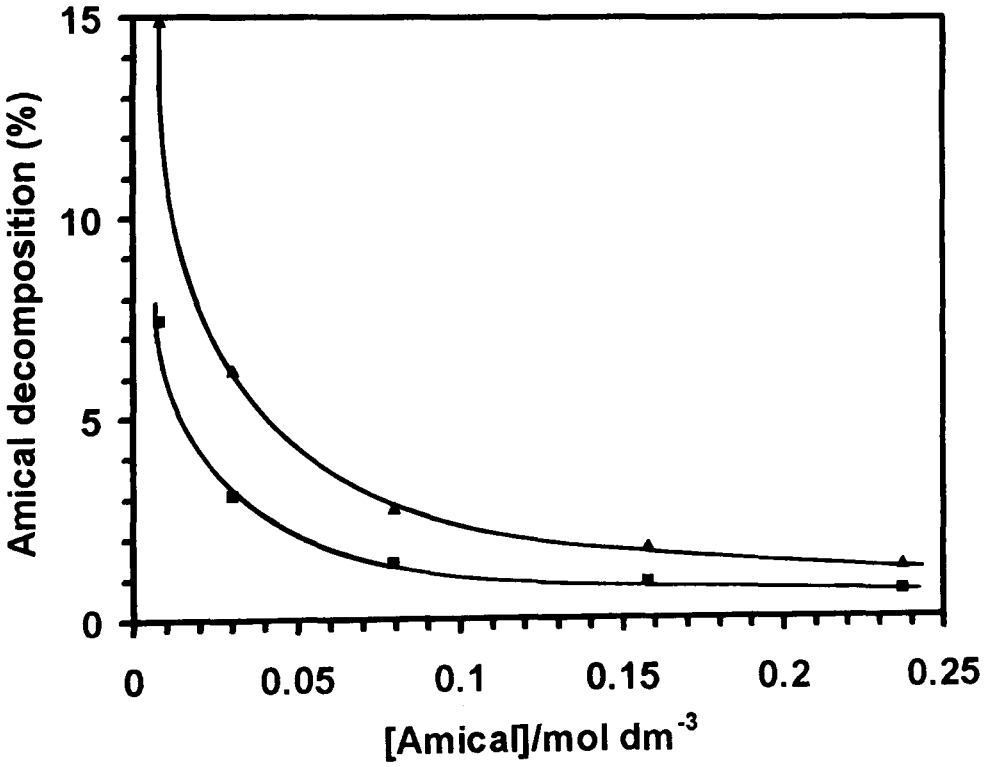

Fig. 38 Plot of Amical **125** (Scheme 10) concentration (in $CHCl_3$) *vs.* percentage of Amical decomposed to I_2. Assumptions: 2 Amical $\rightarrow$ 1 I_2 (▲), 1 Amical $\rightarrow$ 1 I_2 (■). Refer to Table 11 for the raw data.

each of the concentration curves shown in Figure 36. The results are summarized in Table 11. The first column of Table 11 gives the Amical concentration while the second column gives the level-off absorbance value of the 512 nm iodine band. The latter figures were substituted into eqn. (2) and the corresponding iodine concentrations obtained are shown in the third column. With the iodine concentrations now known it is possible to calculate the corresponding percentage decomposition of Amical for each curve in Figure 36. Before this can be done, however, the stoichiometry of the Amical–iodine breakdown process has to be examined more closely.

Leaving aside mechanistic arguments for the moment, consider how many Amical molecules it takes to form one molecule of iodine (I_2) when the former breaks down in solution. One Amical molecule contains two iodine atoms. Firstly, consider the case when both iodine atoms are cleaved in the breakdown process and enter solution. If these atoms each then recombine with another iodine atom the overall effect will be the formation of one molecule of iodine (I_2) for every decomposed Amical molecule. In this case the concentration of decomposed Amical is equivalent to the iodine concentration, *i.e.* $[\text{Amical}]_{\text{decomp}} \equiv [I_2]$. The corresponding percentage of Amical decomposed to iodine can therefore be calculated by simply dividing the iodine concentration (Table 11, column 3) by the Amical solution concentration (column 1) and multiplying the result by 100%. The results of this calculation are shown in the fourth column of Table 11. As can be seen from the data in column four the percentage decomposition of Amical to iodine is inversely proportional to [Amical]. The most concentrated Amical solution examined (0.237 mol dm^{-3}) corresponded to ~0.7% Amical decomposition whereas, at the other end of the scale, the 0.0079 mol dm^{-3} solution corresponded to ~7.5% decomposition. Now consider the case when only one iodine atom is cleaved in the breakdown process. If this atom enters solution and then recombines with another iodine atom the overall effect will be the formation of one molecule of iodine (I_2) for every two decomposed Amical molecules. In this case the concentration of decomposed Amical is equivalent to half the value of the iodine concentration, *i.e.* $[\text{Amical}]_{\text{decomp}} \equiv 0.5[I_2]$. The corresponding percentage of Amical decomposed to iodine can therefore be calculated by multiplying the iodine concentration (Table 11, column 3) by a factor of two and then dividing the result by the Amical solution concentration (column 1). Multiplying the final result by 100% then gives the percentage

decomposition. The results of this calculation are shown in the fifth column of Table 11. As a result of the stoichiometry discussed above, note that the data in the fourth and fifth columns differ by only a factor of two. Figure 38 shows a plot of the calculated percentage decomposition of Amical (Table 11, columns 4 and 5) versus Amical concentration (Table 11, column 1). The conclusion to be made from Figure 38 is that Amical decomposition (whether liberating one or two iodine atoms per molecule) is inversely proportional to concentration, with the nature of the proportionality resembling that of an exponential-like decay curve.

Mechanism of Amical Breakdown

Now consider the mechanism of the breakdown of Amical in solution to form molecular iodine. Suggestions for Amical decomposition modes under acidic, alkaline and photo-chemical conditions are shown in Figure 39, pathways (i)–(iii) respectively. Under acidic conditions, pathway (i), Amical **125** can lose an iodide cation to form the iodo carbanion **130**. The latter can then either protonate to form the mono-iodo Amical analogue **126**, or lose an iodide anion to form the carbene **131**. Carbenes are, typically, highly reactive species. It therefore seems likely that **131** will react or breakdown further. An iodide cation and iodide anion are cleaved in forming **130** and **131** respectively. These can combine to form a molecule of iodine. Under alkaline conditions, pathway (ii), Amical **125** can lose a proton to form the di-iodo carbanion **132**. The latter can then lose an iodide anion to form the iodo carbene **133** which, like **131**, can react or breakdown further. Under photochemical conditions, pathway (iii), Amical **125** can lose an iodide radical to form the iodo radical **134**. The latter can then lose an iodide radical to form the carbene **131**, the latter of which can react or breakdown further as in pathway (i). The iodide radicals cleaved in forming **134** and **131** can combine to form a molecule of iodine. Now reconsider the Amical decomposition curves shown in Figure 38. The results of an earlier experiment (Figure 35) showed that the rate of Amical breakdown to iodine was affected by light. This, coupled with the fact that all UV experiments were conducted under neutral conditions, suggests that Amical forms iodine via the photochemical route shown in Figure 39, pathway (iii). If the mono-iodo radical **134** does not cleave its remaining iodine atom then clearly two molecules of **134**, and therefore two molecules of Amical **125**, are requir-

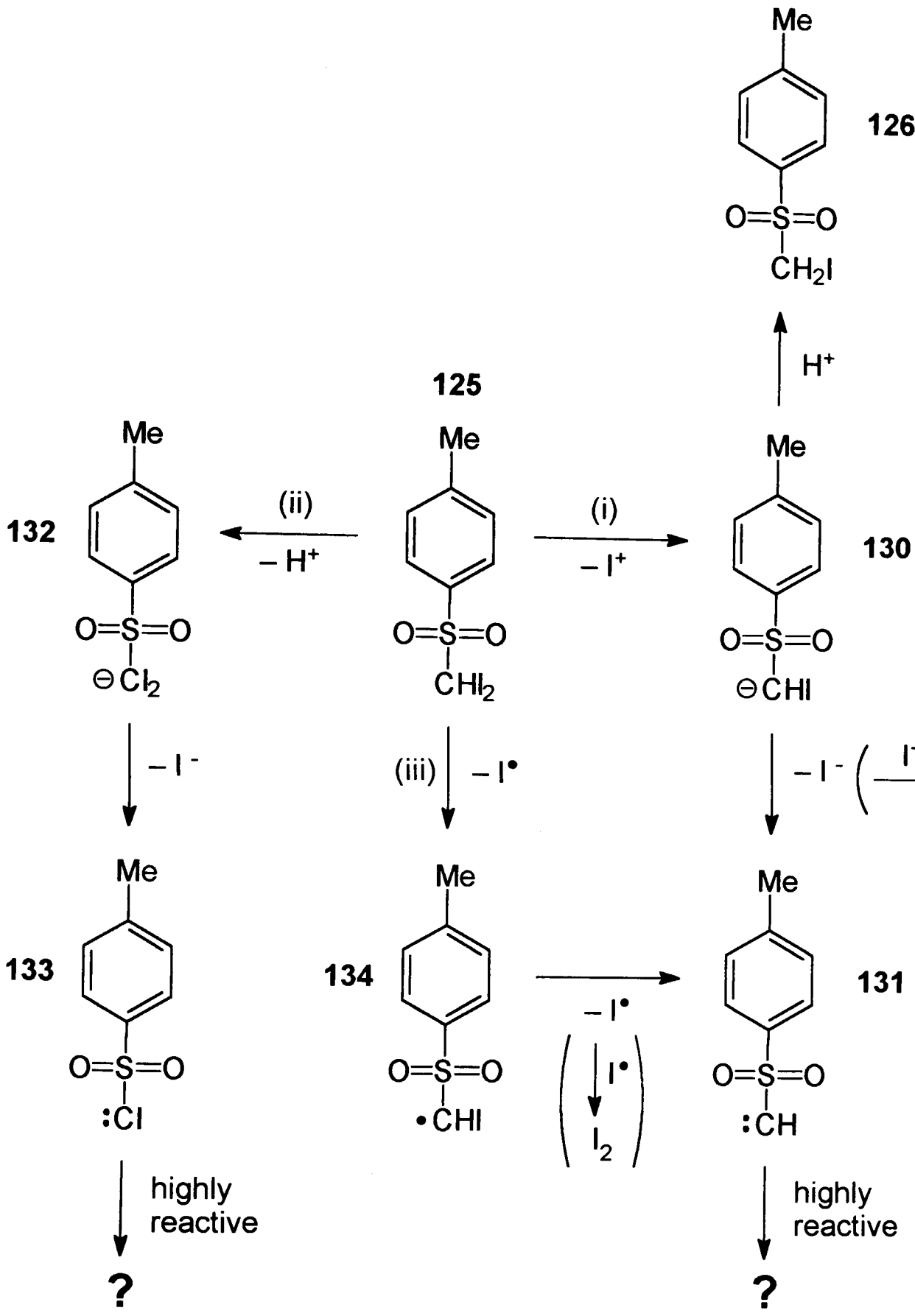

Fig. 39 Suggested decomposition modes of Amical **125** under (i) acidic, (ii) alkaline, and (iii) photochemical conditions.

ed to form one molecule of iodine. This decomposition mode is represented by the upper curve (▲) in Figure 38. If, on the other hand, the mono-iodo radical **134** breaks down further to form the carbene **131** then only one molecule of Amical **125** is required to form one molecule of iodine. This decomposition mode is represented by the lower curve (■) in Figure 38. Although the present UV experiments indicate Figure 39, pathway (iii), to be the likely mechanism of iodine formation, they do not indicate the extent of Amical **125** breakdown, *i.e.* **125→134**, or **125→131**. Consequently, either one of the curves shown in Figure 38 could be correct.

UV Spectrophotometric Studies of Iodomethyl-*p*-tolylsulfone and Iodoform

The question which now arises is whether the breakdown of Amical **125** to iodine in chloroform is a characteristic of Amical, alone, or do other iodomethyl sulfones behave likewise? In an attempt to answer this question a UV spectrophotometric experiment was performed on the mono-iodo Amical analogue **126**, iodomethyl-*p*-tolylsulfone (Scheme 10). A solution was prepared in a UV cuvette of **126** in chloroform (0.0079 mol dm^{-3}). The cuvette was stoppered and the UV spectrum run immediately. The spectrum revealed a single, intense band at 295 nm (Figure 40, broken line). The sample was removed from the UV instrument and left to stand in daylight, at room temperature. The chloroform solution very slowly turned violet in colour over a period of 24 h. The UV spectrum of the solution was taken after 20 h and revealed, in addition to the afore-mentioned 295 nm band, an iodine band at 512 nm (Figure 40, solid line). This experiment proves that **126**, like Amical **125**, breaks down in chloroform to produce molecular iodine. Decomposition therefore occurs in both the mono-iodo and di-iodo compounds. A further series of experiments examined the effect of light on the breakdown of the mono-iodo Amical analogue **126**. A solution was prepared in a UV cuvette of **126** in chloroform (0.0079 mol dm^{-3}). Fixed wavelength (512 nm) absorbance measurements were then taken periodically (in the manner described previously for the Amical UV exper-iments), leaving the cuvette to stand in daylight between measurements. The above experiment was repeated on two further solutions of **126** in chloroform (each, 0.0079 mol dm^{-3}), one solution kept in darkness and the other subjected to UV light (protocol as for the Amical UV experiments). The results obtained from these experiments are

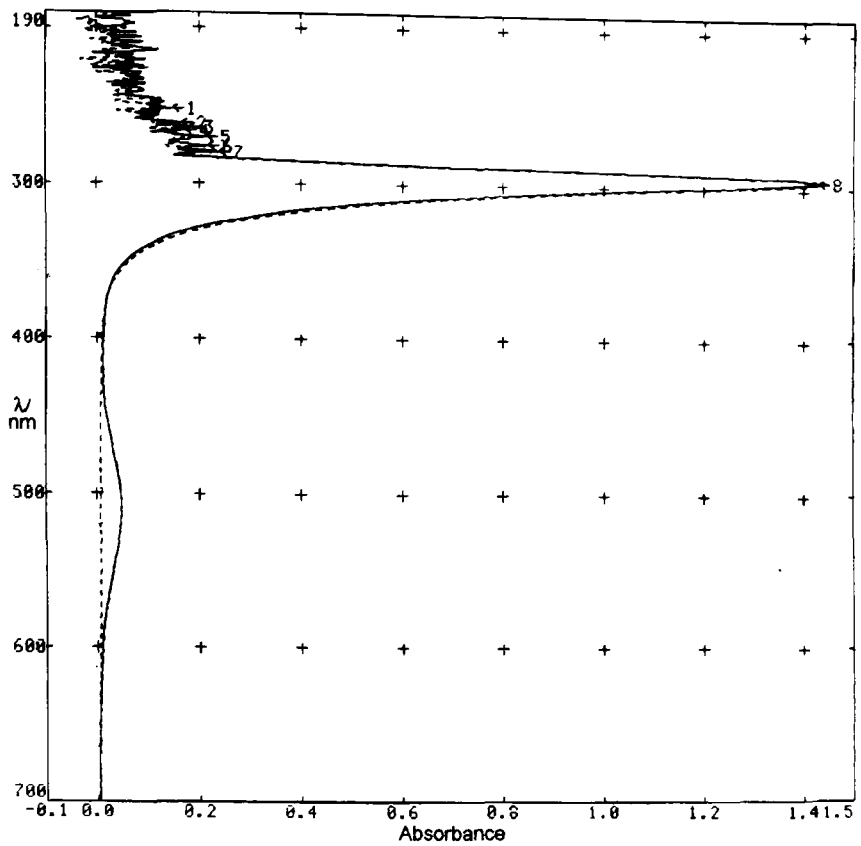

Fig. 40 UV Absorbance spectrum of a solution of the mono-iodo Amical analogue **126** (Scheme 10) in chloroform (0.0079 mol dm^{-3}) left in daylight. Note the appearance, with time, of the I_2 band at 512 nm: broken line, t = 0 min, A_{512} = 0.007; solid line, t = 20 h, A_{512} = 0.047.

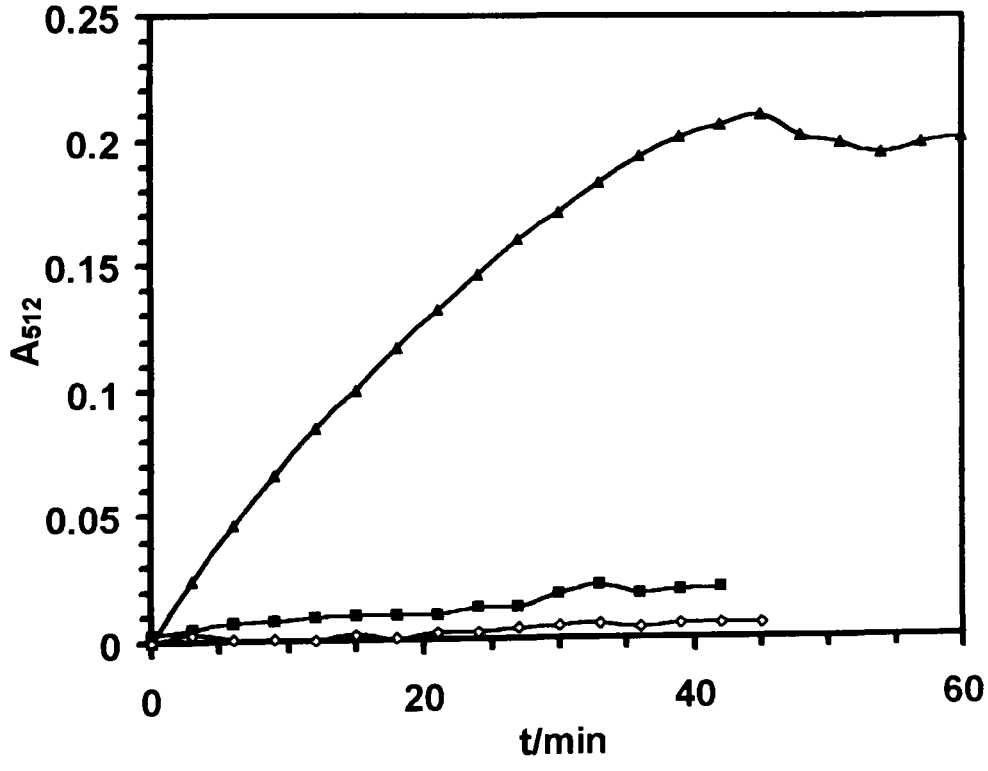

Fig. 41 Plot of I_2 absorbance (A_{512}) *vs.* time for 0.0079 mol dm^{-3} solutions of the mono-iodo Amical analogue **126** (Scheme 10) in $CHCl_3$ subjected to UV_{254} light (▲), daylight (■) and darkness (◊). Refer to Table 12 for the raw data.

shown in Table 12, with the data represented graphically in Figure 41. As can be seen from Figure 41 the rate of breakdown of **126** to iodine increased in the order, darkness < daylight < UV light. In the case of the UV light irradiated sample the rate of iodine production levelled off after ~45 min. With the sample left in daylight iodine production, although heavily suppressed, continued to increase very slowly. When the sample was kept in darkness iodine formation was almost totally suppressed with only a very small, residual absorbance being measured. These results are similar to those obtained for Amical **125** (Figure 35), with two noticeable differences. The first of these concerns the rate of iodine production in daylight. In the case of Amical **125** the rate of iodine production was quite marked in daylight (Figure 35, ■). However, in the case of **126** the rate of iodine production was extremely slow in daylight (Figure 41, ■). The second difference concerns the level-off absorbance values of the UV light curves. In the case of Amical **125** the level-off absorbance value = 0.527 (Figure 35, ▲). However, in the case of **126** the level-off absorbance value = 0.210 (Figure 41, ▲). The experiments performed on **125** and **126** (Figures 35 and 41 respectively) used identical solution concentrations (0.0079 mol dm^{-3}). As a consequence this means that, when subjected to UV light, **125** produced about two-and-a-half times as much iodine as **126** did. In conclusion, therefore, it appears that iodine production, resulting from decomposition, increases with the degree of iodonation.

It has been shown that the iodomethyl sulfones **125** and **126** (Scheme 10) break down in chloroform to form molecular iodine. Do other iodine compounds behave in a similar fashion? In an attempt to answer this question iodoform (CHI_3) was selected as a model compound against which a comparison could be made. The daylight/UV light/ darkness UV spectrophotometric experiments described for the compounds **125** and **126** were repeated on a sample of iodoform. A solution was prepared in a UV cuvette of iodoform in chloroform (0.0019 mol dm^{-3}). The UV spectrum was run immediately and revealed an intense, off-scale band centered at ~332 nm with a prominent shoulder at 376 nm (Figure 42, broken line). The sample was removed from the UV instrument and left to stand in daylight, at room temperature. The chloroform solution very rapidly turned violet in colour in a matter of seconds. The UV spectrum of the solution was taken after 35 min and revealed, in addition to the aforementioned 332 nm band, an iodine band at 512 nm (Figure 42, solid line). This experiment proves that iodoform, like both **125** and

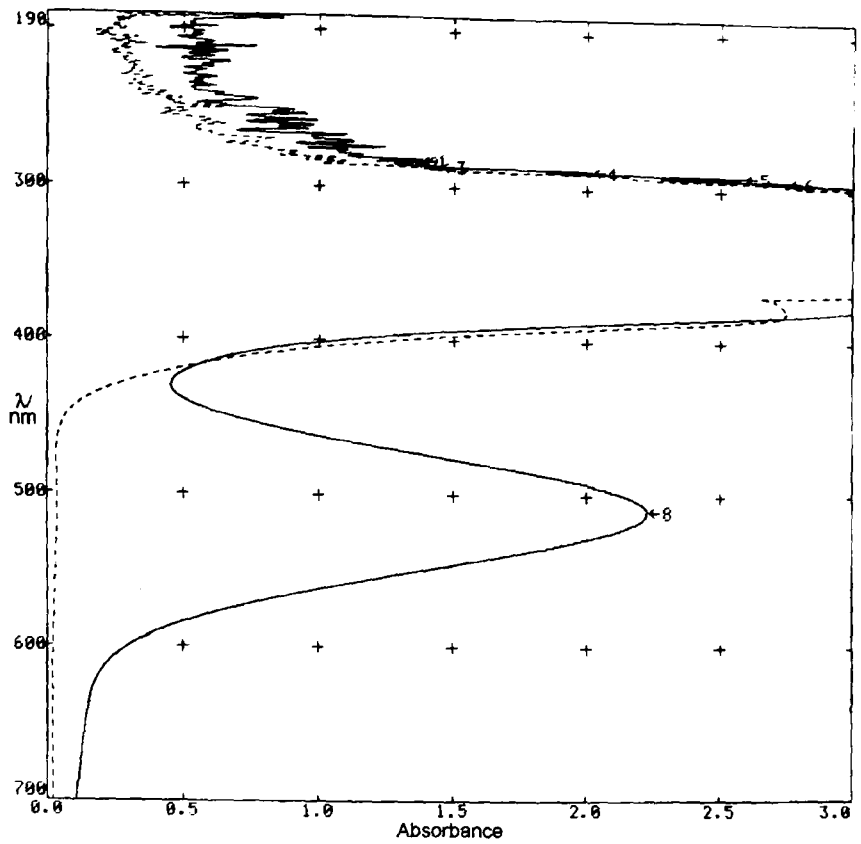

Fig. 42 UV Absorbance spectrum of a solution of iodoform, CHI_3, in chloroform (0.0079 mol dm^{-3}) left in daylight. Note the appearance, with time, of the I_2 band at 512 nm: broken line, t = 0 min, A_{512} = 0.037; solid line, t = 35 min, A_{512} = 2.224.

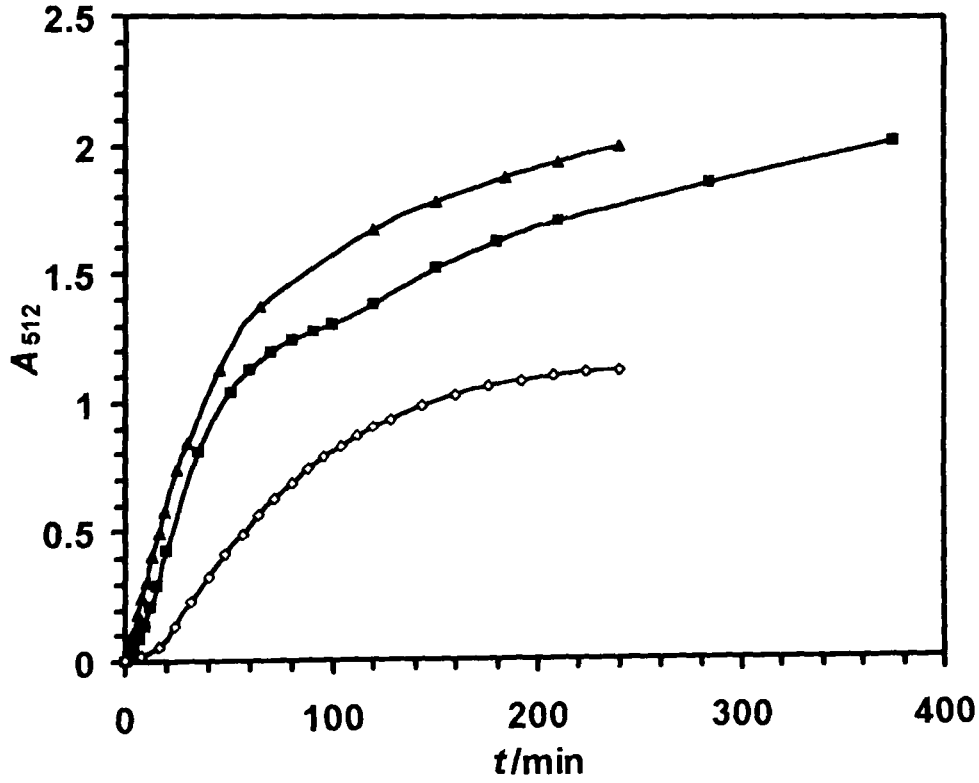

Fig. 43 Plot of I_2 absorbance (A_{512}) *vs.* time for 0.0019 mol dm^{-3} solutions of iodoform (CHI_3) in $CHCl_3$ subjected to UV_{254} light (▲), daylight (■) and darkness (◊). Refer to Table 13 for the raw data.

126, breaks down in chloroform to produce molecular iodine. Periodic, fixed wavelength (512 nm) absorbance measurements were then taken of solutions of iodoform in chloroform (0.0019 mol dm^{-3}) subjected to daylight, darkness and UV light (in a similar manner to the experiments performed on **125** and **126**). The results obtained from these experiments are shown in Table 13, and the data is represented graphically in Figure 43. As can be seen from Figure 43 the rate of breakdown of iodoform to iodine increased in the order, darkness < daylight < UV light. These results are similar to those obtained for both **125** and **126** (Figures 35 and 41 respectively), with some interesting differences. Note, for example, that iodoform breaks down to iodine in the absence of light (Figure 43, ◆). Compare this with **125** and **126** where darkness was found to totally suppress iodine formation in each case (Figures 35 and 41, ◆). Another difference between the iodoform and **125/126** results concerns the absorbance level-off times of the UV light curves. In the case of both **125** and **126** the rate of iodine production had levelled off after 30–45 min (Figures 35 and 41, ▲). With iodoform, however, iodine formation was still prominent even after 4 hours. The final difference, of note, concerns the absorbance values. Despite the iodoform solutions being one quarter as concentrated as the solutions of **125** and **126** (*c.f.* 0.0019 against 0.0079 mol dm^{-3}) the absorbance values, for a given time, obtained for the former were much larger. Consider, for example, the UV light curves obtained for **125**, **126** and iodoform (Figures 35, 41 and 43, ▲). The absorbance values after 45 min are 0.527, 0.210 and 1.127 respectively. Note that iodine production is far greater in the case of the iodoform solution. In conclusion, the breakdown of **125/126**/iodoform in chloroform to produce iodine increases in the order **126** < **125** < iodoform. This order follows the degree of iodonation (1, 2 and 3 respectively). It seems reasonable to assume, therefore, that the more iodine atoms the molecule has the greater will be the rate of decomposition to form iodine. This, however, is not the whole story as stability factors have to be considered too. For example, **125** and **126** (Scheme 10) each contain arylsulfonyl groups attached to the iodomethyl moiety, whereas iodoform only has attached a hydrogen atom. The relative abilities of these groups to stabilize the intermediate(s) resulting from chemical breakdown of the parent molecule are likely to play an important role in determing the rate of iodine production.

Table 8 Variation of I_2 absorbance (A_{512}) with time for 0.0079 mol dm^{-3} solutions of Amical **125** (Scheme 10) in $CHCl_3$ subjected to daylight, darkness and UV_{254} light. Refer to Figure 35 for the graphical output.

	A_{512}		
t/min	Daylight	Darkness[a]	UV_{254} light[b]
0	0.007	0.017	0.009
3	0.025	0.016	0.055
6	0.046	0.017	0.113
9	0.076	0.018	0.213
12	0.114	0.019	0.293
15	0.147	0.018	0.365
18	0.168	0.019	0.413
21	0.186	0.020	0.455
24	0.210	0.021	0.486
27	0.235	0.019	0.506
30	0.261	0.020	0.516
33	0.298	0.021	0.520
36	0.330	0.023	0.521
39	0.362	0.024	0.524
42	0.393	0.024	0.523
45	0.423	0.026	0.527
48	0.446	—	—
54	0.480	—	—
57	0.497	—	—
60	0.513	—	—
63	0.527	—	—

[a]Sample left inside UV instrument. [b]Hand-held UV lamp (254 nm) commonly used for viewing TLC plates.

Table 9 Variation of I_2 absorbance (A_{512}) with time for differently concentrated solutions of Amical **125** (Scheme 10) in $CHCl_3$ subjected to daylight. Refer to Figure 36 for the graphical output.

	A_{512}				
t/min	0.237 M	0.158 M	0.079 M	0.030 M	0.0079 M
0	0.226	0.150	0.075	0.020	0.007
0.5	0.259	—	—	—	—
0.75	—	0.198	—	—	—
1	0.302	—	0.127	—	—
1.5	0.329	0.251	—	0.039	—
2	0.372	—	0.199	—	—
2.25	—	0.312	—	—	—
2.5	0.429	—	—	—	—

Table continued ...

Table 9 (contd.)

	A_{512}				
t/min	0.237 M	0.158 M	0.079 M	0.030 M	0.0079 M
3	0.488	0.394	0.291	0.065	0.025
3.5	0.553	—	—	—	—
3.75	—	0.495	—	—	—
4	0.611	—	0.407	—	—
4.5	0.695	0.627	—	0.093	—
5	0.769	—	0.559	—	—
5.5	—	0.859	—	—	—
6	1.063	—	0.735	0.128	0.046
6.5	—	1.052	—	—	—
7	1.251	—	0.812	—	—
7.5	—	1.112	—	0.183	—
8	1.300	—	0.846	—	—
8.5	—	1.135	—	—	—
9	1.309	—	0.882	0.247	0.076
10	1.312	1.159	0.915	—	—
10.5	—	—	—	0.330	—
11	—	1.168	0.944	—	—
12	1.302	1.180	0.970	0.422	0.114
13	—	1.185	0.986	—	—
13.5	—	—	—	0.515	—
14	1.310	1.194	0.998	—	—
15	—	—	1.005	0.595	0.147
16	1.318	1.198	—	—	—
16.5	—	—	—	0.661	—
17	—	—	1.006	—	—
18	1.328	1.200	—	0.708	0.168
19	—	—	0.994	—	—
19.5	—	—	—	0.755	—
20	1.338	1.203	—	—	—
21	—	—	0.985	0.787	0.186
22	1.344	—	—	—	—
22.5	—	—	—	0.812	—
23	—	—	0.979	—	—
24	1.356	—	—	0.824	0.210
25	—	1.223	0.978	—	—
25.5	—	—	—	0.830	—
26	1.360	—	—	—	—
27	—	—	—	0.833	0.235
28	1.365	—	—	—	—
30	—	1.232	0.975	—	0.261
32	1.375	—	—	0.831	—
33	—	—	—	—	0.298

Table continued ...

Table 9 (contd.)

	A_{512}				
t/min	0.237 M	0.158 M	0.079 M	0.030 M	0.0079 M
35	1.374	—	0.974	—	—
36	—	—	—	—	0.330
37	—	—	—	0.832	—
39	—	—	—	—	0.362
40	1.383	1.247	0.974	—	—
42	—	—	—	—	0.393
45	1.393	—	—	0.842	0.423
48	—	—	—	—	0.446
50	—	1.256	0.975	—	—
54	—	—	—	—	0.480
57	—	—	—	—	0.497
60	—	—	—	—	0.513
63	—	—	—	—	0.527

Table 10 Variation of I_2 absorbance (A_{512}) with concentration for solutions of I_2 in $CHCl_3$. Refer to Figure 37 for the graphical output.

$[I_2]^a$	1	2	4	6	8	10	12	14	16	20
A_{512}	0.091	0.189	0.365	0.535	0.711	0.899	1.087	1.248	1.433	1.777

[a] 10^4 mol dm^{-3}.

Table 11 Variation of Amical **125** (Scheme 10) percentage decomposition to I_2 with concentration (solutions in $CHCl_3$). Measurement of the level-off I_2 absorbance (A_{512}) allowed the $[I_2]$ to be calculated for each Amical solution. With $[I_2]$ known, the percentage of Amical decomposed to I_2 could then be determined. Refer to Figure 38 for the graphical output.

			Amical decomposition (%)	
[Amical]/mol dm^{-3}	A_{512} (max.)[a]	$[I_2]^b$ /10^4 mol dm^{-3}	Am → I_2[c]	2 Am → I_2[d]
0.0079	0.527	5.89	7.46	14.92
0.03	0.832	9.31	3.1	6.2
0.079	0.975	10.9	1.38	2.76
0.158	1.256	14.0	0.89	1.78
0.237	1.393	15.6	0.66	1.31

[a]Refers to the level-off absorbance value (see Figure 36). [b]Calculated from an I_2 absorbance–concentration calibration graph (see Figure 37). [c,d]Assumes one I_2 molecule results from the breakdown of one[c]/two[d] Amical molecule(s) (Am).

Table 12 Variation of I_2 absorbance (A_{512}) with time for 0.0079 mol dm^{-3} solutions of the mono-iodo Amical analogue **126** (Scheme 10) in $CHCl_3$ subjected to daylight, darkness and UV_{254} light. Refer to Figure 41 for the graphical output.

	A_{512}		
t/min	Daylight	Darkness[a]	UV_{254} light[b]
0	0.003	0.0	0.0
3	0.005	0.003	0.024
6	0.007	0.001	0.046
9	0.008	0.001	0.066
12	0.009	0.0	0.085
15	0.01	0.002	0.1
18	0.01	0.001	0.117
21	0.01	0.003	0.132
24	0.013	0.003	0.146
27	0.013	0.004	0.16
30	0.018	0.005	0.171
33	0.021	0.006	0.183
36	0.018	0.004	0.193
39	0.019	0.006	0.201
42	0.02	0.006	0.206
45	—	0.006	0.21
48	—	—	0.202
51	—	—	0.199
54	—	—	0.195
57	—	—	0.199
60	—	—	0.201

[a]Sample left inside UV instrument. [b]Hand-held UV lamp (254 nm) commonly used for viewing TLC plates.

Table 13 Variation of I_2 absorbance (A_{512}) with time for 0.0019 mol dm^{-3} solutions of iodoform (CHI_3) in $CHCl_3$ subjected to daylight, darkness and UV_{254} light. Refer to Figure 43 for the graphical output.

	A_{512}		
t/min	Daylight	Darkness[a]	UV_{254} light[b]
0	0.001	0.007	0.005
2	0.014	—	0.056
4	0.037	—	0.117
6	—	—	0.182
7	0.09	—	—
8	—	0.017	0.247
9	0.133	—	—
10	—	—	0.308
12	0.211	—	—

Table continued ...

Table 13 (contd.)

	A_{512}		
t/min	Daylight	Darkness[a]	UV_{254} light[b]
13	—	—	0.405
15	0.291	—	—
16	—	0.055	0.493
19	—	—	0.577
20	0.428	—	—
24	—	0.133	—
25	—	—	0.739
30	—	—	0.841
32	—	0.228	—
35	0.806	—	—
40	—	0.324	—
45	—	—	1.127
48	—	0.412	—
50	1.041	—	—
56	—	0.492	—
60	1.129	—	—
64	—	0.562	—
65	—	—	1.370
70	1.193	—	—
72	—	0.626	—
80	1.24	0.685	—
88	—	0.738	—
91	1.276	—	—
96	—	0.786	—
100	1.302	—	—
104	—	0.828	—
112	—	0.868	—
120	1.382	0.904	1.673
128	—	0.934	—
144	—	0.987	—
150	1.52	—	1.781
160	—	1.027	—
176	—	1.058	—
180	1.621	—	—
185	—	—	1.875
192	—	1.081	—
208	—	1.099	—
210	1.704	—	1.933
224	—	1.112	—
240	—	1.121	2.0
285	1.855	—	—
375	2.015	—	—

[a]Sample left inside UV instrument. [b]Hand-held UV lamp (254 nm) commonly used for viewing TLC plates.

3.3.5 Towards a Polymer-Supported Diiodomethyl Sulfone

Introduction

The microbiological results obtained for both Amical **125** and the mono-iodo Amical analogue **126** (Scheme 10) proved encouraging. Following on from this research it was decided to synthesize a polymeric analogue of Amical or, at least, a polymeric species carrying the diiodomethyl sulfone moiety (the advantages and merits of *polymeric* antimicrobial agents have been discussed previously in section 1.5).

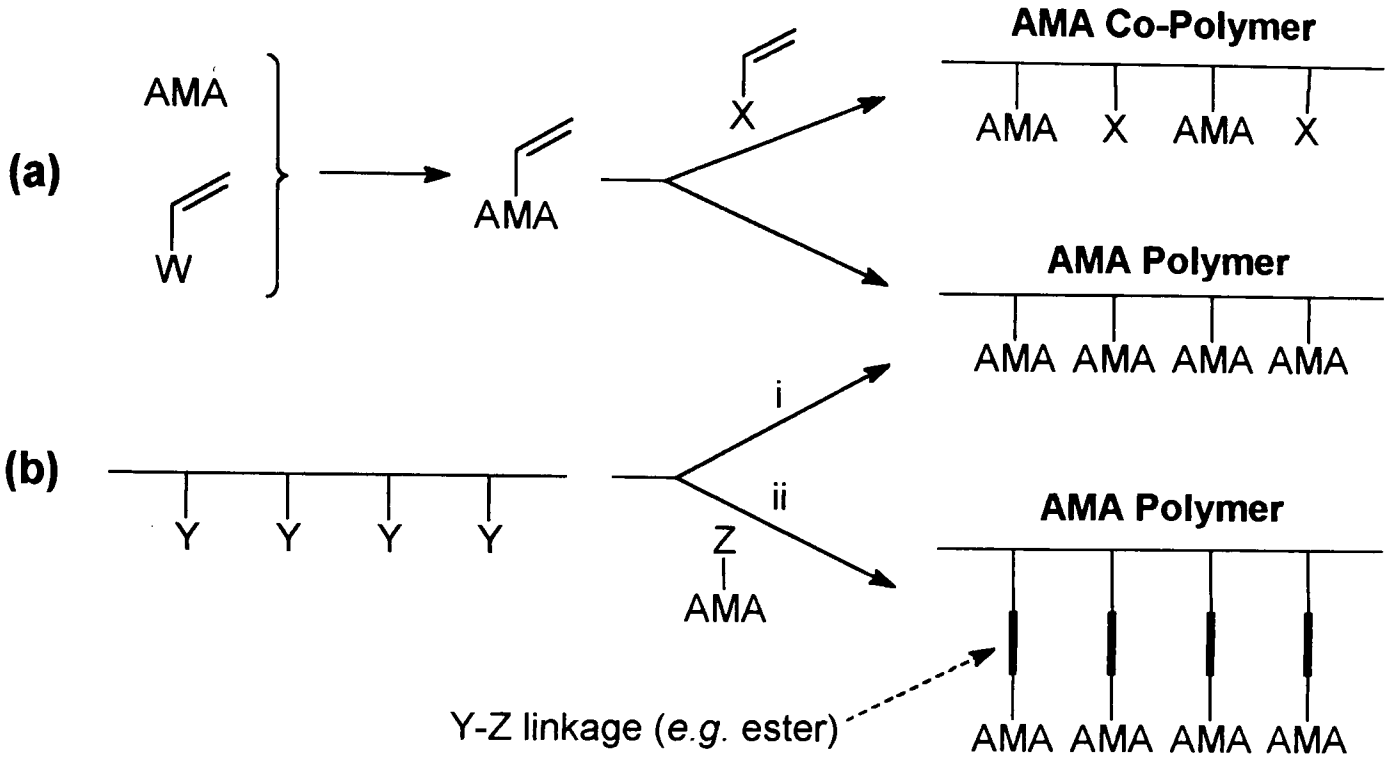

Fig. 44 Synthetic approaches towards polymeric antimicrobial agents: (a) polymerization of monomeric AMAs, (b) chemical modification of existing polymers.

There are, essentially, two basic synthetic approaches towards the synthesis of a polymeric antimicrobial agent (Figure 44). The first of these involves the synthesis of a polymerizable AMA (Figure 44a). For example, a vinyl group could be introduced into an antimicrobial molecule or, alternatively, a vinyl compound with a suitable functionality ('W') could be converted into a polymerizable AMA. The resultant AMA monomer could then be polymerized, or alternatively co-polymerized, to form an AMA (co-)polymer, as shown. Potential routes to polymerizable Amical analogues have been discussed previously in section 3.3.3. The second approach towards a polymeric AMA involves the chemical modification of an existing polymer (Figure

44b). If the polymer contains a suitable functional handle ('Y') then it would be possible, in principle, to use the 'handle' as a synthetic 'linkage' between the polymer and a functionalized antimicrobial agent, AMA–Z (Route ii). For example, Y might be an hydroxyl or an amine group, while Z might be an ester or acid chloride group. The resultant linkage, in this case, would be an ester group. Alternatively, but allowing room for less synthetic scope, the 'handle' could be converted directly into an anti-microbial functionality (Route i).

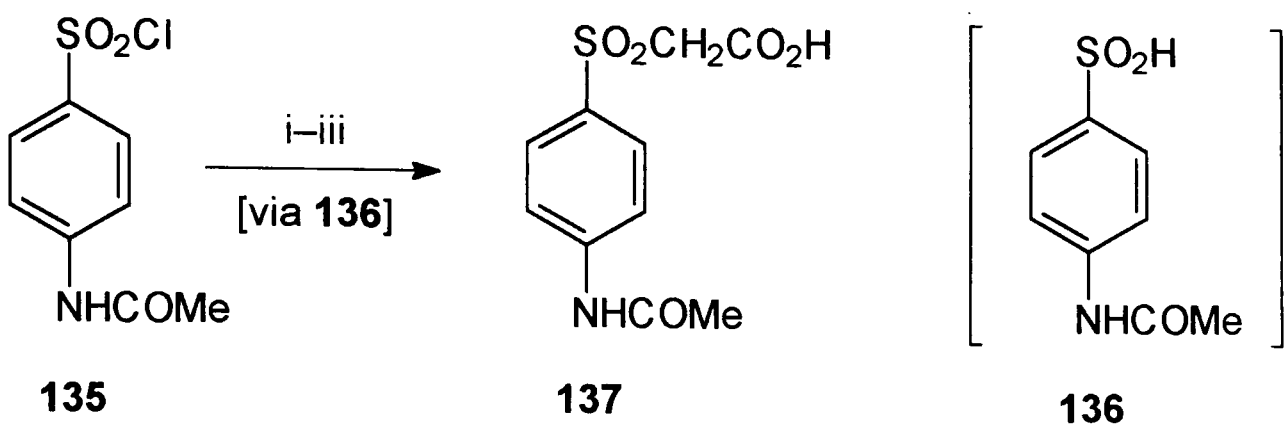

135 **137** **136**

Scheme 11 *Reagents and conditions:* i, Na_2SO_3, H_2O, inert atm., 45–50 °C, 2 h (pH 8.5–9.0); ii, $ClCH_2CO_2H$, then Na_2CO_3 (pH 4.0–4.2), 84–85 °C, 3 h; iii, HCl (aq) (pH 0.3).

It was noticed that the arylsulfonyl portion of the Amical molecule ($-C_6H_4-SO_2-$) bears a structural similarity to a *p*-benzenesulfonic acid group ($-C_6H_4SO_3H$). If the latter group were a pendant function on a polymeric 'bead' the species is what is commonly referred to as an *ion exchange resin* of the sulfonic acid type [Ion exchange resins are highly porous, cross-linked polymer beads (anywhere from millimetres down to microns in diameter). When a solution of ions is passed through an ion exchange resin the latter has the ability to exchange the ions in the solution for ions of its own kind (anions or cations, depending on the resin type)]. The question now arises as to a viable conversion of a $-C_6H_4SO_3H$ group into a $-C_6H_4SO_2CHI_2$ group? If the latter conversion could be effected then it would be possible, in principle, to synthesize a polymer-supported diiodomethyl sulfone in the form of resin beads. Such a polymer-supported AMA seemed a very interesting and potentially technologically useful idea. A synthesis by Courtin[77] was found detailing the conversion of an arylsulfonyl chloride into an arylsulfonylacetic acid. The procedure (Scheme

11) involved the reduction of the sulfonyl chloride **135** with an aqueous solution of sodium sulfite. The resultant sulfinic acid intermediate **136** was then acidified with chloroacetic acid to give the sulfonylacetic acid **137**.

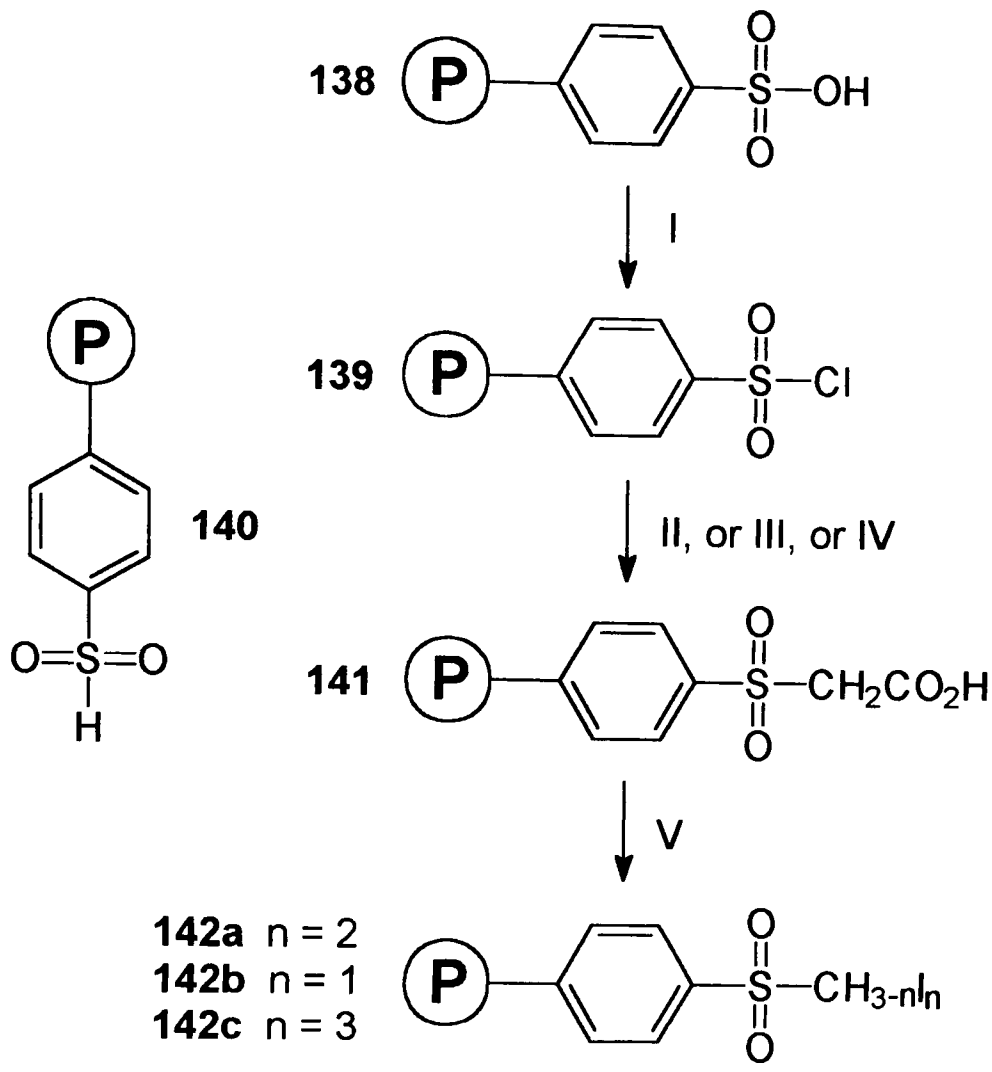

Scheme 12 *Reagents and conditions:* I, $SOCl_2$, Δ, 5 h; II: i, Na_2SO_3, H_2O, 60 °C, 2 h (pH 8); ii, $ClCH_2CO_2H$, 80–95 °C, 3¼ h; iii, HCl (aq) (pH 1); III: i, Na_2SO_3, $ClCH_2CO_2H$, *n*-$Bu_4N^+Cl^-$, CH_2Cl_2–H_2O, 40 °C, 6 h (pH 8); ii, HCl (aq) (pH 2); IV: i, Na_2SO_3, *n*-$Bu_4N^+Cl^-$, CH_2Cl_2–H_2O, 40 °C, 1 h (pH 8); ii, $ClCH_2CO_2H$, CH_2Cl_2, 40 °C, 5 h; iii, HCl (aq) (pH 2); V, I_2, NaOH, *n*-$Bu_4N^+Cl^-$, CH_2Cl_2–H_2O, r.t., 24 h.

In the light of the availability of sulfonic acid ion exchange resins and the aforementioned sulfite reduction method the synthesis of a polymer-supported diiodomethyl sulfone can now be visualized (Scheme 12). The synthesis will be described in principle for the present and the results of the experimental chemistry discussed, in detail, later on in the section: The starting material would be a benzenesulfonic acid ion exchange resin, represented by the structure **138** (Scheme 12). The sulfonic acid

138 would, firstly, be converted to the sulfonyl chloride **139**. The latter would then, in turn, be converted to the sulfonylacetic acid **141** (via the sulfinic acid **140**) using Courtin's reductive method. The final step in the synthesis would involve the halogenation and decarboxylation of the sulfonylacetic acid **141** to form the diiodomethyl-*p*-benzenesulfone resin **142a**. The transformation sulfonylacetic acid → diiodomethyl sulfone has been described previously for the synthesis of Amical **125** and the monoiodo Amical analogue **126** (Scheme 10, Route iii). On paper, at least, the synthesis of the diiodomethyl sulfone resin **142a** looked promising. It was anticipated, however, that problems might arise during the reduction and halogenation reactions (**139** → **141**, and **141** → **142a** respectively). Although both of these reactions are known to work for low molecular weight compounds, it remained to be seen whether the same reactions would work successfully on polymeric resin beads.

Sulfonic Acid Ion Exchange Resins – Technical Specifications and Conditioning

It was decided to attempt the synthesis outlined in Scheme 12 on two different types of ion exchange resin, *Amberlyst 15* and *Dowex 50-X8*. Each of these is a strongly acidic cation exchange resin of the benzenesulfonic acid type ($-C_6H_4SO_3H$). Although both resins have the sulfonic acid group that the synthetic chemistry demands (Scheme 12), the physical characteristics of each resin are markedly different. Ion exchange resins are three-dimensionally cross-linked polymer matrices in bead form. Covalently immobilized onto the polymer is a specific functional group that gives the resin its ion-exchange properties. Ion exchange resins can have the same functional group but constitutionally different polymer matrices. It is these same differences that give resin bead types their own unique set of physical characteristics. For example, Amberlyst 15 is a 'rigid', extremely porous (*macroreticular*) resin that is essentially non-swelling. Dowex 50-X8, on the other hand, is a 'soft', swellable, gel-type resin of low porosity. The technical specifications on Amberlyst 15 and Dowex 50-X8 resins are summarized in Table 14. It was anticipated that the chemistry in Scheme 12 might work successfully on one particular type of resin but not on another type. As a result, Amberlyst 15 and Dowex 50-X8 resins were chosen in order to give the chemistry a better chance to work.

Table 14 Technical specifications on Amberlyst 15 and Dowex 50-X8 ion-exchange resins.

Resin description	Amberlyst 15	Dowex 50-X8
BDH catalogue #	55133	55036
Supplied	Dry	Wet
Exchange type	Cation	Cation
Functionality	$SO_3^- H^+$	$SO_3^- Na^+$
Colour	'cement' grey	orange-red
Physical appearance	rigid & opaque	soft & glassy
Wet exchange capacity/meq cm^{-3}	1.75	1.9
Dry exchange capacity/meq g^{-1}	4.3	3.9 (H^+ form)[a]
Particle size range/mm	0.4–0.5	0.300–0.850
Wet density/g cm^{-3}	0.6	0.85
Maximum operating T/°C	120	150

[a]Experimentally determined after resin conditioning.

Both Amberlyst 15 and Dowex 50-X8 resins were conditioned prior to use according to a standard technique outlined in the BDH Chemicals literature.[78] The Dowex 50-X8 resin was supplied from the manufacturer in the form of its sodium salt. It was therefore converted into the sulfonic acid form. The Amberlyst 15 resin was supplied in the required ionic form. Despite this, it was regenerated to ensure that all the $-SO_3^-$ groups were in protonated form. In a typical resin conditioning experiment the resin was packed into a column and firstly back-washed with water in order to ensure efficient packing of the resin bed. The resin was then pre-washed with deionized water and regenerated with a volume of 5% aqueous hydrochloric acid solution that corresponded to four times the theoretical capacity of the resin bed (as recommended for strongly acidic cation exchange resins[78]). The volumes required of HCl solution to regenerate each resin were calculated as shown below.

	Amberlyst 15	*Dowex 50-X8*
Exchange capacity =	4.3 meq g^{-1} (dry)	1.9 meq cm^{-3} (wet)
Amount of resin conditioned =	30.17 g	50.0 cm^3
⇒ Resin capacity =	4.3 x 30.17 meq	1.9 x 50.0 meq
	= 129.731 meq	95 meq
Now, HCl regenerant solution† =	1371.4 meq dm^{-3}	1371.4 meq dm^{-3}
⇒ Volume to regenerate resin =	(129.731/1371.4) dm^3	(95/1371.4) dm^3

	$= 0.09457\ dm^3$	$= 0.06927\ dm^3$
$\Rightarrow$ 4 x Volume HCl =	$4 \times 0.09457\ dm^3$	$4 \times 0.06927\ dm^3$
	$= 0.3783\ dm^3$	$= 0.2771\ dm^3$
	i.e. $378.3\ cm^3$	*i.e.* $277.1\ cm^3$
Experimental volume used =	$380\ cm^3$	$280\ cm^3$

†The regenerant solution was 5% aq. HCl. This corresponds to (5/36.46) x 10 = 1.3714 mol dm^{-3} HCl. Since eq HCl ≡ mol HCl, 5% HCl ≡ 1371.4 meq dm^{-3}.

After being treated with the regenerant solution the resin was thoroughly washed with deionized water and dried with acetone. For experimental purposes the resins were required in dry form and so were dried *in vacuo* before use and stored over anhydrous calcium chloride. Quantitative recovery and weighing of the Dowex resin enabled the calculation of the resin's dry exchange capacity in the H^+ form: 95 meq of the Na^+ resin were conditioned to yield 24.41 g of dry H^+ resin $\Rightarrow$ dry exchange capacity of Dowex H^+ resin = (95/24.41) = 3.9 meq g^{-1}.

Calculation of Degree of Sulfonation of Sulfonic Acid Resins

The general structure of Amberlyst and Dowex benzenesulfonic acid resins can be represented by the structural formula: $-[CH_2CH(C_6H_4SO_3H)]_\alpha-[CH_2CH(C_6H_5)]_{1-\alpha}-$. In other words, only a fraction of the benzene rings are sulfonated, the fraction being defined by the factor α, where $0 < \alpha < 1$ (the value of α varies from one resin type to another). The fraction of unsulfonated benzene rings is therefore $(1-\alpha)$. Ion exchange resins are cross-linked (usually with divinylbenzene). The above structural formula is therefore only an approximate representation since it does not directly take into account the fraction of benzene rings involved in cross-linking. Assuming the above formula, therefore, the theoretical percentage, *%E*, of an element is given by the expression,

$$\%E = 100E[N_1\alpha + N_2(1-\alpha)] / MW_{ave} \qquad (3)$$

where E is the elemental atomic weight, N_1 is the number of atoms of the element in the sulfonated portion of the structure, N_2 is the number of atoms of the element in the unsulfonated portion, α is the fraction of sulfonated benzene rings, and MW_{ave} is the average

molecular weight of the whole structure. Let Q represent the molecular weight of the sulfonated portion of the molecule corresponding to the formula $CH_2CH(C_6H_4SO_3H)$. Similarly, let R represent the molecular weight of the unsulfonated portion corresponding to the formula $CH_2CH(C_6H_5)$. The average molecular weight of the whole structure can therefore be expressed as,

$$MW_{ave} = Q\alpha + R(1 - \alpha) \tag{4}$$

By substituting this expression for MW_{ave} into eqn (3) the latter becomes,

$$\%E = 100E[N_1\alpha + N_2(1 - \alpha)] \,/\, Q\alpha + R(1 - \alpha) \tag{5}$$

Eqn. (5) can now be used to give expressions for the theoretical percentages of carbon, hydrogen and sulfur in a benzenesulfonic acid resin. In the case of carbon, $N_1 = N_2 = 8$; for hydrogen, $N_1 = N_2 = 8$; and for sulfur, $N_1 = 1$ and $N_2 = 0$. Applying eqn (5) therefore gives the following expressions,

$$\%C = 100C[8\alpha + 8(1 - \alpha)] \,/\, [Q\alpha + R(1 - \alpha)] \tag{6}$$

$$\%H = 100H[8\alpha + 8(1 - \alpha)] \,/\, [Q\alpha + R(1 - \alpha)] \tag{7}$$

$$\%S = 100S\alpha \,/\, [Q\alpha + R(1 - \alpha)] \tag{8}$$

where C, H and S are the elemental weights of carbon, hydrogen and sulfur respectively. It can be shown that rearranging eqns. (6)–(8) in terms of α gives the respective equations,

$$\alpha = (800C - R\%C) \,/\, \%C(Q - R) \tag{9}$$

$$\alpha = (800H - R\%H) \,/\, \%H(Q - R) \tag{10}$$

$$\alpha = R\%S \,/\, [\%S(R - Q) + 100S] \tag{11}$$

The fraction α of sulfonated benzene rings can now be calculated from any one of eqns. (9)–(11) if elemental microanalytical data for the benzenesulfonic acid resin is available. If the experimental elemental microanalytical data are perfectly accurate then, naturally, the values of α determined from eqns. (9)–(11) should all be identical. In practice, however, this is rarely found to be the case. In general, experimental elemental microanalyses on resin beads yield notoriously inaccurate values for the carbon and hydrogen contents. As a

result, it is common practise to use the heteroatom content (%) (*e.g.* sulfur in the present case) for determining α.

Elemental microanalyses were carried out on dry samples of conditioned Amberlyst 15 and Dowex 50-X8 (H^+ form) resins. The elemental contents allowed the factor α to be determined for each resin using eqns. (9)–(11). The results of the calculations are summarized in Table 15.

Table 15 Determination of the fraction α of sulfonated benzene rings in Amberlyst 15 and Dowex 50-X8 sulfonic acid ion exchange resins. Calculations are based on elemental microanalytical data – the most reliable data was obtained from the sulfur content (highlighted).

Amberlyst 15			Dowex 50-X8 (H^+ form)		
Microanalysis	α	Eqn.[a]	Microanalysis	α	Eqn.[a]
%C = 50.60	1.07	(9)	*%C* = 46.41	1.29	(9)
%H = 5.82	0.43	(10)	*%H* = 5.63	0.49	(10)
%S = 13.90	0.69	(11)	*%S* = 12.95	0.62	(11)

[a]The following values were used in eqns. (9)–(11): C = 12.01, H = 1.01, S = 32.06, Q (≡ $C_8H_8O_3S$) = 184.21, and R (≡ C_8H_8) = 104.15.

As explained previously, the most reliable value of α is generally obtained from heteroatomic microanalytical data. In the present case, the value α was based on sulfur content, *i.e.* eqn. (11). For Amberlyst 15 sulfonic acid resin %S = 13.90, corresponding to a value of α = 0.69 (Table 15). Similarly, for Dowex 50-X8 sulfonic acid resin %S = 12.95%, corresponding to a value of α = 0.62. In other words, approximately 69% of the benzene rings in Amberlyst 15 are sulfonated, compared to 62% sulfonation in Dowex 50-X8. As a final point of note, compare the values of α that are based on elemental carbon and hydrogen (Table 15). As mentioned earlier, the carbon and hydrogen contents are generally too unreliable to determine α with. Based on elemental hydrogen, the α values are 38% and 21% out compared, respectively, to the Amberlyst and Dowex α values based on sulfur. However, the elemental carbon data was so inaccurate that the resulting values of α were both > 1.0, which is clearly absurd since, by definition, $0 < \alpha < 1$.

Theoretical Microanalyses of Chemically Modified Amberlyst and Dowex Resins

The calculation of the α value for each of the Amberlyst and Dowex sulfonic acid resins was based on the structural formula: $-[CH_2CH(C_6H_4X)]_\alpha-[CH_2CH(C_6H_5)]_{1-\alpha}-$, X = SO_3H. Now that the α values are known for each resin type it is possible to calculate theoretical elemental microanalyses for structural formulae with X groups other than SO_3H, in other words for the chemically modified resins **139** (X = SO_2Cl), **141** (X = $SO_2CH_2CO_2H$) and **142** (X = $CH_{3-n}I_n$, n = 1–3) (Scheme 12). The theoretical elemental microanalyses calculated for the Amberlyst- and Dowex-derived resins **139**, **141** and **142** are summarized in Table 16. In addition, the theoretical carbon and hydrogen contents (based on experimental %S) are given for Amberlyst 15 and Dowex 50-X8 sulfonic acid resins.

Table 16 Theoretical elemental microanalyses[a] of Amberlyst 15, Dowex 50-X8, and the chemically modified resins **139**, **141** and **142a** (Scheme 12). Analyses are also given (for comparison) for the mono- and tri-iodo species **142b** and **142c**.

Resin type	X	%C	%H	%Cl	%I	%S
Amberlyst 15	SO_3H	60.28	5.07	—	—	13.90[b]
Dowex 50-X8[c]	SO_3H	62.48	5.25	—	—	12.95[d]
Amberlyst **139**	SO_2Cl	55.82	4.29	14.21	—	12.85
Dowex **139**	SO_2Cl	58.15	4.51	13.30	—	12.03
Amberlyst **141**	$SO_2CH_2CO_2H$	59.80	5.03	—	—	11.74
Dowex **141**	$SO_2CH_2CO_2H$	61.70	5.19	—	—	11.05
Amberlyst **142a**	SO_2CHI_2	31.46	2.44	—	52.78	6.67
Dowex **142a**	SO_2CHI_2	33.54	2.62	—	50.98	6.44
Amberlyst **142b**	SO_2CH_2I	42.62	3.58	—	35.75	9.03
Dowex **142b**	SO_2CH_2I	44.89	3.78	—	34.12	8.62
Amberlyst **142c**	SO_2CI_3	24.93	1.76	—	62.75	5.28
Dowex **142c**	SO_2CI_3	26.77	1.93	—	61.03	5.14

[a]Calculations based on the fragment: $-[CH_2CH(C_6H_4X)]_\alpha-[CH_2CH(C_6H_5)]_{1-\alpha}-$ (Amberlyst 15, α = 0.69; Dowex 50-X8, α = 0.62). [b,d]Experimentally determined in order to calculate %C and %H. [c]H^+ form.

The analyses for the resins **139**, **141** and **142** were calculated from the equation,

$$\%E = 100E[N_1\alpha + N_2(1-\alpha)] \,/\, Q\alpha + R(1-\alpha) \qquad (12)$$

This expression is near-identical to eqn. (5) with the exception that Q' represents the molecular weight of the functionalized portion of the molecule corresponding to the general formula $CH_2CH(C_6H_4X)$, X = functional group. Save for Q', the variables in eqn. (12) are identically defined to those in eqn. (5).

Calculation of Exchange Capacity of Sulfonic Acid Resins

Recall the sulfur contents obtained for the Amberlyst and Dowex sulfonic acid resins (Table 15). In addition to allowing α to be calculated, the sulfur data can be used to calculate the resin exchange capacity. The calculations of the exchange capacities of Amberlyst 15 and Dowex 50-X8 sulfonic acid resins are given below.

	Amberlyst 15	*Dowex 50-X8*
1 g dry resin contains:	13.90% S	12.95% S
	$\equiv$ 0.139 g S	$\equiv$ 0.1295 g S
	$\equiv$ (0.139/32.06) moles S	$\equiv$ (0.1295/32.06) moles S
	$\equiv$ (139/32.06) mmol S	$\equiv$ (1295/32.06) mmol S
	= 4.34 mmol S	= 4.04 mmol S
	$\equiv$ 4.34 mmol SO_3H	$\equiv$ 4.04 mmol SO_3H
	$\equiv$ 4.34 meq g^{-1} of H^+	$\equiv$ 4.04 meq g^{-1} of H^+
	c.f. 4.3 meq g^{-1} (BDH lit.)	*c.f.* 3.9 meq g^{-1} (experiment)

For Amberlyst 15 sulfonic acid resin %S = 13.90, corresponding to an exchange capacity of 4.34 meq g^{-1}. This figure is therefore in excellent agreement with the value quoted for Amberlyst 15 in the BDH literature, *viz.* 4.3 meq g^{-1}. For Dowex 50-X8 sulfonic acid resin %S = 12.95%, corresponding to an exchange capacity of 4.04 meq g^{-1}. This figure agrees favourably with the value of 3.9 meq g^{-1} obtained from the resin conditioning experiment (for details, refer to the section *Sulfonic Acid Ion Exchange Resins – Technical Specifications and Conditioning*).

Chemical Modification of Amberlyst and Dowex Sulfonic Acid Resins

The specifications and conditioning of Amberlyst and Dowex sulfonic acid resins have been described in previous sections. Now consider the experimental chemistry. As stated

previously, the aim in this case was to chemically modify the sulfonic acid resin **138** into the diiodomethyl sulfone resin **142a**, via the sulfonylacetic acid resin **141** (Scheme 12). The synthetic pathway **138** → **142a** was carried out in parallel on Amberlyst 15 and Dowex 50-X8 sulfonic acid resins. Identical sets of reaction and experimental conditions were applied to each resin type. At the end of each synthetic step the resin beads were recovered quantitatively, dried (drying pistol) and weighed for use in the next step; in addition, small samples were reserved for elemental microanalysis, FTIR spectroscopy and microbiological testing. Due to the intrinsically insoluble nature of resin beads solution state ^{1}H NMR spectroscopy could not be utilized (solid state ^{13}C NMR spectroscopy, however, would have proved a valuable structural tool for these experiments but it was not available routinely).

The initial step of the synthesis involved the preparation of the sulfonyl chloride resin **139** (Scheme 12). Dry sulfonic acid resin **138** (Amberlyst 15 or Dowex 50-X8) was refluxed with thionyl chloride to yield the sulfonyl chloride resin **139**, the latter of which was dried with dichloromethane ($CaCl_2$–dried). The next step in the synthesis involved the conversion of the sulfonyl chloride resin **139** into the sulfonylacetic acid resin **141**. This synthesis was attempted using three different sets of reaction conditions (Scheme 12, Routes II–IV).

The first set of conditions (Route II) was adapted from the method described by Courtin[77] for the conversion of a low molecular weight arylsulfonyl chloride into an arylsulfonylacetic acid (Scheme 11). In the Courtin synthesis the sulfonyl chloride was stirred in a concentrated solution of sodium sulfite, under an inert atmosphere. Trial experiments on the sulfonyl chloride resin **139** (Scheme 12) revealed that the Courtin synthesis could be applied using a much less concentrated Na_2SO_3 solution (as long as the reductant was used in an excess). In addition, it was not found necessary to either stir the reaction mixture or to use an inert atmosphere. As a result of these findings, the sulfonyl chloride resin **139** was heated, unstirred, in an aqueous solution of sodium sulfite in a stoppered reaction flask. The solution was then acidified with chloroacetic acid and heated further. Finally, the solution was acidified with aq. HCl and the resin beads washed with water and acetone respectively.

The second set of conditions (Route III) adapted Coutin's method in the form of a 'single pot', heterogeneous reaction. It was anticipated that the aqueous reductive system (Route II) might hydrolyse the sulfonyl chloride resin **139** back to the sulfonic acid resin **138**. As a result, a water–dichloromethane/Na_2SO_3 system was used in conjunction with a phase-transfer catalyst (*n*-$Bu_4N^+Cl^-$). This system, hopefully, would help prevent the risk of hydrolysis. An additional advantage of the two-phase system is that the organic component (CH_2Cl_2) would be better able to penetrate the resin beads with the reductant, (*n*-$Bu_4N^+)_2SO_3^{2-}$. In the 'single pot', two-phase experiment sulfonyl chloride resin **139**, sodium sulfite and chloroacetic acid were stirred, and heated, in a solution of water–dichloromethane, with tetra-*n*-butylammonium chloride as the phase-transfer catalyst. The solution was acidified and the resin beads washed as described in the previous paragraph.

The third set of conditions (Route IV) utilized an identical two-phase system to that described above. This time, however, the reaction was carried out in two steps. In the two-step, two-phase experiment sulfonyl chloride resin **139**, sodium sulfite and tetra-*n*-butylammonium chloride were stirred, and heated, in a solution of water–dichloromethane. After a time, a solution of chloroacetic acid in dichloromethane was added and the solution heated further. The solution was acidified and the resin beads washed as described previously.

The final step of the synthetic pathway **138** → **142a** involved the conversion of the sulfonylacetic acid resin **141** into the diiodomethyl sulfone resin **142a**. In a previous section the synthesis of the diiodomethyl sulfone, Amical **125** (Scheme 10), was described. The synthesis[72] involved the addition of molecular iodine to an alkaline solution of the sulfonylacetic acid **124**. A two-phase adaptation of this halogenation synthesis was used in an attempt to form the diiodomethyl sulfone resin **142a** (Scheme 12). As described previously, three different synthetic procedures (Routes II–IV) were used in an attempt to prepare the sulfonylacetic acid resin **141**. The two-phase, halogenation reaction was carried out, separately, on each of the three sulfonylacetic acid resin products (Amberlyst- and Dowex-derived resins). The resin product obtained from the reaction **139** → **141** was added to a solution of iodine, sodium hydroxide and tetra-*n*-butylammonium chloride in water–dichloromethane. The resultant solution was stirred (r.t.) overnight. The Amberlyst-derived resin bead products were washed with water and acetone (respectively) and then

extracted in a Soxhlet with acetone. The Dowex-derived resin bead products, on the other hand, were washed with 50% aqueous methanol and acetone (respectively) and then extracted in a Soxhlet with methanol. The Soxhlet extractions ensured that 'free' iodine trapped in the resin beads would be washed out.

Table 17 Experimental elemental microanalyses of Amberlyst 15 and the chemically modified Amberlyst resins **139**, **141** and **142a** (Scheme 12).

Compound/Group	Remarks	%C	%H	%Cl	%I	%S
Amberlyst 15	—	50.60	5.82	—	—	13.90
139 SO_2Cl	—	50.47	4.59	6.33	—	13.91
141 $SO_2CH_2CO_2H$	Route II	47.28	4.63	—	—	13.32
142a SO_2CHI_2	Crude	44.80	4.43	—	4.31	12.76
142a SO_2CHI_2	Soxhlet[a]	45.41	3.99	—	4.85	9.60
141 $SO_2CH_2CO_2H$	Route III	48.86	4.71	—	—	11.41
142a SO_2CHI_2	Crude	46.38	4.55	—	1.09	12.51
142a SO_2CHI_2	Soxhlet[a]	45.77	4.37	—	0.53	12.89
141 $SO_2CH_2CO_2H$	Route IV	48.85	4.73	—	—	13.10
142a SO_2CHI_2	Crude	45.51	4.45	—	0.85	12.76
142a SO_2CHI_2	Soxhlet[a]	45.77	4.41	—	0.81	13.19

[a]Solvent: acetone.

Table 18 Experimental elemental microanalyses of Dowex 50-X8 and the chemically modified Dowex resins **139**, **141** and **142a** (Scheme 12).

Compound/Group	Remarks	%C	%H	%Cl	%I	%S
Dowex 50-X8[a]	—	46.41	5.63	—	—	12.95
139 SO_2Cl	—	49.17	4.44	8.61	—	14.81
141 $SO_2CH_2CO_2H$	Route II	45.27	4.35	—	—	14.05
142a SO_2CHI_2	Crude	44.48	4.23	—	7.91	13.14
142a SO_2CHI_2	Soxhlet[b]	44.50	4.02	—	8.15	12.82
142a SO_2CHI_2	Soxhlet[c]	44.99	4.31	—	0.91	13.35
141 $SO_2CH_2CO_2H$	Route III	51.16	5.32	—	—	12.90
142a SO_2CHI_2	Crude	48.01	4.68	—	0.81	13.56
142a SO_2CHI_2	Soxhlet[d]	46.92	4.58	—	0.55	13.65
141 $SO_2CH_2CO_2H$	Route IV	51.00	5.18	—	—	13.49
142a SO_2CHI_2	Crude	48.01	4.81	—	1.63	13.10
142a SO_2CHI_2	Soxhlet[d]	47.07	4.57	—	0.81	13.90

[a]H^+ form. [b]Solvent: acetone. [c]Solvents: acetone then methanol. [d]Solvent: methanol.

Elemental microanalytical data for the chemically modified Amberlyst and Dowex resins **139**, **141** and **142a** are summarized in Tables 17 and 18 respectively. FTIR spectroscopy (KBr pellet), in addition to elemental microanalysis, was used to monitor the synthesis **138** → **142a**. In order to confirm that the sulfonylacetic acid resin **141** had been prepared successfully the 1717 cm^{-1} carbonyl absorption of the carboxylic acid group in *p*-tolylsulfonylacetic acid **124** (Scheme 10) was used as a reference. The Amberlyst-derived attempts at **141** revealed absorptions in the carbonyl region at 1717 cm^{-1} (broad, weak to medium intensity; Route II product), 1709 cm^{-1} (sharp, weak intensity; Route III product) and 1709 cm^{-1} (sharp, weak intensity; Route IV product). The Dowex-derived attempts at **141**, on the other hand, revealed either extremely little (Route II & III products) or nothing at all (Route IV product) in the 1700–1720 cm^{-1} region of interest. In addition, the spectrum of the Dowex product derived from Route II was near-identical to the spectrum of the sodium salt form of Dowex 50-X8. In the case of the Amberlyst-derived resins it therefore appeared that a small percentage of sulfonyl chloride groups in **139** had been successfully converted to sulfonylacetic acid groups in **141**. On the basis of the FTIR band intensities the conversion seemed greater when the Route II (aqueous) reduction method was used. In the case of the Dowex-derived resins, however, it appeared that there had been little, if any, successful conversion of **139** into **141**. Spectral evidence suggested that in every attempt to prepare **141** from **139** the latter had either been partially, or completely, hydrolysed to the sodium salt form of the sulfonic acid **138** (aq. NaOH was used as a pH adjuster in Routes II–IV). Now consider the results for the iodonation reaction, **141** → **142a**. FTIR spectroscopy of the Dowex-derived attempts at **142a** (originated from Routes II–IV) revealed spectra that were near-identical to the spectrum of the sodium salt form of Dowex 50-X8. The spectra of the Amberlyst-derived attempts at **142a** (originated from Routes II–IV) were similar, but not identical, to the Dowex 50-X8 sodium salt spectrum. Elemental microanalysis of the Amberlyst-derived attempts at **142a** (after Soxhlet extraction) revealed either low (4.85%; product originated from Route II) or very low (0.53 and 0.81%; products originated from Routes III & IV respectively) iodine contents. Similarly, elemental microanalysis of the Dowex-derived attempts at **142a** (after Soxhlet extraction) revealed very low (0.91, 0.55 and 0.81%; products originated from Routes II–IV respectively) iodine contents. Note the elemental microanalytical data obtained from

the Soxhlet extraction of the Dowex-derived product originated from Route II (Table 18). When acetone was used as the extraction solvent the iodine content did not change very much (7.91→ 8.15%). However, when the extraction solvent was changed to methanol, the iodine content dropped to only 0.91%. Acetone was therefore considered to be an ineffective extraction solvent for the Dowex-derived resins and so methanol was used instead (acetone, on the other hand, was found to be a good extraction solvent for the Amberlyst-derived resins). In conclusion, in the attempted preparation of the diiodomethyl sulfone resin **142a** the highest iodine content (4.85%) was achieved with the Amberlyst-derived resin **141** that originated from Route II.

The overall results for the synthesis **138** → **142a** are disappointing. The iodonation reaction appeared to have worked successfully. However, due to the low conversions achieved in the **139** → **141** step (the aqueous reduction – Route II – appeared the most successful method, though), there were not enough sulfonylacetic acid groups on the resins **141** to undergo iodonation. As a consequence, only low, or very low iodine loadings were achieved for the resins **142**. Theoretical elemental microanalyses for the iodomethyl sulfone resins **142a–c** are shown in Table 16. In the case of the Amberlyst-derived resins the iodine contents are 35.75, 52.78 and 62.75% for the mono-, di- and tri-iodo species respectively. Similarly, for the Dowex-derived resins the iodine contents are 34.12, 50.98 and 61.03% for the mono-, di- and tri-iodo species. Assuming only mono-iodonation of **141** occurred the resultant resin **142b** would still contain a relatively high iodine content (~35%). The highest iodine content obtained for the resin **142** in the present experiments was a value of ~5% (Amberlyst-derived resin originated from Route II). Due, however, to the low percentage of sulfonylacetic acid groups on the resins **141** it is not possible to assess the degree of iodonation (*i.e.* **142a**, **142b** or **142c**) that this 5% value corresponded to.

Microbiological Testing of Chemically Modified Amberlyst and Dowex Resins

Bead samples of Amberlyst 15, Dowex 50-X8 and the chemically modified resins **139**, **141** and **142a** (Scheme 12) were tested for antimicrobial activity using three different methods: the *plate assay technique*, the *liquid assay technique*, and the *supernatant test*. A short summary of each test is given below. For further information, however,

refer to the experimental chapter, section 2.4.2 of which explains in detail the methodology and experimental protocol of each technique.

The *plate assay technique* is a 'dry' test since samples are tested in the dry state (*c.f.* MIC testing). In a typical experiment test samples are arranged on the surface of an inoculated malt extract agar (MEA) plate. The plate is incubated and then examined for inhibitory effects. Uninhibited microbial growth is represented by a 'lawn' of growth of the micro-organism. An active sample would inhibit microbial growth. This is represented by a *zone of inhibition* (diameter measured in millimetres) around the test sample area. An inhibition zone indicates 'leaching' of an active agent from the test sample. The *liquid assay technique* is a 'wet' test since samples are tested in solution. In a typical experiment test samples are added to vials containing the test medium. The samples are then inoculated and incubated. Samples of the test medium are plated out onto MEA plates and viable count determinations performed to determine *cell numbers* The cell number (units, cfu cm^{-3}) indicates the extent of microbial growth: no growth ≡ 0 cfu cm^{-3}; uninhibited growth ≡ 'control' value (for the present tests, ~10^7 cfu cm^{-3}); and inhibited growth ≡ 0 < cell number < 'control' value. Inhibition indicates either direct contact of the cell with the test sample ('contact activity') or 'leaching' of an agent from the test sample. The *supernatant test* is a 'leakage' test and is similar to the liquid assay experiment. In a typical experiment test samples are added to vials containing the test medium. The samples are then incubated *sans* inolculum. Samples of the test medium are then removed, inoculated and incubated further. Viable count determinations are performed to determine cell numbers. Inhibition indicates, unambiguously, 'leaching' of an agent from the test sample.

Microbiological test data for Amberlyst 15, Dowex 50-X8 and the chemically modified Amberlyst and Dowex resins **139**, **141** and **142a** are summarized in Tables 19 and 20 respectively. The headings 'Plate', 'Liquid' and 'S/N' refer to plate assay, liquid assay and supernatant tests respectively. Entries under the plate assay column indicate the diameters (mm) of inhibition zones. The term 'no inh.' refers to samples that displayed no inhibition zone. Entries under both the liquid assay and supernatant columns indicate cell

Table 19 Microbiological testing[a] of Amberlyst 15 and the chemically modified Amberlyst resins **139**, **141** and **142a** (Scheme 12). Columns 4–6 indicate the results of plate assay, liquid assay, and supernatant (S/N) tests respectively.

Entry	Compound/Group	Remarks	Plate[b]	Liquid[c]	S/N[c]
1	Amberlyst 15	—	0.5–1	no growth	1.0×10^3
2	**139** SO_2Cl	—	2	no growth	$\leq 10^2$
3	**141** $SO_2CH_2CO_2H$	Route II	no inh.	com. growth	com. growth
4	**142a** SO_2CHI_2	Crude	no inh.	no growth	com. growth
5	**142a** SO_2CHI_2	Soxhlet[d]	no inh.	no growth	com. growth
6	**141** $SO_2CH_2CO_2H$	Route III	no inh.	$\sim 10^4$	com. growth
7	**142a** SO_2CHI_2	Crude	2–3	2×10^2	inh. growth[e]
8	**142a** SO_2CHI_2	Soxhlet[d]	no inh.	2×10^2	com. growth
9	**141** $SO_2CH_2CO_2H$	Route IV	no inh.	$\sim 10^4$	com. growth
10	**142a** SO_2CHI_2	Crude	3 mm	2×10^2	com. growth
11	**142a** SO_2CHI_2	Soxhlet[d]	3–4	com. growth	com. growth

[a]Test organism, *Saccharomyces cerevisiae* EL1. [b]Entries indicate diameters (mm) of inhibition zones around bead samples on MEA plates; 'no inh.' – no inhibition zone. [c]Cell numbers (cfu cm^{-3}) determined by viable count method: 0 (no growth); 0 < cell number < $\sim 10^7$ (inhibited growth); $\geq \sim 10^7$ (complete growth – 'com. growth'). [d]Solvent: acetone. [e]Inhibited growth (cell number N/A).

numbers (cfu cm^{-3}) as determined by the viable count method. The terms 'no growth' and 'com. growth' refer to cell numbers equal to zero and the 'control' value respectively. Resin samples are numbered from #1–23 for ease of identification. In the discussion to follow a 'positive' result refers to samples that displayed an inhibitory effect (*i.e.* a zone of inhibition in the plate assay test, or a cell number less than the 'control' value in either the liquid assay or supernatant tests). Conversely, a 'negative' result refers to samples that had no inhibitory effect (*i.e.* no zone of inhibition in the plate assay test, or a cell number equal to the 'control' value in either the liquid assay or supernatant tests). The microbiological test results will now be discussed in detail.

For any single resin species there appears, overall, to be little, if any, correlation of the results from the three microbiological tests. Indeed, the results are often contradictory. For example, consider sample #19. The positive result from the plate test indicates leak-

Table 20 Microbiological testing[a] of Dowex 50-X8 and the chemically modified Dowex resins **139**, **141** and **142a** (Scheme 12). Columns 4–6 indicate the results of plate assay, liquid assay, and supernatant (S/N) tests respectively.

Entry	Compound/Group	Remarks	Plate[b]	Liquid[c]	S/N[c]
12	Dowex 50-X8[d]	—	1–2	no growth	$\leq 10^2$
13	**139** SO_2Cl	—	2–3	no growth	$\leq 10^2$
14	**141** $SO_2CH_2CO_2H$	Route II	no inh.	no growth	4.0×10^4
15	**142a** SO_2CHI_2	Crude	3–4	no growth	2.9×10^2
16	**142a** SO_2CHI_2	Soxhlet[e]	3–4	no growth	9.0×10^1
17	**142a** SO_2CHI_2	Soxhlet[f]	no inh.	com. growth	com. growth
18	**141** $SO_2CH_2CO_2H$	Route III	see[g]	$\sim 10^4$–10^5	2.0×10^3
19	**142a** SO_2CHI_2	Crude	5	2×10^2	com. growth
20	**142a** SO_2CHI_2	Soxhlet[h]	no inh.	com. growth	com. growth
21	**141** $SO_2CH_2CO_2H$	Route IV	1	no growth	1.0×10^1
22	**142a** SO_2CHI_2	Crude	no inh.	com. growth	com. growth
23	**142a** SO_2CHI_2	Soxhlet[h]	no inh.	com. growth	com. growth

[a]Test organism, *Saccharomyces cerevisiae* EL1. [b]Entries indicate diameters (mm) of inhibition zones around bead samples on MEA plates; 'no inh.' – no inhibition zone. [c]Cell numbers (cfu cm^{-3}) determined by viable count method: 0 (no growth); 0 < cell number < $\sim 10^7$ (inhibited growth); $\geq \sim 10^7$ (complete growth – 'com. growth'). [d]H^+ form. [e]Solvent: acetone. [f]Solvents: acetone then methanol. [g]Possible inhibition no zone (*i.e.* direct contact inhibition). [h]Solvent: methanol.

age. The liquid test is also positive. However, the supernatant test is negative. In the same way the results obtained for sample #10 are contradictory. Some samples, however, show self-consistency in their results. For example, consider sample #8. The negative result from the plate test indicates no leakage, a result supported by the negative supernatant test. Since the liquid test is positive it can be concluded that the sample displayed contact activity. Similar sets of self-consistent results are also shown by samples #4, 5, 6 and 9. In particular, samples #4 and 5 each showed no growth (*i.e.* total microbial kill) in their liquid assay tests. These samples were therefore very active.

Within any given test there is, again, little correlation with resin structure. It was hoped that the diiodomethyl sulfone resin **142a** would be very active. However, in some instances, the sulfonic acid **138** and sulfonyl chloride **139** forms seemed more active than subsequent species in the plate assay test. Consider, for example, the plate assay results

obtained for the sample progression #1–5. Another example of this 'reverse activity' effect can be seen in the plate assay results for the sample progression #12, 13, 21–23. Now consider the plate assay results for the sample progression #1, 2, 9–11. In this case the desired progression of activity is obtained since the precursors seem less active than subsequent species.

Figures 45 and 46 show photographs that were taken of a pair of agar plates (diameter 88 mm) after a typical plate assay experiment. The test organism, in each case, was the yeast strain, *Saccharomyces cerevisiae* EL1. Samples #7, 8, 10 and 11 (Table 19) are tested in Figure 45, and samples #17, 19, 20, 22 and 23 (Table 20) are tested in Figure 46. In Figure 45, zones of inhibition can be seen around the bead samples #7, 10 and 11. Note that sample #8 has no zone of inhibition. In Figure 46, a large zone of inhibition can be seen around the bead sample #19. Each of the samples #17, 20, 22 and 23 has no inhibition zone.

In conclusion, the results obtained from the microbiological testing of the resins **138**, **139**, **141** and **142a** are, overall, rather disappointing. From the chemistry results there is good evidence for achieving the proposed structural transformations and, in particular, for generating the polymer-supported diiodomethyl sulfone resin **142a**. Unfortunately, however, the results of the chemistry are not reflected consistently in the microbiological data. It is important, here, to mention the reliability of the microbiological results. Living systems are prone to contamination. As a result, microbiological testing is commonly conducted to strict and rigorous protocols. For example, it is standard practice in biochemistry laboratories to test samples in duplicate and then to perform multi-repeat experiments. The data obtained from these experiments is then usually collated and statistically analysed before any conclusions can be drawn from the results. The present microbiological data was limited by both shortage of material and time constraints. As a result, it was not possible to conduct the microbiological tests according to the rigorous protocol defined above.

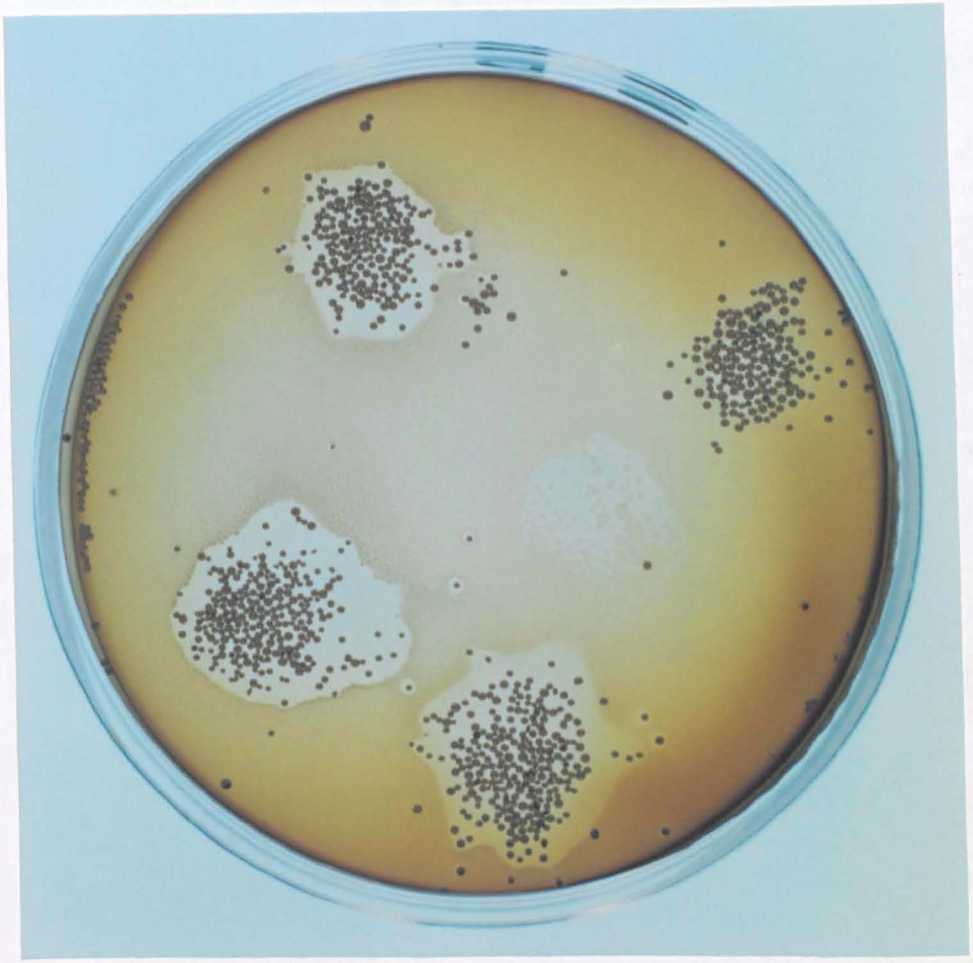

Fig. 45 Photograph of the results of a plate assay experiment. Samples #7 (top left), 10 (bottom left) and 11 (bottom right) display inhibitions zones (⇒ active) whereas sample #8 (top right) does not (⇒ inactive). Samples as in Table 19. Test organism is *Saccharomyces cerevisiae* EL1. Agar plate diameter = 88 mm.

Fig. 46 Photograph of the results of a plate assay experiment. Samples #17 (centre), 20 (top right), 22 (bottom left) and 23 (bottom right) have no inhibition zone (⇒ inactive) but sample #19 (top left) displays a large inhibition zone (⇒ active). Samples as in Table 20. Test organism is *Saccharomyces cerevisiae* EL1. Agar plate diameter = 88 mm.

3.4 Nicotinate Quaternary Ammonium Salts

3.4.1 Introduction

As discussed in chapter 1, antimicrobial activity is strongly influenced by certain key aspects of molecular design. These include physical factors like, for example, molecular shape and size. The most important influence on antimicrobial activity, however, is molecular structure and the key features here include functional group type and the 'architecture' of molecular sub-structure. A well-known, and extensively studied, class of antimicrobial compound that exhibits interesting aspects of molecular design are the *quaternary ammonium compounds* (or *quaternary ammonium salts* – '*quats*' for short).

Quaternary ammonium compounds are commonly used as antibacterial agents and disinfectants.[79] The key structural features of quats appears to be the possession of (i) a positively charged nitrogen atom, and (ii) a hydrophobic group (for example, a hydrocarbon chain). The mode of action of quaternary ammonium compounds has been extensively described[1,35,36,80–82] and involves the following sequential steps:

- Electrostatic attraction between the positive charge of the quat and the negatively charged outer membrane of the cell wall.
- Absorption onto, and diffusion through, the cell wall.
- Binding to the cytoplasmic membrane.
- Disruption of the cytoplasmic membrane followed by the release of cytoplasmic constituents (*e.g.* potassium ions), leading to death of the cell.

Polymeric versions and analogues of quaternary ammonium compounds are potentially very interesting. For example, a polymeric quat could provide the basis for a *controlled release system*.[83,84] In such a system, the antimicrobial agent is covalently immobilized onto a polymeric support via a labile bond (*e.g.* an ester or amide linkage). The agent can then be slowly released, by hydrolysis or decomposition, to give a 'free' active antimicrobial agent. Polymeric quats can be useful in other ways. For example, if the antimicrobial agent is permanently immobilized onto a polymeric support it has claimed that the polymeric quat can bind, irreversibly, to live, bacterial cells.[36] The literature contains

examples of soluble polymeric quaternary ammonium salts that, in addition to being antimicrobially active, are more active than their monomeric analogues.[35,36] There are also many examples of insoluble polymeric quats that have no antimicrobial activity.[85–87] At the present time, it is not fully understood why some polymers are active and others are not.

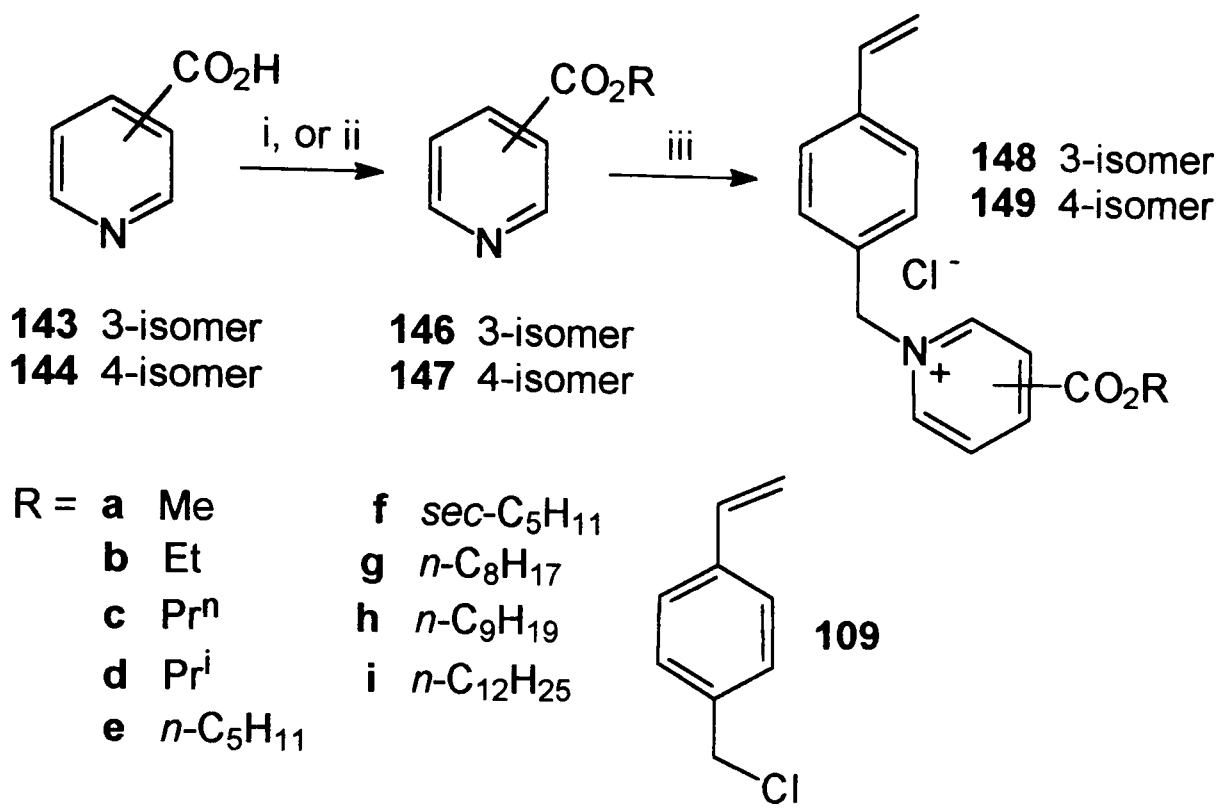

Scheme 13 *Reagents and conditions:* i, ROH **145a–d**, conc. H_2SO_4, Δ, 1 d; ii, $SOCl_2$, py, 100 °C, 1 h, then ROH **145e–i**, 100 °C, 4 h; iii, **109**, neat, 70 °C, 1 d.

Encouraged by the results of previous research,[88] the present studies were concerned with the design and synthesis of a novel polymerizable quaternary ammonium compound. In addition to adhering to the structural criteria discussed above a new quat compound should, ideally, be relatively straightforward to synthesize, from readily available and (preferably) inexpensive starting materials. Additionally, the compound should be as 'bio-friendly' as possible and not be too harmful or toxic. In keeping with these criteria, the series of polymerizable nicotinate quaternary ammonium salts **148** (Scheme 13) were proposed. With regard to structural design, the quat **148** is, essentially, a polymerizable pyridinium salt in the form of an alkyl nicotinate ester that has been quaternized with a vinylbenzyl group, with chloride ion as the counter-ion. Key structural features in the quat **148** include the positively charged nitrogen atom, the alkyl ester and the vinyl group. As

mentioned previously, the first two of these features are known to influence antimicrobial activity. The additional structural feature of a vinyl group in **148** would allow the molecule to be polymerized, the result of which would be a polymeric pyridinium chloride with an alkyl ester side-chain.

It was anticipated that the length and shape of the ester chain in **148** would be key structural influences on antimicrobial activity. As a result, the series of quats **148a–i**, with esters of different chain length (C_{1-12}) and branching (**148d** and **148f**), were synthesized. The position of the ester group on the pyridinium ring was considered an additional factor that might influence antimicrobial activity: the inductive influence of a *para*-substituted ester group in **149** (*c.f.* *meta*-substituted ester in **148**) would, theoretically, have the effect of re-enforcing the positive charge density on the nitrogen atom. Since charge is an important design feature in quaternary ammonium compounds, the quats **148** and **149** should, in theory, exhibit different antimicrobial activities. As a result, a selection of the isonicotinate quat series **149** were synthesized.

3.4.2 Monomer Synthesis

The two-step synthesis of the polymerizable nicotinate quaternary ammonium salts **148a–i** is shown in Scheme 13. The first step involved the preparation of the nicotinate esters **146a–i**. The nicotinate esters **146a–d**, with chain lengths in the range C_{1-3}, were prepared by a standard literature procedure.[89] Nicotinic acid **143** was refluxed, separately, with each of the alcohols **145a–d** in the presence of concentrated sulfuric acid to produce the esters **146a–d** (Scheme 13, Route i). Kugelrohr distillation afforded the following nicotinate esters: methyl **146a** (mp 38–40 °C; 81%), ethyl **146b** (77%), *n*-propyl **146c** (72%), and *iso*-propyl **146d** (57%). The isonicotinate esters **147a–d** were prepared, and purified, in a similar manner to that of the nicotinate esters **146a–d**: methyl **147a** (35%), ethyl **147b** (67%), *n*-propyl **147c** (70%), and *iso*-propyl **147d** (65%). The nicotinate esters **146e–i**, with chain lengths in the range C_{5-12}, were prepared by the published method of Woodward and Badgett.[90] Nicotinic acid **143** was heated with thionyl chloride in pyridine to give nicotinoyl chloride (**143**, but –COCl for $-CO_2H$). The latter was then heated, separately, with each of the alcohols **145e–i** to produce the esters **146e–i** (Scheme 13, Route ii). Kugelrohr distillation afforded the following nicotinate esters: *n*-pentyl **146e** (60%), *sec*-

pentyl **146f** (22%), *n*-octyl **146g** (71%), *n*-nonyl **146h** (86%), and *n*-dodecyl **146i** (85%). The isonicotinate esters **147g** and **147i** were prepared, and purified, in a similar manner to that of the nicotinate esters **146e–i**: *n*-octyl **147g** (66%), and *n*-dodecyl **147i** (76%). Due to time constraints, the isonicotinate esters **147e**, **147f** and **147h** were not prepared.

The final step of the synthesis involved quaternization of the nicotinate esters **146a–i** with *p*-vinylbenzyl chloride **109** (Scheme 13, Route iii). A neat solution of each of the nicotinate esters **146a–i** in *p*-vinylbenzyl chloride **109** was heated at 70 °C for 24 h. Trituration with diethyl ether afforded the following nicotinate quaternary ammonium salts: methyl **148a** (mp 135–137 °C; 74%), ethyl **148b** (mp 46–48 °C; 72%), *n*-propyl **148c** (gum; 99%), *iso*-propyl **148d** (glass; ~100%), *n*-pentyl **148e** (mp 93–97 °C; 60%), *sec*-pentyl **148f** (gum; ~100%), *n*-octyl **148g** [mp 60 (softened)–100 (decomp.); 69%], *n*-nonyl **148h** (mp 111–112 °C; 66%), and *n*-dodecyl **148i** (mp 55 °C; 72%). The isonicotinate quaternary ammonium salts **149a–d**, **149g** and **149i** were prepared, and purified, in a similar manner to that of the nicotinate quaternary ammonium salts **148a–i**: methyl **149a** (mp 142 °C; 61%), ethyl **149b** (mp 73–78 °C; 93%), *n*-propyl **149c** (mp 129–131 °C; 79%), *iso*-propyl **149d** (mp 117–125 °C; ~100%), *n*-octyl **149g** [mp 79 (softened)–87 (melt) °C; 68%], and *n*-dodecyl **149i** (mp 123 °C; 21%). A summary of yields and melting points for the series of nicotinate and isonicotinate quats **148** and **149** is presented in Table 21.

Table 21 Synthesis of polymerizable nicotinate and isonicotinate quaternary ammonium salts **148** and **149** (Scheme 13).

	Nicotinate quat **148**		Isonicotinate quat **149**	
R	Yield (%)[a]	Mp (°C)	Yield (%)[a]	Mp (°C)
a Me	74	135–137	61	142
b Et	72	46–48	93	73–78
c Pr^n	99	gum	79	129–131
d Pr^i	~100	glass	~100	117–125
e *n*-C_5H_{11}	60	93–97	Not synthesized	
f *sec*-C_5H_{11}	~100	gum	Not synthesized	
g *n*-C_8H_{17}	69	60[b]–100[c]	68	79[b]–87
h *n*-C_9H_{19}	66	111–112	Not synthesized	
i *n*-$C_{12}H_{25}$	72	55	21	123

[a]Isolated yield. [b]Softened. [c]Decomposed.

The series of nicotinate and isonicotinate esters **146** and **147** and polymerizable nicotinate and isonicotinate quats **148** and **149** were characterized by elemental micro-analysis and UV, FTIR and ^{1}H NMR spectroscopic techniques. The UV electronic spectra (ethanol; 190–350 nm range) of each compound series **146**, **147**, **148** and **149** showed a pair of bands in the following regions: **146**, 218–222 and 263–264 nm; **147**, 213–219 and 274–275 nm; **148**, 204–207 and 253–254 nm; and **149**, 206–208 and 253–254 nm. The FTIR spectra (KBr pellet, or film; 4000–400 cm^{-1} range) of each compound series **146**, **147**, **148** and **149** showed a strong carbonyl absorption in the following regions: **146**, 1721–1726 cm^{-1}; **147**, 1723–1733 cm^{-1}; **148**, 1726–1747 cm^{-1}; and **149**, 1728–1733 cm^{-1}. ^{1}H NMR spectroscopy (250 MHz, $CDCl_3$) revealed that all members of the quat series **148** and **149** were hydrated to varying degrees, ranging from 0.4–1.6 molecules of water per quat molecule. A summary of FTIR and UV electronic spectral data for the series of nicotinate and isonicotinate quats **148** and **149** is presented in Table 22. Selected ^{1}H NMR spectral data for the same compounds is presented in Tables 23 and 24 respectively.

Table 22 FTIR and electronic spectral data for the polymerizable nicotinate and isonicotinate quaternary ammonium salts **148** and **149** (Scheme 13).

	Nicotinate quat **148**		Isonicotinate quat **149**	
R	ν_{max} (C=O) / cm^{-1} [a]	λ_{max}/nm[b]	ν_{max} (C=O) / cm^{-1} [a]	λ_{max}/nm[b]
a Me	1729	204 and 253	1733	206 and 253
b Et	1739	206 and 254	1729	206 and 253
c Pr^n	1733	205 and 254	1733	206 and 254
d Pr^i	1729	206 and 254	1728	206 and 253
e *n*-C_5H_{11}	1729	205 and 253	Not synthesized	
f *sec*-C_5H_{11}	1729	207 and 254	Not synthesized	
g *n*-C_8H_{17}	1726	205 and 253	1729	208 and 253
h *n*-C_9H_{19}	1747	N/A	Not synthesized	
i *n*-$C_{12}H_{25}$	1746	206 and 253	1733	206 and 253

[a]KBr pellet (solid), film (gum/glass). [b]In ethanol.

Table 23 Partial ^{1}H NMR (δ/ppm; *J*/Hz) spectral data[a] for the polymerizable nicotinate quaternary ammonium salts **148** (Scheme 13).

R	Me	OCH_2	Vinyl H			NCH_2
			$=CHH_{cis}$	$=CHH_{trans}$	–CH=	
a Me	3.98 (s)	—	5.29 (d, *J* 10.9)	5.73 (d, *J* 17.6)	6.64 (dd, *J* 17.6 & 10.9)	6.53 (s)
b Et	1.40 (t, *J* 7.1)	4.43 (q, *J* 7.1)	5.29 (d, *J* 10.9)	5.73 (d, *J* 17.6)	6.64 (dd, *J* 17.6 & 10.9)	6.46 (s)
c Pr^n	0.98 (t, *J* 7.4)	4.31 (t, *J* 6.8)	5.28 (d, *J* 10.9)	5.73 (d, *J* 17.6)	6.64 (dd, *J* 17.6 & 10.9)	6.54 (s)
d Pr^i	1.38[b] (d, *J* 6.3)	—	5.29 (d, *J* 10.8)	5.74 (d, *J* 17.6)	6.64 (dd, *J* 17.5 & 11.0)	6.48 (s)
e *n*-C_5H_{11}	0.90 (br s)	4.36 (t, *J* 6.1)	5.30 (d, *J* 10.7)	5.74 (d, *J* 17.3)	6.65 (dd, *J* 17.4 & 11.0)	6.45 (s)
f *sec*-C_5H_{11}	0.90[c] (t, *J* 7.3), 1.34[d] (d, *J* 6.3)	—	5.29 (d, *J* 10.9)	5.74 (d, *J* 17.6)	6.65 (dd, *J* 17.6 & 10.9)	6.43 (s)
g *n*-C_8H_{17}	0.87 (t, *J* 6.4)	4.36 (t, *J* 6.8)	5.30 (d, *J* 10.9)	5.75 (d, *J* 17.6)	6.66 (dd, *J* 17.6 & 10.9)	6.45 (s)
h *n*-C_9H_{19}	0.87 (t, *J* 6.5)	4.36 (t, *J* 6.9)	5.30 (d, *J* 10.9)	5.75 (d, *J* 17.6)	6.65 (dd, *J* 17.6 & 10.9)	6.45 (s)
i *n*-$C_{12}H_{25}$	0.87 (t, *J* 6.6)	4.37 (t, *J* 6.8)	5.31 (dd, *J* 10.9 & 0.5)	5.76 (dd, *J* 17.6 & 0.5)	6.67 (dd, *J* 17.6 & 10.9)	6.46 (s)

[a]Recorded at 250 MHz in $CDCl_3$. [b]2 x Me. [c]CH_2CH_3. [d]$CHCH_3$.

Table 24 Partial ^{1}H NMR (δ/ppm; *J*/Hz) spectral data[a] for the polymerizable iso-nicotinate quaternary ammonium salts **149** (Scheme 13).

R	Me	OCH_2	Vinyl H			NCH_2
			$=CHH_{cis}$	$=CHH_{trans}$	–CH=	
a Me	3.96 (s)	—	5.25 (d, *J* 10.9)	5.69 (d, *J* 17.6)	6.59 (dd, *J* 17.6 & 10.9)	6.48 (s)

Table continued...

Table 24 (contd.)

R	Me	OCH_2	Vinyl H			NCH_2
			$=CHH_{cis}$	$=CHH_{trans}$	–CH=	
b Et	1.35 (t, *J* 7.1)	4.39 (q, *J* 7.1)	5.22 (d, *J* 10.9)	5.66 (d, *J* 17.6)	6.56 (dd, *J* 17.6 & 10.9)	6.46 (s)
c Pr^n	0.98 (t, *J* 7.4)	4.32 (t, *J* 6.7)	5.26 (d, *J* 10.9)	5.70 (d, *J* 17.6)	6.60 (dd, *J* 17.6 & 10.9)	6.51 (s)
d Pr^i	1.33[b] (d, *J* 6.2)	—	5.22 (d, *J* 10.9)	5.66 (d, *J* 17.6)	6.56 (dd, *J* 17.6 & 10.9)	6.44 (s)
g *n*-C_8H_{17}	0.86 (t, *J* 6.6)	4.35 (t, *J* 6.7)	5.26 (d, *J* 10.9)	5.69 (d, *J* 17.6)	6.60 (dd, *J* 17.6 & 10.9)	6.52 (s)
i *n*-$C_{12}H_{25}$	0.87 (t, *J* 6.6)	4.37 (t, *J* 6.7)	5.29 (d, *J* 10.9)	5.72 (d, *J* 17.6)	6.63 (dd, *J* 17.6 & 10.9)	6.54 (s)

[a]Recorded at 250 MHz in $CDCl_3$. [b]2 x Me.

3.4.3 Microbiological Testing

Introduction

The series of nicotinate and isonicotinate esters **146** and **147** and the polymerizable nicotinate and isonicotinate quats **148** and **149** were tested for antimicrobial activity. The MIC values were determined in NAJ and MOJ media against the yeast strain *Saccharomyces cerevisiae* EL1; the concentration test range was 1000–1 μg cm^{-3}. The data obtained from the MIC tests is summarized in Table 25. In addition, plots of MIC *vs.* chain length, x (*n*-C_xH_{2x+1}), are shown for each compound series **146**, **148** and **149** in Figures 47–49 respectively. The plots include only MIC data for compounds with *straight-chain* esters. Note that data points corresponding to MIC values >1000 μg cm^{-3} are plotted as '1000' μg cm^{-3} values but are represented by white squares (□) in order to differentiate them from other data points (black squares, ■).

As mentioned previously, key features of quaternary ammonium compounds are the possession of a positively charged nitrogen atom and a hydrophobic group. As a result, the MIC data will be analysed in order to see how antimicrobial activity is affected by each of the following:

(a)

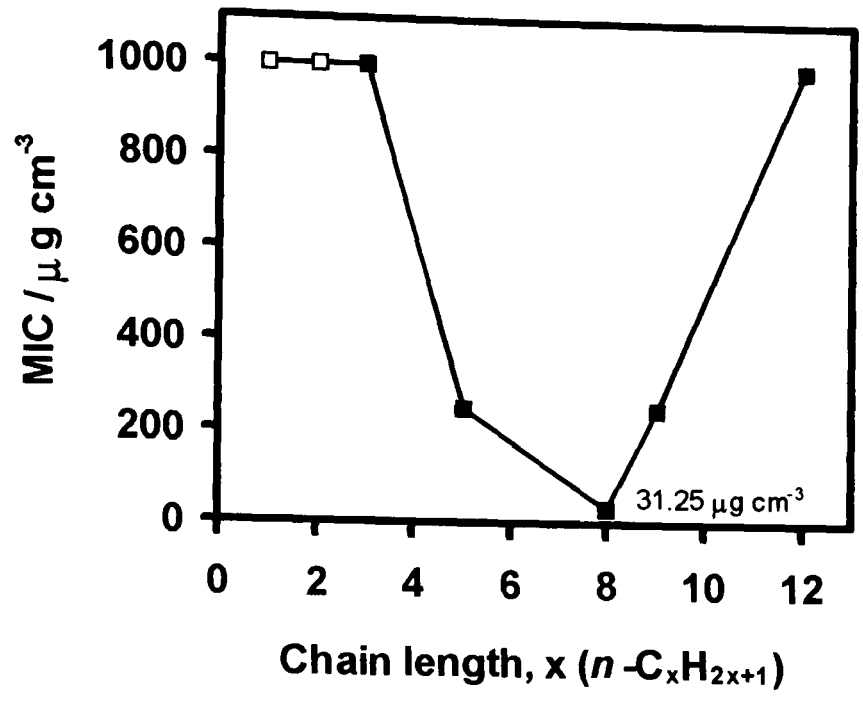

(b)

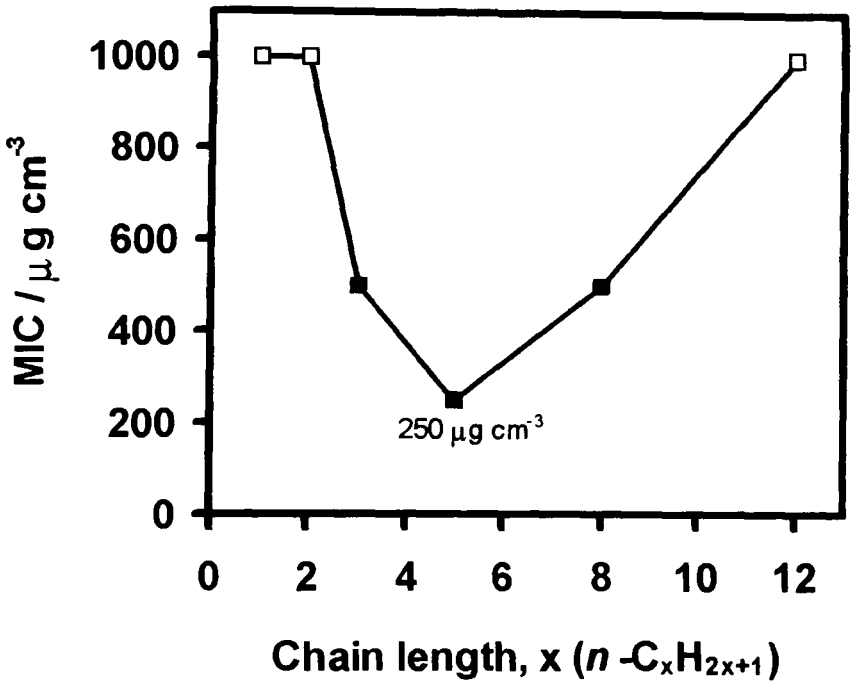

Fig. 47 Plot of MIC *vs.* chain length for the nicotinate esters **146** (Scheme 13); test organism, *Saccharomyces cerevisiae* EL1; test media: (a) NAJ, (b) MOJ. Data points corresponding to MIC values >1000 μg cm^{-3} are represented by white squares (□). See also Table 25.

(a)

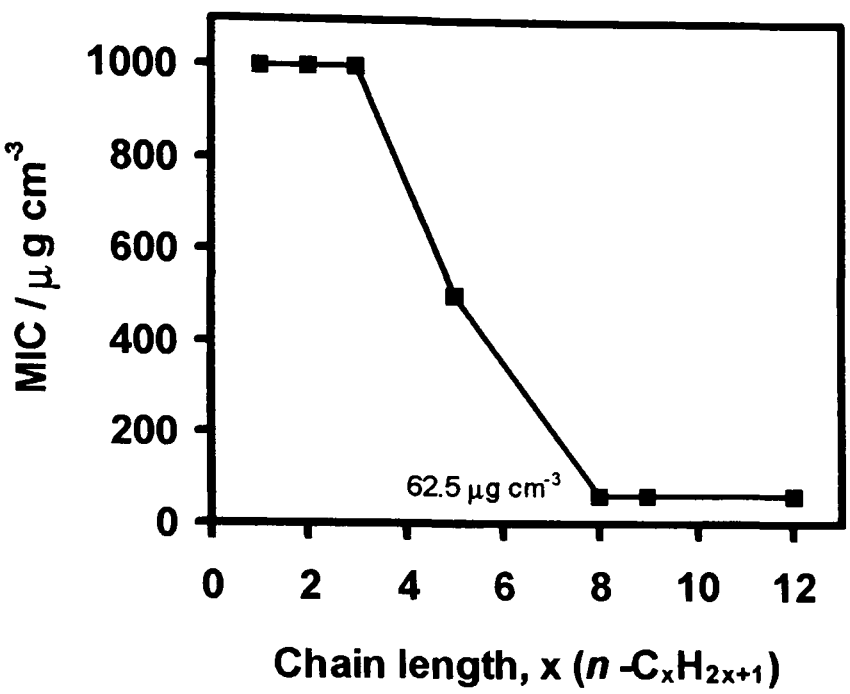

(b)

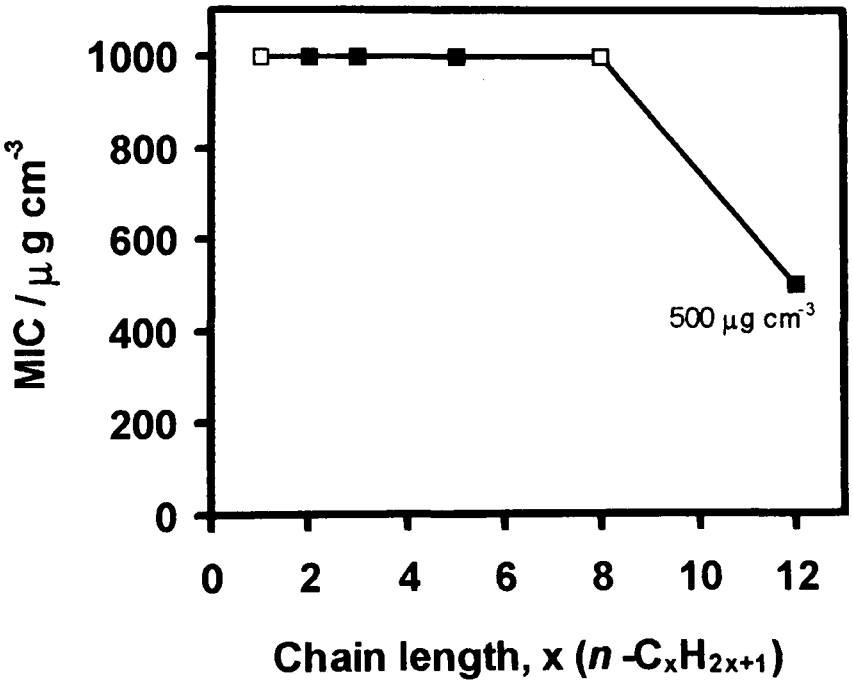

Fig. 48 Plot of MIC *vs.* chain length for the polymerizable nicotinate quats **148** (Scheme 13); test organism, *Saccharomyces cerevisiae* EL1; test media: (a) NAJ, (b) MOJ. Data points corresponding to MIC values >1000 μg cm^{-3} are represented by white squares (□). See also Table 25.

(a)

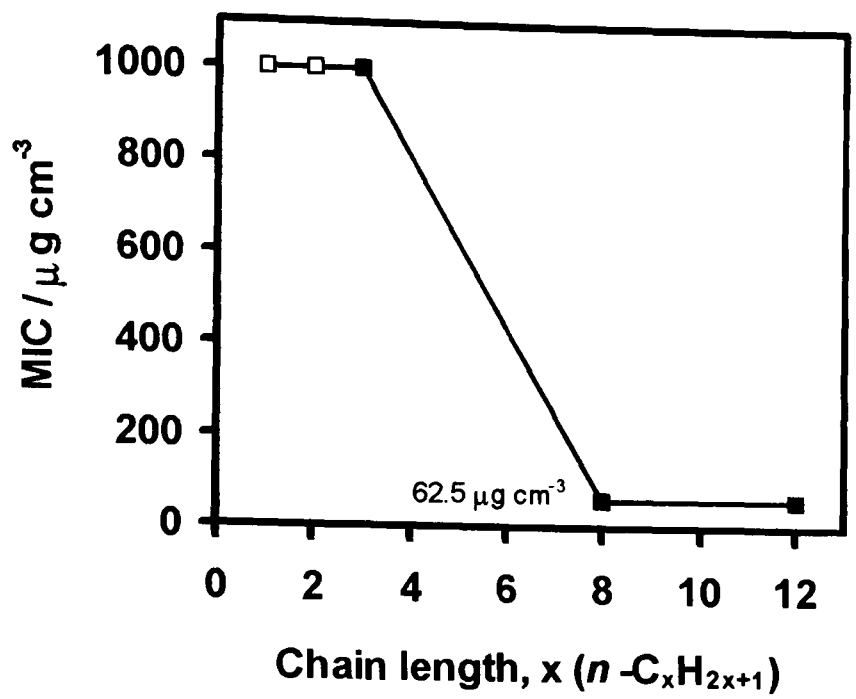

(b)

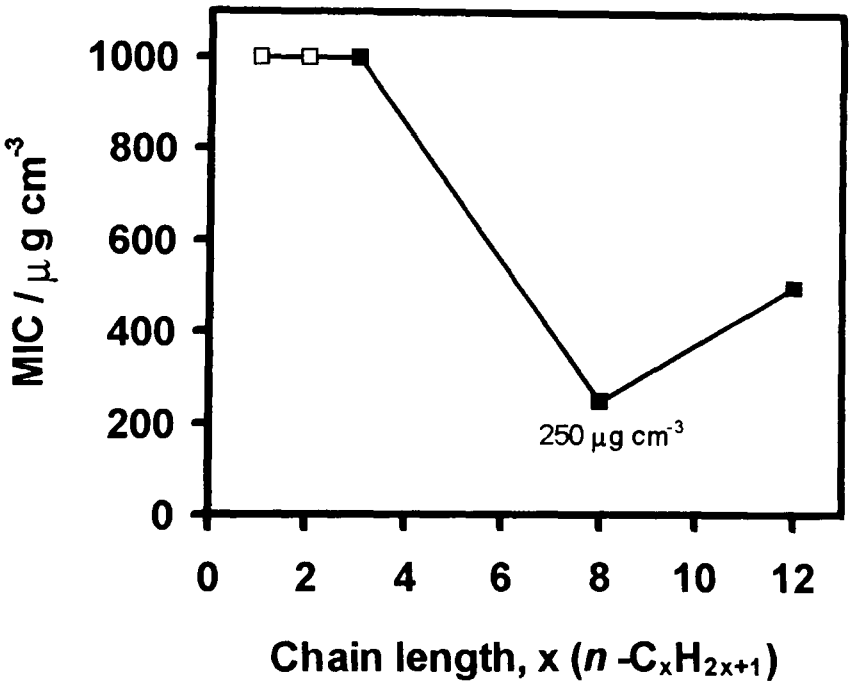

Fig. 49 Plot of MIC *vs.* chain length for the polymerizable isonicotinate quats **149** (Scheme 13); test organism, *Saccharomyces cerevisiae* EL1; test media: (a) NAJ, (b) MOJ. Data points corresponding to MIC values >1000 μg cm^{-3} are represented by white squares (□). See also Table 25.

- Ester chain length: C_{1-12} straight-chain esters.
- Structure of ester chain: branched *vs.* straight-chain ester.
- Position of ester group on pyridinium ring: *meta- vs. para*-substitution.

Table 25 MIC data[a] for the nicotinate and isonicotinate esters **146** and **147**, and the polymerizable nicotinate and isonicotinate quats **148** and **149** (Scheme 13). *N.b.* '—' – not synthesized.

	NAJ[b]: MIC/μg cm^{-3}				MOJ[c]: MIC/μg cm^{-3}			
R	**146**	**147**	**148**	**149**	**146**	**147**	**148**	**149**
a Me	$>10^3$	$>10^3$	10^3	$>10^3$	$>10^3$	$>10^3$	$>10^3$	$>10^3$
b Et	$>10^3$	$>10^3$	10^3	$>10^3$	$>10^3$	$>10^3$	10^3	$>10^3$
c Pr^n	10^3 [d]	10^3 [e]	10^3 [e]	10^3 [e]	500	500	10^3	10^3
d Pr^i	$>10^3$	10^3 [f]	10^3	$>10^3$ [e]	$>10^3$	500	10^3	10^3
e *n*-C_5H_{11}	250	—	500	—	250	—	10^3	—
f *sec*-C_5H_{11}	500	—	10^3	—	500	—	10^3	—
g *n*-C_8H_{17}	31.25	N/A	62.5	62.5	500	N/A	$>10^3$	250
h *n*-C_9H_{19}	250	—	62.5	—	N/A	—	N/A	—
i *n*-$C_{12}H_{25}$	10^3	N/A	62.5	62.5	$>10^3$	N/A	500	500

[a]Test organism, *Saccharomyces cerevisiae* EL1. [b]Norwegian apple juice. [c]Mills orange juice. [d-f]Inhibitory effect down to: [d]15.6, [e]125, [f]62.5 μg cm^{-3}.

Ester Chain Length

In NAJ, the nicotinate ester series **146** showed an increase in activity from C_1 to C_8 (maximum activity at C_8, MIC = 31.25 μg cm^{-3}), followed by a decrease in activity from C_8 to C_{12} (Figure 47a). A similar minimum in MIC (maximum in microbiological activity) was observed for the series **146** in MOJ, with maximum activity at C_5, MIC = 250 μg cm^{-3} (Figure 47b). In NAJ, the nicotinate quat series **148** showed an increase in activity from C_1 to C_{12}. Maximum activity was observed for the C_8, C_9 and C_{12} quats, each with an MIC value of 62.5 μg cm^{-3} (Figure 48a). A similar activity pattern was observed for the series **148** in MOJ, with maximum activity at C_{12}, MIC = 500 μg cm^{-3} (Figure 48b). Note, however, that the activity momentarily decreased at C_8, MIC = > 1000 μg cm^{-3}. This apparently erroneous result could be due to experimental error in the MIC test. In NAJ, the isonicotinate quat series **149** showed an increase in activity from C_1 to C_{12}. Maximum activity was observed for the C_8 and C_{12} quats, each with an MIC value of 62.5 μg cm^{-3} (Figure 49a). In MOJ, however, the isonicotinate quat series **149** showed an increase in activity

from C_1 to C_8 (maximum activity at C_8, MIC = 250 μg cm^{-3}), followed by a decrease in activity at C_{12} (Figure 49b).

In conclusion, the activity in each of the quat series **148** and **149** was found to increase with an increase in chain length from C_1 to C_{12}. In general, maximum activity was observed for the C_8, C_9 and C_{12} compounds. For the nicotinate ester series **146**, maximum activity peaked for compounds with chains of moderate length (C_5 and C_8).

Structure of Ester Chain

A comparison was made between compounds with *iso*-propyl and *sec*-pentyl alkyl chains (Table 25, R = **d** and **f** respectively) and their straight-chain counterparts, *n*-propyl and *n*-pentyl (R = **c** and **e** respectively). Consider, first, the results obtained for the isomeric C_3 alkyl chains. In both NAJ and MOJ, *n*-propyl nicotinate **146c** was more active than *iso*-propyl nicotinate **146d** (*e.g.* in MOJ: **146c**, MIC = 500 μg cm^{-3}; **146d**, MIC = >1000 μg cm^{-3}). In the case of the isonicotinates, however, *n*-propyl isonicotinate **147c** and *iso*-propyl isonicotinate **147d** had identical activities in each test medium (MICs of 1000 μg cm^{-3} in NAJ, and MICs of 500 μg cm^{-3} MOJ). The *n*-propyl nicotinate quat **148c** and *iso*-propyl nicotinate quat **148d** had identical activities in each test medium (MICs of 1000 μg cm^{-3} in NAJ, and MICs of 1000 μg cm^{-3} in MOJ). In the case of the isonicotinate quats, however, the *n*-propyl isonicotinate quat **149c** was more active than the *iso*-propyl isonicotinate quat **149d** in NAJ (**149c**, MIC = 1000 μg cm^{-3}; **149d**, MIC = >1000 μg cm^{-3}). In MOJ, **149c** and **149d** had identical activities (MICs of 1000 μg cm^{-3}). Now consider the results obtained for the isomeric C_5 alkyl chains (data for the nicotinate species, only). In both NAJ and MOJ, *n*-pentyl nicotinate **146e** was more active than *sec*-pentyl nicotinate **146f** (**146e**, MIC = 250 μg cm^{-3} in both NAJ and MOJ; **146f**, MIC = 500 μg cm^{-3} in both NAJ and MOJ). The *n*-pentyl nicotinate quat **148e** was more active than the *sec*-pentyl nicotinate quat **148f** in NAJ (**148e**, MIC = 500 μg cm^{-3}; **148f**, MIC = 1000 μg cm^{-3}). In MOJ, however, **148e** and **148f** had identical activities (MICs of 1000 μg cm^{-3}).

In conclusion, the straight-chain ester and quat compounds were generally found to be more active than their branched-chain counterparts. At worst, the straight-chain and branched-chain species had similar activities.

Position of Ester Group on Pyridinium Ring

Although the MIC data for the isonicotinate compound series **147** and **149** was incomplete (Table 25) it appeared that, for a given chain length and test medium, the nicotinate and isonicotinate species (whether ester or quat) had comparable activities. A notable exception to this, however, is the octyl quats **148g** and **149g**. In this case, the isonicotinate quat **149g** (MIC = 250 μg cm^{-3}) is considerably more active than its nicotinate counterpart **148g** (MIC >1000 μg cm^{-3}) in MOJ. In NAJ, however, both compounds have identical activities (MICs of 62.5 μg cm^{-3}). There are other examples of nicotinate and isonicotinate compound pairs with different activities (*e.g.* in MOJ: **148b**, MIC = 1000 μg cm^{-3}; **149b**, MIC = >1000 μg cm^{-3}) but, in general, the data is not consistent enough to form any concrete conclusions. As a result, the influence of the position of the ester group on antimicrobial activity is not entirely clear.

General Conclusions

From the MIC test results (Table 25), the following general conclusions can be drawn:

- An increase in ester chain length leads to an increase in antimicrobial activity. Compounds with chain lengths in the range C_8 to C_{12} are the most active.
- Straight-chain compounds have greater antimicrobial activities than their branched-chain counterparts.
- The position (*meta- vs. para*-substitution) of the ester group on the pyridinium ring does not appear to significantly influence antimicrobial activity.

A final conclusion to make concerns the testing media. It was found that, in general, for a given compound, smaller MIC values were recorded in NAJ than in MOJ. In general, compounds therefore tested more active in Norwegian apple juice than in Mills orange juice.

The first conclusion therefore supports the finding that antimicrobial activity in quaternary ammonium compounds is enhanced by a hydrophobic group (for example, an

alkyl chain). In addition, the second conclusion supports the view that straight-chains are more readily able to insert into cell membranes than branched-chains.

3.4.4 Polymer and Co-polymer Synthesis

As mentioned in the introduction to this section there is strong evidence to suggest that soluble polymeric quaternary ammonium compounds are effective and potentially very versatile antibacterial agents. It was decided to select one of the nicotinate quats **148a–i** and investigate its polymerization reactions with the aim of producing a water-soluble polymeric pyridinium salt.

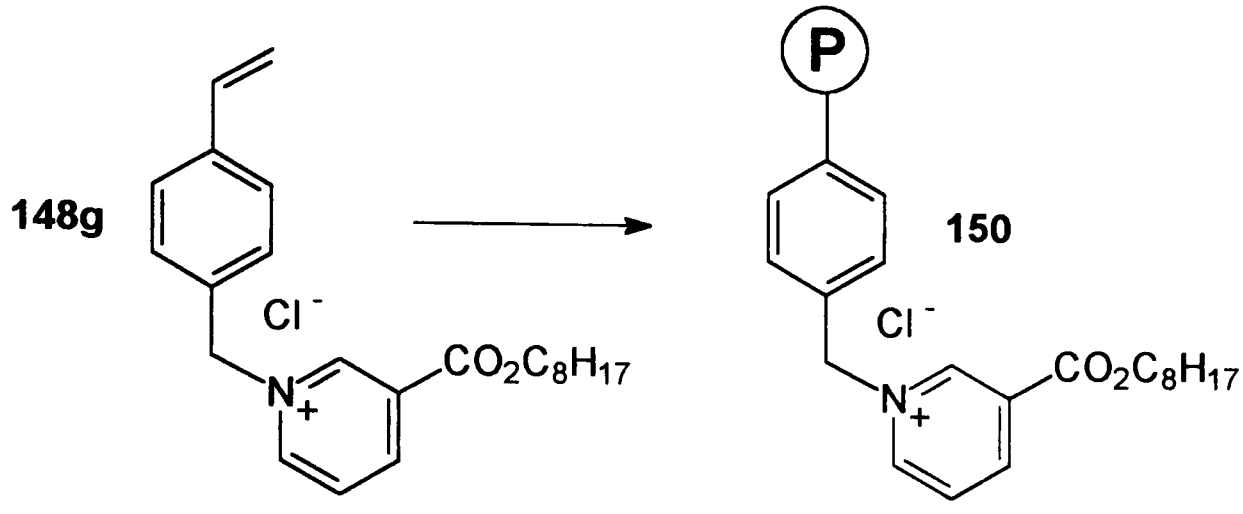

Scheme 14 *Reagents and conditions:* AIBN, THF, 60 °C, 18 h.

Encouraged by favourable MIC data (Table 25), the *n*-octyl nicotinate quat **148g** was selected for polymerization studies. The homo-polymerization of the monomer **148g** is shown in Scheme 14. Monomer **148g** and initiator, azobis-*iso*-butyronitrile (AIBN), were dissolved in tetrahydrofuran and the solution degassed (freeze-pump-thaw method). The solution was then heated at 60 °C for 18 h. Repeated trituration of the crude product with diethyl ether afforded the homo-polymer **150** as a tan powder (mp 127–135 °C; 27% conversion). ^{1}H NMR spectroscopy (250 MHz, $CDCl_3$) of **150** revealed a series of broad signals, characteristic of those found in typical polymer spectra. Notably prominent signals were those due to the C_8 ester chain: δ 0.86 (CH_3), 1.27 [$(CH_2)_5CH_3$] and 1.77 (OCH_2CH_2) ppm. The OCH_2 signal was less prominent but could be seen at δ ~4.3 ppm. The methine and methylene peaks due to the polymer backbone appeared in the range δ 2.0–3.6 ppm. The

aromatic protons appeared as a series of very broad signals in the range δ 5.5–10.0 ppm. FTIR spectroscopy (KBr pellet) of **150** revealed a strong carbonyl absorption at 1724 cm^{-1} (*c.f.* 1726 cm^{-1} in the monomer **148g**). It came as a disappointment to find that the polymer **150** was very insoluble in water. An MIC test revealed that **150** was inactive: MIC = >1000 [31.25] μg cm^{-3} in NAJ, and MIC = >1000 μg cm^{-3} in MOJ.

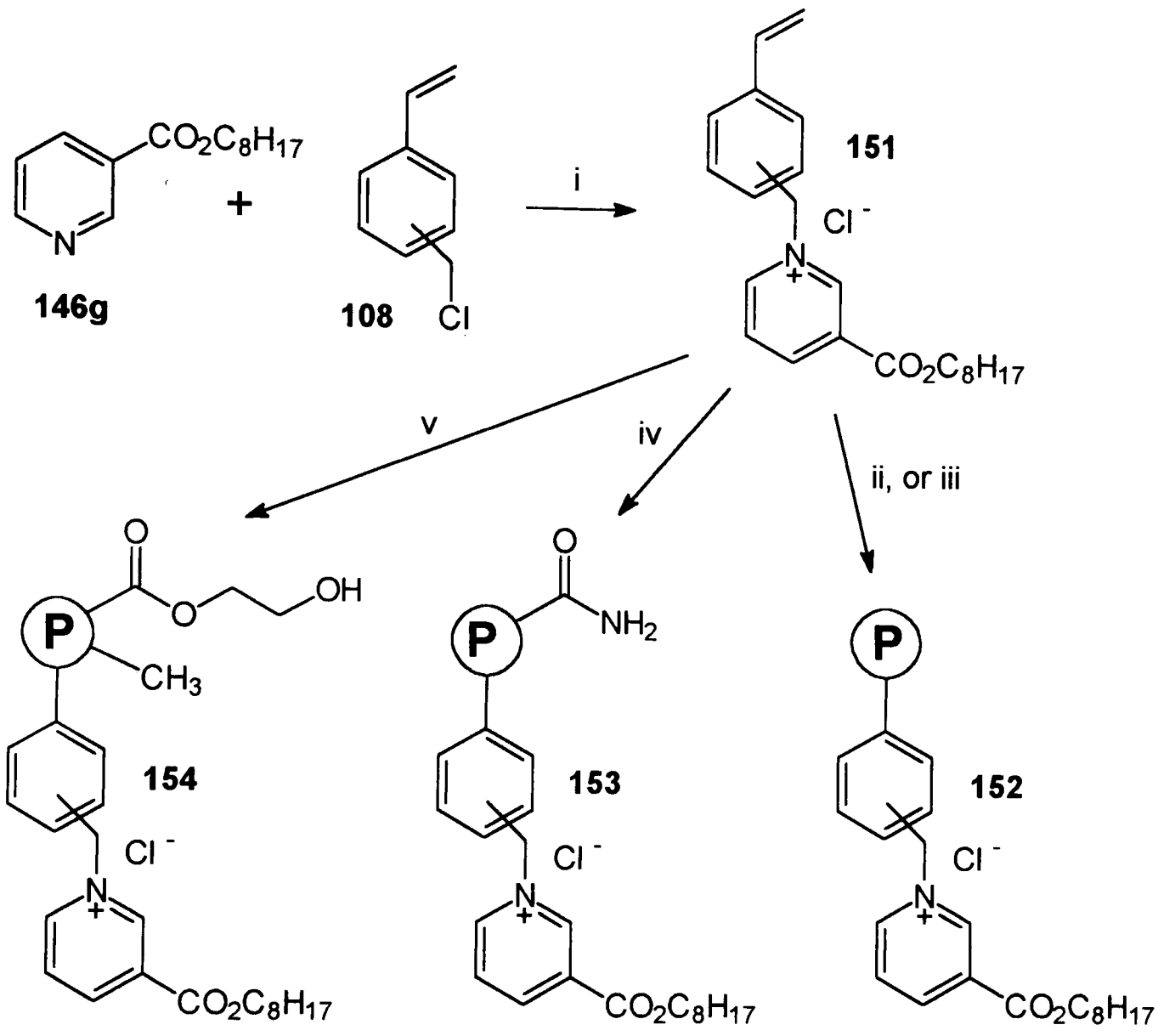

Scheme 15 *Reagents and conditions:* i, neat, 66 °C, 18 h; ii, $K_2S_2O_8$, H_2O, 66 °C, 19 h; iii, AIBN, THF, 78 °C, 20 h; iv, AAm, AIBN, THF, 64 °C, 19 h; v, HEMA, AIBN, THF, 64 °C, 19 h.

It was decided to co-polymerize **148g** with a water-soluble co-monomer with the aim of producing a water-soluble pyridinium salt co-polymer. However, owing to shortage of sample **148g** a batch of the isomeric nicotinate quat monomer **151** was prepared (Scheme 15). Recall that the quat **148g** was prepared by the quaternization of *n*-octyl nicotinate **146g** with *p*-vinylbenzyl chloride **109** (Scheme 13). The quat **151**

was prepared in an identical manner to that of **148g** with the exception that the ester **146g** was quaternized with the isomeric mixture, *m/p*-vinylbenzyl chloride **108** (Scheme 15). The isomeric mixture **108** was used in preference to the pure isomer **109** because none of the latter was available at the time; in addition, it was more economic to use the considerably less expensive isomeric mixture. The sample of *m p*-vinylbenzyl chloride **108** (Aldrich) was confirmed by ^{1}H NMR spectroscopy (250 MHz, $CDCl_3$) to consist of an approximate 7:3 mixture of *meta-/para*-isomers. The quat **151** was purified by trituration with diethyl ether and afforded a gum (63%). The ^{1}H NMR spectrum (250 MHz, $CDCl_3$) of **151** was similar to that of the quat **148g** with the exception that the former spectrum showed an additional set of signals due to the *meta*-quat component. In addition, the spectrum revealed that the quat **151** was hydrated with 1.5 molecules of water per molecule of **151**. The FTIR spectrum (film) of **151** revealed a strong carbonyl absorption at 1731 cm^{-1} (*c.f.* 1726 cm^{-1} in the monomer **148g**).

Before proceeding with co-polymer studies, the quat **151** was homo-polymerized (Scheme 15). The homo-polymerization of **151** was attempted in both aqueous (Route ii) and organic (Route iii) solvents. In the aqueous system, potassium persulfate ($K_2S_2O_8$) initiator was added to a solution of the monomer **151** in deionized water. Upon addition of the persulfate the solution turned milky white in colour. Despite this, the solution was degassed and then heated at 66 °C for 19 h. At the end of the reaction a water-insoluble gelatinous material had formed. This gel-like residue was dried and examined further. It was found to be completely insoluble in all the common bench solvents. A series of swelling tests were then conducted. The gel was found to swell in *N,N*-dimethylformamide, dimethylsulfoxide, ethanol, methanol and tetrahydrofuran (slight swelling), but did not swell in acetone, benzene, dichloromethane, diethyl ether, ethyl acetate, *n*-hexane, toluene and water. It was concluded from these observations that the gel-like material was the polymer **152** in the form of either a very high molecular weight species or, alternatively, a cross-linked gel.

The organic system (Route iii) used to homo-polymerize **151** was identical to that used for the homo-polymerization of **148g** (Scheme 14). A solution of monomer **151** and AIBN in tetrahydrofuran was degassed and then heated at 78 °C for 20 h.

Work-up afforded the homo-polymer **152** as a sandy powder (mp >340 °C; 7% conversion). ^{1}H NMR spectroscopy (250 MHz, $CDCl_3$) of **152** revealed the following key signals: δ 0.87 (CH_3), 1.27 [$(CH_2)_5CH_3$], 1.78 (OCH_2CH_2), 1.9–3.6 (CH_2CH of polymer backbone), ~4.3 (OCH_2), 5.8–6.5 (ex br, NCH_2) and 6.5–10.5 (several signals, v br, Ar–H) ppm. FTIR spectroscopy (KBr pellet) of **152** revealed a strong carbonyl absorption at 1727 cm^{-1} (*c.f.* 1731 cm^{-1} in the monomer **151**). Like **150** (Scheme 14), the polymer **152** was insoluble in water. As a result, and owing to the poor MIC results obtained for **150**, the polymer **152** was not tested for antimicrobial activity.

The monomer **151** was co-polymerized, separately, with two different water-soluble co-monomers, acrylamide (AAm) and 2-hydroxyethyl methacrylate (HEMA). As already mentioned, the homo-polymer **152** was found to be insoluble in water. It was hoped that by introducing the hydrophilic AAm and HEMA functionalities into the polymer **152** the water solubility of the resultant co-polymers would be improved. The co-polymerization of **151** with acrylamide is shown in Scheme 15. A solution of AIBN and equimolar amounts of monomer **151** and acrylamide in tetrahydrofuran was degassed and then heated at 64 °C for 19 h. Work-up afforded the AAm co-polymer **153** as a tan powder (28% conversion). ^{1}H NMR spectroscopy (250 MHz, $CDCl_3$) of **153** revealed the following key signals: δ 0.87 (CH_3), 1.27 [$(CH_2)_5CH_3$], 1.73 (OCH_2-CH_2), 1.6–3.9 (CH_2CH of polymer backbone), ~4.3 (OCH_2) and 5.5–10.5 (several signals, v br, Ar–H) ppm. The NH_2 signal could not be clearly identified; in theory, $RCONH_2$ protons resonate in the range δ 5–12 ppm.[62] FTIR spectroscopy (KBr pellet) of **153** revealed a pair of strong carbonyl absorptions at 1724 cm^{-1} (ester C=O; *c.f.* 1727 cm^{-1} in the homo-polymer **152**) and 1666 cm^{-1} (AAm C=O). In addition, there was a medium intensity band at 3209 cm^{-1}, assigned to N–H stretching. Unfortunately, the co-polymer **153** was found to be insoluble in water. As a result, and owing to insufficient sample weight, **153** was not tested for antimicrobial activity.

The conditions for the co-polymerization of **151** with 2-hydroxyethyl methacrylate (Scheme 15) were identical to those used in the acrylamide co-polymerization reaction. Work-up afforded the HEMA co-polymer **154** as a sandy-brown powder [mp 78 (softened)–110 °C; 8% conversion]. ^{1}H NMR spectroscopy (250 MHz,

$CDCl_3$) of **154** revealed the following key signals: δ 0.88 (with sh, CH_3), 1.28 [$(CH_2)_5CH_3$], 1.73 (OCH_2CH_2), 1.6–4.1 (CH_2CH of polymer backbone, and CH_2CH_2 of HEMA), ~4.3 (OCH_2) and 5.6–10.0 (several signals, v br, Ar–H) ppm. FTIR spectroscopy (KBr pellet) of **154** revealed a strong carbonyl absorption at 1724 cm^{-1} (*c.f.* 1727 cm^{-1} in the homo-polymer **152**). Like **153**, the co-polymer **154** was insoluble in water. As a result, and owing to insufficient sample weight, **154** was not tested for antimicrobial activity.

The experimental conditions used for the preparation of the homo-polymers **150** (Scheme 14) & **152** (Scheme 15) and the co-polymers **153** & **154** (Scheme 15) are summarized in Table 26. A summary of elemental microanalytical data and selected FTIR data for the same compounds is shown in Table 27.

Table 26 Polymerization of nicotinate quaternary ammonium salts **148g** (Scheme 14) and **151** (Scheme 15).

P[a]	M[b]	[M]/mol dm^{-3}	Co-M[c]	[Co-M] / mol dm^{-3}	[Initiator]/ mol dm^{-3}	Conditions: Solvent, *T*, *t*.	Con.[d] (%)
150	**148g**	0.43	None	—	0.021[e]	THF, 60 °C, 18 h	27
152[f]	**151**	0.22	None	—	0.0062[g]	H_2O, 66 °C, 19 h	—
152	**151**	0.32	None	—	0.015[e]	THF, 78 °C, 20 h	7
153	**151**	0.25	AAm[h]	0.25	0.014[e]	THF, 64 °C, 19 h	28
154	**151**	0.25	HEMA[i]	0.25	0.014[e]	THF, 64 °C, 19 h	8

[a]Polymer. [b]Monomer. [c]Co-monomer. [d]Conversion. [e]AIBN. [f]Either a very high molecular weight species or a cross-linked gel. [g]$K_2S_2O_8$. [h]Acrylamide. [i]2-Hydroxyethyl methacrylate.

Table 27 Elemental microanalytical data and selected FTIR data for the polymeric pyridinium salts **150** (Scheme 14) and **152–154** (Scheme 15).

	Elemental microanalysis				
Polymer	%C	%H	%Cl	%N	ν_{max}/cm^{-1} [a]
150	63.60	7.65	4.63	2.74	1724 (C=O)
152[b]	66.96	7.62	7.38	2.75	N/A
152[c]	63.81	7.39	5.22	2.53	1727 (C=O)
153	63.47	7.52	4.33	4.09	3209 (N–H), 1724 (ester C=O), 1666 (AAm C=O)
154	63.86	7.68	3.38	2.22	1724 (C=O)

[a]KBr pellet. [b,c]Scheme 15, Routes ii[b] and iii.[c]

In conclusion, the results of the above co-polymer studies came as somewhat of a disappointment. Owing to the water-insolubility of the homo-polymer **152** (Scheme 15) it had been hoped that co-polymerization of the monomer **151** with the hydrophilic monomers acrylamide and 2-hydroxyethyl methacrylate would lead to a water-soluble polymeric pyridinium salt. However, neither the AAm co-polymer **153** or the HEMA co-polymer **154** were soluble in water. In addition, the yields obtained of **153** and **154** were very low (28% and 8% respectively).

3.4.5 Other Polymerizable Nicotinate Quaternary Ammonium Salts

The key structural features of the nicotinate quat **148** (Scheme 13) are the hydrophobic alkyl chain and the vinyl group. As mentioned previously, the hydrophobic group in quaternary ammonium compounds plays a principle role in the compound's mode of action against bacterial cells. The vinyl group of **148** is a useful, additional feature that allows the molecule to be polymerized (the merits of polymeric quats were discussed earlier). With these key features in mind, now consider the possibilities for other types of polymerizable nicotinate quaternary ammonium compounds.

Shown in Figure 50 is a suggested route to the polymerizable pyridinium salt **157**. The monomer **157** is structurally similar to that of the quat **148** (Scheme 13), with two notable exceptions. The first of these concerns the alkyl chain. In **148**, the alkyl chain is part of the ester group. In **157**, however, the alkyl group is attached to nitrogen, forming a pyridinium salt. The second structural difference between **148** and **157** concerns the location of the vinyl group. In **148**, the vinyl group is attached to nitrogen in the nicotinate ring, whereas in **157** it is located at the other end of the ester chain. In other words, on comparing **157** to **148**, the positions of the alkyl and vinyl groups are switched around. The monomer **157** has the same key structural features as **148** and so would make an ideal candidate for a new quaternary ammonium compound. The synthesis of **157**, however, would not be as straightforward as that of **148**. Nicotinic acid **143** could be converted to the nicotinate alcohol **155** using the di-alcohol **81**. The hydroxyl group of **155** could then be acrylated with acryloyl chloride to give the acrylate **156**. Finally, quaternization of **156** with an alkyl halide (RX) would give the polymerizable pyridinium salt **157**. Alkyl groups with different chain

lengths could be used to generate a series of compounds **157** in a similar manner to that of **148**. This would allow the correlation of chain length with antimicrobial activity. The advantage of the structure **157**, over that of **148**, is that the di-alcohol **81**

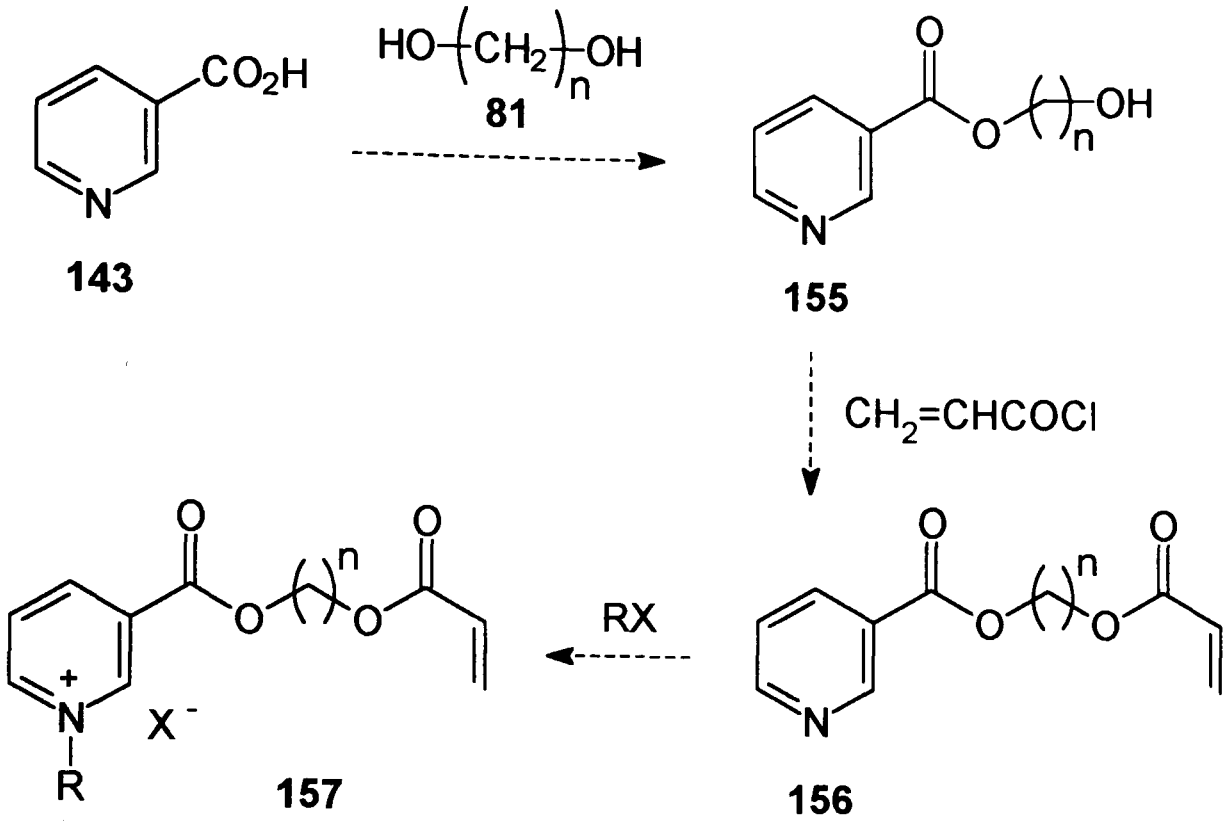

Fig. 50 Suggested route to a polymerizable pyridinium salt.

acts as a 'spacer' group, effectively separating the polymerizable group from the anti-microbially active part of the molecule. The length, n, of the spacer group therefore acts as an additional structural 'variable'. Also, the spacer group need not be derived from the di-alcohol **81**. Instead, it might prove interesting to use a more hydrophilic spacer, *e.g.* a poly(ethylene glycol) ('PEG'), $HO(CH_2CH_2O)_nH$. Introducing a spacer, such as this, would make the resultant monomer more hydrophilic. This would be particularly advantageous if the ultimate aim was to produce a water-soluble polymer (or co-polymer) of **157**. Another alternative spacer group might be the amino-alcohol, $HO(CH_2)_nNH_2$. This could be attached to the carboxylic acid group of nicotinic acid **143**, via oxygen or nitrogen, to ultimately give the monomer **157** but with one of the C(O)O groups replaced by C(O)NH. The monomer **157** is just one example of a potentially interesting group of polymerizable quaternary ammonium compounds which would make useful targets for extensions of this work.

4. FUTURE WORK

Each section of the *Results and Discussion* chapter concluded with suggested avenues of research for future study. The potentially more attractive, and profitable, of these research areas are summarized below.

The 'model' compounds benzofuroxan **71** (Scheme 3), 3-amino parabens **78** (Scheme 4) and benzokathon **99** (Scheme 6) all displayed antimicrobial activity against *Saccharomyces cerevisiae* EL1. The synthesis of benzofuroxan and benzokathon heterocyclic ring systems are based on *ortho*-substituted benzene rings. An *ortho*-substituted aromatic compound with a residual functional group (*e.g.* an hydroxy or an amino group) would therefore serve as a precursor towards polymerizable derivatives. In this way, acrylate and acrylamido monomers of both benzofuroxan (Figure 24, **72b** and **73b** respectively) and benzokathon (Figure 28, **100b** and **101b** respectively) might be realized. Vinylbenzofuroxan **74** (Figure 24) and vinylbenzokathon **102** (Figure 28) are also potentially interesting monomers, but their syntheses may be more problematical. The synthesis of a monomer based on the 3-amino parabens ester **78** could be undertaken by modifying either the amino or carboxylic acid groups. Using the former strategy, it would be possible, using protection chemistry, to prepare the acrylamido monomer **79** (Figure 25). Alternatively, a 'spacer' function with a polymerizable end group could be attached to the carboxylic acid group to produce the novel acrylate monomer **83** (Figure 25).

A relatively new class of cationic biocides are the phosphonium salts. These compounds serve as an interesting, and novel, alternative to the more conventional cationic biocides, the quaternary ammonium salts. The present studies were concerned with the polymerizable phosphonium salts **105** and **111** (Scheme 7). The polymerizable function in these compounds is a vinylbenzyl group. The methacrylate monomer **113** and the methacrylamide monomer **114** (Figure 30) have been proposed as hydrophilic variants of **105** and **111**. Alternatives to the methacrylate monomers **113** and **114** would be the phosphonium salt vinyl ethers **115** and **116** (Figure 30). The vinyl ether **116** contains an ethoxy spacer group and therefore serves as a more hydrophilic variant of **115**.

Of the compounds tested in the present studies, Amical **125** and the monoiodo analogue **126** (Scheme 10) proved to be the most potently active against *Saccharo-*

myces cerevisiae EL1. The diiodomethyl sulfone moiety of Amical can be formed from an aromatic thiol group. A thiophenol with a residual functional group (*e.g.* an hydroxy or an amino group) would therefore serve as a precursor towards polymerizable Amical derivatives. Targets worthy of future study might include the acrylate-, acrylamido- and vinyl- diiodomethyl sulfone monomers **127b**, **128b** and **129b** (Figure 32) respectively.

Amical is an example of a class of antimicrobial agents referred to as *activated halogen compounds*. The biologically active part of the Amical molecule is the diiodomethyl sulfone ($-SO_2CHI_2$) moiety – the diiodomethyl group is activated by the sulfonyl portion. The structure of diiodomethyl compounds can therefore be generalized to $X-CHI_2$, where X is an activating group of some description. It may prove interesting to study diiodomethyl compounds that contain different activating groups. Examples of conventional 'X' groups worth investigating are –C(O)R, –C(O)Ar and $-CO_2R$. An example of a more exotic, and novel, X-functionality might be the phosphorous (V) group, –P(O)(OH)R.

The present studies indicate good evidence for achieving the chemical modification of the sulfonic acid ion exchange resin **138** to the diiodomethyl sulfone resin **142a** (Scheme 12). An 'antimicrobial resin' is a very desirable target since it has the potential of being technologically very useful. It would prove both beneficial and logical, therefore, to optimize the chemistry shown in Scheme 12 with the aim of producing a resin **142a** with a high iodine loading. Rigorous microbiological testing of the resin would then allow its antimicrobial potential to be fully realized.

Nicotinic acid **143** (Scheme 13) proved a useful precursor in the synthesis of the polymerizable nicotinate quaternary ammonium salts **148a–i** (Scheme 13). Nicotinic acid could also serve as a precursor towards the preparation of the polymerizable pyridinium salt **157** (Figure 50). The acrylate monomer **157** is an interesting structural variant of the nicotinate quats **148** because the roles of the ester moiety and the nitrogen atom are complimentary. In the quats **148**, the polymerizable group is attached via the nitrogen atom and the all-important alkyl chain forms part of the ester group. In the monomer **157**, however, the nitrogen atom bears the alkyl chain and the polymerizable group is attached to an alkyl spacer which, in turn, forms part of the

ester group. The spacer group therefore serves as an additional structural 'variable'. For example, it may prove interesting to prepare a more hydrophilic version of **157** by employing a poly(ethylene glycol) spacer group, $HO(CH_2CH_2O)_nH$.

The logical conclusion to the above research would be the preparation and microbiological testing of homo-polymers and co-polymers. The co-monomers need not be non-antimicrobial compounds. Alternatively, it may prove interesting to produce co-polymers derived from different antimicrobial monomers (a 'mixed' anti-microbial polymer). Additionally, if a series of co-polymers are prepared using different co-monomer ratios then microbiological activity could be correlated with co-polymer composition. This would give the optimum co-polymer ratio required for maximum antimicrobial effectiveness.

5. REFERENCES AND NOTES

1 T. J. Franklin and G. A. Snow, *Biochemistry of Antimicrobial Action*, Chapman and Hall, London, 4th edition, 1989.

2 F. E. Hahn, *Antibiotics (N.Y.)*, 1975, **5**, 353.

3 W. Hofheinz and B. Merkli, *Handbook Expl. Pharmacol.*, 1984, **68**, 61.

4 R. S. Gupta, *Antibiotics (N.Y.)*, 1983, **6**, 46.

5 K. K. Bhutani, G. L. Sharma and M. Ali, *Planta Med.*, 1987, **53**, 532.

6 K. Thoma and D. Steinbach, *Pharm. Ind.*, 1975, **37**, 455.

7 A. S. Levinson, *J. Chem. Educ.*, 1987, **54**, 98.

8 J. Dressel, *J. Chem. Educ.*, 1961, **38**, 620.

9 J. G. Olenick, *Antibiotics (N.Y.)*, 1975, **3**, 699.

10 *Martindale, The Extra Pharmacopoeia*, Pharmaceutical Press, London, 28th/29th editions, 1982/1989, p. 4797.

11 German Patent 3 142 854, *Chem. Abs.*, 1983, **99**, 53790h.

12 N. X. Chin and H. C. Neil, *Antimicrob. Agents Chemother.*, 1984, **25**, 319.

13 G. J. Manius, *Anal. Profiles Drug Subst.*, 1978, **7**, 445.

14 C. H. O'Callaghan, P. Acred, P. B. Harper, D. M. Ryan, S. M. Kirby and S. M Harding, *Antimicrob. Agents Chemother.*, 1980, **17**, 876.

15 B. R. Smith, *Clin. Pharm.*, 1984, **3**, 373.

16 N. A. Campbell, *Biology*, Benjamin/Cummings Publishing Company, Inc., California, 4th edition, 1996.

17 T. M. Devlin (editor), *Textbook of Biochemistry*, Wiley-Liss (John Wiley & Sons), New York, 3rd edition, 1992.

18 D. Voet and J. G. Voet, *Biochemistry*, John Wiley & Sons, New York, 2nd edition, 1995.

19 D. I. Edwards, *Antimicrobial Drug Action*, Macmillan Press Ltd., London, 1st edition, 1980.

20 S. M. L. Hammond, *Antibiotics and Antimicrobial Action*, Arnold, London, 1st edition, 1978.

21 V. M. Dillon and R. G. Board (editors), *Natural Antimicrobial Systems and Food Preservation*, CAB International, Wallingford, U.K., 1st edition, 1994.

22 H.–G. Schmitt, *The Action of Antimicrobial Substances (Parfümerie + Kosmetik, No. 1/1987)*, Bayer AG, Organic Chemicals Group, Leverkusen, March 1988.

23 J. Elks and C. R. Ganellin (editors), *Dictionary of Drugs*, Chapman and Hall, London, 1st edition, 1990.

24 W. B. Hugo and A. D. Russell, *Pharmaceutical Microbiology*, Blackwell Scientific Publications, Oxford, 1980, Chapter 9.

25 H. Tripathy, D. G. Pradham, B. C. Dash and G. N. Mahapatra, *Agric. Biol. Chem.*, 1973, **37**, 1375.

26 R. A. Coburn, A. J. Batista, R. T. Evans and R. J. Genco, *J. Med. Chem.*, 1981, **24**, 1245.

27 H. C. Stecker and R. E. Faust, *J. Soc. Cosmetic Chemists*, 1960, **11**, 347.

28 A. Kraushaar, *Arzneim.-Forsch.*, 1954, **4**, 548.

29 A. D. Russell, *Infection*, 1986, **14**, 212.

30 W. D. Crow and N. J. Leonard, *J. Org. Chem.*, 1965, **30**, 2660.

31 J. M. G. Cowie, *Polymers: Chemistry and Physics of Modern Materials*, Blackie, Glasgow, 2nd edition, 1991.

32 H. R. Allcock and F. W. Lampe, *Contemporary Polymer Chemistry*, Prentice-Hall, Englewood Cliffs, New Jersey, 2nd edition, 1990.

33 H.–G. Elias, *Macromolecules*, Plenum Press, New York, 2nd edition, 1984.

34 F. W. Billmeyer, *Textbook of Polymer Science*, Wiley-Interscience, New York, 3rd edition, 1984.

35 T. Ikeda, S. Tazuke and Y. Suzuki, *Makromol. Chem.*, 1984, **185**, 869.

36 N. Kawabata and M. Nishiguchi, *Appl. Environ. Micro.*, 1988, **54**, 2532.

37 A. Kanazawa, T. Ikeda and T. Endo, *J. Appl. Polym. Sci.*, 1994, **53**, 1245.

38 C. U. Pittman, *J. Appl. Polym. Sci.*, 1981, **26**, 2403.

39 A. W. Sheldon, *J. Paint Technol.*, 1975, **47**, 54.

40 J. A. Montemarano and E. J. Dyckman, *J. Paint Technol.*, 1975, **47**, 59.

41 E. J. Dyckman, J. A. Montemarano and E. C. Fisher, *Nav. Eng. J.*, 1973 (December), **33**.

42 M. D. Steele and R. W. Drisko, *J. Coatings Technol.*, 1976, **48**, 59.

43 T. Ikeda, H. Yamaguchi and S. Takzuke, *J. Bioact. Comp. Polym.*, 1986, **1**, 301.

44 A. Kanazawa, T. Ikeda and T. Endo, *J. Polym. Sci., Part A: Polym. Chem.*, 1993, **31**, 1467.

44A D. W. Emerson, *Ind. Eng. Chem. Res.*, 1988, **27**, 1797.

44B D. W. Emerson, *Ind. Eng. Chem. Res.*, 1990, **29**, 448.

44C D. W. Emerson, D. Gaj, C. Grigorian and J. E. Turek, *Polym. Prepr. Am. Chem. Soc. Div. Polym. Chem.*, 1982, **23**, 289.

44D D. W. Emerson, *Ind. Eng. Chem. Res.*, 1993, **32**, 1228.

44E D. W. Emerson, D. T. Shea and E. M. Sorensen, *Ind. Eng. Chem. Prod. Res. Dev.*, 1978, **17**, 269.

44F Y. Nakamura, *J. Chem. Soc. Japan, Ind. Chem. Sect.*, 1954, **57**, 818; *Chem. Abs.*, 1955, **58**, 10661g.

44G R. Bogoczek and E. Kociolek–Balawejder, *Vysokomol. Soedin. Ser. A.*, 1987, **29**, 2346; *Chem. Abs.*, 1988, **108**, 38845.

45 R. J. Fort and T. M. Polyzoidis, *Eur. Poly. J.*, 1976, **12**, 685; see also P. Štrop, F. Mikeš and J. Kálal, *J. Phys. Chem.*, 1976, **80**, 694.

46 MIC test developed by Angela Brown, Department of Biosciences, University of Strathclyde.

47 W. J. Cho, C. S. Ha, B. K. Min and S. T. Oh, *J. Appl. Polym. Sci.*, 1994, **52**, 583.

48 D. C. Sherrington, P. Snedden and A. Sneddon, *Project Spider: Synthetic Chemistry Report, Review Meeting*, June 1994.

49 A. G. Green and F. M. Rowe, *J. Chem. Soc.*, 1912, **63**, 2452.

50 D. L. Hammick, W. A. M. Edwardes and E. R. Steiner, *J. Chem. Soc.*, 1931, **96**, 3308.

51 A. J. Boulton, P. B. Ghosh and A. R. Katritzky, *J. Chem. Soc.(C)*, 1966, **10**, 971.

52 E. Lück, *Antimicrobial Food Additives – Characteristics, Uses, Effects*, Verlag, New York, 1980, p. 223.

53 I. F. Nes and T. Eklund, *J. Appl. Bacteriol.*, 1983, **54**, 237.

54 N. D. Shiralkar and D. V. Rege, *Indian Food J.*, 1978, **32**, 34.

55 J. R. Furr and A. D. Russell, *Microbios.*, 1972, **5**, 189.

56 K. Tatsuguchi, S. Kuwamoto, M. Ogomori, T. Ide and T. Watanabe, *Shotokuhin Eiseigaku Zasshi*, 1991, **32**, 121; *Chem. Abs.*, 1991, **115**, 174137h.

57 E. Freese, C. W. Sheu and E. Galliers, *Nature (London)*, 1973, **241**, 321.

58 A. A. Brown, M. Catlin, B. Kristiansen, W. M. M^{c}Gregor, B. M^{c}Neil, M. Mattey, B. Rowatt, D. C. Sherrington and A. Sneddon, *Synthesis and Antimicrobial Activity of 3-Substituted Parabens Esters*, unpublished paper.

59 Further information on flash-column chromatography techniques can be found in: W. C. Still, M. Kahn and A. Mitra, *J. Org. Chem.*, 1978, **43**, 2923.

60 TCI, *Catalogue of Organic Chemicals*, 1992.

61 S. N. Lewis, G. A. Miller, M. Hausman and E. C. Szamborski, *J. Het. Chem.*, 1971, **8**, 571.

62 D. H. Williams and I. Fleming, *Spectroscopic Methods in Organic Chemistry*, McGraw–Hill, London, 3rd edition, 1980.

63 Further information and details on the benzokathon family and its derivatives can be found in: L. L. Bambas, *The Chemistry of Heterocyclic Compounds, Vol. IV: Five-membered Heterocyclic Compounds with N and S or N, S and O (except thiazole)*, Interscience Publishers Inc., New York, p. 253.

64 M. M^{c}Kibben and E. W. M^{c}Clelland, *J. Chem. Soc.*, 1932, **123**, 170.

65 Aldrich, *Catalogue Handbook of Fine Chemicals*, 1994–1995.

66 R. Elsmore, *Israel J. Med. Sci.*, 1986, **22**, 647.

67 A. Kanazawa, T. Ikeda and T. Endo, *J. Polym. Sci., Part A: Polym. Chem.*, 1993, **31**, 335.

68 A. Kanazawa, T. Ikeda and T. Endo, *J. Polym. Sci., Part A: Polym. Chem.*, 1993, **31**, 1441.

69 A. Kanazawa, T. Ikeda and T. Endo, *J. Appl. Polym. Sci.*, 1994, **53**, 1237.

70 A. J. Crovetti, German Patent 2,011,052, *Chem. Abs.*, 1971, **74**, P55266z.

71 A. J. Crovetti, US Patent 3,632,859, 1972.

72 T. Ammo, M. Tamagishi, S. Kouchiwa, S. Ukai, H. Hayashi and Y. Tobari, Japanese Patent 6806,609, *Chem. Abs.*, 1968, **69**, P96242d.

73 F. M. H. Cavati, A. J. Crovetti, B. E. Melin and R. A. Smith, EP 258,878, *Chem. Abs.*, 1988, **109**, P33869n.

74 W. J. Kenney, J. A. Walsh and D. A. Davenport, *J. Am. Chem. Soc.*, 1961, **83**, 4019.

75 *Amical 48 Data Sheet*, Angus Chemical Company.

76 Microsoft *Excel* (version 5.0), 'LINEST' function.

77 A. Courtin, *Helv. Chim. Acta.*, 1983, **66**, 1046.

78 Further information on resin types and resin conditioning techniques can be found in: *Ion Exchange Resins Handbook*, BDH.

79 A. N. Petrocci, *Disenfection, Sterilization and Preservation*, Philadelphia, 2nd edition, 1977, p. 325.

80 I. Lacko, *Z. Naturforsch., Teil C.*, 1979, **34(C)**, 485.

81 S. Osanai and Y. Abe, *J. Chem Tech. Biotechnol.*, 1985, **35(B)**, 43.

82 J. Kolodynski, S. Ulaszewski, D. Grobelny, R. Witowska, S. Witek and T. Lachowicz, *Acta. Micro. Pol.*, 1984, **33**, 119.

83 A. J. Isquith, E. A. Abbott and P. A. Walters, *Appl. Micro.*, 1973, **24**, 859.

84 D. L. Price, A. D. Sawant and D. G. Ahearn, *J. Ind. Micro.*, 1991, **8**, 83.

85 N. V. Kolokolkina, E. F. Panarin, M. A. Penenzhik, N. S. Plotkina, M. V. Solovskii, and A. D. Virnik., *J. Appl. Chem. USSR.*, 1985, **58**, 1474.

86 P. Messinger and A. Schimpke–Meier, *Arch. Pharm.*, 1988, **321**, 89.

87 K. Nagai, Y. Ohishi, H. Inaba and S. Kudo, *J. Polym. Sci., Polym. Chem. Ed.*, 1985, **23**, 1221.

88 W. M. M^{c}Gregor, A. Sneddon, D. C. Sherrington and B. Rowatt, *Effect of Chemical Structure on Antimicrobial activity of Quaternary Ammonium Hydroxides*, unpublished paper.

89 A. I. Vogel (revised by B. S. Furniss *et al.*), *Vogel's Textbook Of Practical Organic Chemistry*, Longman Scientific & Technical (John Wiley & Sons, Inc.), New York, 5th edition, p. 1078.

90 C. F. Woodward and C. O. Badgett, US Patent 2,150,164, *Chem. Abs.*, 1950, **44**, 8378d.

6. APPENDIX

Selected ^{1}H NMR Spectra

Reproduced in the following pages are ^{1}H NMR spectra (Figures 51–59) of a selection of important compounds featured in this thesis. The spectra are listed in Table 28.

Table 28 ^{1}H NMR Spectra.

Compound	Section	Scheme	Spectrum
Nonyl 3-amino parabens ester **78**	3.1.4	4	Fig. 51
Chloropropyl thiol **94**	3.1.5	5	Fig. 52
Bromoethyl-dithiodipropionamide **92b**	3.1.5	5	Fig. 53
Diiodomethyl sulfone **125**	3.3.2	10	Fig. 54
Monoiodomethyl sulfone **126**	3.3.2	10	Fig. 55
Octyl nicotinate quat **148g**[a]	3.4.2	13	Fig. 56
Homo-polymer **150** of octyl nicotinate quat **148g**	3.4.4	14	Fig. 57
Co-polymer **153** of octyl nicotinate quat **151**[b] and acrylamide	3.4.4	15	Fig. 58
Co-polymer **154** of octyl nicotinate quat **151** and 2-hydroxyethyl methacrylate	3.4.4	15	Fig. 59

[a] *p*-Isomer. [b] *m*/*p*-Isomeric mixture.

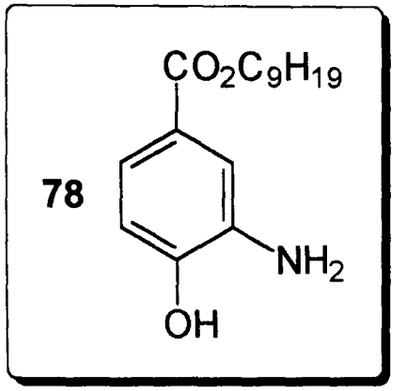

Fig. 51 ^{1}H NMR Spectrum (250 MHz, $CDCl_3$) of the nonyl 3-amino parabens ester **78** (Scheme 4).

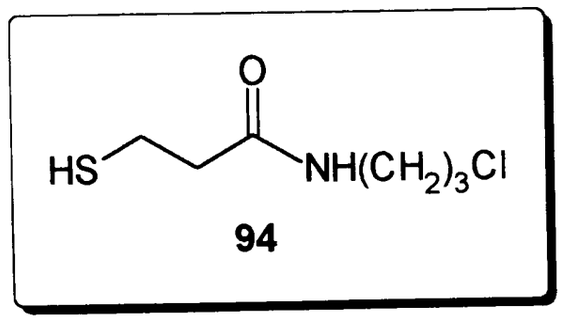

94

Fig. 52 ^{1}H NMR Spectrum (250 MHz, $CDCl_3$) of the chloropropyl thiol **94** (Scheme 5).

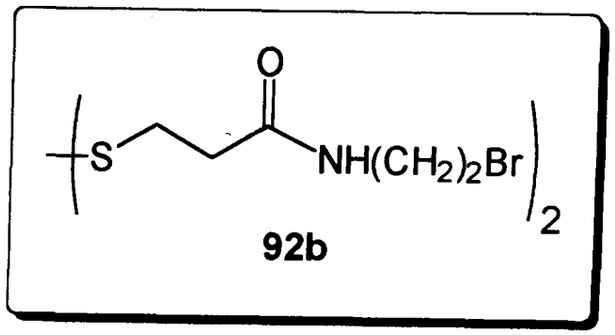

92b

Fig. 53 ^{1}H NMR Spectrum (250 MHz, C_5D_5N) of the bromoethyl-dithiodipropionamide **92b** (Scheme 5).

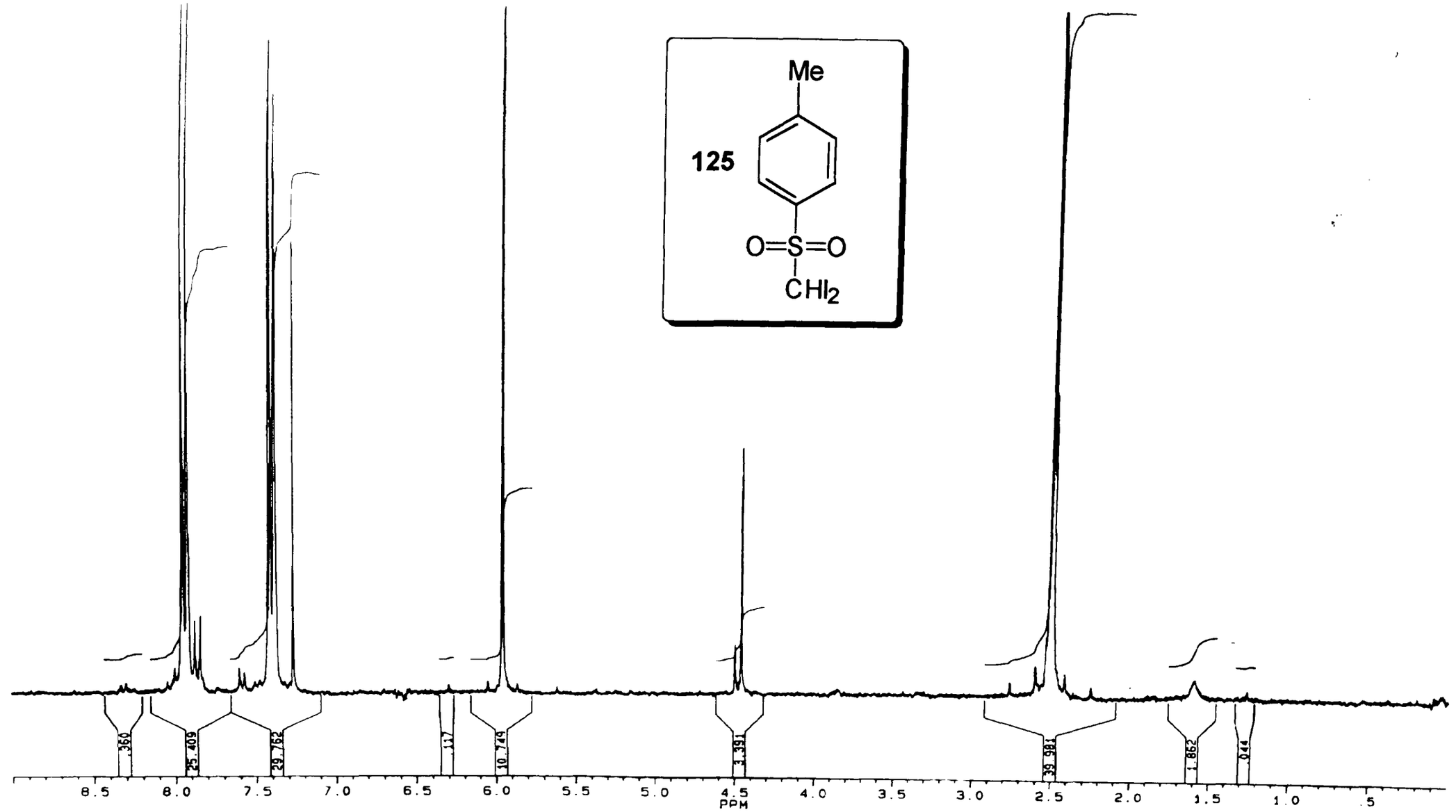

Fig. 54 ^{1}H NMR Spectrum (250 MHz, $CDCl_3$) of the diiodomethyl sulfone **125** (Scheme 10).

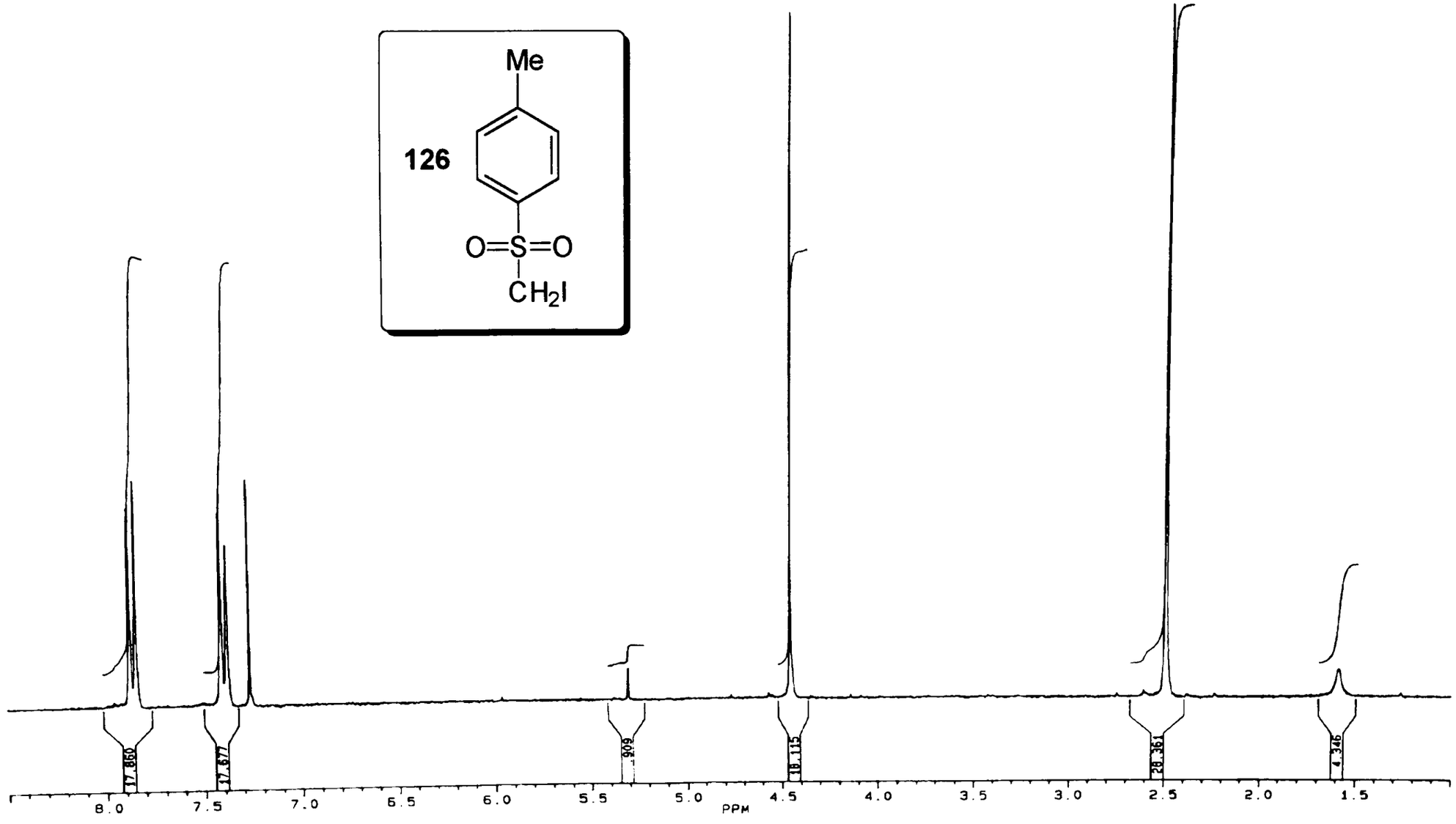

Fig. 55 ^{1}H NMR Spectrum (250 MHz, $CDCl_3$) of the monoiodomethyl sulfone **126** (Scheme 10).

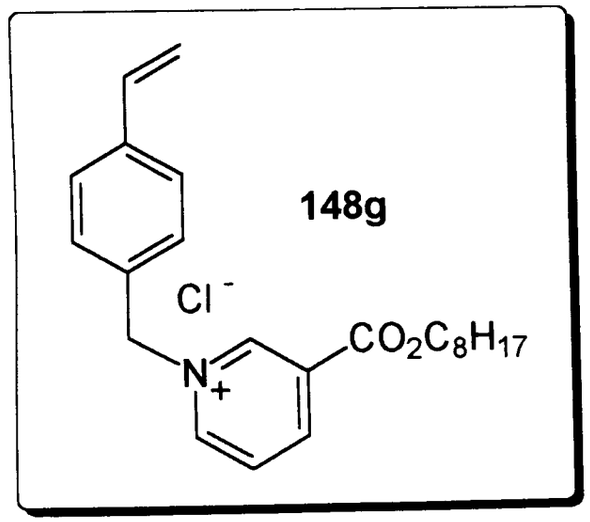

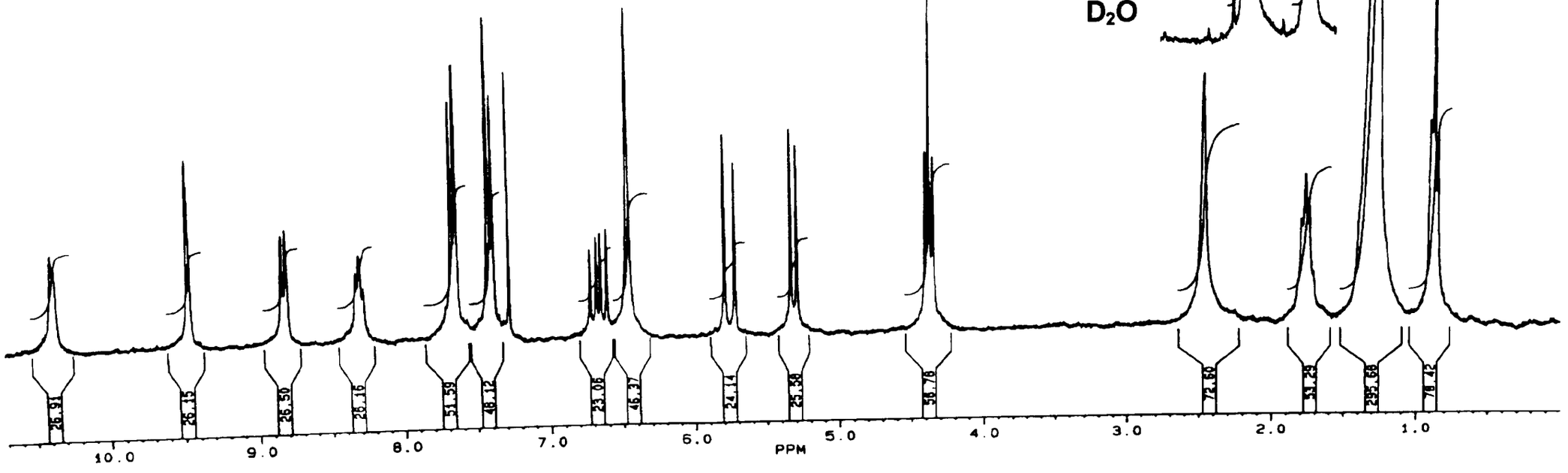

Fig. 56 ^{1}H NMR Spectrum (250 MHz, $CDCl_3$) of the octyl nicotinate quat **148g** (Scheme 13).

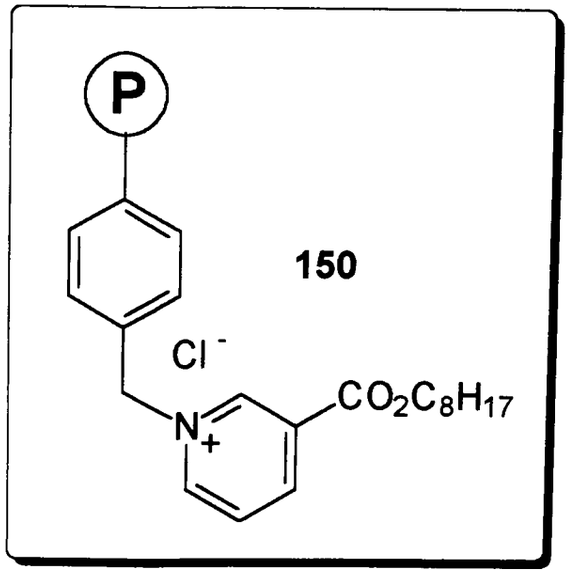

Fig. 57 ^{1}H NMR Spectrum (250 MHz, $CDCl_3$) of the homo-polymer **150** of the octyl nicotinate quat **148g** (Scheme 14).

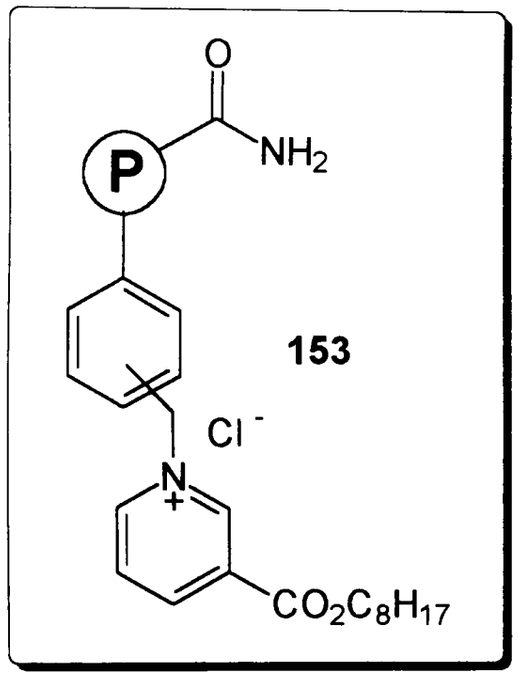

Fig. 58 ^{1}H NMR Spectrum (250 MHz, $CDCl_3$) of the co-polymer **153** of the octyl nicotinate quat **151** and AAm (Scheme 15).

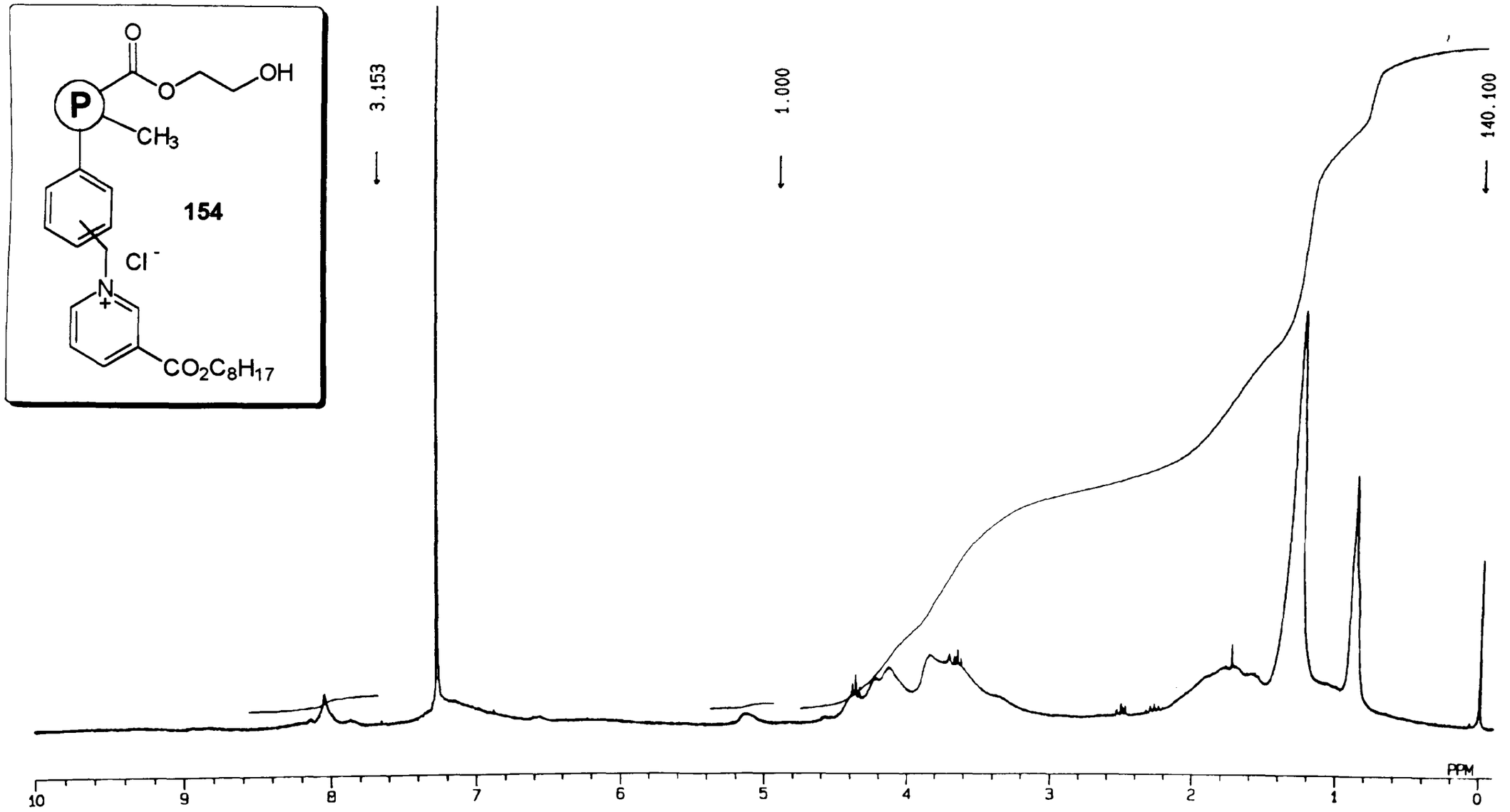

Fig. 59 ^{1}H NMR Spectrum (250 MHz, $CDCl_3$) of the co-polymer **154** of the octyl nicotinate quat **151** and HEMA (Scheme 15).